SERDP

FINAL REPORT

Variation in Phenological Shifts: How Do Annual Cycles and Genetic Diversity Constrain or Enable Responses to Climate Change?

Julie Heath
Boise State University

Richard Fischer
U.S. Army Engineer Research & Development Center

July 2022

SERDP Project RC-2702

REPORT DOCUMENTATION PAGE

Form Approved
OMB No. 0704-0188

1. REPORT DATE *(DD-MM-YYYY)*	**2. REPORT TYPE**	**3. DATES COVERED** *(From - To)*
20-07-2022	SERDP Final report	03-08-2017 to 20-07-2022

4. TITLE AND SUBTITLE
Variation in phenological shifts: How do annual cycles and or enable responses to climate change?

5a. CONTRACT NUMBER
W912HQ17C0047

5b. GRANT NUMBER

5c. PROGRAM ELEMENT NUMBER

6. AUTHOR(S)
Julie A. Heath, Christen M. Bossu, Kathleen R. Callery, Richard A. Fisher, Stephanie J. Galla, Anjolene R. Hunt, Christopher J.W. McClure, M. David Oleyar, Benjamin P. Pauli, Breanna F. Powers, Kristen C. Ruegg, Sarah E. Schwiltz, Jason M. Winiarski

5d. PROJECT NUMBER RC-2702

5e. TASK NUMBER

5f. WORK UNIT NUMBER

7. PERFORMING ORGANIZATION NAME(S) AND ADDRESS(ES)
Boise State University
1910 University Dr.
Boise, ID 83725

8. PERFORMING ORGANIZATION REPORT NUMBER
RC-2702

9. SPONSORING / MONITORING AGENCY NAME(S) AND ADDRESS(ES)
Strategic Environment Research and Development Program
4800 March Center Drive Suite 16F16
Alexandria, VA 22350-3605

10. SPONSOR/MONITOR'S ACRONYM(S)

11. SPONSOR/MONITOR'S REPORT NUMBER(S) RC-2702

12. DISTRIBUTION / AVAILABILITY STATEMENT
DISTRIBUTION STATEMENT A. Approved for public release: distribution unlimited.

13. SUPPLEMENTARY NOTES

14. ABSTRACT

Effective management of wildlife on Department of Defense lands requires identifying which species, or populations, may be vulnerable to climate-driven phenological mismatch. We studied the ecological and genetic correlates of American kestrel (*Falco sparverius*) phenology and developed an individual-based model to test hypotheses about mechanisms underlying phenology shifts. We found that the effects of mismatch on adult survival and competition for mates and nest sites were the strongest drivers of early nesting, not the effects of mismatch on productivity, as commonly reported. Further, seasonal trade-offs between reproduction and survival limited nesting phenology shifts. We identified genetic variants within candidate genes that modulate the circannual rhythms of American kestrels. Genetic variants showed both multi- and single-gene effects on the timing of nesting and migration passage. However, genetic composition and diversity had only very small effects on nesting phenology shifts. Finally, we demonstrated the portability of our model by parameterizing it for species of concern. The creation of an individual-based model that integrates functional genetic and ecological information, and simulates both evolutionary and ecological processes, was an important advancement for understanding and predicting population responses to environmental change and increases our understanding of the mechanisms underlying phenology shifts.

15. SUBJECT TERMS

Installation Resilience, Threatened and endangered species and invasive species, habitat, restoration, phenological shifts, genetic diversity, adaptive capacity, American kestrel, burrowing owl, Canada warbler, chronotypes, climate change, functional genetics, individual-based model, migratory bird, mismatch, productivity, species of concern, survival, timing

16. SECURITY CLASSIFICATION OF:			**17. LIMITATION OF ABSTRACT**	**18. NUMBER OF PAGES**	**19a. NAME OF RESPONSIBLE PERSON**
a. REPORT	**b. ABSTRACT**	**c. THIS PAGE**			Julie Heath
UNCLASS	UNCLASS	UNCLASS	UNCLASS	212	**19b. TELEPHONE NUMBER** *(include area code)* 208-426-3208

Table of Contents

List of Tables

List of Figures

List of Acronyms

AHY: after hatch year
AIC_c: Akaike's information criterion corrected for small sample size
AKP: American Kestrel Partnership
BBL: Bird Banding Laboratory
BUOW: burrowing owl
CAWA: Canada warbler
CI: confidence interval
DNA: deoxyribonucleic acid
DoD: Department of Defense
EPA: Environmental Protection Agency
FCPP: full-cycle phenology project
GRF: Gaussian random fields
HY: hatch-year
IBM: individual-based model
INLA: integrated nested Laplace approximation
LPML: log pseudo-marginal likelihood
MAPS: Monitoring Avian Productivity and Survivorship
MODIS: Terra Moderate Resolution Imaging Spectroradiometer
MSS: mission sensitive species
NA-CORDEX: North American Coordinated Regional Downscaling Experiment
NDVI: Normalized Difference Vegetation Index
ODD: overview, design concepts, details
PC: principal component
PIF: Partners in Flight
RAD: Restriction-site Associated
RCM: regional climate models
RCP: representative concentration pathways
SCOPE: simulation of carry-over and phenological effects
SD: standard deviation
SI-x: extended spring index
SNP: single-nucleotide polymorphisms
SPDE: stochastic partial differential equation
STR: short tandem repeats
TRACE: transparent and comprehensive model evaludation
USA: United States of America
USGS: United States Geological Survey

Keywords

adaptive capacity, American kestrel, burrowing owl, Canada warbler, chronotypes, climate change, functional genetics, individual-based model, migratory bird, mismatch, productivity, species of concern, survival, timing

Acknowledgments

Thank you to our collaborators and coauthors who made important contributions to this project including providing samples and sharing data, assisting with fieldwork, logistics and permitting, analyzing samples and data, and co-authoring publications that resulted from this research: E. Anderson, R. Bailey, R. Bay, E. Bayne, M. Blom, C. Boal, T. Booms, M. Brinkmeyer, J. Clarke, R. Dawson, A. Eschenbauch, J. Eschenbauch, D. Espinosa, B. Helm, P. Jeurgens, J. Jung, G. Kaltenecker, J. Kennedy, M. Kohn, Little Gap Raptor Research, W. Le, E. Luttmann, H. McCaslin, K. Miller, R. Miller, J. Morrow, L. Morrow, J. Ng, J. Pagel, N. Paprocki, R. Porter, J. Rajbhandary, B. Ralph, L. Reitsma, J.M. Requena-Mullor, T. Schweizer, S. Simmonds, J.A. Smallwood, T. Smith, E.R. Snyder, K. Steenhof, T. Swem, J.-F. Therrien, W.L. Underwood, R. van Buskirk, M. Warne, J. Watson, and K. Wolfe.

We are indebted to our partners on DoD installations for providing invaluable on-the-ground assistance with logistics, installation access and nest box monitoring: W. Berry, J. Bolsinger, P. Cutler, A. Dankert, R. Felix, J. Ferrer-Perez, T. Filkins, M. Gagnier, J. Haddix, M. Houck, K. Hyde, K. Karssen, R. Knight, C. Leingang, J. Mangelinckx, D. Moon, K. Murdock, M. Parks, S. Phillips, C. Plimpton, D. Rees, J. Robb, B. Rossi, J. Schillaci, A. Schultz, S. Stratton, S. Sullivan, and K. White.

Thank you to our wonderful field team and students whose tireless efforts, adaptability, and field skills allowed us to collect data across the United States: K. Dreher, E. Hirsh, A. Johns, H. McCaslin, C. Pozzanghera, S. Ranck, C. Rankin, A. Santiago, S. Shively. Thank you to B. Myers, S. Edralin, and J. Jenkins for help with data entry and organization. We are grateful for the researchers and community scientists who contributed samples and data to the phenology project, or through American Kestrel Partnership, eBird, and Cornell NestWatch databases, without whom a project of this scale would not be possible. Thank you to landowners for allowing access to their property.

This project leveraged funding from several other awards including the California Energy Commission (EPC-15-043), National Geographic (WW-202R-17), First Solar Incorporated, Raptor Research Foundation's Dean Amadon grant, Natural Sciences and Engineering Research Council of Canada (122981-2005), Canada Foundation for Innovation, British Columbia Knowledge Development Fund (202580), University of Northern British Columbia, National Science Foundation (NSF-1942313), the National Science Foundation (REU Site Award DBI: 1852133), Boise State and American Kestrel Partnership's Adopt-a-box program, generous donations from S. Radford, J. Ellis, HawkWatch International, and contributors to the genoscape crowdsourcing campaign via Go-Fund-Me. We acknowledge NSF Track I and 2 EPSCoR Programs (award number OIA-1757324 and OIA-1826801, respectively) for their support of S. Galla.

Thank you to the MakerLab staff at Boise State University, DNA Technologies and Expression Analysis Cores at the UC Davis Genome Center, computational allocations from the Extreme Science and Engineering Discovery Environment (Xsede) and UCLA's Shared Hoffman2 Cluster. We would like to acknowledge high-performance computing support of the Borah compute cluster (DOI: 10.18122/oit/3/boisestate) provided by Boise State University's Research Computing Department and K. Shannon's help with scripts for extended spring index estimates.

We thank SERDP for the support to conduct this research, K. Preston for his excellent guidance and stewardship of the program, and S. Lawless and the Noblis team for helping with logistical support.

Abstract

Introduction and Objectives. Effective wildlife management requires identifying which species, or populations, may be vulnerable to climate-driven phenological mismatch. Critical knowledge gaps remain, however, about the underlying genetic and environmental factors that affect the adaptive potential of populations to shift phenology. We addressed these gaps by accomplishing four objectives. First, we conducted a large-scale investigation of the demographic consequences of phenological mismatch on a migratory bird, the American kestrel (*Falco sparverius*). Second, we investigated the genetic variants associated with the nesting and migration phenology of kestrels. Third, we developed an individual-based simulation model to test hypotheses about mechanisms underlying phenology shifts. We used American kestrels as a focal species for these objectives because western kestrels show evidence of phenology shifts (i.e., are nesting earlier) whereas eastern kestrels do not. Finally, we parameterized the model a Department of Defense (DoD) Partners in Flight (PIF) Mission-sensitive Species, burrowing owl (*Athene cunicularia*), and a DoD PIF Tier 2 species, Canada warblers (*Cardellina canadensis*).
Technical Approach. We added avian monitoring capacity at several DoD installations and leveraged research networks to sample American kestrels' environmental, phenological, demographic, and genetic information across their entire North American range. These data were used to develop SCOPE (Simulation of Carry-Over and Phenological Effects), an individual-based model to test hypotheses about phenology shifts in response to climate change. Once SCOPE was developed, we used published research and data mining approaches to parameterize SCOPE for Canada warblers and burrowing owls.
Results. Western kestrels had concomitant declines in reproduction and survival during the breeding season, whereas eastern kestrels showed seasonal trade-offs between reproduction and survival, with early nesters having higher productivity and lower survival than later nesters. We identified genetic variants within candidate genes that modulate the circannual rhythms of American kestrels. Genetic variants showed both multi- and single-gene effects on the timing of nesting and migration passage. Further, heterozygosity at individual loci of candidate genes differed between western kestrels and eastern kestrels. However, when population-specific genotypes were seeded in SCOPE, genetic composition and diversity had only very small effects on nesting phenology shifts. Alternatively, results from SCOPE showed that seasonal declines in adult survival, as well as competition for nest sites and mates, were strong drivers of earlier nesting. Finally, results from the Canada warbler SCOPE model showed that their nesting phenology did not keep pace with climate-driven advances in spring, suggesting that they are vulnerable to mismatch. Burrowing owl SCOPE results suggested owls might be resilient to mismatch.
Benefits. Results suggest that large populations that lack seasonal trade-offs in reproduction and survival are likely to be resilient to phenological mismatch. Alternatively, populations that have seasonal trade-offs between reproduction and survival, declining populations where density-dependent processes like competition for nest sites and mates is lower, or small populations with limited genetic potential are likely to be vulnerable to mismatch. Genetic results suggest that future research on the genes that modulate the metabolic and light input pathways to biological clocks will be helpful for revealing variants associated with phenology. Finally, we provide methodological approaches for integrating genetic and ecological information into models that simulate both evolutionary and ecological processes, which is an important advancement for understanding and predicting population responses to environmental change and increases our understanding of the mechanisms underlying phenology shifts.

Executive Summary

Introduction

Changes in phenology—the timing of life cycle events—are one of the most notable responses to climate change (Thackeray et al. 2016). In particular, birds are nesting earlier to synchronize energetically expensive reproduction with peaks in food resources that are advancing with earlier springs (Both et al. 2004). Changes in nesting phenology are not homogenous, however, as many populations have not shifted clutch initiation dates to keep pace with advancing springs (Visser and Both 2005). Lack of phenology shifts can lead to temporal decoupling of reproduction and food resources (i.e., phenological mismatch) that affect nesting productivity (Visser et al. 2006), adult survival (Callery et al. 2022), and population viability (Møller et al. 2008). Therefore, it is important to understand population characteristics associated with vulnerability to phenological mismatch. This information will help us predict whether species of concern on Department of Defense (DoD) lands may, or may not, be sensitive to climate-driven changes in spring or have the capacity to shift the timing of life cycle events in response to climate change.

Although phenology shifts are widespread in birds, the pace of the shifts, the strength of mismatch effects, and the capacity of individuals to shift their timing of reproduction may depend on regional patterns of climate and resource availability, species life-history traits, or variability in adaptive capability among individuals within a population (Visser et al. 2003, Both et al. 2004). Growing seasons and climatic conditions vary widely across North America (Eastman et al. 2013). Individuals breeding in some regions may experience narrow, peaked resource availability during the breeding season (i.e., short nesting window), whereas individuals in other regions may experience a prolonged, dampened resource curve (i.e. long nesting window), or milder, more predictable weather patterns. The former may result in higher fitness for individuals that optimally time breeding, but may have extreme fitness consequences for individuals that mistime breeding. Conversely, the latter may result in lower productivity peaks, but mistiming effects may be less severe (Garcia-Heras et al. 2016). Further, birds that nest in highly seasonal environments are often migratory, which may have carry-over effects (i.e., events in one season affecting events in subsequent seasons, (Sherry and Holmes 1996), Webster et al. 2002) on nesting phenology shifts (Williams et al. 2015). For example, long-distance migrants may not cue into earlier growing seasons on the breeding ground because they are away on their winter grounds, thus limiting their ability to nest earlier (Both et al. 2010). Finally, the timing of clutch initiation (Sheldon et al. 2003, Postma 2014) and plasticity in timing (Nussey et al. 2005) are heritable traits, suggesting an underlying role of genetics. Polymorphisms in genes that underlie daily (circadian) and yearly (circannual) rhythms create distinct early or late circannual phenotypes (chronotypes, Liedvogel et al. 2009, Saino et al. 2019) that are likely to affect timing across the annual cycle. The prevalence of particular chronotypes and their underlying genetic mechanisms can vary spatially (Johnsen et al. 2007) and within populations (Bossu et al. 2022). This variation can lead to the differential capacity for phenological responses and resilience to climate change if chronotypes are heritable and favored by selection (Nussey et al. 2005, Helm et al. 2019). Because DoD installations are located in diverse geographic and climatic regions across the nation and managers must effectively manage species with a wide variety of migratory strategies, it is important to understand how variation in these factors impacts vulnerability to climate-driven phenological mismatch.

American kestrels (*Falco sparverius)* are widespread, generalist predators that breed across much of North America (Smallwood and Bird 2020). Kestrels are leap-frog migrants with northern populations being more migratory and migrating farther distances than southern populations (Heath et al. 2012). Kestrels are dietary generalists and prey on insects, small mammals, birds, and lizards (Smallwood and Bird 2020). Clutch initiation of kestrels is positively correlated with the start of spring and is timed so that raising broods corresponds with the timing of peaks in small mammals. Western and eastern kestrel populations are spatially and genetically distinct (Ruegg et al. 2021) and show differences in phenological responses to climate change. Kestrel clutch initiation dates are advancing with earlier springs in western populations (Smith et al. 2017), but remain unchanged in eastern populations, despite advancing springs (Del Corso 2016). The causes of variation in phenological shifts between populations, and potential fitness consequences are unknown. Further, geographic variation in population trends, specifically steeper declines in eastern populations (Smallwood et al. 2009, McClure et al. 2017), emphasizes the importance of understanding population characteristics associated with vulnerability to mismatch consequences. We used American kestrels as a focal species to examine how phenological mismatch affects productivity and survival across a large spatial scale, to identify the genetic basis of intraspecific variation in seasonal timing, and to develop an individual-based model (IBM) to evaluate and test these potential mechanisms underlying shifts in bird breeding phenology. Finally, we demonstrated the value of full annual cycle modeling by parameterizing the IBM for a DoD Partners in Flight (PIF) Mission-sensitive Species (burrowing owl, Athene cunicularia), and a DoD PIF Tier 2 species (Canada warbler, Cardellina canadensis) (DoD PIF 2019).

Objectives

We accomplished four objectives to address critical knowledge gaps and to develop a portable modeling framework for investigating phenological shifts across annual cycles. First, we conducted a large-scale investigation of the demographic consequences of phenological mismatch on American kestrels (Chapter 1). Second, we investigated the genetic variants associated with the nesting and migration phenology of kestrels (Chapter 2). Third, we developed an individual-based simulation model to test hypotheses about mechanisms underlying phenology shifts (Chapter 3). Finally, we parameterized the model for two species of high management importance to DoD for meeting testing and training missions (Chapter 4).

This project was developed to meet the DoD FY2017 Statement of Need (SON) 17−01 by improving our fundamental and applied understanding of the abiotic and biotic factors that affect the phenology of migratory land birds, the consequences of phenology shifts (or lack thereof), and forecasting how land bird populations may change under non-stationary climate conditions. Specifically, we addressed three research needs (abbreviated in italics below) listed in the SON.

Research Need: develop monitoring protocols for tracking of phenological changes, trends, and their implications. We used long-term research sites, widespread citizen science programs, and systematically selected study sites on multiple DoD installations to collect spatially and temporally comprehensive data on phenology, productivity, and genetics (Chapters 1 and 2). In addition, we used a unique combination of in-person and virtual monitoring for data collection. We used these data to test the following hypotheses in Chapter 1:

- Mistimed individuals have lower productivity and survival, likely because of lower resource availability.

- The strength of mistiming effects would vary spatially because of regional differences in seasonally abundant resources.
- Mistimed individuals compensate for low resource availability by altering the onset of incubation, advancing the average hatch date, and spreading-out offspring needs.

Research Need: Increase understanding of specific genetic factors.

We identified polymorphisms in candidate genes that are linked to circadian rhythms, demonstrated their association to the timing of clutch initiation and migration, and showed differences in genetic composition and diversity across populations responding differently to climate change (Chapter 2). Further, we explored how genetic diversity at seven loci within candidate genes (*top1*, *peak1*, *nacc2*, *mybbp1a*, *scn5a1*, *cpne4*, *cry1*) affected the potential for evolutionary adaptation under a resource concentration pathway (RCP) 8.5 climate scenario (Chapter 3). Finally, we developed methods for incorporating functional genetics into IBMs (Chapter 3). In Chapter 2 we addressed the following hypotheses:

- Genetic mechanisms underlie phenology.
- Genetic variation in candidate genes modulates individual responses to environmental conditions resulting in different timing phenotypes.
- Populations showing different responses to climate change have different standing genetic diversity at clock-linked genes.

In Chapter 3 we addressed the hypothesis:

- Composition and diversity within circadian rhythm candidate genes affect nesting phenology shifts.

Research Need: Life-cycle modeling to (a) assess emerging theoretical understanding of phenology and its role in maintaining species viability and (b) address resultant conservation and management challenges within relevant, testable, and adaptable conceptual frameworks.

A fundamental theme in our research approach was the need to study phenology shifts within the context of a full annual cycle. For example, to study the factors that affect phenology shifts in avian nesting seasons, we also studied the factors associated with inter-annual variation in migration strategies. We created the Simulation of Carry-Over and Phenological Effects (SCOPE) modeling framework, used SCOPE to test hypotheses about mechanisms underlying phenology shifts (Chapter 3), and then demonstrated the model's portability for additional species (Chapter 4). In Chapter 3, we addressed the following hypotheses:

- Seasonal timing effects on nesting success facilitate earlier nesting (i.e., advancing nesting phenology is driven by earlier nesting birds having higher nesting success than later nesters).
- Seasonal timing effects on adult survival facilitate earlier nesting (i.e., advancing nesting phenology is driven by earlier nesting birds having higher survival than later nesters).
- Carry-over effects from migration strategy, migration distance affect nesting phenology shifts.

In Chapter 4, we hypothesized that once developed, a modeling framework that represents the full annual cycle of a migratory land bird could be parameterized for different species using data mining approaches. We parameterized SCOPE with data for Canada warblers and burrowing owls to forecast changes in phenology, phenological mismatch, nest success, survival, and population sizes from 1980 – 2099 under resource concentration pathways (RCP) 4.5 and 8.5.

Technical Approach

Research on factors affecting phenology shifts can be challenging because significant shifts in the timing of annual-cycle events are likely to occur over time scales that are greater than the period of a single research project. At the same time, there is a pressing need to identify vulnerable species and develop management strategies for systems that are changing relatively rapidly in ecological-time frames. Our approach for overcoming this challenge and providing information to DoD managers in a timely fashion was to design a project that is conducted on a scale that will capture spatial-temporal variation in annual cycles and genetic diversity and then use the empirical information to develop a simulation model to test hypotheses about the causes and consequences of phenology shifts across extended temporal scales (Figure A).

We broadly monitored and sampled American kestrels across their North American range and across the annual cycle. Also, we leveraged data and samples from research projects and citizen science communities (i.e., the Cornell Lab of Ornithology's NestWatch program and The Peregrine Fund's American Kestrel Partnership) to create a powerful network for phenology research. We used longitudinal data to examine relationships between mismatch and survival, and large-coverage spatial data to examine mismatch and productivity. We identified several single-nucleotide polymorphisms (SNPs) within candidate genes associated with circannual rhythms; specifically, variants within genes associated with metabolic and light input pathways that modulate the biological pacemaker. Then, we created genetic assays to screen thousands of samples from nesting and migratory kestrels and linked genotypes to the timing of clutch initiation and migration. We used the ecological and genetic information to parameterize our individual-based model, SCOPE. The model was tested and calibrated through iterative comparisons with empirical information. We parameterized the virtual environment with data from global climate models. Then, we tested several ecological and evolutionary hypotheses about the mechanisms underlying phenology shifts. Finally, we demonstrated the portability of the model for other land bird species and forecast population changes at RCPs 4.5 and 8.5.

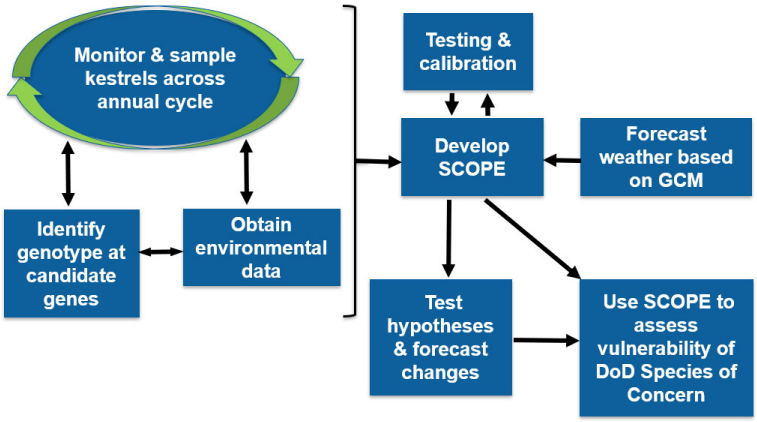

Figure A Overview of the technical approach for SERDP RC-2702 project *Variation in phenological shifts: How do annual cycles and genetic diversity constrain or enable responses to climate change?*

Results and Discussion

In our continent-wide study on phenology and American kestrel productivity (Chapter 1), we found seasonal declines in productivity across the breeding range. Specifically, kestrels nesting before the start of spring had higher nest success and productivity than later nesters, with the most severe effects of timing occurring in the Northeast. Also, phenological mismatch affected the apparent survival of adult birds that raised young, but the direction of the effect

differed between kestrel populations (Figure B). In the west, early nesting individuals had higher survival than later nesters, whereas in the east later nesters had higher survival than earlier nesters. Finally, males from later breeding pairs started incubating sooner than males from earlier breeding pairs, resulting in increased hatching asynchrony and age spread of young.

Concomitant seasonal declines in reproduction and survival in western populations may facilitate population-level responses to earlier springs, whereas seasonal trade-offs and high risks associated with mistiming may constrain phenology shifts for eastern populations. Indeed, clutch initiation dates are advancing at western sites, but remain static at eastern sites. Different patterns of seasonal changes in reproductive success and survival between populations may be related to the duration of growing seasons and nesting windows at each site. In the west, the growing season is long and kestrels have a long (~4 month) nesting window. In the east, the growing season is shorter and kestrels have a shorter (~2 month) nesting window. Although the early onset of incubation may be an adaptive behavior that advances the average hatch date and spreads out energetic demands, it is unknown how impactful this will be in mitigating the fitness consequences of phenology mismatch.

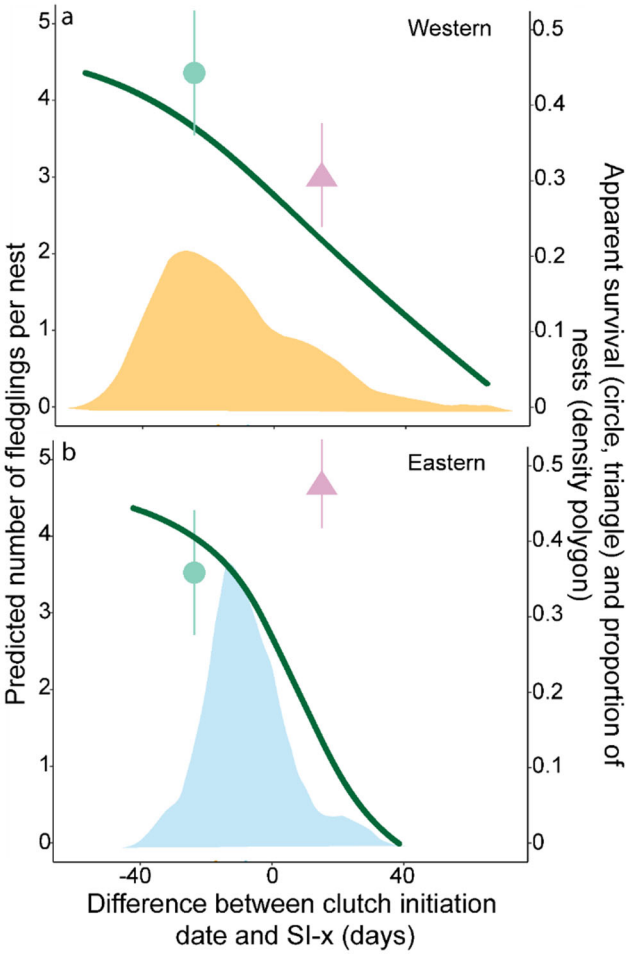

Figure B The density distributions of the difference between clutch-initiation (CI) dates and the extended spring index (SI-x) in polygons, apparent survival estimates (mean and 85% confidence interval) of an early (green point and line) and late (coral triangle and line) successful, adult females, and seasonal trends in productivity (dark green line) for the western (Idaho) site (a) and eastern (New Jersey) site (b). At the western site, seasonal declines in both productivity and apparent survival may be allowing for earlier nesting in response to climate change via directional selection, whereas at the eastern site an inverse pattern between apparent survival and productivity may create a constraint for earlier nesting.

In Chapter 2, we estimated the heritability of American kestrel clutch initiation and found that clutch initiation was highly heritable ($h^2 = 0.42$), supporting the hypothesis of underlying genetic mechanisms. Our F_{ST} analysis revealed 7,227 polymorphic loci in 1843 genes. We identified links to seasonal behavior for 21 of these genes using a literature search. Because assay design for specific loci of interest is not always possible, we were only able to design targeted assays for loci in 10 of the 21 total genes of interest. These included: 2 core clock genes (*cry1*, *npas2*), 4 clock-linked genes (*top1*, *cpne4*, *mybpp1a,* and *phlpp1*), 2 genes linked to morphological differentiation potentially important to avian migration (*lmbr1* and *nacc2*), and the remaining 2 genes (*peak1* and *scn5a*) were known to

be differentially expressed in the hypothalamus in Swainson's thrushes (*Catharus ustulatus*) during non-migratory and migratory states (Johnston et al. 2016).

We genotyped 971 American kestrel nestlings at the 10 loci. An ordinal principal component (PC) analysis showed strong correlations among genotypes, and $PC_{nesting}$ 1 accounted for 17.7% of the variance and with high loadings *top1* and *peak1* and low on *cpne1* and *cry1*. Further, there was an interaction between $PC_{nesting}$ 1 scores and the start of spring (SI-x, Figure C). Specifically, the SI-x effect was greater for individuals with higher $PC_{nesting}$ 1 values and lower for individuals with low $PC_{nesting}$ 1 values. Genes with high loadings on $PC_{nesting}$ 1 may govern sensitivity to environmental cues, like vegetation green-up. If true, individuals with high $PC_{nesting}$ 1 scores may show more plasticity because of interannual differences in environmental conditions compared to individuals with lower $PC_{nesting}$ 1 scores. Finally, there was some evidence of single gene effects on clutch initiation. Birds that were homozygous minor for *mybbp1a* and *nacc2* tended to initiate clutches earlier. These results suggest that genetic variants underlie variation in clutch initiation phenology and that some genotypes may be more sensitive to environmental cues than others, resulting in different capacities (i.e., plasticity) to shift phenology in response to environmental change.

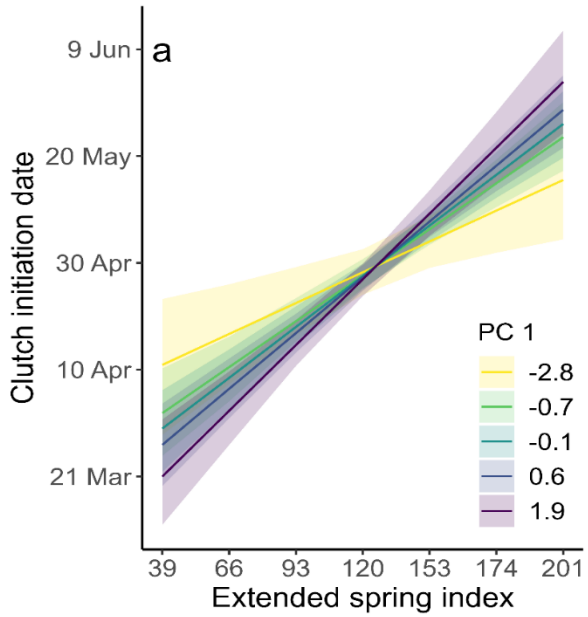

Figure C Predicted clutch initiation dates of American kestrels based on an interaction between candidate gene $PC_{nesting}$ 1 and the extended spring index (SI-x). The effect of SI-x depended on $PC_{nesting}$ 1 scores. Specifically, effects of the SI-x were strongest in individuals with higher $PC_{nesting}$ 1 scores (homozygous minor in *peak1* and *top1*, homozygous major *cry1* and *cpne4*); whereas the effects of the SI-x were weaker in individuals with low $PC_{nesting}$ 1 scores (homozygous major in *peak1* and *top1*, homozygous minor in *cry1* and *cpne4*).

In addition to nesting samples, we genotyped 165 American kestrels during autumn migration passage through Boise, Idaho. Similar to the clutch initiation results, categorical principal component analysis of genetic variation demonstrated high collinearity between certain genes (*top1, peak1, phlpp1*) and there was a significant correlation between $PC_{migration}$ 1 and migration passage date. Genotypes associated with early migration were similar to genotypes associated with early clutch initiation. Our results highlight a strong association between timing and genetic variation in clock-linked genes (*top1*, for migration and clutch initiation, *mybpp1a* for clutch initiation, and to a lesser extent, *phlpp1* for migration) known to entrain the core clock pathway. Here, we document what is, to the best of our knowledge, the first example of an association between intra-population genetic variation in genes that entrain biological clocks, and the existence of early and late migratory chronotypes (timing phenotypes) *within* populations.

Finally, $PC_{nesting}$ 1 scores were higher in the eastern population compared to the western population. This difference likely comes from the lack of lower scores (i.e., homozygous major *top1* and *peak1* individuals) in the east compared to the west (Figure D). Further, western

individuals tended to have higher mean heterozygosity than eastern individuals at two genes that had high loadings on PC 1, *top1* and *peak1*. These results suggest that eastern populations may have less overall genetic diversity within candidate genes than western populations, which could limit the capacity for phenological responses and resilience to climate change – a hypothesis we tested in Chapter 3.

We successfully developed a full flyway-scale model for American kestrels that incorporates genetic and life-history traits, and evolutionary and ecological processes (Chapter 3). Patterns from SCOPE simulations from 1980 – 2019 matched observed patterns of nesting phenology shifts, average nest success, productivity, migration distances and distance changes, and ecoregion population trends. In addition, we developed a set of assumptions and criteria to consider when developing an IBM with functional genetics. This was the first IBM to represent allele inheritance, functional effects on traits (nesting phenology), and selection pressures at a large spatial and temporal scale with realistic dispersal patterns and processes.

We created experiments within SCOPE to examine how genetic composition and diversity, and demographic and life-history traits affect nesting phenology shifts and population trends. Interestingly, genetic composition and diversity had small effects on nesting phenology shifts. In the western, eastern, and heterozygous seed experiments, all loci trended towards fixation for alleles favorable for earlier egg-laying dates, with *cpne4*, *cry1*, *mybbp1a*, *peak1*, and *top1* trending towards fixation for major or minor alleles. Strong fitness advantages of early nesting individuals compared to later nesting individuals created strong directional selection for early nesting, and allele frequencies trended toward fixation of an early chronotype. Experiments performed here do not support the hypothesis that genetic diversity or composition of eastern American kestrels are constraining their ability to nest earlier. However, if heritability and genetic mechanisms were removed from the model, advancement of egg-laying was slower and populations tended to decline, reflecting the importance of representing evolutionary processes in biological IBMs.

In another set of experiments, we ran seven versions of SCOPE to summarize changes across the western range and one experiment across the eastern range. We considered the model with all effects "on" as the baseline model. We considered another experiment with all the climate and genetic effects "off" as a static-environmental model (i.e., no climate change). In the remaining experiments, we turned off different effects of the environment or traits one-by-one to test hypotheses. In the baseline model, individuals advanced their nesting by a day every 5 years and with climate change turned off, egg-laying dates did not advance over time (Figure D). Interestingly, when the effect of phenological

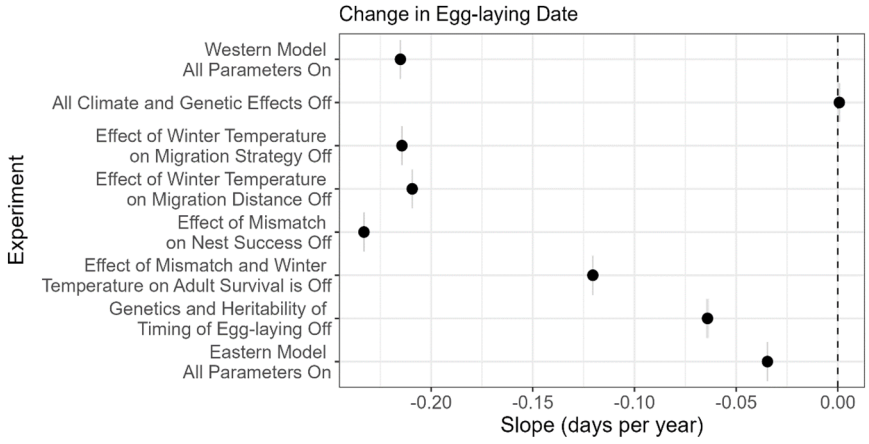

Figure D Average change in egg-laying date per year (dark circle) and standard error (gray line width) of American kestrels during a 120-year (1980 – 2099) simulation for eight different ecological experiments. More negative values reflect faster advancement of egg-laying dates compared to no shift (0 value).

mismatch on nesting success was turned off, kestrels advanced egg-laying dates at a faster rate compared to the baseline scenario. With the effect of phenological mismatch on productivity turned off, kestrels had higher nesting success and the population size grew larger than in any other scenario. At higher population sizes there was higher competition for mates and nest sites compared to lower population sizes. This density-dependent effect created additional selection pressure to nest earlier, thus driving the faster advancement of nesting. This result was unexpected because the effect of mismatch on nesting success and productivity is thought to be one of the main drivers of earlier nesting. However, if populations are declining because of mismatch effects on nest success or productivity, then it is less likely that density-dependent effects, such as competing for nest sites or mates, would drive earlier nesting. Thus, contrary to current belief, the effect of phenological mismatch on productivity may not be the main driver of earlier nesting.

In general, adult survival increased in experimental runs because of increasing winter minimum temperatures. Interestingly, when the effects of phenological mismatch and minimum temperatures on adult and juvenile survival were removed, the rate of egg-laying advancement drastically slowed, suggesting that mismatch effects on survival are important drivers of earlier nesting, even more so than the effects of phenological mismatch on productivity. This conclusion is further supported by the results from the eastern flyway model. The eastern model has similar sub-models to the western model, with the exception of the survival model which reflects the seasonal trade-off between productivity and adult survival (Figure B). In this case, successful adults that nest earlier, have lower survival than successful adults that nest later. The trade-off between survival and reproduction constrained egg-laying advancement, resulting in declining nest success as individuals became more mismatched, and populations declined. Results from SCOPE reinforce that seasonal trade-offs are likely to limit changes in nesting phenology and may be a reliable indicator of phenological vulnerability in migratory birds. Finally, carry-over effects from changes in migration tendency and distance had a small effect on the rate of egg-laying phenology advancement, suggesting that migration does not constrain earlier nesting, as previously hypothesized. Results from SCOPE experiments reinforce the risk assessment and management recommendations in Chapter 1. Specifically, large populations that lack seasonal trade-offs in reproduction and survival are likely to be resilient. Whereas large populations that have seasonal trade-offs between reproduction and survival, declining populations where competition for nest sites and mates is decreased, or small populations with limited genetic potential are likely to be vulnerable to mismatch.

In Chapter 4, we collated data for each species from previous research, used data mining approaches, and collected expert opinions from collaborators. Then, we re-parameterized SCOPE with the appropriate spatial, climate, and environmental variables and the species-specific biology-environmental parameters for each model sub-process. We obtained high-quality data on Canada warbler biology from Monitoring Avian Productivity and Survival (MAPS) sites and other sources and learned that Canada warbler reproduction and survival were sensitive to phenology. Within SCOPE simulations, we found that Canada warbler nesting phenology did not advance at the same pace as climate-driven advances in spring, leading to increased mismatch over time, decreased adult survival, and declining population trends. It was challenging to find high-quality raw data on burrowing owl life history. To parameterize SCOPE, we used published information about nest success and survival that contained little to no information about sensitivity to mismatch. Within SCOPE simulations, burrowing owls did not advance their phenology to keep pace with earlier springs, but their populations remained

relatively stable, likely because of inadequate representation of sensitivity to mismatch. Together, these results highlight the importance of data curation and availability. Developing tools to assess climate vulnerability will require access to longitudinal data that can be challenging for individuals to manage and share. Improved resources for data management could aid in capturing archival data that would be useful for creating natural resource management tools. In sum, though SCOPE was initially developed for a data-rich species, American kestrels, the sub-processes within the model were made to be generalizable to other species of migratory birds. Parameterization of SCOPE for Canada warblers revealed that phenological mismatch is likely to become a threat for this species. Alternatively, parameterization of SCOPE for burrowing owls suggested the phenological mismatch would not be an emerging threat for owls, but challenges in obtaining quality data for burrowing owls make this result tenuous.

Implications for Future Research and Benefits

We met our objectives to quantify the effects of phenological mismatch on productivity and survival of American kestrels and to uncover potential behavioral adaptations to mismatch. American kestrels proved to be a valuable model species to study these concepts. Our results suggest that *whether* populations adapt by shifting phenology can differ geographically depending on regional environmental conditions, nesting window constraints, and trade-offs between fitness components. Furthermore, *how* they adapt can differ, with some individuals or populations shifting phenology to keep pace with advancing spring, while others may alter incubation behavior to mitigate mismatch impacts. Further research is needed to determine the extent to which similar regional variation of mismatch consequences exist for other species, particularly specialist species that must closely track specific resources, and imperiled species for which fitness consequences could be particularly detrimental to their recovery. Distributions of seasonal breeding windows may help to assess mismatch vulnerability or potential for seasonal trade-offs. Eastern kestrels had very narrow and peaked nesting window compared to western kestrels (Figure B). Data collection on the distribution of clutch initiation dates for DoD species of concern could be an important first step toward identifying species that have constraining selection on nesting timing and may indicate seasonal trade-offs.

We successfully estimated the heritability of nesting phenology, identified genetic variants with targeted candidate gene analysis to document significant correlations between genetic variation and the timing of clutch initiation and migration of American kestrels, and directly compared gene complexes and heterozygosity of individual loci between western and eastern kestrels. We found support for the hypothesis that phenology is governed by genetic mechanisms. Further, this study is the first to document the intra-population genetic that creates early and late migratory chronotypes (timing phenotypes) *within* populations. These results are particularly important in light of the absence of information on intrinsic factors affecting phenology shifts. While we have successfully identified some genes of small effect, we are missing others and may not be accounting for potential epigenetic effects. Repeating this analysis with whole-genome sequencing may reveal additional clock-linked genes that contribute to the observed patterns. Finally, we showed that western and eastern kestrels have different genetic diversity at these important loci, supporting the hypothesis that differences in genetics may affect the adaptive capacity of populations to respond to climate change. Understanding species and population-level adaptive capacity for phenological responses to climate change will help DoD managers assess and prioritize management actions for DoD PIF Mission-sensitive Species (MSS, DoD PIF 2019). Our work showed that underlying genetics play an important role in

phenology and capacity to shift phenology, but that adaptive capacity could vary regionally, or even within a population. Although these processes are intrinsic to populations, external stressors (natural and anthropogenic) can limit the realization of potential adaptive capacity. Hence, resource managers can play an important role in reducing anthropogenic stressors (e.g. pollution, land-use change) to reduce barriers to dispersal and gene flow for populations with fundamental adaptive capacity, and to limit controllable pressures for more vulnerable populations with less adaptive capacity.

Our work provided methodological approaches for integrating genetic and ecological information into models that simulate both evolutionary and ecological processes, which is an important advancement for understanding and predicting population responses to environmental change and increases our understanding of the mechanisms underlying phenology shifts. Further, we tested several hypotheses about the mechanisms underlying phenology shifts. We found no evidence that, in large populations, composition or diversity within circadian rhythm candidate genes limit nesting phenology shifts. If ecological patterns (seasonal declines in nesting success and adult survival) were present, allele frequencies quickly trended towards earlier nesting phenotypes. This conclusion may not be true for all populations, though. For example, if populations experienced a bottleneck and were significantly smaller (e.g., <500 individuals), some of these alleles may move towards fixation because of drift, as opposed to selection.

We found that the effect of phenology mismatch on adult survival, competition for nest sites and mates, and evolutionary processes are key mechanisms driving earlier nesting. The effect of phenological mismatch on nesting success was not a strong driver of earlier nesting, and migration was only a weak constraint to earlier nesting. In addition to this new knowledge, these experiments provide DoD land managers insight into populations that are resilient to and those that are vulnerable to climate-driven phenological mismatch. Results from SCOPE experiments reinforce the risk assessment and management recommendations in Chapter 1. Specifically, large populations that lack seasonal trade-offs in reproduction and survival are likely to be resilient. Whereas large populations that have seasonal trade-offs between reproduction and survival, declining populations where competition for nest sites and mates is decreased, or small populations with limited genetic potential are likely to be vulnerable to mismatch. Finally, SCOPE provided the ability to directly compare two hypotheses to explain why eastern American kestrels are not advancing their egg-laying dates: 1) lack of genetic diversity, or 2) seasonal trade-offs between reproduction and survival. Results clearly demonstrate that seasonal trade-offs constrain phenology shifts and eastern kestrels are not limited by genetic diversity (see Eastern Seed experiment).

We demonstrated the portability of SCOPE by parameterizing SCOPE for DoD species on concern. Parameterization of SCOPE for Canada warblers revealed that phenological mismatch is likely to become a threat for this species. Alternatively, parameterization of SCOPE for burrowing owls suggested the phenological mismatch would not be an emerging threat for owls, but challenges in obtaining quality data for burrowing owls make this result tenuous. Though SCOPE was initially developed for a data-rich species, American kestrels, the sub-processes within the model were made to be generalizable to other species of migratory birds, but challenges in data accessibility and small sample sizes limited our ability to use SCOPE to the full extent. Developing tools to assess climate vulnerability will require access to longitudinal data that can be challenging for individuals to manage and share. Improved resources for data management could aid in capturing archival data that would be useful for creating natural resource management tools.

Literature Cited

Bossu, C. M., Heath, J. A., Kaltenecker, G. S., Helm, B., & Ruegg, K. C. (2022). Clock-linked genes underlie seasonal migratory timing in a diurnal raptor. *Proceedings of the Royal Society B*, *289*(1974), 20212507.

Both, C., Artemyev, A. V., Blaauw, B., Cowie, R. J., Dekhuijzen, A. J., Eeva, T., ... & Visser, M. E. (2004). Large–scale geographical variation confirms that climate change causes birds to lay earlier. *Proceedings of the Royal Society of London. Series B: Biological Sciences*, *271*(1549), 1657-1662.

Both, C., Van Turnhout, C. A. M., Bijlsma, R. G., Siepel, H., Van Strien, A. J., and Foppen, R. P. B. (2010). Avian population consequences of climate change are most severe for long-distance migrants in seasonal habitats. *Proceedings of the Royal Society B: Biological Sciences*, 277(1685), 1259-1266.

Callery, K. R., Smallwood, J. A., Hunt, A. R., Snyder, E. R., & Heath, J. A. (2022). Seasonal trends in adult apparent survival and reproductive trade-offs reveal potential constraints to earlier nesting in a migratory bird. *Oecologia*, *199*(1), 91-102.

Del Corso, M. (2016). Warmer temperatures on American kestrel (*Falco sparverius*) breeding grounds associated with earlier laying and successful reproduction. Master thesis, Department of Biology, Montclair State University, Montclair, New Jersey, USA.

Department of Defense Partners in Flight. (2019). Annal Report. https://partnersinflight.org/resources/dod-pif-annual-report-2019/

Eastman, J. R., Sangermano, F., Machado, E. A., Rogan, J., & Anyamba, A. (2013). Global trends in seasonality of normalized difference vegetation index (NDVI), 1982–2011. *Remote Sensing*, *5*(10), 4799-4818.

Garcia-Heras, M. S., Arroyo, B., Mougeot, F., Amar, A., & Simmons, R. E. (2016). Does timing of breeding matter less where the grass is greener? Seasonal declines in breeding performance differ between regions in an endangered endemic raptor. *Nature Conservation, 15*, 23–45.

Heath, J. A., Steenhof, K., & Foster, M. A. (2012). Shorter migration distances associated with higher winter temperatures suggest a mechanism for advancing nesting phenology of American kestrels *Falco sparverius*. *Journal of Avian Biology*, *43*(4), 376-384.

Helm, B., Van Doren, B. M., Hoffmann, D., & Hoffmann, U. (2019). Evolutionary response to climate change in migratory pied flycatchers. *Current Biology*, *29*(21), 3714-3719.

Johnsen, A., Fidler, A. E., Kuhn, S., Carter, K. L., Hoffmann, A., Barr, I. R., ... & Kempenaers, B. (2007). Avian Clock gene polymorphism: evidence for a latitudinal cline in allele frequencies. *Molecular Ecology*, *16*(22), 4867-4880.

Johnston, R. A., Paxton, K. L., Moore, F. R., Wayne, R. K., & Smith, T. B. (2016). Seasonal gene expression in a migratory songbird. *Molecular Ecology*, *25*(22), 5680-5691

Liedvogel, M., Szulkin, M., Knowles, S. C., Wood, M. J., & Sheldon, B. C. (2009). Phenotypic correlates of Clock gene variation in a wild blue tit population: evidence for a role in seasonal timing of reproduction. *Molecular Ecology*, *18*(11), 2444-2456.

McClure, C. J., Schulwitz, S. E., Van Buskirk, R., Pauli, B. P., & Heath, J. A. (2017). Commentary: Research recommendations for understanding the decline of American Kestrels (*Falco sparverius*) across much of North America. *Journal of Raptor Research*, *51*(4), 455-464.

Møller, A. P., Rubolini, D., & Lehikoinen, E. (2008). Populations of migratory bird species that did not show a phenological response to climate change are declining. *Proceedings of the National Academy of Sciences*, *105*(42), 16195-16200.

Nussey, D. H., Postma, E., Gienapp, P., & Visser, M. E. (2005). Selection on heritable phenotypic plasticity in a wild bird population. *Science*, *310*(5746), 304-306.

Postma, E. (2014). Four decades of estimating heritabilities in wild vertebrate populations: improved methods, more data, better estimates. *Quantitative Genetics in the Wild*, *16*, 33.

Saino, N., Albetti, B., Ambrosini, R., Caprioli, M., Costanzo, A., Mariani, J., ... & Bollati, V. (2019). Inter-generational resemblance of methylation levels at circadian genes and associations with phenology in the barn swallow. *Scientific Reports*, *9*(1), 1-16.

Ruegg, K. C., Brinkmeyer, M., Bossu, C. M., Bay, R. A., Anderson, E. C., Boal, C. W., ... & Heath, J. A. (2021). The American Kestrel (*Falco sparverius*) genoscape: Implications for monitoring, management, and subspecies boundaries. *The Auk*, *138*(2), ukaa051.

Sheldon, B. C., Kruuk, L. E. B., & Merila, J. (2003). Natural selection and inheritance of breeding time and clutch size in the collared flycatcher. *Evolution*, *57*(2), 406-420.

Sherry, T. W., & Holmes, R. T. (1996). Winter habitat quality, population limitation, and conservation of Neotropical-Nearctic migrant birds. *Ecology*, *77*(1), 36-48.

Smallwood, J. A., Causey, M. F., Mossop, D. H., Klucsarits, J. R., Robertson, B., Robertson, S., ... & Boyd, K. (2009). Why are American Kestrel (*Falco sparverius*) populations declining in North America? Evidence from nest-box programs. *Journal of Raptor Research*, *43*(4), 274-282.

Smallwood, J. A., Bird, D. M. (2020). American Kestrel (*Falco sparverius*), version 10. In: Poole AF, Gill FB (eds) Birds of the World. *Cornell Lab of Ornithology*, Ithaca. https://doi.org/10. 2173/bow.amekes. 01

Smith, S. H., Steenhof, K., McClure, C. J., & Heath, J. A. (2017). Earlier nesting by generalist predatory bird is associated with human responses to climate change. *Journal of Animal Ecology*, *86*(1), 98-107.

Thackeray, S. J., Henrys, P. A., Hemming, D., Bell, J. R., Botham, M. S., Burthe, S., ... & Wanless, S. (2016). Phenological sensitivity to climate across taxa and trophic levels. *Nature*, *535*(7611), 241-245.

Visser, M. E., Adriaensen, F., van Balen, J. H., Blondel J., Dhondt A. A., van Dongen, S., du Feu, C., Ivankina, E. V., Kerimov, A. B., de Laet, J., Matthysen, E., McCleery, R., Orell, M., and Thomson, D. L. (2003) Variable responses to large-scale climate change in European Parus populations. *Proceedings of the Royal Society of London. Series B: Biological Sciences*, *270*(1513), 367-372.

Visser, M. E., & Both, C. (2005). Shifts in phenology due to global climate change: the need for a yardstick. *Proceedings of the Royal Society B: Biological Sciences*, *272*(1581), 2561-2569.

Visser, M. E., Holleman, L. J., & Gienapp, P. (2006). Shifts in caterpillar biomass phenology due to climate change and its impact on the breeding biology of an insectivorous bird. *Oecologia*, *147*(1), 164-172.

Webster, M. S., Marra, P. P., Haig, S. M., Bensch, S., & Holmes, R. T. (2002). Links between worlds: unraveling migratory connectivity. *Trends in Ecology & Evolution*, *17*(2), 76-83.

Williams, T. D., Bourgeon, S., Cornell, A., Ferguson, L., Fowler, M., Fronstin, R. B., & Love, O. P. (2015). Mid-winter temperatures, not spring temperatures, predict breeding phenology in the European starling Sturnus vulgaris. *Royal Society Open Science*, *2*(1), 140301.

Chapter 1. Effects of phenological mismatch on American kestrel (*Falco sparverius*) demography

Kathleen R. Callery, John A. Smallwood, Sarah E. Schulwitz, Anjolene R. Hunt, Jason M. Winiarski, Emilie R. Snyder, Christopher J. W. McClure, Richard A. Fischer, Julie A. Heath

Abstract

Timing of avian reproduction coincides with peak food availability to optimize resources for raising young and self-maintenance. When reproduction is mistimed, birds could incur costs that affect their productivity or survival. Climate-driven advances in spring are increasing this phenological mismatch in some regions, which can result in decreased individual fitness, and subsequent population declines. We quantified the relationship between phenological mismatch and productivity of American kestrels (*Falco sparverius*) across their breeding range in the United States and southern Canada using nest observations from long-term nest box monitoring, remote trail cameras on Department of Defense (DoD) sites, and community-scientist-based programs. In addition, we studied whether phenological mismatch affected the apparent survival of American kestrels in two intensively-monitored populations in the western (Idaho) and eastern (New Jersey) United States. Lastly, we quantified the relationship between phenological mismatch, parental incubation behavior, and hatch asynchrony to examine whether behavioral adaptations may mitigate demographic costs associated with mistiming. We found seasonal declines in productivity across the breeding range. Specifically, kestrels nesting before the start of spring had higher nest success and productivity than later nesters, with the most severe effects of timing occurring in the Northeast. Also, phenological mismatch affected the apparent survival of adult birds that raised young, but the direction of the effect differed between populations. In the west, early nesting individuals had higher survival than later nesters, whereas in the east later nesters had higher survival than earlier nesters. Finally, males from later breeding pairs started incubating sooner than males from earlier breeding pairs, resulting in increased hatching asynchrony and age spread of young. Concomitant seasonal declines in reproduction and survival in western populations may facilitate population-level responses to earlier springs, whereas seasonal trade-offs and high risks associated with mistiming may constrain phenology shifts for eastern populations. Indeed, clutch initiation dates are advancing at the western site, but remain static at the eastern site. Different patterns of seasonal changes in reproductive success and survival between populations may be related to the duration of growing seasons and nesting windows at each site. In the west, the growing season is long and kestrels have a long (~4 month) nesting window. In the east, the growing season is shorter and kestrels have a shorter (~2 month) nesting window. Although the early onset of incubation may be an adaptive behavior that advances the average hatch date and spreads out energetic demands, it is unknown how impactful this will be in mitigating the fitness consequences of phenology mismatch. In sum, we demonstrate that American kestrels are vulnerable to demographic consequences of phenological mismatch and that this vulnerability varies across space. Our research suggests that northeastern populations could be more vulnerable to mismatch than western populations, which may be one factor contributing to the steep population declines documented in the northeast. Length of nesting windows and growing seasons may be a useful indicator to survey for migratory species that may be vulnerable to phenological mismatch.

Objectives

In this chapter, we aimed to improve our fundamental and applied understanding of the consequences of phenological mismatch on the demographics of migratory land birds. We used American kestrels as a focal species because this species shows phenology variation and differential responses to climate change across its range. Specifically, our objectives were to: 1) quantify the effects of phenological mismatch on the productivity of American kestrels on DoD sites and nest monitoring sites across the breeding range, 2) quantify the effects of phenological mismatch on the survival of American kestrels in two intensively-monitored populations in eastern and western North America, and 3) investigate whether American kestrels altered incubation behavior to mitigate the effects of mistiming on fitness. We tested the following hypotheses:

H1: Mistimed individuals have lower productivity and survival, likely because of lower resource availability.

H2: The strength of mistiming effects would vary spatially because of regional differences in seasonally abundant resources

H3: Mistimed individuals compensate for low resource availability by altering the onset of incubation, advancing the average hatch date, and spreading-out offspring needs.

We predicted that productivity and survival would decline as phenological mismatch increased, and that these effects would be steepest in regions with narrow, peaked resource availability during the breeding season (i.e., short nesting window). Further, we predicted that individuals that mistimed nesting (i.e., initiated clutches later) would start incubating earlier in the egg-laying sequence than well-timed individuals.

This research addressed two research needs within the SERDP Statement of Need (SON) 17-01: **Develop monitoring protocols for tracking of phenological changes, trends, and their implications**. We used long-term research sites, widespread citizen science programs, and systematically placed study sites on DoD installations to collect spatially and temporally comprehensive data on phenology and productivity. In addition, we used a unique combination of in-person and virtual monitoring for data collection.

Life-cycle modeling to assess emerging theoretical understanding of phenology and its role in maintaining species viability. Though many studies have looked at the effects of nesting phenology on productivity, few have examined the effects of nesting phenology on survival – an important fitness component and population demographic. Further, no other migratory bird studies have aimed to combine results from both productivity and survival models to demonstrate how these important demographics may interact and affect population vulnerability to phenological mismatch.

Background

Optimal reproductive performance occurs when birds time reproduction to coincide with peak food availability (Lack 1968). Within a population, variation in nesting phenology (i.e., the timing of clutch initiation) relative to prey phenology may result in variation in individual fitness (Visser and Gienapp 2019). Specifically, deviations from optimal timing, or mismatch, can affect productivity (Both and Visser 2005, Visser and Gienapp 2019). As climate change advances the onset of spring across temperate regions (Schwartz et al. 2006, Christiansen et al. 2011), unequal phenology shifts among different taxa and trophic levels have resulted in mismatches between animal breeding seasons and food availability (Visser and Gienapp 2019). In birds, the resource-

limited conditions of this phenological mismatch can result in lower survival (Golet et al. 1998, Lof et al. 2012), lower productivity (Both and Visser 2005, Visser and Gienapp 2019), or trade-offs between these fitness components (Reed et al. 2013, Bastianelli et al. 2021). Ultimately, these impacts may contribute to population declines, especially when the rate of spring advancement outpaces species' capacities for adaptation (Visser et al. 2012). Indeed, species that have shifted timing the least in response to climate change have experienced more severe population declines than species that have shifted the most (Møller et al. 2008). Therefore, it is important to understand population characteristics associated with vulnerability to phenological mismatch. This information will help us predict whether species of concern on DoD lands may, or may not, be sensitive to climate-driven changes in spring or have the capacity to shift the timing of life cycle events in response to climate change.

Although phenological mismatch effects are widespread in birds, the strength of effects and the capacity of individuals to shift their timing of reproduction may depend on regional patterns of climate and resource availability, species life-history traits, or variability in adaptive capability among individuals within a population (Visser et al. 2003, Both et al. 2004). Growing seasons and climatic conditions vary widely across North America (Eastman et al. 2013). Individuals breeding in some regions may experience narrow, peaked resource availability during the breeding season (i.e., short nesting window), or may face increased thermoregulation costs, lasting snow cover, low food availability, and inclement spring weather that may inhibit early nesting (Stevenson and Bryant 2000, Irons et al. 2017). Individuals in other regions may experience a prolonged, dampened resource curve (i.e. long nesting window), or milder, more predictable weather patterns. The former may result in higher fitness for individuals that optimally time breeding, but may have extreme fitness consequences for individuals that mistime breeding. Conversely, the latter may result in lower productivity peaks, but mistiming effects may be less severe (Garcia-Heras et al. 2016). Seasonal declines in productivity (Garcia-Heras et al. 2016) and population declines (Both et al. 2010) are both more pronounced for species breeding in regions with strong seasonality and shorter nesting windows than those breeding in regions with weaker seasonality and longer nesting windows. In North America, climate change effects also vary regionally, with the steepest spring warming and increases in frost-free days occurring in northern and western regions (Easterling 2002, Peterson et al. 2013), extreme temperatures and drought occurring in southern and western regions (Peterson et al. 2013), and increasing extreme precipitation events occurring in eastern regions (Kunkel et al. 2013, Huang et al. 2017). Further, the capacity of individuals to shift phenology may also be affected by life-history traits such as migratory strategy. Migrant individuals, that often breed in highly seasonal environments, have incomplete knowledge of breeding ground conditions, which may impede their ability to adjust the timing of migration departure, duration, and arrival to match resource peaks (Rubolini et al. 2010), which can result in fewer, weaker phenological responses (Rubolini et al. 2010, Samplonius et al. 2018), and stronger negative population effects of climate change compared to residents (Møller et al. 2008, Both et al. 2010). Because DoD installations are located in diverse geographic and climatic regions across the nation and managers must effectively manage species with a wide variety of migratory strategies, it is important to understand how variation in these factors impacts vulnerability to climate-driven phenological mismatch.

When mismatch does occur, behavioral plasticity of individuals offers one potential mechanism for species to respond and adapt to resource-limited conditions. For example, initiating continuous incubation before clutch completion results in earlier average hatch date

(i.e., less mismatched, Both and Visser 2005), and staggers egg hatching dates and nestling development in a phenomenon called "hatch asynchrony" (Clark and Wilson 1981). Having offspring that reach their peak growth rate at different times lessens the *per diem* energy burden on parents during brood-rearing (Wiebe and Bortolotti 1994, Mainwaring et al. 2014), which could be adaptive if brood-rearing is occurring under mismatched, resource-limited conditions. However, little research exists on the relationship between phenological mismatch and hatch asynchrony.

American kestrels (*Falco sparverius)* are widespread, generalist predators that breed across much of North America (Smallwood and Bird 2020). Kestrels are leap-frog migrants with northern populations being more migratory and migrating farther distances than southern populations (Heath et al. 2012). Kestrels are dietary generalists and prey on insects, small mammals, birds, and lizards (Smallwood and Bird 2020). Clutch initiation of kestrels is positively correlated with the start of spring (estimated from the extended spring index, SI-x, Appendix 1) and Normalized Difference Vegetation Index (NDVI) values, which are a good proxy for small mammals (Smith et al. 2017) and insect (Lafage et al. 2014) abundance. Specifically, the timing of NDVI peaks is positively correlated with the timing of peaks in small mammals, regardless of land cover type (Smith et al. 2017). Furthermore, the median timing of kestrel clutch initiation is 12 days before the SI-x (Figure A1.1), suggesting that incubation and brood-rearing would coincide with increasing and relatively high NDVI values (Figure A1.2) and prey abundance based on known durations of egg-laying (8 – 12 days) and incubation (26 – 32 days) for the species (Smallwood and Bird 2020). Kestrel clutch initiation dates are advancing with earlier springs in western populations (Smith et al., 2017), but remain unchanged in eastern populations, despite advancing springs (Del Corso 2016). The causes of geographic variation in phenological shifts, and potential fitness consequences are unknown. Further, geographic variation in population trends, specifically steeper declines in eastern populations (Smallwood et al. 2009, McClure et al. 2017), emphasizes the importance of understanding population characteristics associated with vulnerability to mismatch consequences. Here we used American kestrels as a focal species to examine how phenological mismatch affects productivity and survival across a large spatial scale so that we can better understand population characteristics associated with vulnerability to mismatch consequences and how climate-driven changes in spring might impact land bird populations.

Materials and Methods

Productivity

We obtained nest records from the Cornell Lab of Ornithology's NestWatch program (1997 – 2018; https://nestwatch.org/) and The Peregrine Fund's American Kestrel Partnership (AKP, 2007 – 2019; https://kestrel.peregrinefund.org/), which collects data across North America. Additionally, we collected data as part of our long-term *Southwestern Idaho Kestrel Study* (2008 – 2018), and the *Full Cycle Phenology Project* (2018 – 2019) where we monitored nest boxes on Department of Defense (DoD) installations in Washington, New Mexico, California, New York, North Carolina, and Kansas (Figure 1.1).

Data collection protocols varied depending on the monitoring program, but nest records were typically collected through repeat nest monitoring by community science volunteers, professional biologists, time-lapse camera imagery, or a combination of these approaches. Additional details on data collection for each of these nest monitoring programs, data processing steps, and determination of breeding parameters are provided in Appendix 1. We restricted our

analysis to nests in which 1) eggs or nestlings were observed and the date on which the first egg of the clutch was laid (clutch initiation date) was directly observed or could be reliably back-

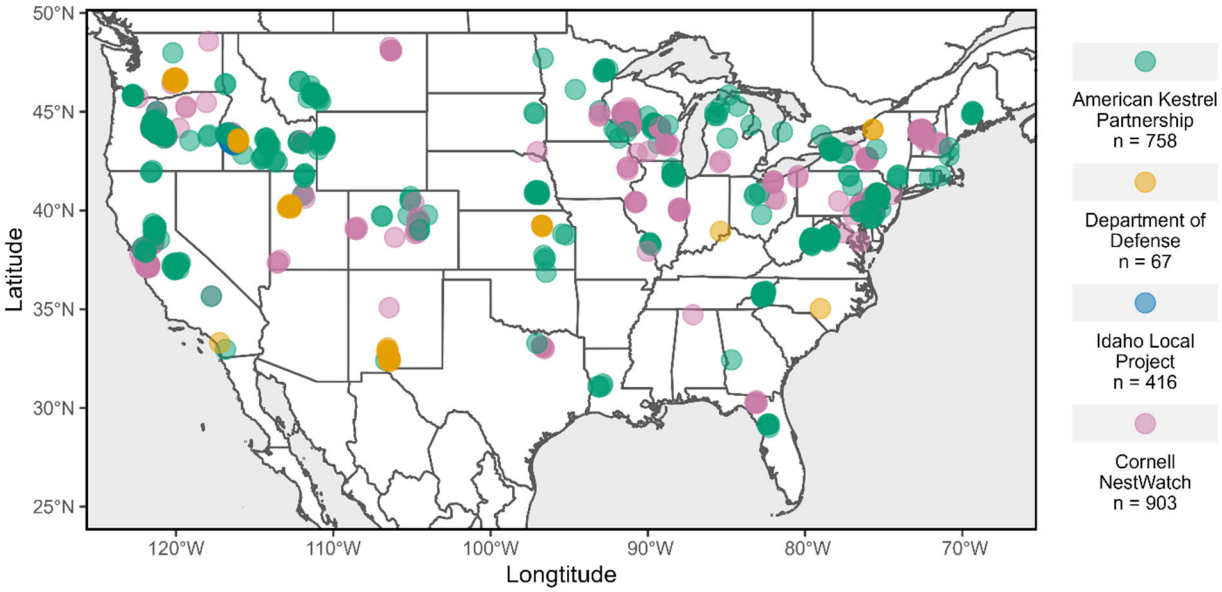

Figure 1.1 Map of American kestrel nests included in the productivity analysis (n = 2144). Each point represents one nest, darker points represent multiple nests, and the color of the point indicates the source of data: the American Kestrel Partnership (2007 – 2019, n = 758), the Full Cycle Phenology Project on Department of Defense land (2018 – 2019, n = 67), the long-term monitoring site in southwestern Idaho (2008 – 2018, n = 416), or Cornell NestWatch (1997 – 2018, n = 903).

calculated from the information provided, 2) nest outcome could be assigned from nestling age or participant comments, and 3) the number of young fledged was provided.

Survival

We collected mark-and-recapture data from American kestrels nesting in nest box networks in Idaho (*Southwestern Idaho Kestrel Study*) and New Jersey (Figure 1.2a) with long-term monitoring programs. The study site in southwestern Idaho (43° N, 116° W) encompasses approximately 1000 km^2 within a mixture of sagebrush steppe, agriculture, and rangelands, alongside exurban and suburban areas in the municipalities of Kuna, Meridian, and Boise. The number of nest boxes at this study site ranged from 98 to 113, depending on the year. Occupancy averaged 42% (± 14.4 SD) and, on average, occupied boxes (i.e., American kestrels with ≥ 1 egg) were 1.5 km apart. The magnitude of seasonal changes in primary productivity is relatively low and variable across landscapes and years (Figure 1.2b, see Appendix 1 for NDVI methods). The study site in northwestern New Jersey (41° N, 74° W) encompasses approximately 200 km^2 and is comprised of agricultural lands with open fields embedded within forested areas in Sussex and Warren counties (Smallwood et al. 2009). The number of nest boxes at this study site ranged from 96 to 127, depending on the year. Occupancy averaged 28% (± 9.5 SD) and, on average, occupied boxes were 1.5 km apart. Seasonal changes in primary productivity at the New Jersey site are relatively higher in magnitude and consistent from year to year (Figure 1.2c). We captured and marked adult American kestrels in nest boxes in Idaho from 2008 to 2017, and in New Jersey from 1997 to 2017. We monitored nest boxes from March to July and systematically checked for occupancy (every 1–3 weeks in Idaho; every 3–4 weeks in New Jersey). We hand-captured adults in nest boxes during the incubation stage, attached United States Geological

Survey (USGS) aluminum bands, measured and sexed (by plumage) individuals, and returned them to the nest box. Recaptured adults, or individuals that had been banded previously elsewhere, were recorded as already banded. On average, we trapped 80% (± 7.4 SD) and 39% (± 16.6 SD) of nesting adults in Idaho and New Jersey, respectively. Unless individuals were first captured and marked as nestlings, we were unable to age after-hatch-year (adult, AHY) birds to more specific age categories. We returned to the nest box to band, measure, and sex nestlings when they were between 18 and 25 days old. We considered a nesting attempt to be

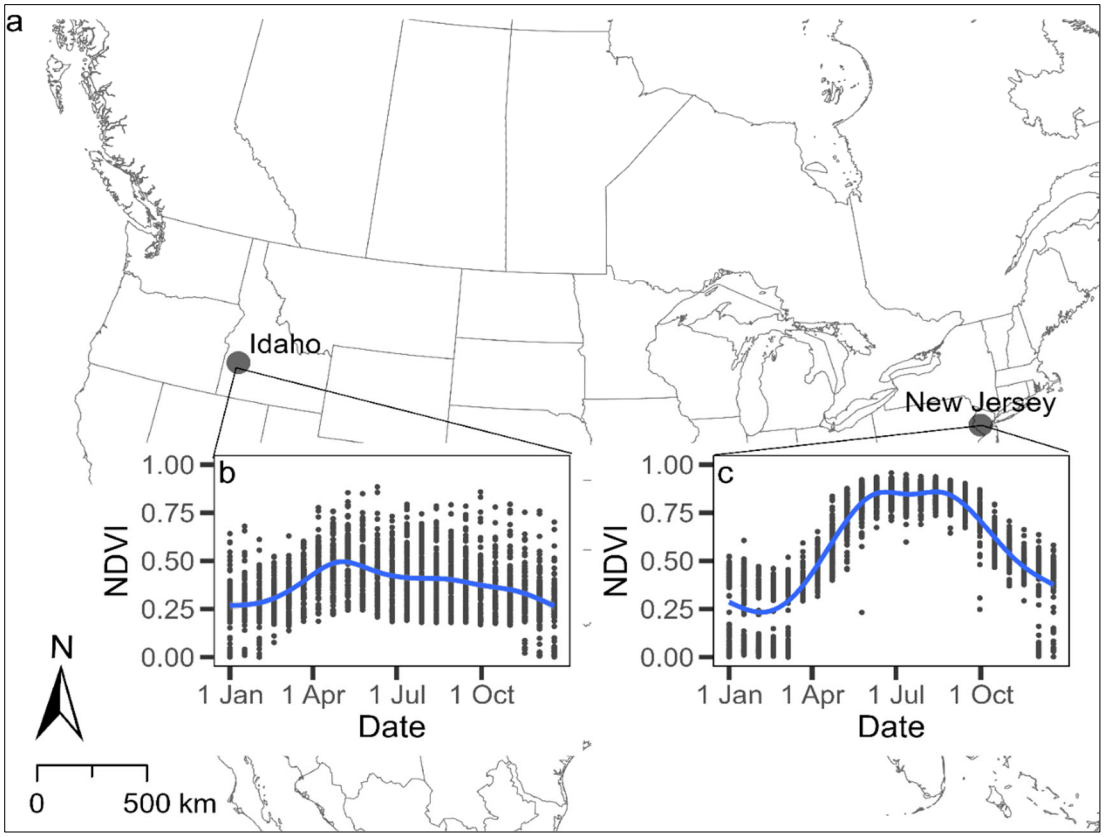

Figure 1.2 Locations (a) of the long-term mark and recapture studies used to estimate apparent survival of American kestrels with insets of annual normalized difference vegetation index (NDVI) from Jan 1 – Dec 31 (2001 – 2020) from five locations within 1 km of nest boxes within the western site (Idaho, b) and eastern site (New Jersey, c). The blue lines represent a smoothed average. Though the study sites are at a similar latitude, growing seasons are more pronounced at the eastern site compared to the western site where vegetation green-up is more heterogeneous and less peaked.

successful if it produced at least one young that reached 25 days old (Anderson et al. 2016, Smallwood 2016) and recorded the clutch-initiation date for each nesting attempt (see Appendix 1).

We calculated winter minimum temperature anomalies for each study site to determine winter severity. We used minimum temperatures because, especially in winter months, minimum temperatures limit species distributions (Root 1988, Zuckerberg et al. 2011) and lower minimum temperatures affect energetic requirements associated with thermoregulation (Meijer et al. 1999). The use of anomaly values allowed for standardized representation of climate change across locations with different minimum temperatures. We used Google Earth Engine (Gorelick et al.

2017) to extract minimum temperatures from the Daymet dataset, which provides daily gridded climate data at 1-km resolution (Thornton et al. 2018). For each year, we averaged daily minimum temperature values within a minimum bounding box of all nest box locations for each study area. For each study site, we calculated winter minimum temperature anomalies for each year as the difference between the mean winter minimum temperature and the mean winter minimum temperature from a 30-year (1981–2010) baseline period.

Incubation onset and hatch asynchrony

We quantified incubation onset and hatch asynchrony at a subset of DoD nest boxes equipped with cellular or non-cellular trail cameras (Spypoint, see Appendix 1) that captured complete time-lapse imagery from clutch initiation date through the end of the incubation period (Figure 1.3). Cameras were initially programmed to capture three images per day, but cellular cameras were switched remotely via the Spypoint website to take hourly images once the clutch was initiated. We defined the relative onset of incubation behavior as the difference in days between clutch initiation and the first day in which each parent began incubation (i.e., laying prone over the eggs and the majority of the eggs are covered). For hatch asynchrony, we calculated the variation in plumage-determined ages (Griggs and Steenhof, 1993) among nestlings approximately 23 – 25 days after the first egg hatched.

Figure 1.3 Images collected by trail cameras in American kestrel nest boxes were used to record nesting phenology and adult incubation behavior. Images progress from left to right then top to bottom, showing mate pairing, egg-laying, and brood rearing.

Phenology mismatch

We estimated the start of spring using extended spring-index (SI-x) models. These models predict the first-bloom dates of lilac (*Syringa chinensis* and *S. vulgaris*), and honeysuckle cultivars (*Lonicera tatarica* and *L. korolkowii*) using daily maximum and minimum surface temperatures (Schwartz and Hanes 2010, Rosemartin et al. 2015). Lilac and honeysuckle first-bloom dates have been used to indicate the onset of spring, and the ubiquitous distribution of these ornamental plants allows for the meaningful comparison of spring phenology across space, time, and different biomes (Schwartz and Hanes 2010). SI-x models have been validated across North America and provide fine-scale (1 km) estimates of the start of spring (Izquierdo-Verdiguier et al. 2018). SI-x measures are highly correlated with land surface metrics (e.g.,

NDVI; Zurita-Milla et al. 2017), and in North America SI-x has proven more predictive of bird phenology than NDVI (Kelly et al. 2016). Further, the timing of American kestrel clutch initiation was positively associated with SI-x (Figure A1.4). We used NDVI to represent seasonal patterns in primary productivity because NDVI captures year-round green-up and senescence (Appendix 1). We extracted SI-x dates derived from Daymet climate datasets (Thornton et al. 2018) at the latitude and longitude of each occupied nest box per year using Google Earth Engine code modified from Izquierdo-Verdiguier et al. (2018). For the productivity analysis, we created an index of phenology mismatch by calculating the difference in days between the clutch initiation date and the SI-x date. For multi-state survival models, which require individual time-varying covariates to be categorical, we calculated the difference (in days) between the clutch-initiation date and the year-specific SI-x date for each nest attempt and compared the difference to the median difference for each study site. Then, we categorized nesting attempts as "early" (before the median) or "late" (after the median). If an individual attempted to nest more than once in a season (n = 16), the latest successful nesting attempt was considered when assigning the individual to a timing group for that year (n = 8), or if both nesting attempts were unsuccessful (n = 8), the latest nesting attempt was considered.

Statistical analyses

We used a zero-inflated generalized linear mixed-effect model with a Generalized Poisson distribution and log-link to evaluate candidate model sets for predicting productivity in the *glmmTMB* package (Brooks et al. 2017) for R (R Core Team 2020). This model included two sub-models: (1) a zero-inflation to model the probability of nest failure, and (2) a conditional generalized Poisson to model count data (i.e., number of young fledged from successful nests). Each sub-model included a random effect of categorical year. Covariates included in the conditional and zero-inflation model candidate sets for productivity were phenological mismatch, latitude, and longitude. All covariates were scaled and centered. We assessed correlations among covariates and all were $|r| < 0.5$. Candidate models included all possible combinations of the three covariates. We evaluated candidate models for the zero-inflation model with an intercept-only conditional model first. Then, we used the best supported zero-inflated model to evaluate candidate models for the conditional model. We examined dispersion and residuals of the top model using the *DHARMa* package (Hartig 2020) to check model assumptions.

For the survival analysis, we created mark-recapture models using the multi-state model framework in Program MARK (White and Burnham 1999), using the *RMark* package and interface (Laake and Rexstad 2008). Multistate mark-recapture models estimate apparent survival (S), and capture probability (p) similar to Cormack–Jolly–Seber mark-recapture survival models (Lebreton and Pradel 2002); additionally, these models estimate transition probability (Ψ) between categorical states (Schwarz et al. 1993). We created six states, hereafter referred to as strata, to represent nesting timing, age, and nesting success of adults:

1) hatch-year (HY) from a brood initiated "early"
2) HY from a brood initiated "late"
3) a successful after-hatch-year (AHY) that initiated egg-laying "early"
4) a successful AHY that initiated egg-laying "late"
5) an unsuccessful AHY that initiated egg-laying "early"
6) an unsuccessful AHY that initiated egg-laying "late"

In addition to individual strata, we included sex as an individual-level, static covariate and winter minimum temperature anomaly as a population-level, time-varying covariate to explain apparent survival. We created capture histories for each individual by coding their presence or absence in each year of the study and assigning the appropriate stratum according to their age, timing category, and nesting success, for each year they were present. Most (> 85%) American kestrels breed in their second year, and clutch-initiation dates do not differ between second year and older individuals (Steenhof and Heath 2009). We had few known-age individuals, so we did not consider age effects other than categorical HY and AHY designations. We designed a model set for apparent survival that included all additive and interactive models of the multi-state variable stratum, sex, and annual minimum winter temperature anomaly ("winter temperature"). We examined models for p that included the covariates of winter temperature and sex because we typically capture a higher proportion of females compared to males (Steenhof and Heath 2013), and we created a candidate model set for Ψ that included an intercept-only model and an effect of current stratum membership. We did not have the sample size to build more complex models for Ψ. We fixed the Ψ estimates of transition from AHY to HY and between HY strata to 0 (Figure A1.7). We used an iterative process to find the best model by selecting the top model for p, then the best model for Ψ, and used the top models for p and Ψ to build models for S. We ran separate mark-recapture analyses for western and eastern sites, using the same model set for each analysis. We ran goodness of fit tests on survival models with the variable 'strata' using functions from the package *R2UCare* (Gimenez et al. 2018). Specifically, we used the functions overall_JWV to test the fit of the model, test3Gsr to test for the presence of transients, and test3Gwbwa to test for the presence of memory. For all tests we failed to reject the null hypotheses ($p > 0.05$) indicating model fit, and lack of issues with transients and memory. We examined temporal trends in clutch initiation dates for each study site using generalized linear models with Gamma distributions and log link functions in the R package *glmmTMB* (Brooks et al. 2017). We used a Gamma distribution because clutch initiation dates are positive data. We plotted residual dispersion to check model assumptions.

We created gamma-distributed generalized linear models with log links to examine the relationship between within-brood variation in nestling age and the onset of incubation behavior for each parent. One male did not incubate until 20 days after clutch initiation, much later than the other males. We ran models with and without this observation to ensure the value did not have an undue influence on results. We used generalized linear models with negative binomial distributions and a log link to determine if male incubation behavior (number of days between clutch initiation date and the first day of incubation) was predicted by phenological mismatch or location (latitude and longitude). For these models, we used data from both successful and unsuccessful nesting attempts with complete photographic records of incubation behavior.

For each of the three analyses (i.e., productivity, survival, hatch asynchrony), we compared models using Akaike's information criterion corrected for small sample size (AIC_c), and considered the models with the lowest AIC_c to be most informative (Anderson and Burnham 2004). We estimated 85% confidence intervals for model parameters to be compatible with model selection criteria (Arnold 2010), and we considered effects statistically unclear if 85% confidence intervals overlapped zero (Dushoff et al. 2019). We report parameters as estimates ± standard error and with their 85% confidence intervals. We conducted all analyses in R (R Core Team 2021, version 4.0.5).

Results and Discussion

Productivity

We collected data from 2144 American kestrel nesting attempts that occurred between 1997 and 2019 in the contiguous United States and southern Canada (Figure 1.1). Most nests were successful (n = 1642, 77%) and raised 1 – 7 young (mean = 3.9, standard deviation = 1.1). Clutch initiation dates ranged from 1 March – 14 June (Figure A1.1). The median timing of clutch initiation was 12 days before SI-x (range -67 to 64, Figure A1.1).

The best zero-inflation model for predicting nest failure included all two-way interactions between phenological mismatch, latitude, and longitude (Table 1.1a). Nests were more likely to fail if they were initiated after the SI-x, and this effect was strongest in the northeast (Table 1.2a). The best conditional model for productivity was the additive effect of phenological mismatch with an interaction between latitude and longitude (Table 1.1b, Table 1.2b). These results suggest that productivity was lower for successful pairs that nested after the SI-x, regardless of location. When nesting earlier relative to the SI-x, individuals in the northeast had more young per brood than individuals in the west and southwest (Figure 1.4). However, northeastern individuals experienced a sharper decline in productivity with increasing mismatch than individuals from other regions included in our study (Figure 1.4).

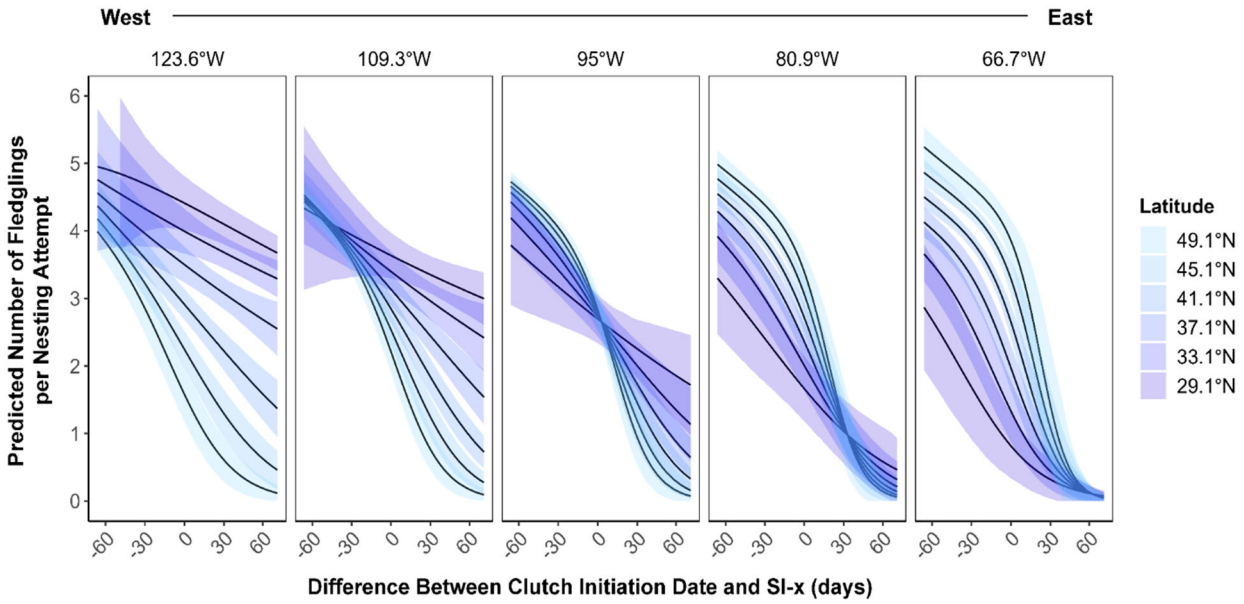

Figure 1.4 The predicted number of American kestrel fledglings per nesting attempt was best predicted by the additive effect of phenological mismatch (the difference in days between the clutch initiation date and the extended spring index date, SI-x) and the interactive effect of latitude and longitude. The lines represent the model predictions, the shaded regions are the 85% confidence intervals, the panels show predictions at different longitudes from west to east, and the colors indicate predictions at different latitudes. The number of young fledged per nesting attempt decreased as pairs laid eggs after the SI-x. The effect of late clutch initiation was strongest in the northeast, where productivity was high then steeply declined.

Table 1.1 Candidate models for predicting the number of American kestrel young fledged per nesting attempt. Zero-inflated generalized Poisson mixed-effect linear models included the covariates of phenological mismatch (the difference between the clutch initiation date and the SI-x), longitude in °W, and latitude in °N. During evaluation of zero-inflated models (a) the conditional model was an intercept-only model. All conditional models (b) included the top model for zero-inflation (all two-way interactions among mismatch, latitude and longitude). Each conditional and zero-inflation model included a random effect of year. Tables show models with weights > 0.01 and an intercept-only model, number of parameters estimated (K), ΔAIC_c, and model weights (wi). We evaluated 15 candidate models for each sub-model.

a. Zero-Inflation Models	K	ΔAIC_c	w_i
Mismatch*Latitude + Latitude*Longitude + Mismatch*Longitude	11	0.0[a]	0.70
Mismatch*Latitude*Longitude	12	1.9	0.27
Mismatch*Longitude + Latitude*Longitude	10	6.4	0.03
Intercept-only	5	159.1	0
[a]AICc = 7040.9			
b. Conditional Models	K	ΔAIC_c	w_i
Mismatch + Latitude*Longitude	15	0.0[a]	0.64
Mismatch*Latitude + Latitude*Longitude + Mismatch*Longitude	17	1.9	0.25
Mismatch*Latitude*Longitude	18	3.4	0.12
Intercept-only	11	64.0	0
[a]AICc = 6976.9			

Table 1.2 Parameter estimates, standard errors, and 85% confidence intervals (CI) from the top zero-inflation model (a), and the top conditional model (b) explaining American kestrel productivity 1997 – 2019 across North America.

a. Parameters	Estimate	85% CI	85% CI	Std. Error
(Intercept)	-1.33	-1.58	-1.07	0.18
Mismatch	0.98	0.85	1.12	0.10
Latitude	-0.01	-0.11	0.09	0.07
Longitude	-0.29	-0.38	-0.19	0.07
Mismatch*Latitude	0.18	0.09	0.27	0.07
Mismatch*Longitude	0.40	0.26	0.54	0.10
Latitude*Longitude	-0.33	-0.45	-0.22	0.08
b. Parameters	Estimate	85% CI	85% CI	Std. Error
(Intercept)	1.365	1.35	1.38	0.01
Mismatch	-0.067	-0.08	-0.05	0.01
Latitude	0.001	-0.01	0.01	0.01
Longitude	0.004	-0.01	0.01	0.01
Latitude*Longitude	0.034	0.02	0.04	0.01

Survival

We captured and marked 1430 (first marked as AHY = 507, HY = 923) individuals at the western site in Idaho and 1405 (first marked as AHY = 284, HY = 1121) individuals at the eastern site in New Jersey that were associated with 369 nest attempts from 2008 to 2017, and 301 nest attempts from 1997 to 2017, at western and eastern sites, respectively. At the western site, clutch initiation dates ranged from early March through late June (Figure 1.5), and the median difference between clutch initiation and the start of spring was -17 days (std. deviation = 21 days, Figure 1.5). At the eastern site, clutch initiation dates ranged from late March through early June (Figure 1.5), and the median difference between clutch initiation and the start of spring was -8 days (std. deviation = 12 days, Figure 1.5). The best-supported model for recapture probability contained a covariate for sex. Western males were more likely to be recaptured than females (β = 0.44; 85% CI 0.06–0.81, Table A1.3) and eastern males were less likely to be recaptured than females (β = -1.21; 85% CI -1.7–0.71, Table A1.4). The best-supported model for the transition probability was the intercept-only model (Table A1.5, Table A1.6). Previous strata state did not explain the transition probability to alternate states. The best-supported model for apparent survival at the western site included additive effects for the multi-state variable stratum (includes nesting timing, age, and nesting success), sex, and winter temperature (Table 1.3). The best-supported model for apparent survival at the eastern site contained the stratum and sex covariates (Table 1.4). Successful "early" nesting individuals had higher apparent survival rates compared to successful "late" nesters in the West (Figure 1.6, Table 1.5). Successful "late" nesting individuals had higher apparent survival rates compared to successful "early" nesters in the East (Figure 1.6, Table 1.5). At both sites, successful adults had higher apparent survival rates than unsuccessful adults, and there was no difference in apparent survival of unsuccessful "early" and "late" adults. Also, there was no difference in apparent survival of "early" versus "late" HY individuals. Overall, HY individuals had lower apparent survival estimates than AHY individuals. Winter minimum temperature anomalies were positively associated with higher

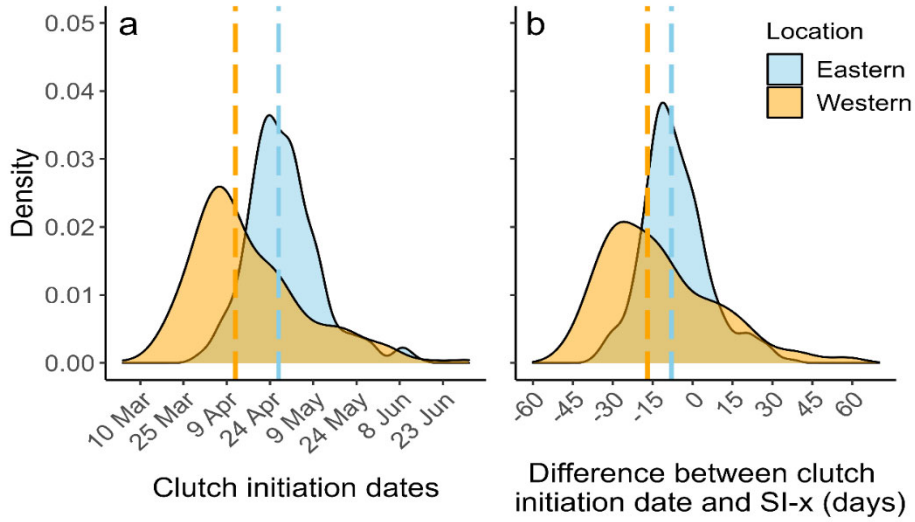

Figure 1.5 Density distributions of the clutch initiation dates (a), and the difference between clutch-initiation date and extended spring index date (SI-x, b) for nests at western (Idaho, shaded orange, n = 369, 2008 – 2017) and eastern (New Jersey, shaded blue, n = 301, 1997 – 2017) sites. The orange dashed line represents the median overall clutch initiation date for western nests in "a" (April 12th) and the overall median difference between clutch initiation and SI-x in "b" (-17 days). The blue dashed line represents the overall median clutch initiation date for eastern nesting attempts in A (April 27th) and the overall median difference between clutch initiation and SI-x in B (-8 days).

apparent survival estimates (β = 0.43; 85% CI 0.21–0.64, Figure 1.6) in the West, and males tended to have higher survival estimates than females, but the 85% confidence interval for sex crossed zero, so we considered this effect statistically unclear (β = 0.11; 85% CI -0.23–0.45). The top model did not include winter temperature in the East. It did include sex, but the confidence interval for sex crossed zero (β = − 1.04; 85% CI -1.30–0.01), so we considered this effect statistically unclear. Clutch initiation date advanced (β = -0.009; 85% CI -0.014–0.003) over the nine-year study period in the West (Figure 1.7), whereas clutch initiation dates did not change over the 20-year study period in the East (β = 0.003; 85% CI -0.002–0.004, Figure 1.7).

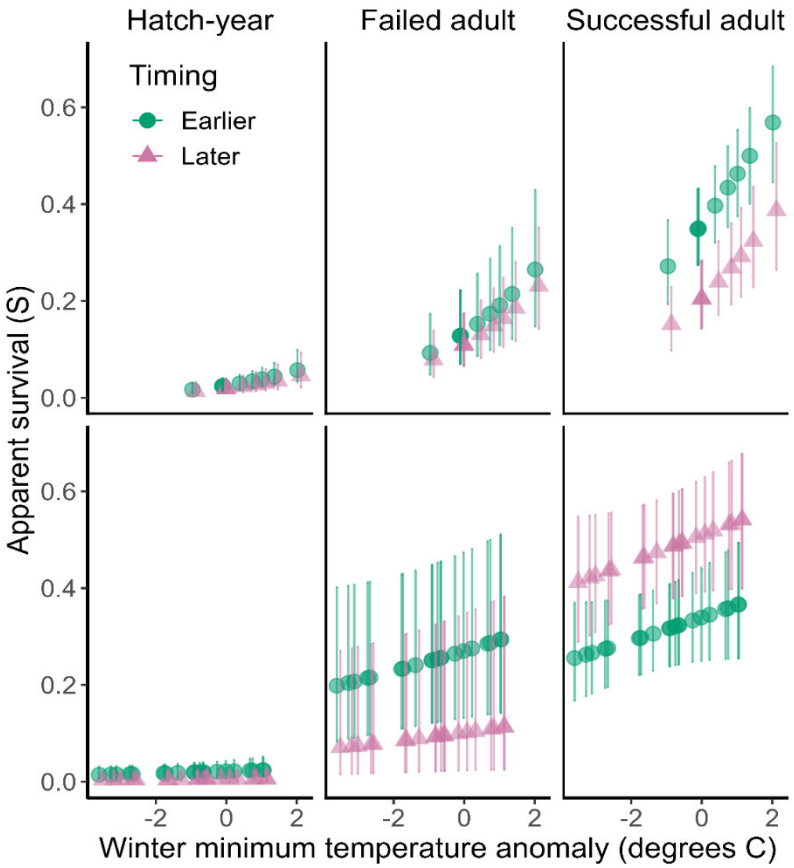

Figure 1.6 Apparent survival estimates for female western (Idaho) American kestrels from 2008 –2017 (top) and eastern (New Jersey) American kestrels from 1997 – 2017 (bottom) categorized by age, whether or not an adult successfully raised young, and nesting timing category across winter minimum temperature anomalies. Circles and triangles are mean estimates and bars represent 85% confidence intervals. Apparent survival of successful adults depended on whether they were in the early (green) or late (coral) nesting timing category. Nesting timing did not affect apparent survival rates of hatch-year individuals or adults that did not successfully rear offspring. Apparent survival rates of western kestrels increased as winter minimum temperature anomaly increased, but this result was statistically unclear for eastern kestrels.

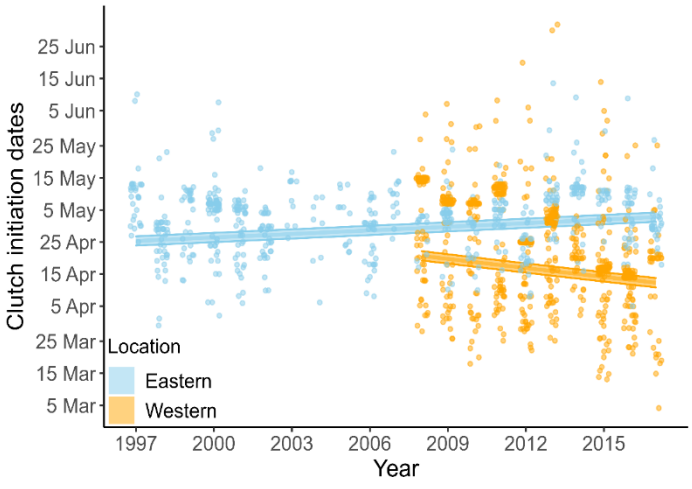

Figure 1.7 Trends in clutch initiation dates of American kestrel nests at the western (Idaho) site from 2008 – 2017 (blue) and eastern (New Jersey) site from 1997 – 2017 (orange). The shaded areas represent the 85% confidence interval around the predicted line, and each point represents the clutch initiation date at an occupied nest box. American kestrels are nesting earlier at the western site, but there is no change in nesting phenology at the eastern site.

Table 1.3 Candidate model set to estimate apparent survival (S) of western American kestrels in Idaho captured between 2008 – 2017. The table includes the model, number of model parameters (K), delta AIC_c (ΔAIC_c), and model weights (w_i). The recapture probability submodel contained a covariate for sex and the transition probability submodel included an intercept-only term for all apparent survival models. See methods for levels of the stratum variable.

Apparent Survival (S)	K	ΔAIC_c	w_i
Stratum + Sex + Winter temperature	30	0	0.57
Stratum + Sex * Winter temperature	31	1.4	0.28
Stratum	28	3.7	0.09
Stratum + Sex	29	5.6	0.03
Stratum * Winter temperature	34	6.3	0.02
Stratum * Sex + Winter temperature	35	8.8	0.01
Stratum * Sex	34	14.4	0
Stratum * Sex * Winter temperature	46	17.3	0
Stratum + Winter temperature	29	51.7	0
Sex + Winter temperature	25	123.4	0
Sex * Winter temperature	26	125.1	0
Intercept only	23	126.4	0
Sex	24	128.3	0
Winter temperature	23	157.4	0

Table 1.4 Candidate model set to estimate apparent survival (S) of eastern American kestrels in New Jersey captured between 1997 – 2017. The table includes the model, number of model parameters (K), delta AICc ($\Delta AICc$), and model weights (w_i). The recapture probability submodel contained a covariate for sex and transition probability submodel included an intercept-only term for all apparent survival models. See methods for levels of the stratum variable.

Apparent Survival (S)	K	$\Delta AICc$	w_i
Stratum + Sex	30	0.0	0.55
Stratum + Sex + Winter temperature	31	1.0	0.33
Stratum + Sex * Winter temperature	32	3.0	0.12
Stratum	29	25.1	0
Stratum + Winter temperature	30	26.5	0
Stratum * Winter temperature	35	31.8	0
Stratum * Sex	35	44.0	0
Stratum * Sex + Winter temperature	36	45.1	0
Stratum * Sex * Winter temperature	47	58.9	0
Sex	25	129.3	0
Intercept only	24	130.2	0
Sex + Winter temperature	26	130.4	0
Sex * Winter temperature	27	132.5	0
Winter temperature	24	141.2	0

Table 1.5 Effect size (β) for each covariate in the top apparent survival model for American kestrels captured at the western (Idaho) and eastern (New Jersey) site. Hatch-year individuals had lower apparent survival rates than adults. Among successful adults, nesting timing had different effects between sites. Winter temperatures had a positive effect on apparent survival rates of western kestrels but that variable was not in the top model for eastern kestrels.

	Western (Idaho) Site			Eastern (New Jersey) Site		
Covariate	β	Lower CI (85%)	Upper CI (85%)	β	Lower CI (85%)	Upper CI (85%)
Stratum						
Earlier hatch-year	-3.52	-4.05	-2.99	-3.95	-4.66	-3.23
Later hatch-year	-3.76	-4.48	-3.05	-5.32	-6.80	-3.85
Earlier adult, nest-success	-0.44	-0.81	-0.07	-0.80	-1.19	-0.41
Later adult, nest-success	-1.18	-1.56	-0.80	-0.10	-0.53	0.34
Earlier adult, nest-failure	-1.74	-2.40	-1.08	-1.06	-1.94	-0.18
Later adult, nest failure	-1.91	-2.45	-1.37	-2.31	-3.86	-0.76
Sex (male)	0.11	-0.23	0.45	-1.04	-1.30	0.01
Winter Temperature (min anomaly °C)	0.43	0.21	0.64	-	-	-

Incubation onset and hatch asynchrony

There were 27 nests with complete photographic records of incubation to use for our analysis of incubation behavior. The onset of male incubation was 1 – 20 days (mean = 8.0, standard deviation = 4.2) after clutch initiation whereas onset of female incubation was 0 – 8 days (mean = 2.0, standard deviation = 2.3) after clutch initiation. Of the 27 nests, we had 16 successful nests where we measured variance in nestling age within broods. Within-brood nestling age variance ranged from 1 to 4 days (mean = 2.1, standard deviation = 1.0) and was best explained by the onset of male incubation behavior (β = -0.33, 85% CI: -0.47 to -0.19, Table 1.6, Figure 1.8). The early onset of male incubation resulted in more asynchronous hatching, producing a greater variance in nestling ages. The onset of male incubation was best predicted by the additive effects of phenological mismatch (β = -0.33, 85% CI: -0.51 to -0.14) and latitude (β = -0.34, 85% CI -0.52 to -0.16, Table 1.7, Figure 1.9). Males from breeding pairs that initiated clutches after the SI-x began incubating sooner than males from breeding pairs that initiated clutches before the SI-x. Males breeding at higher latitudes were more likely to initiate incubation soon after clutch initiation, whereas males breeding at lower latitudes were more likely to delay the onset of incubation.

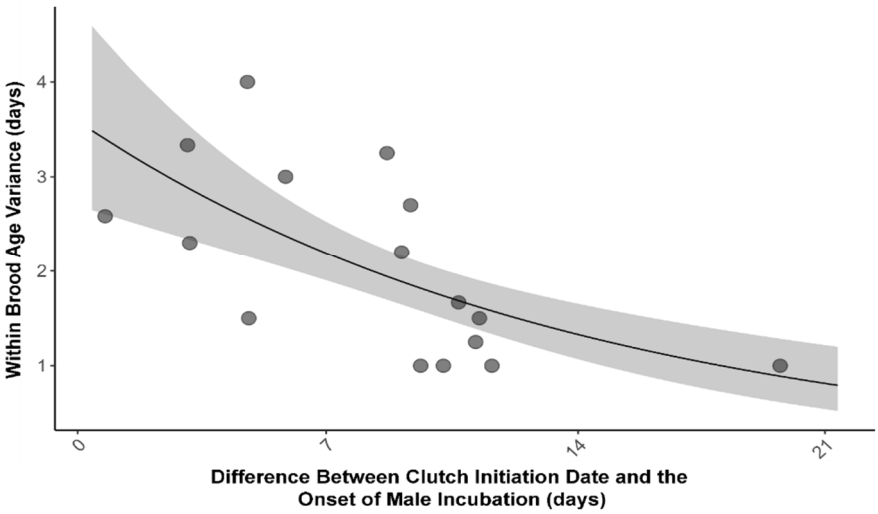

Figure 1.8 Within brood age variance was best predicted by the difference in days between the clutch initiation date and the onset of male incubation. Each point represents a nest with complete incubation data that had at least two fledglings during the breeding seasons of 2018 (n = 8) and 2019 (n = 8). The line represents the model prediction, and the shaded region is the 85% confidence interval.

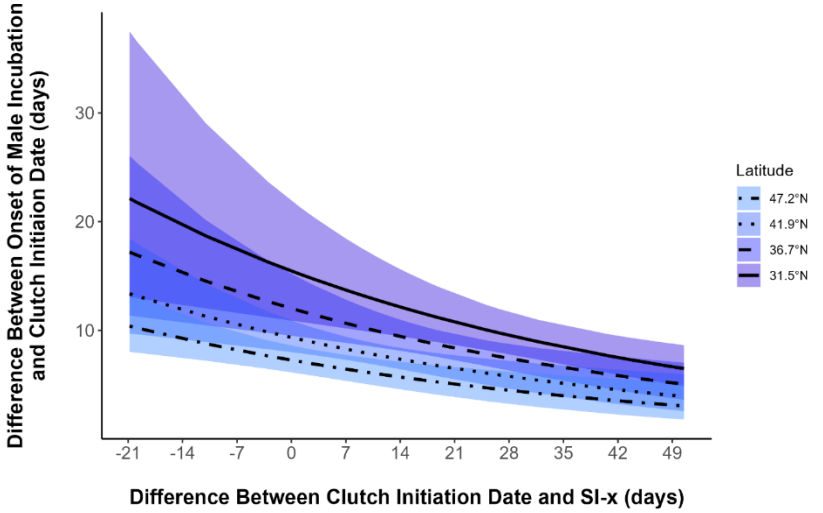

Figure 1.9 The predicted relationships between phenological mismatch (the difference between clutch initiation date and SI-x) and the onset of male incubation relative to clutch initiation date (days) for different latitudes. The line represents the model predictions, the shaded regions are the 85% confidence interval for each prediction, and the line type of each prediction and the color surrounding it represent predictions at different latitudes.

Table 1.6 Candidate models to explain age variation within broods of American kestrels. Covariates included the difference between the clutch initiation and incubation onset dates for male and female American kestrels. Models were generalized linear models with a Gamma distribution to represent age variance within broods. Tables show models, number of parameters estimated (K), ΔAIC_c, and model weights (wi).

Candidate model	K	ΔAIC_c	w_i
Male Incubation	3	0.0[a]	0.79
Male Incubation + Female Incubation	4	3.2	0.16
Intercept-only	2	6.2	0.04
Female Incubation	3	8.6	0.01

[a]$AIC_c = 40.3$

Table 1.7 Candidate models to explain the difference between clutch initiation date and the onset of male incubation in American kestrels. The covariates included are phenological mismatch (the difference between the clutch initiation date and the SI-x), latitude, and longitude. Models were generalized linear models with a negative binomial distribution to represent the difference between clutch initiation date and onset of male incubation. The table shows model, number of parameters estimated (K), ΔAIC_c, and AIC_c weights (w_i).

Candidate model	K	ΔAIC_c	w_i
Mismatch + Latitude	4	0.0[a]	0.42
Mismatch + Latitude + Longitude	5	0.7	0.29
Intercept-only	2	3.2	0.09

[a]AICc = 150.5

Synthesis

Consistent with previous literature (Goodenough et al. 2010, Bowers et al. 2016, Taylor et al. 2021), we showed that mismatch, specifically initiating clutches after the start of spring, decreased nest success and productivity of American kestrels across their range. Regional variation in the strength of mismatch effects (i.e., stronger effects in the Northeast) may be related to differences in growing seasons and climate change impacts (Both et al. 2010, Garcia-Heras et al. 2016). Growing seasons in the Northeast have a higher but narrower peak in productivity in the spring than in the West, where green-up is less peaked and more heterogeneous. This may explain why "on-time" nesters in the Northeast have higher productivity peaks, but face steeper productivity declines due to mistimed breeding (i.e., shorter nesting window), compared to those nesting in regions where less-peaked, but prolonged growing seasons allow more flexibility in breeding time (i.e., longer nesting window).

In addition to regional trends in phenology and productivity, we showed differing effects of mismatch on apparent survival at two distinct long-term monitoring sites in western and eastern North America. Nesting phenology affected the apparent survival of adult kestrels that raised young, but the direction of the effect differed between populations, with earlier nesters having higher apparent survival than later nesters in the West, and later nesters having higher apparent survival than earlier nesters in the East. Given the seasonal declines in productivity, these results suggest that condition-dependent trade-offs between reproduction and survival exist for eastern kestrels, whereas this trade-off is not apparent for western kestrels. Furthermore, despite advancing springs across North America, clutch initiation dates tended not to change at

the eastern site, but they are advancing at the western site. Seasonal trade-offs may constrain shifts in nesting phenology in response to earlier springs in the eastern population, whereas the high apparent survival and productivity of early nesters in the West may make that population well-suited to respond to directional pressure to breed earlier (Figure 1.10).

Although we would expect seasonal declines in productivity and survival to drive birds to breed earlier, there are also constraints to early nesting. Extreme winter and early season temperatures and storms increase costs of self-maintenance, egg production, incubation, and raising young due to thermoregulation requirements and low food availability (Stevenson and Bryant 2000, Visser et al. 2012, Woodworth et al. 2017) thereby decreasing fitness outcomes of many species, including American kestrels (Dawson and Bortolotti 2000, Shipley et al. 2020). So, although the higher survival we documented in later nesting compared to earlier nesting individuals in New Jersey (i.e., eastern population) is contrary to our initial predictions, this relationship is consistent with early nesting constraints. Spring green-up is advancing in the Northeastern US (Ellwood et al. 2013), but this region is also experiencing other impacts of climate change such as increased severity and frequency of blizzards (Cohen et al. 2018) and extreme precipitation events (Huang et al. 2017). Thus, northeastern kestrels may be experiencing an increasingly inflexible and narrow time window (e.g. ~2 month lay date range in New Jersey, Del Corso 2016) within which they can breed without experiencing a decrease in productivity. Conversely, in Idaho (i.e., western population), patterns of seasonal survival were consistent with our predictions, wherein early nesters had higher survival than later nesters, which is consistent with a release of early season nesting constraints. In western North America winters are becoming milder (Kunkel et al. 2004, Heath et al. 2012), the onset of spring is advancing rapidly (Schwartz et al. 2006, Allstadt et al. 2015) and farmers are advancing the start of their planting season (Christiansen et al. 2011, Smith et al. 2017), resulting in wider prey

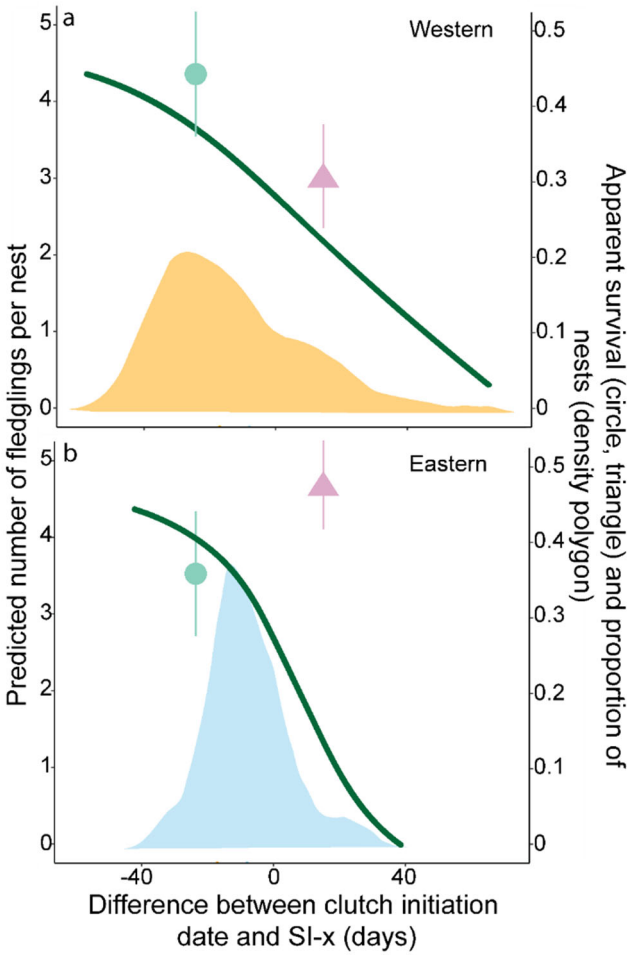

Figure 1.10 The density distributions of the difference between clutch-initiation dates and the start of spring (SI-x) in polygons, apparent survival estimates (mean and 85% confidence interval) of an early (green point and line) and late (coral triangle and line) successful, adult females, and seasonal trends in productivity (dark green line) for the western (Idaho) site (a) and eastern (New Jersey) site (b). At the western site, seasonal declines in both productivity and apparent survival may be allowing for earlier nesting in response to climate change via directional selection, whereas at the eastern site an inverse pattern between apparent survival and productivity may create a constraint for earlier nesting.

peaks and long nesting windows (e.g. ~ 4 months clutch initiation range in southwestern Idaho; Steenhof and Peterson 2009). These changes have removed previous constraints on earlier nesting, leading to shorter migration distances (Heath et al. 2012), northward shifts in wintering distributions (Paprocki et al. 2014), and earlier breeding (Heath et al. 2012) in American kestrels. Alternatively, or in addition to this, the West may also be experiencing increased late-season breeding constraints. Late summer in the West is subject to extreme heat and drought conditions, increasingly so with climate change (Sohrabi et al. 2013), which may have negative effects on both the survival and productivity of later breeders (Albright et al. 2010), increasing the pressure to breed earlier in these regions.

The differing strength of mismatch effects on productivity and different directions of effects on survival from West to East is interesting not only in the context of regionally-specific environmental conditions but also in light of differences in migratory phenotypes and genetic composition. In the partially-migratory populations in the West, earlier breeders tend to be residents, whereas later breeders tend to be migrants (Anderson et al. 2016), likely because migration increases energy demands, constrains arrival time, and decreases the ability to track local resources to breed at the optimal time (Rubolini et al. 2010, Samplonius et al. 2018). In the Northeast, where American kestrels are highly migratory, individuals may be constrained early in the season by arrival time at the nesting site, and later in the season by the need to accrue fuel and complete molt before migration or winter weather arrives (Stutchbury et al. 2011). Migration is also the life history stage with the highest mortality rate in many bird species (Klaassen et al. 2014), so migrants may be less likely to survive to breed in the subsequent season, and highly migratory populations may have lower survival rates than resident or partially-migratory populations. Finally, genetic differences between earlier and later breeders (Saino et al. 2017), between migrants and residents (Ruegg et al. 2021), and between western and eastern populations (Chapter 2) suggest that underlying genetic composition may result in differing levels of adaptive capacity to shift phenology (though see Chapter 3).

Similar to other species, we demonstrated that early-onset of continuous incubation is a mechanism for producing hatching asynchrony in American kestrels (Clark and Wilson 1981). Males from breeding pairs that laid eggs late relative to the start of spring began incubating shortly after the first eggs were laid, which advanced the average hatch date of later broods and increased nestling age variance, consistent with the "hurry-up" hypothesis (Clark and Wilson 1981). This relationship between mismatch and incubation onset suggests that hatching asynchrony may be an adaptation to low food resources resulting from sub-optimal breeding timing. Indeed, asynchronous hatching in American kestrels has been documented more frequently in years of food scarcity, and asynchronous broods need less provisioning per day than synchronous broods (Wiebe and Bortolotti 1994). Our results also showed that males breeding at higher latitudes were more likely to initiate incubation earlier in the laying order than those at lower latitudes. Selection pressure for optimal breeding time is stronger at higher latitudes compared to lower latitudes (Shave et al. 2019) due to narrow, peaked resource availability. However, because of constraints of long-distance migration (Heath et al. 2012), incomplete knowledge of breeding ground conditions (Samplonius et al. 2018), and early season weather stochasticity, high latitude breeders may be unable to adjust their breeding time to match resource peaks (Hurlbert and Liang 2012, Powers et al. 2021). Hence, early-onset incubation to induce hatch asynchrony could be an alternative strategy for high latitude individuals to cope with phenological mismatch.

In summary, although climate change is advancing the timing of spring green-up across North America, regional populations of American kestrels are responding differently. Western populations are nesting earlier, whereas nesting phenology is not changing in eastern populations. In the West, flexible migratory strategies and warmer winters may widen nesting windows and allow individuals to maximize fitness by nesting earlier when both productivity and survival rates are highest. Hence, western populations may be well-suited to respond to directional pressure to breed earlier with a warming climate. Conversely, in eastern populations, environmental constraints and high survival risks associated with early nesting may constrain shifts in nesting phenology. This is particularly concerning in light of population declines in the East. Lastly, although early onset of incubation may be an adaptive behavior to advance the average hatch date and spread out offspring demands, it is unknown how impactful this will be in mitigating the fitness consequences of phenology mismatch.

Conclusions and Implications for Future Research and Implementation

We met our objectives to quantify the effects of phenological mismatch on productivity and survival of American kestrels and to uncover potential behavioral adaptations to mismatch. We have shown that this widespread, generalist species is vulnerable to negative impacts of mismatch on fitness outcomes across its breeding range. Northeastern populations appear to be particularly vulnerable due to trade-offs between steep decreases in productivity with later nesting and low survival with earlier nesting. We suggest that this trade-off in the Northeast may be because of narrow nesting windows resulting from narrow, peaked resource availability and extreme, stochastic early-season weather, and could explain why Northeastern populations have not shifted phenology, despite advancing springs. Furthermore, the lack of shift, and the clear fitness consequences of increasing mismatch, could be contributing to steeply declining population trends in Northeastern populations.

This research has made important contributions to our understanding of factors underlying populations' vulnerability to impacts of climate change, and filled critical knowledge gaps about mechanisms and constraints underlying phenology shifts (or lack thereof). To identify vulnerable species, particularly those with the potential to constrain military testing and training, managers need reliable predictive models of *whether* and *how* populations may cope or adapt to environmental changes associated with non-stationary climate conditions. American kestrels proved to be a valuable model species to study these concepts. Our results suggest that *whether* populations adapt by shifting phenology can differ geographically depending on regional environmental conditions, nesting window constraints, and trade-offs between fitness components. Furthermore, *how* they adapt can differ, with some individuals or populations shifting phenology to keep pace with advancing spring, while others may alter incubation behavior to mitigate mismatch impacts. Further research is needed to determine the extent to which similar regional variation of mismatch consequences exist for other species, particularly specialist species that must closely track specific resources, and imperiled species for which fitness consequences could be particularly detrimental to their recovery. Distributions of seasonal breeding windows may help to assess mismatch vulnerability or potential for seasonal trade-offs. Eastern kestrels had very narrow and peaked nesting window compared to western kestrels (Figure 1.10). Data collection on the distribution of clutch initiation dates for DoD species of concern could be an important first step toward identifying species that have constraining selection on nesting timing and may indicate seasonal trade-offs. The importance of parallel

declines in seasonal productivity and survival compared to seasonal trade-offs on population resilience is discussed in Chapter 3.

Literature Cited

Albright, T. P., Pidgeon, A. M., Rittenhouse, C. D., Clayton, M. K., Wardlow, B. D., Flather, C. H., ... & Radeloff, V. C. (2010). Combined effects of heat waves and droughts on avian communities across the conterminous United States. *Ecosphere*, *1*(5), 1-22.

Allstadt, A. J., Vavrus, S. J., Heglund, P. J., Pidgeon, A. M., Thogmartin, W. E., & Radeloff, V. C. (2015). Spring plant phenology and false springs in the conterminous US during the 21st century. *Environmental Research Letters*, *10*(10), 104008.

Anderson, D., & Burnham, K. (2004). Model selection and multi-model inference. *Second. NY: Springer-Verlag*, *63*(2020), 10.

Anderson, A. M., Novak, S. J., Smith, J. F., Steenhof, K., & Heath, J. A. (2016). Nesting phenology, mate choice, and genetic divergence within a partially migratory population of American Kestrels. *The Auk: Ornithological Advances*, *133*(1), 99-109.

Arnold, T. W. (2010). Uninformative parameters and model selection using Akaike's Information Criterion. *The Journal of Wildlife Management*, *74*(6), 1175-1178.

Bastianelli, O., Charmantier, A., Biard, C., Bonamour, S., Teplitsky, C., & Robert, A. (2021). Is earlier reproduction associated with higher or lower survival? Antagonistic results between individual and population scales in the blue tit. *bioRxiv*.

Both, C., Artemyev, A. V., Blaauw, B., Cowie, R. J., Dekhuijzen, A. J., Eeva, T., ... & Visser, M. E. (2004). Large–scale geographical variation confirms that climate change causes birds to lay earlier. *Proceedings of the Royal Society of London. Series B: Biological Sciences*, *271*(1549), 1657-1662.

Both, C., & Visser, M. E. (2005). The effect of climate change on the correlation between avian life-history traits. *Global Change Biology*, *11*(10), 1606-1613.

Both, C., Van Turnhout, C. A., Bijlsma, R. G., Siepel, H., Van Strien, A. J., & Foppen, R. P. (2010). Avian population consequences of climate change are most severe for long-distance migrants in seasonal habitats. *Proceedings of the Royal Society B: Biological Sciences*, *277*(1685), 1259-1266.

Bowers, E. K., Grindstaff, J. L., Soukup, S. S., Drilling, N. E., Eckerle, K. P., Sakaluk, S. K., & Thompson, C. F. (2016). Spring temperatures influence selection on breeding date and the potential for phenological mismatch in a migratory bird. *Ecology*, *97*(10), 2880-2891.

Brooks, M. E., Kristensen, K., Van Benthem, K. J., Magnusson, A., Berg, C. W., Nielsen, A., ... & Bolker, B. M. (2017). glmmTMB balances speed and flexibility among packages for zero-inflated generalized linear mixed modeling. *The R Journal*, *9*(2), 378-400.

Callery, K. R., Smallwood, J. A., Hunt, A. R., Snyder, E. R., & Heath, J. A. (2022). Seasonal trends in adult apparent survival and reproductive trade-offs reveal potential constraints to earlier nesting in a migratory bird. *Oecologia*, *199*(1), 91-102.

Christiansen, D. E., Markstrom, S. L., & Hay, L. E. (2011). Impacts of climate change on the growing season in the United States. *Earth Interactions*, *15*(33), 1-17.

Clark, A. B., & Wilson, D. S. (1981). Avian breeding adaptations: hatching asynchrony, brood reduction, and nest failure. *The Quarterly Review of Biology*, *56*(3), 253-277.

Cohen, J., Pfeiffer, K., & Francis, J. A. (2018). Warm Arctic episodes linked with increased frequency of extreme winter weather in the United States. *Nature Communications*, *9*(1), 1-12.

Dawson, R. D., & Bortolotti, G. R. (2000). Reproductive success of American kestrels: the role of prey abundance and weather. *The Condor*, *102*(4), 814-822.
Del Corso, M. (2016). Warmer Temperatures on American Kestrel (*Falco sparverius*) Breeding Grounds Associated with Earlier Laying and Successful Reproduction. Master thesis, Department of Biology, Montclair State University, Montclair, New Jersey, USA.
Dushoff, J., Kain, M. P., & Bolker, B. M. (2019). I can see clearly now: reinterpreting statistical significance. *Methods in Ecology and Evolution*, *10*(6), 756-759.
Easterling, D. R. (2002). Recent changes in frost days and the frost-free season in the United States. *Bulletin of the American Meteorological Society*, *83*(9), 1327-1332.
Eastman, J. R., Sangermano, F., Machado, E. A., Rogan, J., & Anyamba, A. (2013). Global trends in seasonality of normalized difference vegetation index (NDVI), 1982–2011. *Remote Sensing*, *5*(10), 4799-4818.
Ellwood, E. R., Temple, S. A., Primack, R. B., Bradley, N. L., & Davis, C. C. (2013). Record-breaking early flowering in the eastern United States. *PloS one*, *8*(1), e53788.
Garcia-Heras, M. S., Arroyo, B., Mougeot, F., Amar, A., & Simmons, R. E. (2016). Does timing of breeding matter less where the grass is greener? Seasonal declines in breeding performance differ between regions in an endangered endemic raptor. *Nature Conservation, 15*, 23–45.
Gimenez, O., Lebreton, J. D., Choquet, R., & Pradel, R. (2018). R2ucare: An R package to perform goodness-of-fit tests for capture-recapture models. *bioRxiv*, 192468.
Golet, G. H., Irons, D. B., & Estes, J. A. (1998). Survival costs of chick rearing in black-legged kittiwakes. *Journal of Animal Ecology*, *67*(5), 827-841.
Goodenough, A. E., Hart, A. G., & Stafford, R. (2010). Is adjustment of breeding phenology keeping pace with the need for change? Linking observed response in woodland birds to changes in temperature and selection pressure. *Climatic Change*, *102*(3), 687-697.
Gorelick, N., Hancher, M., Dixon, M., Ilyushchenko, S., Thau, D., & Moore, R. (2017). Google Earth Engine: Planetary-scale geospatial analysis for everyone. *Remote Sensing of Environment*, *202*, 18-27.
Griggs GR, Steenhof K (1993) Photographic guide for aging nestling American kestrels. USDI Bureau of Land Management Raptor Research Technical Assistance Center, Boise, Idaho, USA.
Hartig, F. (2020). DHARMa: residual diagnostics for hierarchical (multi-level/mixed) regression models. *R Package Version 0.3*, *3*.
Heath, J. A., Steenhof, K., & Foster, M. A. (2012). Shorter migration distances associated with higher winter temperatures suggest a mechanism for advancing nesting phenology of American kestrels *Falco sparverius*. *Journal of Avian Biology*, *43*(4), 376-384.
Huang, H., Winter, J. M., Osterberg, E. C., Horton, R. M., & Beckage, B. (2017). Total and extreme precipitation changes over the northeastern United States. *Journal of Hydrometeorology*, *18*(6), 1783-1798.
Hurlbert, A. H., & Liang, Z. (2012). Spatiotemporal variation in avian migration phenology: citizen science reveals effects of climate change. *PloS One*, *7*(2), e31662.
Irons, R. D., Harding Scurr, A., Rose, A. P., Hagelin, J. C., Blake, T., & Doak, D. F. (2017). Wind and rain are the primary climate factors driving changing phenology of an aerial insectivore. *Proceedings of the Royal Society B: Biological Sciences*, *284*(1853), 20170412.

Izquierdo-Verdiguier, E., Zurita-Milla, R., Ault, T. R., & Schwartz, M. D. (2018). Development and analysis of spring plant phenology products: 36 years of 1-km grids over the conterminous US. *Agricultural and Forest Meteorology*, *262*, 34-41.

Kelly, J. F., Horton, K. G., Stepanian, P. M., de Beurs, K. M., Fagin, T., Bridge, E. S., & Chilson, P. B. (2016). Novel measures of continental-scale avian migration phenology related to proximate environmental cues. *Ecosphere*, *7*(9), e01434.

Klaassen, R. H., Hake, M., Strandberg, R., Koks, B. J., Trierweiler, C., Exo, K. M., ... & Alerstam, T. (2014). When and where does mortality occur in migratory birds? Direct evidence from long-term satellite tracking of raptors. *Journal of Animal Ecology*, *83*(1), 176-184.

Kunkel, K. E., Easterling, D. R., Hubbard, K., & Redmond, K. (2004). Temporal variations in frost-free season in the United States: 1895–2000. *Geophysical Research Letters*, *31*(3).

Kunkel, K. E., Karl, T. R., Easterling, D. R., Redmond, K., Young, J., Yin, X., & Hennon, P. (2013). Probable maximum precipitation and climate change. *Geophysical Research Letters*, *40*(7), 1402-1408.

Laake, J., & Rexstad, E. (2008). RMark–an alternative approach to building linear models in MARK. *Program MARK: a gentle introduction*, C1-C113.

Lebreton, J. D., & Cefe, R. P. (2002). Multistate recapture models: modelling incomplete individual histories. *Journal of Applied Statistics*, *29*(1-4), 353-369.

Lof, M. E., Reed, T. E., McNamara, J. M., & Visser, M. E. (2012). Timing in a fluctuating environment: environmental variability and asymmetric fitness curves can lead to adaptively mismatched avian reproduction. *Proceedings of the Royal Society B: Biological Sciences*, *279*(1741), 3161-3169.

Mainwaring, M. C., Lucy, D., & Hartley, I. R. (2014). Hatching asynchrony decreases the magnitude of parental care in domesticated zebra finches: empirical support for the peak load reduction hypothesis. *Ethology*, *120*(6), 577-585.

Meijer, T., Nienaber, U., Langer, U., & Trillmich, F. (1999). Temperature and timing of egg-laying of European starlings. *The Condor*, *101*(1), 124-132.

Møller, A. P., Rubolini, D., & Lehikoinen, E. (2008). Populations of migratory bird species that did not show a phenological response to climate change are declining. *Proceedings of the National Academy of Sciences*, *105*(42), 16195-16200.

Paprocki, N., Heath, J. A., & Novak, S. J. (2014). Regional distribution shifts help explain local changes in wintering raptor abundance: Implications for interpreting population trends. *PLoS One*, *9*(1), e86814.

Peterson, T. C., Heim Jr, R. R., Hirsch, R., Kaiser, D. P., Brooks, H., Diffenbaugh, N. S., ... & Wuebbles, D. (2013). Monitoring and understanding changes in heat waves, cold waves, floods, and droughts in the United States: state of knowledge. *Bulletin of the American Meteorological Society*, *94*(6), 821-834.

Powers, B. F., Winiarski, J. M., Requena-Mullor, J. M., & Heath, J. A. (2021). Intra-specific variation in migration phenology of American Kestrels (*Falco sparverius*) in response to spring temperatures. *Ibis*, *163*(4), 1448-1456.

R Core Team. (2021). R: A language and environment for statistical computing. *R Foundation for Statistical Computing.* Vienna, Austria. https://www.R- project.org/

Reed, T. E., Jenouvrier, S., & Visser, M. E. (2013). Phenological mismatch strongly affects individual fitness but not population demography in a woodland passerine. *Journal of Animal Ecology*, *82*(1), 131-144.

Root, T. (1988). Energy constraints on avian distributions and abundances. *Ecology*, *69*(2), 330-339.

Rosemartin, A. H., Denny, E. G., Weltzin, J. F., Lee Marsh, R., Wilson, B. E., Mehdipoor, H., ... & Schwartz, M. D. (2015). Lilac and honeysuckle phenology data 1956–2014. *Scientific Data*, *2*(1), 1-8.

Rubolini, D., Saino, N., & Møller, A. P. (2010). Migratory behaviour constrains the phenological response of birds to climate change. *Climate Research*, *42*(1), 45-55.

Ruegg, K. C., Brinkmeyer, M., Bossu, C. M., Bay, R. A., Anderson, E. C., Boal, C. W., ... & Heath, J. A. (2021). The American Kestrel (*Falco sparverius*) genoscape: Implications for monitoring, management, and subspecies boundaries. *The Auk*, *138*(2), ukaa051.

Saino, N., Ambrosini, R., Albetti, B., Caprioli, M., De Giorgio, B., Gatti, E., ... & Rubolini, D. (2017). Migration phenology and breeding success are predicted by methylation of a photoperiodic gene in the barn swallow. *Scientific Reports*, *7*(1), 1-10.

Samplonius, J. M., Bartošová, L., Burgess, M. D., Bushuev, A. V., Eeva, T., Ivankina, E. V., ... & Both, C. (2018). Phenological sensitivity to climate change is higher in resident than in migrant bird populations among European cavity breeders. *Global Change Biology*, *24*(8), 3780-3790.

Schwartz, M. D., Ahas, R., & Aasa, A. (2006). Onset of spring starting earlier across the Northern Hemisphere. *Global Change Biology*, *12*(2), 343-351.

Schwartz, M. D., & Hanes, J. M. (2010). Intercomparing multiple measures of the onset of spring in eastern North America. *International Journal of Climatology*, *30*(11), 1614-1626.

Schwarz, C. J., Schweigert, J. F., & Arnason, A. N. (1993). Estimating migration rates using tag-recovery data. *Biometrics*, 177-193.

Shave, A., Garroway, C. J., Siegrist, J., & Fraser, K. C. (2019). Timing to temperature: egg-laying dates respond to temperature and are under stronger selection at northern latitudes. *Ecosphere*, *10*(12), e02974.

Shipley, J. R., Twining, C. W., Taff, C. C., Vitousek, M. N., Flack, A., & Winkler, D. W. (2020). Birds advancing lay dates with warming springs face greater risk of chick mortality. *Proceedings of the National Academy of Sciences*, *117*(41), 25590-25594.

Smallwood, J. A., Causey, M. F., Mossop, D. H., Klucsarits, J. R., Robertson, B., Robertson, S., ... & Boyd, K. (2009). Why are American Kestrel (*Falco sparverius*) populations declining in North America? Evidence from nest-box programs. *Journal of Raptor Research*, *43*(4), 274-282.

Smallwood, J. A. (2016). Effects of researcher-induced disturbance on American Kestrels breeding in nest boxes in northwestern New Jersey. *Journal of Raptor Research*, *50*(1), 54-59.

Smallwood, J. A., Bird, D. M. (2020). American Kestrel (*Falco sparverius*), version 10. In: Poole AF, Gill FB (eds) Birds of the World. *Cornell Lab of Ornithology*, Ithaca. https://doi.org/10. 2173/bow.amekes. 01

Smith, S. H., Steenhof, K., McClure, C. J., & Heath, J. A. (2017). Earlier nesting by generalist predatory bird is associated with human responses to climate change. *Journal of Animal Ecology*, *86*(1), 98-107.

Sohrabi, M. M., Ryu, J. H., Abatzoglou, J., & Tracy, J. (2013). Climate extreme and its linkage to regional drought over Idaho, USA. *Natural Hazards*, *65*(1), 653-681.

Steenhof, K., & Heath, J. A. (2009). American Kestrel reproduction: evidence for the selection hypothesis and the role of dispersal. *Ibis*, *151*(3), 493-501.
Steenhof, K., & Heath, J. A. (2013). Local recruitment and natal dispersal distances of American kestrels. *The Condor*, *115*(3), 584-592.
Steenhof, K., & Peterson, B. E. (2009). American Kestrel reproduction in southwestern Idaho: annual variation and long-term trends. *Journal of Raptor Research*, *43*(4), 283-290.
Stevenson, I. R., & Bryant, D. M. (2000). Climate change and constraints on breeding. *Nature*, *406*(6794), 366-367.
Stutchbury, B. J., Gow, E. A., Done, T., MacPherson, M., Fox, J. W., & Afanasyev, V. (2011). Effects of post-breeding moult and energetic condition on timing of songbird migration into the tropics. *Proceedings of the Royal Society B: Biological Sciences*, *278*(1702), 131-137.
Taylor, J., Nicoll, M. A., Black, E., Wainwright, C. M., Jones, C. G., Tatayah, V., ... & Norris, K. (2021). Phenological tracking of a seasonal climate window in a recovering tropical island bird species. *Climatic Change*, *164*(3), 1-19.
Thornton, P. E., Thornton, M., Mayer, B. W., Wei, Y., Devarakonda, R., Vose, R. S., Cook, R. B. (2018). Daymet: Daily Surface Weather Data on a 1-km Grid for North America, Version 3. *ORNL DAAC*, Oak Ridge, Tennessee, USA.
Visser, M. E., Adriaensen, F., van Balen, J. H., Blondel J., Dhondt A. A., van Dongen, S., du Feu, C., Ivankina, E. V., Kerimov, A. B., de Laet, J., Matthysen, E., McCleery, R., Orell, M., and Thomson, D. L. (2003) Variable responses to large-scale climate change in European Parus populations. *Proceedings of the Royal Society of London. Series B: Biological Sciences*, *270*(1513), 367-372.
Visser, M. E., te Marvelde, L., & Lof, M. E. (2012). Adaptive phenological mismatches of birds and their food in a warming world. *Journal of Ornithology*, *153*(1), 75-84.
Visser, M. E., & Gienapp, P. (2019). Evolutionary and demographic consequences of phenological mismatches. *Nature Ecology & Evolution*, *3*(6), 879-885.
White, G. C., & Burnham, K. P. (1999). Program MARK: survival estimation from populations of marked animals. *Bird Study*, *46*(sup1), S120-S139.
Wiebe, K. L., & Bortolotti, G. R. (1994). Food supply and hatching spans of birds: energy constraints or facultative manipulation. *Ecology*, *75*(3), 813-823.
Woodworth, B. K., Wheelwright, N. T., Newman, A. E., Schaub, M., & Norris, D. R. (2017). Winter temperatures limit population growth rate of a migratory songbird. *Nature Communications*, *8*(1), 1-9.
Zuckerberg, B., Bonter, D. N., Hochachka, W. M., Koenig, W. D., DeGaetano, A. T., & Dickinson, J. L. (2011). Climatic constraints on wintering bird distributions are modified by urbanization and weather. *Journal of Animal Ecology*, *80*(2), 403-413.
Zurita-Milla, R., Goncalves, R., Izquierdo-Verdiguier, E., & Ostermann, F. O. (2017). Exploring vegetation phenology at continental scales: linking temperature-based indices and land surface phenological metrics. In *Proceedings of the 2017 Conference on Big Data from Space, Toulouse, France* (pp. 28-30).

Chapter 2. Genetic correlates of avian phenology

Julie A. Heath, Christen M. Bossu, Stephanie J. Galla, Barbara Helm, Anjolene R. Hunt, Richard Fischer, M. David Oleyar, Kristen C. Ruegg

Abstract

Changes in phenology are one of the most predominant, and consequential, avian responses to climate change. Extensive within- and between- species variation in the rate of phenology shifts suggest that exogenous and endogenous (i.e., genetic) mechanisms underlie changes in phenology. Unfortunately, the genetic basis of biological timekeeping is poorly understood. Specifically, critical knowledge gaps remain about the underlying genetic factors that affect the potential for populations to undergo phenological shifts. In this chapter, we estimated the heritability of the timing of clutch initiation for American kestrels (*Falco sparverius*) – our focal study species, identified genetic variants associated with different phenological phenotypes (i.e., chronotypes), explored associations between genetic variants and the timing of reproduction and migration, and compared genetic composition and diversity between populations showing different phenological responses to climate change. We used long-term mark and recapture data from a study site in southern Idaho to estimate the heritability of American kestrel clutch initiation and found that clutch initiation was highly heritable ($h^2 = 0.42$), supporting the hypothesis of underlying genetic mechanisms. We broadly sampled American kestrels across their North American breeding range and identified several single-nucleotide polymorphisms (SNPs) within candidate genes associated with circannual rhythms; specifically, variants were within genes associated with metabolic and light input pathways that modulate the biological pacemaker. These genetic variants showed both multi-gene and single-gene effects on the timing of clutch initiation and on the timing of migration passage. Interestingly, genotype-phenology relationships were consistent across phases of the annual cycle. For example, genotypes associated with early clutch initiation were also associated with early migration passage. Finally, principal component scores that represented multi-gene effects and heterozygosity at individual loci differed between western kestrels that show phenological shifts (i.e., are nesting earlier) and eastern kestrels that do not show evidence of phenology shifts. These results support the hypothesis that phenology is a heritable trait governed by genetics. Furthermore, diversity within candidate genes may impact the adaptive capacity of populations to respond to climate-driven changes in spring phenology and may increase population vulnerability to phenological mismatch.

Objectives

Here, we sought to better understand the role of genetic mechanisms in limiting (or facilitating) phenological shifts. We investigated variants in candidate genes related to the circadian/circannual rhythm oscillator because these genes have been identified as potentially important to the timing of reproduction and migration across organisms (Fitzpatrick et al. 2005, Johnsen et al. 2007, O'Malley et al. 2008, Ruegg et al. 2014, Bourret and Garant 2015). Our objectives were to: 1) estimate heritability in the timing of clutch initiation, 2) identify genetic variants associated with the timing of clutch initiation and migration, and 3) compare composition and diversity in candidate genes between populations showing different phenological responses to climate change. We addressed the following hypotheses:

H1: Genetic mechanisms underlie phenology

H2: Genetic variation in candidate genes modulates individual responses to environmental conditions resulting in different timing phenotypes.
H3: Reduced genetic diversity at clock-linked genes can limit the adaptive potential of populations

We predicted that if phenology had underlying genetic mechanisms, then clutch initiation dates would be heritable and genetic variation would result in individuals that are relatively early or late within each season. Also, we predicted that eastern American kestrels that do not show phenology shifts would have lower genetic diversity in candidate genes than western American kestrels that show evidence of phenology shifts.

This research addresses the following SERDP SON 17-01:
Increase understanding of specific genetic factors. We identified polymorphisms at candidate genes that are linked to circadian rhythms, demonstrated their association to the timing of clutch initiation and migration, and showed differences in genetic composition and diversity across populations responding differently to climate change.

Background

Changes in phenology—the timing of life cycle events—are one of the most notable responses to climate change (Thackeray et al. 2016). In particular, birds are nesting earlier to synchronize energetically expensive reproduction with peaks in food resources that are advancing with earlier springs (Both et al. 2004) and to maintain thermal niches (Socolar et al. 2017). Changes in nesting phenology are not homogenous, however, as many populations have not shifted clutch initiation dates to keep pace with advancing springs (Visser and Both 2005). Lack of phenology shifts can lead to temporal decoupling of reproduction and food resources (i.e., phenological mismatch) that affect nesting productivity (Visser et al. 2006), adult survival (Chapter 1), and population viability (Møller et al. 2008). Therefore, understanding the mechanisms underlying phenology shifts is important to identify populations that may be vulnerable to phenological mismatch. For Department of Defense (DoD) managers, it may be particularly important to determine whether Mission Sensitive Species (MSS - those which have the potential to constrain military missions if federally listed under the Endangered Species Act) have the intrinsic capacity to shift phenology, because this could impact potential management strategies and priorities.

Shifts in phenology may be the result of phenotypic plasticity, adaptive evolution, or both (Hoffmann and Sgrò 2011). The timing of clutch initiation (Sheldon et al. 2003, Postma 2014) and plasticity in timing (Nussey et al. 2005) are heritable traits, suggesting an underlying role of genetics. Further, the timing of behavioral and physiological changes associated with breeding and migration are partly genetically hardwired via circannual clocks with multiple environmental input pathways (Gwinner 1996, Visser et al. 2010, Åkesson and Helm 2020). Polymorphisms in genes that underlie daily (i.e., circadian) and yearly (i.e., circannual) rhythms create distinct early or late circannual phenotypes (hereafter: chronotypes, Liedvogel et al. 2009, Saino et al. 2019) that are likely to affect timing across the annual cycle. For example, methylation (Saino et al. 2019) of clock genes, or length of short tandem repeats (STR) in the poly-Q region (Liedvogel et al. 2009, Caprioli et al. 2012) of the *clock* gene correlates with clutch initiation date in some birds (reviewed in Bourret and Garent 2015). Further, the length of the clock poly-Q allele positively correlates with the activation of the hypothalamic-pituitary-gonad axis responsible for the production of hormones that support reproduction (Zhang et al. 2017). Finally, the length

polymorphisms in *clock* and *npas2* genes can interact with environmental conditions (e.g. breeding density) to affect clutch initiation dates (Bourret and Garent 2015). The prevalence of particular chronotypes and their underlying genetic mechanisms can vary spatially (Johnsen et al. 2007) and within populations (Bossu et al. 2022). This variation can lead to the differential capacity for phenological responses and resilience to climate change if chronotypes are heritable and favored by selection (Nussey et al. 2005, Helm et al. 2019).

Candidate genes that underlie chronotypes may exist in the multiple pacemakers of the circadian system that receive and decode photoperiodic information (Cassone 2014, Stevenson and Kumar 2017). Circadian rhythms are generated by interlocking transcription-translation feedback loops and post-translational modification, driven by canonical clock genes (Bell-Pedersen et al. 2005, Mohawk et al. 2012, Cassone 2014), hereafter called "core" clock genes. The circadian system is mainly entrained by light, and there is some evidence from mammal research that temperature and stress sensors may also play a pivotal modulating role (Albrecht 2012, Ribas-Latre and Eckel-Mahan 2016). Thus, core clock genes are regulated by "clock-linked" genes involved in receiving and decoding photoperiodic and metabolic environmental cues. The absence of decisive consistent linkages between genetic variation in clock genes and phenological variability in birds may the result of a focus on core clock genes rather than genes that entrain and modulate the clock pathway, limitations in detection methods that focus only on highly significant outlier loci, thus ignoring genes of small effect or both (Lundberg et al. 2013, Fudickar et al. 2016, Franchini et al. 2017, Towes et al. 2019). Further, studies to date have investigated genetic correlates of phenology through contrasting individuals from different seasonal environments or with different migration strategies. We sought to identify phenology variants both within and across populations.

American kestrels are an ideal model species to study genetic mechanisms of phenology patterns. Spatially and genetically distinct (Ruegg et al. 2021) populations in eastern and western North America show differences in phenological responses to climate change (Chapter 1), fitness consequences of phenological mismatch (Chapter 1), and population trends (Smallwood et al. 2009), creating a unique opportunity for comparative studies. Western populations, which appear to be stable (Steenhof and Peterson 2009, McClure et al. 2017), show evidence of earlier clutch initiation (Heath et al. 2012, Smith et al. 2017) and breeding season declines in both reproduction and survival suggest these populations are well-suited to respond to directional selection from climate-driven advances in spring (Chapter 1). Conversely, eastern populations, which are steeply declining (Smallwood et al. 2009, McClure et al. 2017), do not show evidence of clutch initiation shifts and earlier nesters appear to experience a trade-off between higher productivity and lower adult survival (Chapter 1). Finally, kestrels exhibit different migratory phenotypes across the North American range, from long-distance migrants in the north to short-distance migrants and non-migrant residents in the south (Smallwood and Bird 2020) providing the opportunity for comparisons between populations with distinct migratory strategies

We took an integrative approach to identify the genetic basis of intraspecific variation in seasonal timing that reflects the polygenic nature of chronotypes. First, we estimated the heritability of clutch initiation dates. Then, we analyzed a high-density restriction-site associated (RAD)-sequencing dataset using an F_{ST}-based analysis with relaxed detection thresholds to identify highly polymorphic core clock and clock-linked genes. We hypothesized that if phenology is controlled by many loci of small effect, then relaxed detection thresholds will identify potential candidate loci that may otherwise be missed using stringent thresholds. Based on the results of this analysis, we developed a suite of genetic assays to test the role of candidate

loci in phenology of American kestrel clutch initiation and migration. We hypothesized that if genetic variation within core clock or clock-linked genes was important to regulating reproductive or migratory timing in American kestrels, then we would find significant correlations between allele frequencies at these loci and clutch initiation dates, and correlations between allele frequencies and migration passage dates. Finally, we compared regional differences in allele frequencies and heterozygosity in American kestrels to better understand the mechanisms underlying different patterns in phenology shifts between eastern and western populations.

Materials and Methods

Heritability

We conducted heritability analyses using clutch initiation data collected from a long-term nest monitoring program in southwestern Idaho. From 1992 to 2019 (except for 2007) we visited boxes every 7 – 21 days starting in March to determine kestrel occupancy and clutch size. We estimated clutch initiation dates by counting backward from the number of eggs in the box upon nest discovery [day of nest discovery - (number of eggs in the nest box upon nest discovery * 2)]. If a pair was found with a complete clutch of eggs (5 or more), we back-calculated clutch initiation from the date of the first egg hatching by subtracting 30 days plus (number of eggs * 2) days from the hatch date (Anderson et al. 2016). We captured and individually marked adults and nestlings with a USGS aluminum band and sexed individuals based on plumage.

We used an 'animal' model to estimate clutch initiation heritability (R package *MCMCglmm*, Hadfield 2010). Unlike other methods of estimating heritability, animal models can cope with missing data in the pedigree and use relationships beyond parents and offspring (e.g., siblings, half-siblings, and cousins; Postma and Charmantier 2007, Wilson et al. 2010). We used data from both male and female individuals because the timing of clutch initiation depends on both sexes (Smallwood and Bird 2020). We log-transformed clutch initiation dates to meet normality assumptions. We used priors following de Villemereuil et al. (2018), with random effect parameters $V = 1$, $nu = 1$, $alpha.mu = 0$, and $alpha.V = 1000$, and residual variance parameters set for $V=1$ and $nu=0.02$. We included a numerical year variable as a fixed effect because nesting phenology is advancing in this population (Smith et al. 2017). We included bird identity as a random effect to account for repeated measures over years. The final model was run for 500,000 iterations, with a thinning interval of 50 and a burn-in of 80,000 to improve trace and ensure sufficient sampling size (i.e., >1000) for all parameters. We used the R package *coda* (Plummer et al. 2006) to assess convergence, using the Heidelberger and Welch test (Heidelberger and Welch 1983). We calculated estimates of heritability using the posterior mode of the formula $h^2 = V_A / V_P$, where h^2 is heritability, V_A is the additive genetic variance, and V_P is the sum of random effects and residual variance.

We ran post-hoc power analysis (using methods by de Villemereuil et al. 2018) simulation of our heritability model to determine whether our estimate was biased because of a low sample size. We generated analyses with different parameters for V_A (additive genetic variance), V_{PE} (permanent environmental variance from repeated measures), and V_R (residual variance) to simulate heritability of clutch initiation at 0.42 (posterior mode for our heritability analysis), 0.25, and 0.1. Simulations used average log clutch initiation date and variance of clutch initiation date (*mu*) and pedigree data for American kestrels. For each heritability power analysis, we ran 100 iterations of MCMCglmm using the same prior, number of iterations,

thinning interval, and burn-in as the original model. We calculated the average posterior mode and compared it to the expected heritability to find bias.

Sample collection, DNA extraction, and variant discovery

We collaborated with several non-profit organizations, state agencies, university researchers, and citizen scientists to sample 197 unrelated breeding adult or nestling American kestrels from eight sites throughout the USA and Canadian breeding range in 2015 and 2016. These sites were within the range of fully migratory and partially migratory American kestrels and 2 sites (Texas and Florida) fell within the range of resident (i.e., non-migratory) American kestrels (Ruegg et al. 2021). We extracted the DNA from the resulting samples using Qiagen DNeasy Blood and Tissue Kits and then used RAD DNA sequencing (Ali et al. 2016) to scan the genome for signals of selection across the breeding range. RAD-sequences were aligned to an assembly of the American kestrel genome (Ruegg et al. 2021) and a total of 72,263 single-nucleotide polymorphisms (SNPs) were identified after quality filtering.

We used F_{ST}-based analyses with low detection thresholds to identify candidate loci associated with timing and migratory behavior. We created custom R scripts to identify loci with F_{ST} estimates that fell within a relaxed 90th percentile F_{ST} outlier threshold between the resident and migratory populations (i.e., Florida and Texas vs. all other populations). We used this contrast because of known phenology (i.e., clutch initiation is earlier in resident than migrant individuals, Anderson et al. 2016) and migratory differences between these groups. The F_{ST} threshold was to identify many polymorphic loci of potential small effect that were linked to timing and migratory behavior. For one of our sampling sites (i.e., California) it was unclear whether individuals were residents, migrants or partial migrants and to avoid potential confusion this population was excluded from the F_{ST} analysis.

We designed Fluidigm SNPtype assays and screened additional breeding and migrating American kestrels that were independent of the RAD-seq analyses (above). Specifically, we used the R package snps2assays (Anderson et al. 2015) to evaluate the efficacy of designing assays for candidate loci. We considered the assays designable if GC content was less than 0.65, there were no insertions or deletions (indels) within 30bp of the target variant, and there were no additional variants within 20bp of the targeted variable site. We filtered out assays with primers that mapped to multiple locations in the genome (Li and Durbin 2009), resulting in assays for ten loci in ten candidate genes. We used the Fluidigm assays to genotype the ten candidate genes for the clutch initiation analysis and nine of the ten candidate genes for the migration analysis. We assayed one additional locus for the clutch initiation analysis (i.e., *mybbpla*) because it met F_{ST} selection criteria and we overcame challenges with developing an assay of this gene that we had during the migration genotyping.

Genetic correlates of clutch initiation

We worked with a team of collaborators to collect blood and feather samples from a single American kestrel nestling per brood at field sites throughout North America from 1998 – 2020 (Figure 1.2). We collected samples from nestlings instead of adults because nestling genotypes reflect their parents' genotype and nestlings are easier to capture and sample across a wide geographic range. Blood samples were stored in -80˚C freezers until analysis. Feathers (collected from 2016 – 2020) were stored in paper envelopes at room temperature until analysis. For each genetic sample, we collected information about the location and timing of clutch initiation. We used the methods described above (see Heritability) for estimating clutch initiation

dates or we subtracted the age of the nestling (based on plumage), 30 days for incubation, and the clutch size * 2 from the sampling date.

We grouped individual samples separated by < 150 km into spatial clusters to account for potentially related samples (Figure 2.1). We used the 150 km cut-off because 90% of kestrel dispersal distances are < 150 km (McCaslin et al. 2020). Cluster identity was used to group individuals for heterozygous and allele frequency analyses and as a random factor in mixed models to account for potential non-independence of samples. In addition to genetic samples, we estimated the start of the growing season using the extended spring index (SI-x) to account for spatiotemporal patterns in environmental cues (i.e., the timing of spring) in models of clutch initiation. Further, SI-x dates are positively correlated with the timing of American kestrel clutch initiation (Chapter 1). We used Google Earth Engine code modified from Izquierdo-Verdiguier et al. (2018) to extract SI-x dates derived from Daymet climate datasets (Thornton et al. 2018) at the latitude and longitude of each individual nest.

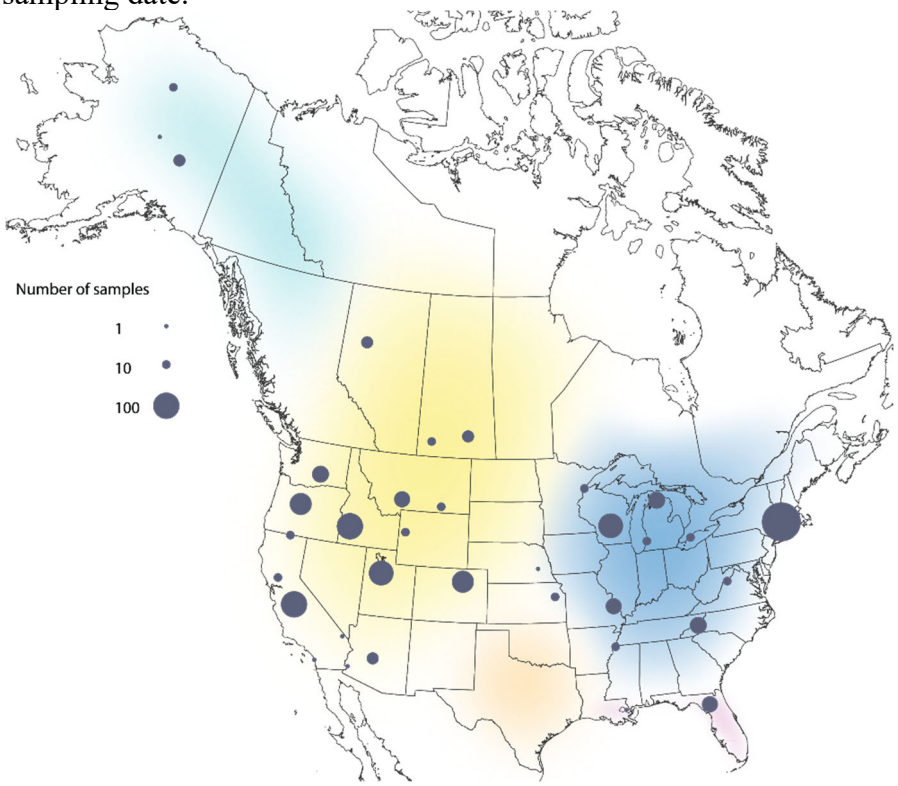

Figure 2.1 A map of locations where American kestrel genetic samples and nesting phenology data were collected. Samples collected within 150 km of each other were grouped to clusters (represented by points). Point size represents the number of samples per cluster. Shading on the map represents assignments to genetically distinct groups described in Ruegg et al. (2021).

We used an ordinal principal component (PC) analysis using the R package *gifi* (Mair et al. 2019) to examine covariance between genes and generated PC scores for each individual from the top three axes. We tested whether multi-gene complexes were associated with the timing of clutch initiation using scores for $PC_{nesting}$ 1 and $PC_{nesting}$ 2 with a linear mixed model. All models included an environmental covariate (SI-x), and a random effect of cluster identity. In addition to additive effects we looked at interactions between $PC_{nesting}$ scores and SI-x. We built a second linear mixed model to examine associations between individual genes and clutch initiation. We included an additive effect of SI-x to account for variation in nesting dates across the sample sites and a random effect of cluster identity. The SI-x variable was centered and scaled before analyses.

Genetic correlates of migration timing

For the migration study, we collected feather samples from a fall migration station near Boise, Idaho, and recorded the day of capture, sex of the bird, and band number. We also collected feather samples from breeding American kestrels across a latitudinal gradient in western North America to ensure that temporal patterns in migrant genotypes were not the result of the latitudinal variation. We used a multi-gene and single-gene framework, similar to the clutch initiation study, to determine whether migratory timing was associated with allele frequencies in the nine candidate genes. We used an ordinal principal component analysis using the R software package *gifi* (Mair et al. 2019) to broadly determine how the nine candidate genes covaried. We ran separate PC analyses for clutch initiation and migration timing because of the different number of loci included in each project. We used linear regression to evaluate whether migration timing (i.e., day of year when a fall migrant was captured) was associated with genetic variation as measured by $PC_{migration}$ 1 and $PC_{migration}$ 2, and included a covariate of sex to account for the potential influence of differential migration between sexes on migration timing. To investigate single gene effects, we fit linear regression models of each allele frequency of the top 4 candidate genes (i.e., those that loaded strongly on $PC_{migration}$ 1, *top1*, *peak1, phlpp1* and *cpne4*, Table S2), to migration timing as defined by the midpoint day of each week during the autumn migration period and using the lm function in the R software package. The nonlinear decline in allele frequency over autumn migration of three of the top candidate genes, *top1*, *peak1*, and *cpne4* prompted the fitting of a curved regression model, and we tested whether this linear regression polynomial model provided a better fit using a likelihood ratio test in the R package *lmtest* (Zeileis and Hothorn 2002). We examined the association between $PC_{nesting}$ 1 and nest latitude of individuals breeding across the west to test whether seasonal allele frequency trends result from different populations migrating through the migration station at different times or distinct migratory chronotypes.

Genetic differences between populations

We categorized nestling samples as "west" or "east" based on the genoscape (Ruegg et al. 2021) to compare genetic composition and diversity between breeding populations (Figure 2.1). We did not include samples between longitudes -104.40 and -97.20 to avoid areas where west and east populations may be mixing and assignment to west or east subgroups was more ambiguous. We compared $PC_{nesting}$ 1 and $PC_{nesting}$ 2 scores between western and eastern populations using a linear mixed model with the population as a predictor and cluster identity as a random effect. We estimated allele frequencies and mean heterozygosity (as per Nei 1987) for nestlings in eastern and western populations using R packages *PopGenReport* (Adamack and Gruber 2014) and *pegas* (Paradis 2010), respectively. We removed population clusters with sample sizes of less than 10 individuals to avoid bias in mean heterozygosity and allele frequencies. We compared allele frequencies and heterozygosity between western and eastern populations using a generalized linear model with a beta distribution for response variables and a categorical predictor of population.

All analyses were conducted in R (R Core Team, 2019). We used a frequentist framework to test statistical null hypotheses with *P-values*, with the exception of the heritability analysis (see above). We considered P-values < 0.05 to be statistically significant. We mention results where P-values > 0.05 and < 0.15 and the parameter estimate indicated a possible effect to avoid being overly conservative and making Type II errors. We report effect sizes and standard error, or 95% confidence intervals.

Results and Discussion

Heritability

Our pedigree contained information from 1318 nesting attempts and among these records 99 kestrels had known relationships. The 95% heritability posterior distribution for h^2 was from 0.24 – 0.53, with a h^2 posterior mode of 0.42 (h^2 SD ± 0.08, over 8400 iterations; Figure 2A.1). Heritability power analysis simulations showed that empirical heritability estimates were robust, despite the relatively small sample size used here. Simulated high heritabilities (e.g., $h^2 = 0.42$) were slightly underestimated in simulations (average posterior mode h^2 ± SD = 0.4 ± SD 0.13, over 100 simulations). Lower heritabilities were more substantially underestimated (Table 2A.1).

The timing of clutch initiation is a heritable trait for American kestrels, and the heritability estimate was high (0.42) compared to other bird species ($h^2 = 0.04 – 0.30$, Teplitsky et al. 2009, Thorley and Lord 2015), though there was substantial variation in the 95% heritability posterior distribution (range = 0.29). While the sample size for this analysis was low, power analysis simulations indicate that the pedigree was robust for providing higher heritability estimates. Previous repeatability analyses of clutch initiation dates in western American kestrels were high in males (0.37) compared to females (0.08, Anderson et al. 2016). While some suggest repeatability as an upper limit for heritability, it is important to note that these estimates were produced with different sample sizes and may be impacted by interactions between genes and the environment (Dohm 2002). Further, there is potential for heritability to be overestimated because of shared genes and shared environments, in the instance where offspring choose to breed in the same area (Postma and Charmantier 2007). Regardless, these results indicate that underlying genetics contribute to the timing of clutch initiation in American kestrels.

Variant discovery

Our F_{ST} analysis revealed 7,227 polymorphic loci in 1843 genes. A subsequent literature search identified 21 of these genes with links to different aspects of seasonal behavior. These 21 candidate genes were grouped into four major categories, including: 1) timing (circannual and circadian rhythm, including metabolic sensors and photoperiodic pathways); 2) morphological differentiation (i.e., cytoskeleton organization, muscle development, and contraction, and bone metabolism that can increase bone density and strength); 3) migratory restlessness (i.e., regulation of sleep and locomotor activity); and 4) physiology (i.e., lipid metabolism and

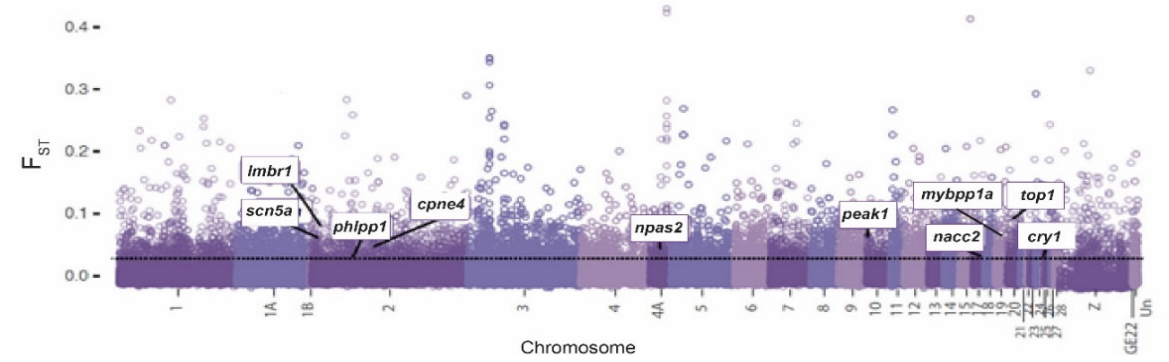

Figure 2.2 Genomic position of the ten validated candidate genes on a Manhattan plot of F_{ST} between resident populations and migrant populations of American kestrels. Candidate genes that fell within the relaxed outlier detection threshold (*e.g.* 90th percentile) and genotyped in this study are labeled. The 90th percentile is marked with a dashed line.

increased fat storage, Bossu et al. 2022). Because assay design for specific loci of interest is not always possible (see methods), we were only able to design targeted assays for loci in 10 of the 21 total genes of interest (Figure 2.2). These included: 2 core clock genes (*cry1*, *npas2*), 4 clock-linked genes (*top1*, *cpne4*, *mybpp1a,* and *phlpp1*), 2 genes linked to morphological differentiation potentially important to avian migration (*lmbr1* and *nacc2*), and the remaining 2 genes (*peak1* and *scn5a*) were known to be differentially expressed in the hypothalamus in Swainson's thrushes (*Catharus ustulatus*) during non-migratory and migratory states (Johnston et al. 2016).

Genetic correlates of clutch initiation

We genotyped 971 American kestrel nestlings at loci within 10 candidate genes associated with circannual and circadian rhythms or migratory timing of American kestrels. We sampled kestrels across North America and grouped samples into 32 spatial clusters based on the nearest neighbor distance of < 150 km (Figure 2.1).

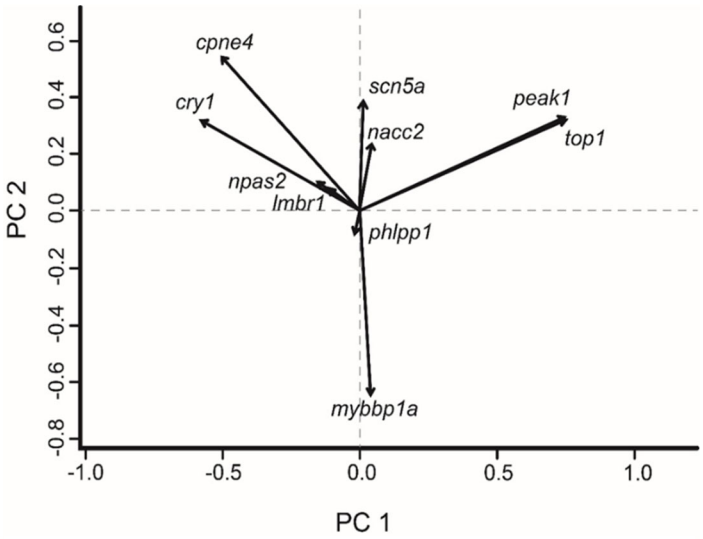

Figure 2.3 Eigenvectors of the first two principal components from an analysis of 10 clock-linked candidate genes based on 971 genetic samples collected from American kestrel nestlings. PC scores were used to study genetic correlates of the timing of clutch initiation.

An ordinal principal component analysis showed strong correlations among genotypes (Figure 2.3). The first principal component ($PC_{nesting}$ 1) accounted for 17.7% of the variance and loadings were high on *top1* and *peak1* and low on *cpne1* and *cry1* (Table 2A.2). $PC_{nesting}$ 2 accounted for 12.6% of variance and loadings on the second PC were high on *cpne4* and low on *mybbp1a* (Table 2A.2). The third explained 11.0% of the variance, respectively, but the loadings for the third $PC_{nesting}$ were high (> |0.5|) on only one gene (Table 2A.2). Therefore, we did not evaluate the relationships between $PC_{nesting}$ 3 and clutch initiation dates because those relationships would be better captured in the single-gene analysis.

American kestrels nested from 2 Mar to 13 Jun with a median clutch initiation date of 20 Apr (n = 844). There was an interaction between $PC_{nesting}$ 1 scores and the SI-x that positively correlated with clutch initiation dates ($\beta = 1.38 \pm 0.55$, $P = 0.01$, Figure 2.4a). There tended to be a negative relationship between $PC_{nesting}$ 2 scores and clutch initiation dates, but that effect was not significant ($\beta = -0.74 \pm 0.52$, $P = 0.15$, Figure 2.4b).

There was some evidence of single gene effects on clutch initiation. The *mybbp1a* ($\beta = -3.36 \pm 1.40$, $P = 0.02$) was negatively associated with clutch initiation date and *nacc2* tended to negatively correlate with clutch initiation date ($\beta = -2.07 \pm 1.26$, $P = 0.10$). Specifically, birds

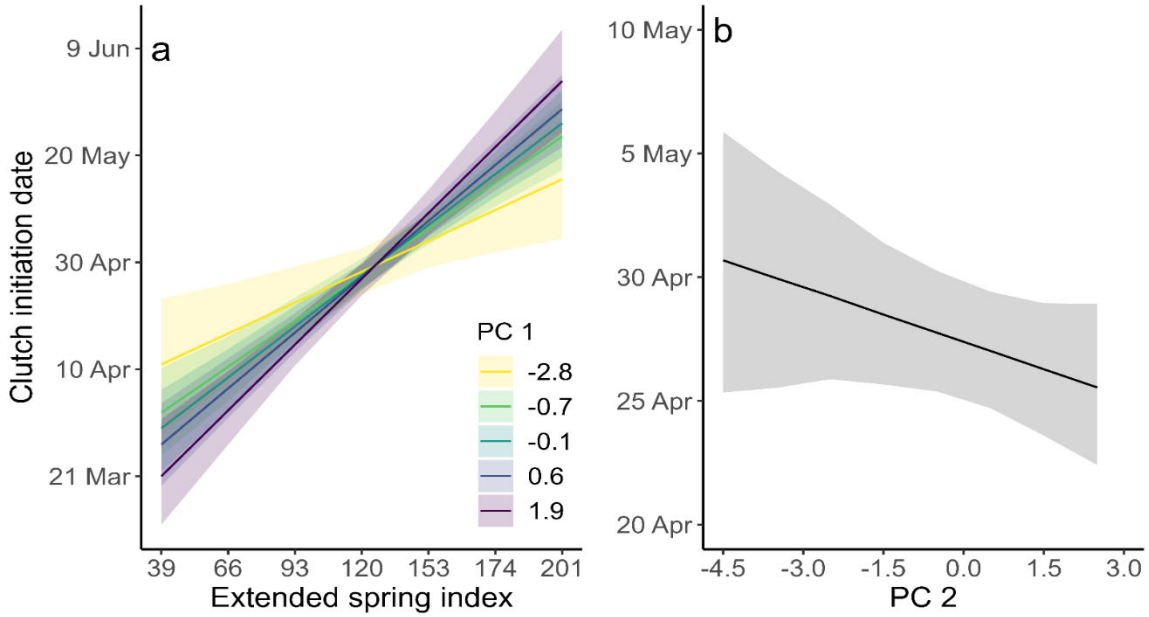

Figure 2.4 Predicted clutch initiation dates of American kestrels based on an interaction between candidate gene $PC_{nesting}$ 1 and the extended spring index (a) and candidate gene $PC_{nesting}$ 2 (b). The effect of the extended spring index (SI-x) depended on $PC_{nesting}$ 1 scores. Specifically, effects of the SI-x were strongest in individuals with higher $PC_{nesting}$ 1 scores (homozygous minor in *peak1* and *top1*, homozygous major *cry1* and *cpne4*); whereas the effects of the SI-x were weaker in individuals with low $PC_{nesting}$ 1 scores (homozygous major in *peak1* and *top1*, homozygous minor in *cry1* and *cpne4*). Individuals with lower $PC_{nesting}$ 2 scores (homozygous minor *mybbp1a*, homozygous major *cpne4*) tended to nest later than individuals with higher $PC_{nesting}$ 2 scores (homozygous major *mybbp1a*, homozygous minor *cpne4*).

that were homozygous minor for *mybbp1a* and *nacc2* tended to initiate clutches earlier. All other single-gene effects were small ($\beta <$ |0.6|) and not significant. These results suggest that genetic variants underlie variation in clutch initiation phenology, and that some genotypes may be more sensitive to environmental cues than others, resulting in different capacities (i.e. plasticity) to shift phenology in response to environmental change.

Genetic correlates of migration timing

We genotyped 165 American kestrels during autumn migration passage through Boise, Idaho and, in addition, 738 breeding American kestrels from 83 sites across the west) to ensure that temporal patterns in migrant genotypes were not the result of the latitudinal variation. A categorical principal

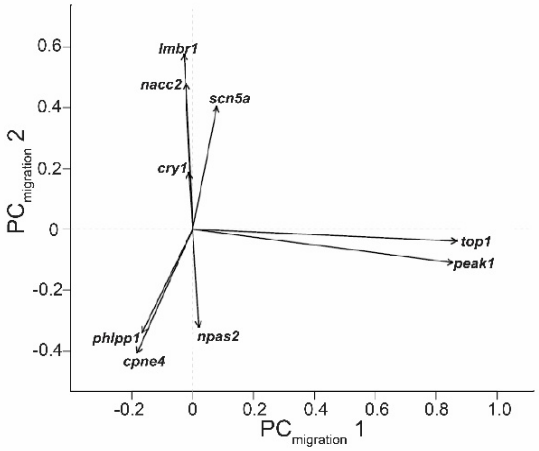

Figure 2.5 Eigenvectors of the first two principal components from an analysis of 9 clock-linked candidate genes based on 165 migration and 738 breeding samples collected from American kestrels. $PC_{migration}$ scores were used to study genetic correlates of migration timing.

component analysis of genetic variation in the nine-candidate genes used in this analysis demonstrated high collinearity between certain genes (Figure 2.5). More specifically, $PC_{migration}$ 1 explained 17.5% of the genetic variation and was weighted by variation in 3 clock-linked genes, *top1*, *cpne4*, *phlpp1* and 2 genes associated with migration *peak1* and *scn5a*. $PC_{migration}$ 2 explained 13.1% of total genetic variation and was driven by variation in 8 of the 9 genes, including the 2 core clock genes *cry1* and *npas2* (Figure 2.5, Table 2A.3). There was a significant correlation between $PC_{migration}$ 1 and migration passage date in 165 individuals captured in the time series (β = -0.94 ± 0.22, $P < 0.01$, Figure 2.6), but no correlation between $PC_{migration}$ 2 and migration passage date ($P > 0.15$). There was no association between $PC_{migration}$ 1 and breeding latitude in western North America breeding samples ($P = 0.17$, Figure 2A.2), suggesting that the relationship between migration timing and $PC_{migration}$ 1 was not the result of migration passage of individuals from different regions. Finally, the effect of PC1 on autumn migration timing did not depend on sex ($P = 0.19$) and it did not differ between females and males ($P = 0.17$, Figure 2A.3).

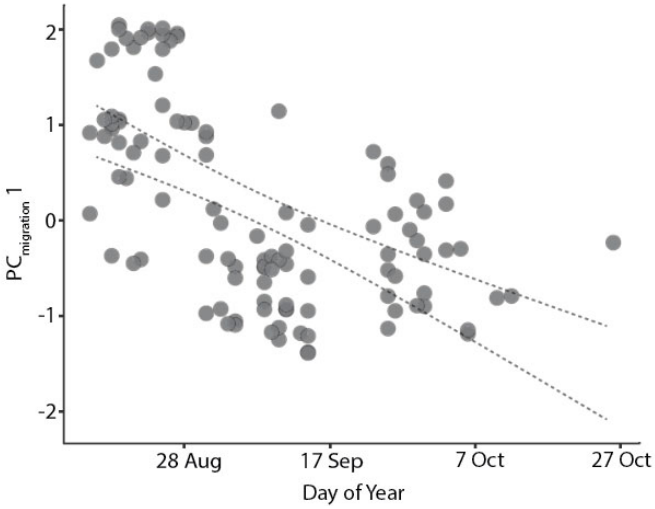

Figure 2.6 The relationship between migration passage date and candidate gene $PC_{migration}$ 1 for American kestrels. Individuals with higher $PC_{migration}$ 1 scores migrated earlier than individuals with lower $PC_{migration}$ 1 scores.

Single gene analyses further support the results from the multi-locus analyses and help elucidate which genes in particular are driving the observed patterns. The single-gene analyses demonstrated that allele frequencies in three

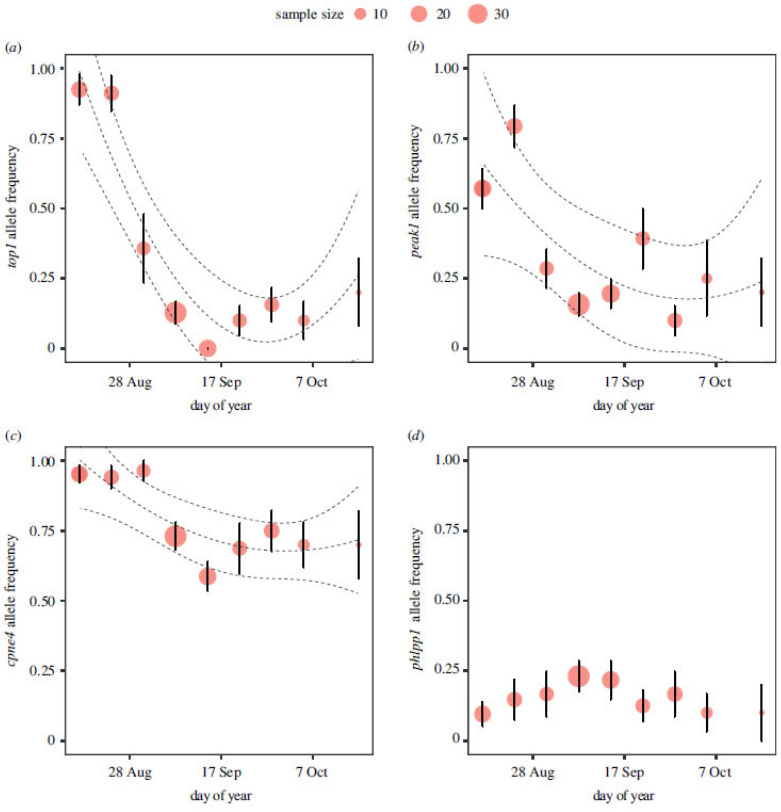

Figure 2.7 Allele frequency (i.e., proportion of major allele) of *top1*, *peak1*, *cpne4* and *phlpp1* as a function of week across autumn migration (Day of Year) of American kestrels at an Idaho migration station. Point sizes are proportional to sample size (n) with the bars showing ± standard error of the mean.

of the top four genes that loaded highest on $PC_{migration}$ 1, *top1*, *peak1*, and *cpne4*, were strongly associated with migration timing in a distinctly, non-linear fashion (*top1* $P < 0.001$, *peak1* $P < 0.001$, and *cpne4* $P < 0.001$, Figure 2.7). In particular, the observed correlations appear to be driven by a shift in allele frequency early in migration. These results suggest that genetic variation underlies autumn migration phenology, with early and late migratory chronotypes passing through at different times.

Genetic differences between populations

$PC_{nesting}$ 1 scores differed between western and eastern individuals (western $\beta = -0.39 \pm 0.18$, $P = 0.03$, Figure 2.8a). $PC_{nesting}$ 1 scores were higher in the eastern population compared to the western population. This difference likely comes from the lack of lower scores (i.e., homozygous major *top1* and *peak1* individuals) in the east compared to the west (Figure 2.8). $PC_{nesting}$ 2 scores tended to differ between populations, but the difference was small and not significant (western $\beta = -0.20 \pm 0.13$, $P = 0.12$, Figure 2.8b).

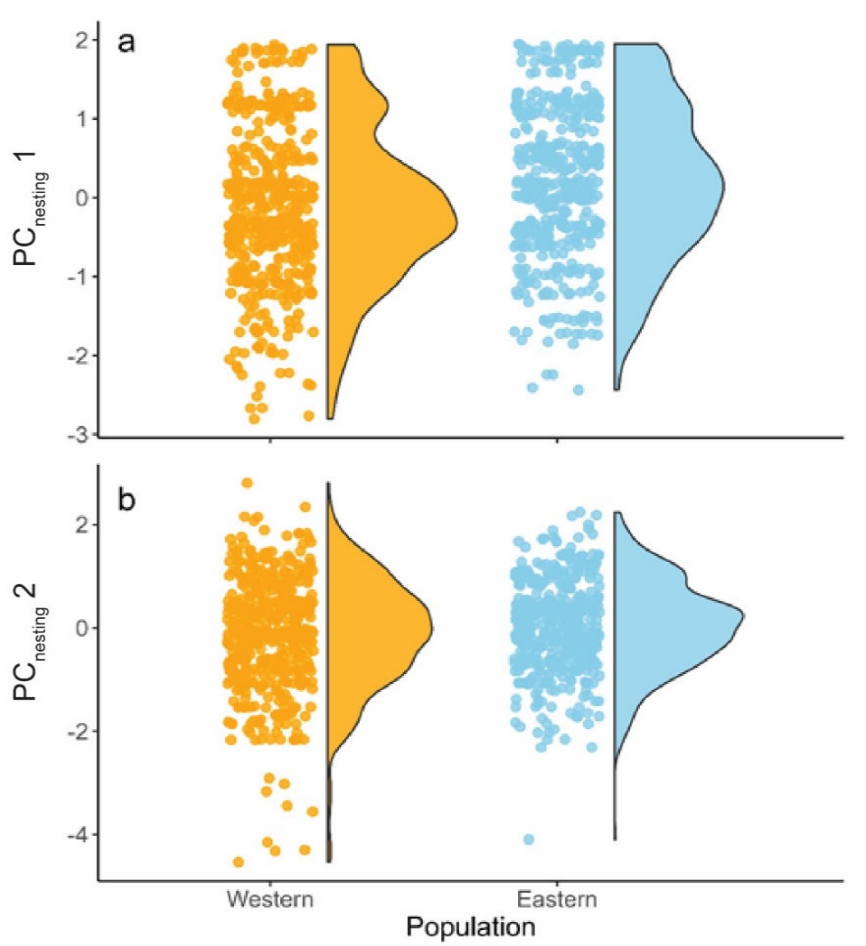

Figure 2.8 Scores on the first principal component (a) and second principal component (b) represent variation in genotypes that correlate with the timing of clutch initiation for western (n = 478) and eastern (n = 433) American kestrels. Western individuals tended to have more diverse principal component scores than eastern individuals.

We calculated the allele frequencies of eight eastern clusters (total individuals = 478) and 13 western clusters (total individuals = 433). There were no significant differences in major allele frequencies between eastern and western populations (Table 2A.4). Western individuals tended to have higher mean heterozygosity than eastern individuals at two genes that had high loadings on PC 1, *top1* ($H_{east} = 0.29$, $H_{west} = 0.33$, $P = 0.07$), *peak1* ($H_{east} = 0.40$, $H_{west} = 0.42$, $P = 0.07$) and *phllp1* ($H_{east} = 0.23$, $H_{west} = 0.26$, $P = 0.06$, Table 2A.5). Eastern individuals had higher mean heterozygosity at *cry1* ($H_{east} = 0.28$, $H_{west} = 0.27$, $P = 0.03$) and *nacc2* ($H_{east} = 0.21$, $H_{west} = 0.19$, $P = 0.02$). These results suggest that eastern populations may have less overall genetic diversity

within candidate genes than western populations, which could limit the capacity for phenological responses and resilience to climate change (Nussey et al. 2005, Helm et al. 2019).

Synthesis

The timing of clutch initiation was a heritable trait for American kestrels, suggesting that genetics play a role in modulating phenology. Genetic variants covaried with the timing of nesting and the timing of migration. Specifically, an interaction between $PC_{nesting}$ 1 and SI-x suggests that some genotypes may be more sensitive to environmental cues than other genotypes. The variation in sensitivity to environmental cues could result in individuals that are relatively early or late within breeding populations. Alternatively, there was a direct correlation between $PC_{migration}$ 1 and migratory timing, with earlier migrating individuals having higher $PC_{migration}$ 1 scores (homozygous minor in *top1* and *peak1*) than later migrating individuals. Together, results from both the clutch initiation analysis and migration analysis, demonstrate the role of genetic variants in seasonal timing and the underlying mechanism that creates chronotypes within populations.

For clutch initiation, the $PC_{nesting}$ 1 interacted with SI-x to predict clutch initiation. Specifically, the SI-x effect was greater for individuals with higher $PC_{nesting}$ 1 values and lower for individuals with low $PC_{nesting}$ 1 values. Genes with high loadings on $PC_{nesting}$ 1 (*top1, peak1, cry1, cpne1*) may govern sensitivity to environmental cues, like vegetation green-up. If true, individuals with high $PC_{nesting}$ 1 scores may show more plasticity because of interannual differences in environmental conditions compared to individuals with lower $PC_{nesting}$ 1 scores. Plasticity in clutch initiation has been shown to be highly heritable (h^2= 0.3) in great tits (*Parus major*), and selection favoring highly plastic individuals has increased as climate change has caused a mismatch between tits and their prey (Nussey et al. 2005). Diversity in $PC_{nesting}$ 1 may play a key role in the adaptive capacity of phenological plasticity. The second $PC_{nesting}$ tended to correlate with the timing of clutch initiation. Individuals with low $PC_{nesting}$ 2 scores tended to initiate clutches later than individuals with high $PC_{nesting}$ 2 scores. Further, there was evidence that one gene with high loadings on $PC_{nesting}$ 2, *mybbp1a* (and to some extent *nacc2*), had a single gene effect on the timing of clutch initiation. Together, these results suggest that the candidate genes identified here may affect phenotypic plasticity (through changing the effect size of SI-x) and directly affect phenotype for the timing of clutch initiation.

In the migration analysis, we found that variation in three genes (*top1*, *peak1*, *cpne4*) was strongly associated with migration passage date. Further, all migrating individuals in our study were genetically identified as originating from a single panmictic source population (Bossu et al. 2022) and no correlation was found between $PC_{migration}$ 1 and breeding latitude, ruling out the possibility that early and late migrants represent individuals from distinct geographic regions. We did not investigate gene and environmental interactions in the migration study, in part because environmental cues of migration timing are less clear than environmental cues of reproduction. The genes represented by $PC_{migration}$ 1 may play a similar role in migration timing, as $PC_{nesting}$ 1 does in clutch initiation – individuals that were more plastic or sensitive to environmental cues could have migrated later than less sensitive individuals. Future work on the environmental correlates of migration would help to tease apart whether candidate genes are affecting phenotypic plasticity or migration timing directly.

We found that *top1, peak1,* and *cpne4* variants played an important role in migration and clutch initiation timing. Specifically, individuals that were homozygous minor in *top1* and *peak1,* and homozygous major in *cpne4* tended to migrate earlier and, in some cases, nest earlier. Though studies on a diversity of organisms have found significant associations between

migratory timing and genetic variation in core clock-linked genes (*clock* and *npas2*- Liedvogel et al. 2009, O'Malley et al. 2010, Bazzi et al. 2015, Saino et al. 2015), we found no association between variation in two core clock genes, *npas2* and *cry1*, and migratory timing, though *cry1* did play a role in the timing of clutch initiation. While our result may seem counterintuitive, further information on the circadian clock feedback loops and the metabolic sensors and light pathways they interact with can help put our results into context (Bell-Pedersen et al. 2005, Cassone et al. 2014). For example, circadian rhythms underlying vertebrate locomotion, physiology, behavior and gene expression are known to be controlled by a core set of genes which make up positive and negative feedback loops. In the positive limb of the feed-back loop, *clock*, *npas2*, and *bmal1* form a complex that activates transcription of CRY and PER (Mohawk et al. 2012). In the negative limb of the feedback loop, CRY and PER repress transcriptional activity of the CLOCK/NPAS2-BMAL1 complex and facilitate daily rhythms in the expression of countless clock-controlled genes (Bell-Pedersen et al. 2005). Thus, one explanation for the lack of an association between migratory timing and genetic variation in core clock genes (*npas2*) found herein is that core genes remain highly conserved to preserve their central role in biological time-keeping and associated physiological processes (Bradshaw and Holzapfel 2007, Krabbenhoft and Turner 2014).

In contrast, our results highlight a strong association between timing and genetic variation in clock-linked genes (*top1*, for migration and clutch initiation, *mybpp1a* for clutch initiation, and to a lesser extent, *phlpp1* for migration) known to entrain the core clock pathway. More specifically, the CLOCK/NPAS2-BMAL1 complex promotes transcription of metabolic sensors, RORs and REV-ERBs, known to fine-tune the circadian clock (Everett and Lazar 2014, Kim and Lazar 2020). *Top1*, the gene with a strong association with clutch initiation and migration timing, is a key regulator of these metabolic sensors, such that knockout of *top1* results in lengthening of the circadian period in mice (Onishi and Kawano 2012). *Mybbp1a* interacts with *cry1* to repress PER2, resulting in down-regulation of PER2 expression (Hara et al. 2009). In turn, *phlpp1* plays a role in light input pathways such that its deletion in mice results in the inability to properly calibrate the circadian clock to light (Masubuchi et al. 2010). Thus, while none of these genes has previously been linked to avian phenology, it makes sense that genetic variation within these genes could result in differences in period length, photic entrainment, and subsequent seasonal timing. While more research is needed, our results highlight the potentially important role of genetic variation in metabolic and light input pathway genes (*top1*, *mybbp1a* and *phlpp1*) in regulating seasonal timing in birds.

The links between the two other genes that were also associated with migratory timing, *peak1* and *cpne4*, and biological clocks remain more tenuous. *Peak1* is a pseudokinase, which was previously found to be differentially expressed in Swainson's thrushes in relation to migratory state (Johnston et al. 2016), but no associations with this gene and biological clocks have been identified. One potential avenue for future work is to investigate the known associations between this gene and key signaling pathways that play a role in circadian and photic regulation (Weber 2009, Herzog et al. 2017). For example, *peak1* is known to interact with ERK, a kinase that is involved in photic resetting of the clock in rodents (Butcher et al. 2002, Bell-Pedersen 2013), and is modulated by the retinoic acid signaling pathway. Genetic changes in another kinase gene, *rock1*, were also recently found to be associated in Chinook salmon (*Oncorhynchus tshawytscha*) with run timing (e.g., spring vs fall migration timing), as well as the timing of final ascent to spawning grounds in the Snake River (Koch and Narum 2020, Thompson et al. 2020). Alternatively, *cpne4* has been associated with migratory

restlessness in birds (Jones et al. 2008), and with sleep-wake cycle regulation, a core circadian process, in reptiles (Norimoto et al. 2020).

While chronotypes often refer to variation in the timing of daily events between individuals, recent behavioral studies on birds have elucidated the link between the timing of daily events and the timing of seasonal migration at the phenotypic level (Rittenhouse et al. 2019). Further research on birds and fish has demonstrated a link between circadian and circannual rhythms, where the hormonal pathways triggered by a photoperiod signal, for example via melatonin and thyroid hormones, results in a seasonal phenotype (Sur et al. 2021, Doyle et al. 2021). At the genotypic level, previous work on *clock* provided a tenuous link between genetic variation in genes central to daily rhythms and the timing of seasonal events, but this work was performed across rather than within populations (O'Malley et al. 2010). Here, we document what is, to the best of our knowledge, the first example of an association between intra-population genetic variation in genes that entrain biological clocks, and the existence of early and late migratory chronotypes *within* populations.

In addition to helping unravel the genetic basis of phenology, the identification of a genetic polymorphism underlying early and late migratory chronotypes in American kestrels has importance for our understanding of how this species may or may not be able to shift migratory timing in the face of climate change (Visser et al. 2010). Previous work has shown that the degree of standing genetic variation in migration-linked genes can have significant fitness consequences in rapidly changing environments. For example, work in Dutch pied flycatchers (*Ficedula hypoleuca*) suggested that the lack of genetic variation underlying the timing of spring migration constrained the advancement of breeding dates, despite earlier onset of spring (Both et al. 2005). In contrast, a recent study of hand-raised German pied flycatchers suggested that the advancement of lay dates in wild populations over a 20-year period was almost completely explained by selection on the underlying circannual clock itself (Helm et al. 2019). We found that western and eastern kestrels had different distributions of $PC_{nesting}$ 1 and tended to have different $PC_{nesting}$ 2 scores. In both cases, eastern kestrels had fewer low-scoring genotypes than western kestrels. Differences in scores may indicate that eastern kestrels have overall less genetic diversity at these loci than western kestrels. Eastern kestrels have a narrower nesting window (~two months) compared to western kestrels (~four months, Chapter 1). Further, we found evidence that eastern kestrels experience a within-season trade-off between reproduction and survival, with earlier nesters having higher productivity and lower survival compared to later nesters (Chapter 1). Taken together, these results suggest that nesting phenology in the east may be (or was) under stabilizing selection, resulting in a narrower window for clutch initiation and less genetic diversity in clock-linked genes. Though, eastern kestrels did have higher heterozygosity at the *cry1* and *nacc2* loci, both of which tended to covary with the timing of clutch initiation.

Population differences in the clock-linked genes described here may limit the capacity of eastern individuals to shift the timing of clutch initiation. Monitoring genotypic and phenological change in natural populations may provide insight into whether there are genetic constraints on adaptive capacity. Alternatively, in the next chapter, we will test whether genetic composition or diversity limits the adaptive capacity of these populations through the use of a genetically-explicit individual-based model.

Conclusions and Implications for Future Research and Implementation

We successfully achieved our objectives of: 1) demonstrating that the timing of important life-history events, like nesting, is heritable in American kestrels, 2) identifying genetic variants with targeted candidate gene analysis to document significant correlations between genetic variation within metabolic and light input pathway genes known to entrain circannual clocks and the timing of clutch initiation and migration of American kestrels, and 3) directly comparing gene complexes (PC values) and allele frequencies and heterozygosity of individual loci between western and eastern kestrels. We found support for the hypothesis that phenology is governed by genetic mechanisms, and that variation within candidate genes can produce chronotypes within populations. Finally, we showed that western and eastern kestrels have different genetic diversity at these important loci, supporting the hypothesis that differences in genetics may affect the adaptive capacity of populations to respond to climate change. Our results support the hypothesis that phenology is a heritable trait governed by genetics. Furthermore, diversity within candidate genes may impact the adaptive capacity of populations to respond to climate-driven changes in spring phenology and may affect population vulnerability to phenological mismatch.

Understanding species and populations vulnerability to – and adaptive capacity in response to – climate change will help DoD managers assess and prioritize management actions for MSS. Our work showed that underlying genetics play an important role in phenology and capacity to shift phenology, but that adaptive capacity could vary regionally, or even within a population. Although these processes are intrinsic to populations, external stressors (natural and anthropogenic) can limit the realization of potential adaptive capacity (Beever et al. 2016). Hence, resource managers can play an important role in reducing anthropogenic stressors (e.g. pollution, land-use change) to reduce barriers to dispersal and gene flow for populations with fundamental adaptive capacity, and to limit controllable pressures for more vulnerable populations with less adaptive capacity (Beever et al. 2016). Overall, this work advances our understanding of the genetic complexities underlying timing in a diurnal migratory raptor and provides, to the best of our knowledge, the first documentation of a genetic basis for early and late migratory chronotypes within populations of a migratory bird. Results support the idea that genetic variation in clock-linked, rather than core clock genes result in the existence of early and late chronotypes within American kestrels. Further, results provide important insights into the factors controlling avian phenology. These results are particularly important in light of the absence of information on intrinsic factors affecting phenology shifts. While we have successfully identified some genes of small effect, we are missing others and may not be accounting for potential epigenetic effects (Vogt 2015). Repeating this analysis with whole-genome sequencing may reveal additional clock-linked genes that contribute to the observed patterns. In the next chapter, we will develop a better understanding of the linkages between climate-induced selection for phenological shifts, genetic variation in clock-linked genes, and population trends of American kestrels. New knowledge presented in this chapter combined with results from Chapter 3 can help to guide DoD Natural Resource Managers in addressing questions about the adaptive potential of migratory birds to respond to climate-driven shifts in seasons.

Literature Cited

Adamack, A. T., & Gruber, B. (2014). PopGenReport: simplifying basic population genetic analyses in R. *Methods in Ecology and Evolution*, *5*(4), 384-387.

Åkesson, S., & Helm, B. (2020). Endogenous programs and flexibility in bird migration. *Frontiers in Ecology and Evolution*, *8*, 78.

Albrecht, U. (2012). Timing to perfection: the biology of central and peripheral circadian clocks. *Neuron*, *74*(2), 246-260.

Ali, O. A., O'Rourke, S. M., Amish, S. J., Meek, M. H., Luikart, G., Jeffres, C., & Miller, M. R. (2016). RAD capture (Rapture): flexible and efficient sequence-based genotyping. *Genetics*, *202*(2), 389-400.

Anderson, E. C. (2015). snps2assays: Prepare SNP assay orders from ddRAD or RAD loci. (doi:10.5281/zenodo.4072250).

Anderson, A. M., Novak, S. J., Smith, J. F., Steenhof, K., & Heath, J. A. (2016). Nesting phenology, mate choice, and genetic divergence within a partially migratory population of American Kestrels. *The Auk: Ornithological Advances*, *133*(1), 99-109.

Bazzi, G., Ambrosini, R., Caprioli, M., Costanzo, A., Liechti, F., Gatti, E., ... & Rubolini, D. (2015). Clock gene polymorphism and scheduling of migration: a geolocator study of the barn swallow *Hirundo rustica*. *Scientific Reports*, *5*(1), 1-7.

Beever, E. A., O'leary, J., Mengelt, C., West, J. M., Julius, S., Green, N., ... & Hofmann, G. E. (2016). Improving conservation outcomes with a new paradigm for understanding species' fundamental and realized adaptive capacity. *Conservation Letters*, *9*(2), 131-137.

Bell-Pedersen, D., Cassone, V. M., Earnest, D. J., Golden, S. S., Hardin, P. E., Thomas, T. L., & Zoran, M. J. (2005). Circadian rhythms from multiple oscillators: lessons from diverse organisms. *Nature Reviews Genetics*, *6*(7), 544-556.

Bourret, A., & Garant, D. (2015). Candidate gene–environment interactions and their relationships with timing of breeding in a wild bird population. *Ecology and Evolution*, *5*(17), 3628-3641.

Bossu, C. M., Heath, J. A., Kaltenecker, G. S., Helm, B., & Ruegg, K. C. (2022). Clock-linked genes underlie seasonal migratory timing in a diurnal raptor. *Proceedings of the Royal Society B*, *289*(1974), 20212507.

Both, C., Artemyev, A. V., Blaauw, B., Cowie, R. J., Dekhuijzen, A. J., Eeva, T., ... & Visser, M. E. (2004). Large–scale geographical variation confirms that climate change causes birds to lay earlier. *Proceedings of the Royal Society of London. Series B: Biological Sciences*, *271*(1549), 1657-1662.

Both, C., G. Bijlsma, R., & E. Visser, M. (2005). Climatic effects on timing of spring migration and breeding in a long-distance migrant, the pied flycatcher *Ficedula hypoleuca*. *Journal of Avian Biology*, *36*(5), 368-373.

Bradshaw, W. E., & Holzapfel, C. M. (2007). Evolution of animal photoperiodism. *Annual Review of Ecology, Evolution, and Systematics*, 1-25.

Butcher, G. Q., Dziema, H., Collamore, M., Burgoon, P. W., & Obrietan, K. (2002). The p42/44 mitogen-activated protein kinase pathway couples photic input to circadian clock entrainment. *Journal of Biological Chemistry*, *277*(33), 29519-29525.

Caprioli, M., Ambrosini, R., Boncoraglio, G., Gatti, E., Romano, A., Romano, M., ... & Saino, N. (2012). Clock gene variation is associated with breeding phenology and maybe under directional selection in the migratory barn swallow. *PLoS One*, *7*(4), e35140.

Cassone, V. M. (2014). Avian circadian organization: a chorus of clocks. *Frontiers in Neuroendocrinology*, *35*(1), 76-88.

Dohm, M. R. (2002). Repeatability estimates do not always set an upper limit to heritability. *Functional Ecology*, 273-280.

Doyle, A., Cowan, M. E., Migaud, H., Wright, P. J., & Davie, A. (2021). Neuroendocrine regulation of reproduction in Atlantic cod (*Gadus morhua*): Evidence of Eya3 as an integrator of photoperiodic cues and nutritional regulation to initiate sexual maturation. *Comparative Biochemistry and Physiology Part A: Molecular & Integrative Physiology*, *260*, 111000.

Everett, L. J., & Lazar, M. A. (2014). Nuclear receptor Rev-erbα: up, down, and all around. *Trends in Endocrinology & Metabolism*, *25*(11), 586-592.

Fitzpatrick, M. J., Ben-Shahar, Y., Smid, H. M., Vet, L. E., Robinson, G. E., & Sokolowski, M. B. (2005). Candidate genes for behavioural ecology. *Trends in Ecology & Evolution*, *20*(2), 96-104.

Franchini, P., Irisarri, I., Fudickar, A., Schmidt, A., Meyer, A., Wikelski, M., & Partecke, J. (2017). Animal tracking meets migration genomics: transcriptomic analysis of a partially migratory bird species. *Molecular Ecology*, *26*(12), 3204-3216.

Fudickar, A. M., Peterson, M. P., Greives, T. J., Atwell, J. W., Bridge, E. S., & Ketterson, E. D. (2016). Differential gene expression in seasonal sympatry: mechanisms involved in diverging life histories. *Biology letters*, *12*(3), 20160069.

Gwinner, E. (1996). Circadian and circannual programmes in avian migration. *The Journal of Experimental Biology*, *199*(1), 39-48.

Hadfield, J. D. (2010). MCMC methods for multi-response generalized linear mixed models: the MCMCglmm R package. *Journal of Statistical Software*, *33*, 1-22.

Hara, Y., Onishi, Y., Oishi, K., Miyazaki, K., Fukamizu, A., & Ishida, N. (2009). Molecular characterization of Mybbp1a as a co-repressor on the Period2 promoter. *Nucleic Acids Research*, *37*(4), 1115-1126.

Heath, J. A., Steenhof, K., & Foster, M. A. (2012). Shorter migration distances associated with higher winter temperatures suggest a mechanism for advancing nesting phenology of American kestrels *Falco sparverius*. *Journal of Avian Biology*, *43*(4), 376-384.

Heidelberger, P., & Welch, P. D. (1983). Simulation run length control in the presence of an initial transient. *Operations Research*, *31*(6), 1109-1144.

Helm, B., Van Doren, B. M., Hoffmann, D., & Hoffmann, U. (2019). Evolutionary response to climate change in migratory pied flycatchers. *Current Biology*, *29*(21), 3714-3719.

Herzog, E. D., Hermanstyne, T., Smyllie, N. J., & Hastings, M. H. (2017). Regulating the suprachiasmatic nucleus (SCN) circadian clockwork: interplay between cell-autonomous and circuit-level mechanisms. *Cold Spring Harbor Perspectives in Biology*, *9*(1), a027706.

Hoffmann, A. A., & Sgrò, C. M. (2011). Climate change and evolutionary adaptation. *Nature*, *470*(7335), 479-485.

Izquierdo-Verdiguier, E., Zurita-Milla, R., Ault, T. R., & Schwartz, M. D. (2018). Development and analysis of spring plant phenology products: 36 years of 1-km grids over the conterminous US. *Agricultural and forest meteorology*, *262*, 34-41.

Johnsen, A., Fidler, A. E., Kuhn, S., Carter, K. L., Hoffmann, A., Barr, I. R., ... & Kempenaers, B. (2007). Avian Clock gene polymorphism: evidence for a latitudinal cline in allele frequencies. *Molecular Ecology*, *16*(22), 4867-4880.

Johnston, R. A., Paxton, K. L., Moore, F. R., Wayne, R. K., & Smith, T. B. (2016). Seasonal gene expression in a migratory songbird. *Molecular Ecology*, *25*(22), 5680-5691.

Jones, S., Pfister-Genskow, M., Cirelli, C., & Benca, R. M. (2008). Changes in brain gene expression during migration in the white-crowned sparrow. *Brain Research Bulletin*, *76*(5), 536-544.

Kim, Y. H., & Lazar, M. A. (2020). Transcriptional control of circadian rhythms and metabolism: a matter of time and space. *Endocrine Reviews*, *41*(5), 707-732.

Krabbenhoft, T. J., & Turner, T. F. (2014). Clock gene evolution: seasonal timing, phylogenetic signal, or functional constraint? *Journal of Heredity*, *105*(3), 407-415.

Koch, I. J., & Narum, S. R. (2020). Validation and association of candidate markers for adult migration timing and fitness in Chinook Salmon. *Evolutionary Applications*, *13*(9), 2316-2332.

Li, H., & Durbin, R. (2009). Fast and accurate short read alignment with Burrows–Wheeler transform. *Bioinformatics*, *25*(14), 1754-1760.

Liedvogel, M., Szulkin, M., Knowles, S. C., Wood, M. J., & Sheldon, B. C. (2009). Phenotypic correlates of Clock gene variation in a wild blue tit population: evidence for a role in seasonal timing of reproduction. *Molecular Ecology*, *18*(11), 2444-2456.

Lundberg, M., Boss, J., Canbäck, B., Liedvogel, M., Larson, K. W., Grahn, M., ... & Wright, A. (2013). Characterisation of a transcriptome to find sequence differences between two differentially migrating subspecies of the willow warbler *Phylloscopus trochilus*. *BMC genomics*, *14*(1), 1-11.

Mair, P., De Leeuw, J., & Groenen, P. (2019). Gifi: Multivariate analysis with optimal scaling. *R package version 0.3–9*.

Masubuchi, S., Gao, T., O'Neill, A., Eckel-Mahan, K., Newton, A. C., & Sassone-Corsi, P. (2010). Protein phosphatase PHLPP1 controls the light-induced resetting of the circadian clock. *Proceedings of the National Academy of Sciences*, *107*(4), 1642-1647.

McCaslin, H. M., Caughlin, T. T., & Heath, J. A. (2020). Long-distance natal dispersal is relatively frequent and correlated with environmental factors in a widespread raptor. *Journal of Animal Ecology*, *89*(9), 2077-2088.

McClure, C. J., Schulwitz, S. E., Van Buskirk, R., Pauli, B. P., & Heath, J. A. (2017). Commentary: Research recommendations for understanding the decline of American Kestrels (*Falco sparverius*) across much of North America. *Journal of Raptor Research*, *51*(4), 455-464.

Mohawk, J. A., Green, C. B., & Takahashi, J. S. (2012). Central and peripheral circadian clocks in mammals. *Annual Review of Neuroscience*, *35*, 445.

Møller, A. P., Rubolini, D., & Lehikoinen, E. (2008). Populations of migratory bird species that did not show a phenological response to climate change are declining. *Proceedings of the National Academy of Sciences*, *105*(42), 16195-16200.

Nei, M. (1987). *Molecular evolutionary genetics*. Columbia university press.

Norimoto, H., Fenk, L. A., Li, H. H., Tosches, M. A., Gallego-Flores, T., Hain, D., ... & Laurent, G. (2020). A claustrum in reptiles and its role in slow-wave sleep. *Nature*, *578*(7795), 413-418.

Nussey, D. H., Postma, E., Gienapp, P., & Visser, M. E. (2005). Selection on heritable phenotypic plasticity in a wild bird population. *Science*, *310*(5746), 304-306.

O'Malley, K. G., & Banks, M. A. (2008). A latitudinal cline in the Chinook salmon (*Oncorhynchus tshawytscha*) Clock gene: evidence for selection on PolyQ length variants. *Proceedings of the Royal Society B: Biological Sciences*, *275*(1653), 2813-2821.

O'Malley, K. G., Ford, M. J., & Hard, J. J. (2010). Clock polymorphism in Pacific salmon: evidence for variable selection along a latitudinal gradient. *Proceedings of the Royal Society B: Biological Sciences*, *277*(1701), 3703-3714.
Onishi, Y., & Kawano, Y. (2012). Rhythmic binding of Topoisomerase I impacts on the transcription of Bmal1 and circadian period. *Nucleic Acids Research*, *40*(19), 9482-9492.
Paradis, E. (2010). pegas: an R package for population genetics with an integrated–modular approach. *Bioinformatics*, *26*(3), 419-420.
Plummer, M., Best, N., Cowles, K., & Vines, K. (2006). CODA: convergence diagnosis and output analysis for MCMC. *R News*, *6*(1), 7-11.
Postma, E., & Charmantier, A. (2007). What 'animal models' can and cannot tell ornithologists about the genetics of wild populations. *Journal of Ornithology*, *148*(2), 633-642.
Postma, E. (2014). Four decades of estimating heritabilities in wild vertebrate populations: improved methods, more data, better estimates. *Quantitative Genetics in the Wild*, *16*, 33.
Ribas-Latre, A., & Eckel-Mahan, K. (2016). Interdependence of nutrient metabolism and the circadian clock system: importance for metabolic health. *Molecular Metabolism*, *5*(3), 133-152.
Rittenhouse, J. L., Robart, A. R., & Watts, H. E. (2019). Variation in chronotype is associated with migratory timing in a songbird. *Biology Letters*, *15*(8), 20190453.
Ruegg, K., Anderson, E. C., Boone, J., Pouls, J., & Smith, T. B. (2014). A role for migration-linked genes and genomic islands in divergence of a songbird. *Molecular Ecology*, *23*(19), 4757-4769.
Ruegg, K. C., Brinkmeyer, M., Bossu, C. M., Bay, R. A., Anderson, E. C., Boal, C. W., ... & Heath, J. A. (2021). The American Kestrel (*Falco sparverius*) genoscape: Implications for monitoring, management, and subspecies boundaries. *The Auk*, *138*(2), ukaa051.
R Core Team (2019) R: A language and environment for statistical computing. *R Foundation for Statistical Computing.* Vienna, Austria. https://www.R- project.org/
Saino, N., Bazzi, G., Gatti, E., Caprioli, M., Cecere, J. G., Possenti, C. D., ... & Spina, F. (2015). Polymorphism at the Clock gene predicts phenology of long-distance migration in birds. *Molecular Ecology*, *24*(8), 1758-1773.
Saino, N., Albetti, B., Ambrosini, R., Caprioli, M., Costanzo, A., Mariani, J., ... & Bollati, V. (2019). Inter-generational resemblance of methylation levels at circadian genes and associations with phenology in the barn swallow. *Scientific Reports*, *9*(1), 1-16.
Sheldon, B. C., Kruuk, L. E. B., & Merila, J. (2003). Natural selection and inheritance of breeding time and clutch size in the collared flycatcher. *Evolution*, *57*(2), 406-420.
Smallwood JA, Bird DM (2020) American Kestrel (*Falco sparverius*), version 1.0. In Birds of the World (Poole AF, Gill FB, eds.). Cornell Lab of Ornithology, Ithaca, NY, USA. https://doi.org/10.2173/bow.amekes.01
Smallwood, J. A., Causey, M. F., Mossop, D. H., Klucsarits, J. R., Robertson, B., Robertson, S., ... & Boyd, K. (2009). Why are American Kestrel (*Falco sparverius*) populations declining in North America? Evidence from nest-box programs. *Journal of Raptor Research*, *43*(4), 274-282.
Smith, S. H., Steenhof, K., McClure, C. J., & Heath, J. A. (2017). Earlier nesting by generalist predatory bird is associated with human responses to climate change. *Journal of Animal Ecology*, *86*(1), 98-107.
Socolar, J. B., Epanchin, P. N., Beissinger, S. R., & Tingley, M. W. (2017). Phenological shifts conserve thermal niches in North American birds and reshape expectations for climate-

driven range shifts. *Proceedings of the National Academy of Sciences*, *114*(49), 12976-12981.
Steenhof, K., & Peterson, B. E. (2009). American Kestrel reproduction in southwestern Idaho: annual variation and long-term trends. *Journal of Raptor Research*, *43*(4), 283-290.
Stevenson, T. J., & Kumar, V. (2017). Neural control of daily and seasonal timing of songbird migration. *Journal of Comparative Physiology A*, *203*(6), 399-409.
Sur, S., Sharma, A., Malik, I., Bhardwaj, S. K., & Kumar, V. (2021). Daytime light spectrum affects photoperiodic induction of vernal response in obligate spring migrants. *Comparative Biochemistry and Physiology Part A: Molecular & Integrative Physiology*, *259*, 111017.
Teplitsky, C., Mills, J. A., Yarrall, J. W., & Merilä, J. (2009). Heritability of fitness components in a wild bird population. *Evolution: International Journal of Organic Evolution*, *63*(3), 716-726.
Thackeray, S. J., Henrys, P. A., Hemming, D., Bell, J. R., Botham, M. S., Burthe, S., ... & Wanless, S. (2016). Phenological sensitivity to climate across taxa and trophic levels. *Nature*, *535*(7611), 241-245.
Thompson, N. F., Anderson, E. C., Clemento, A. J., Campbell, M. A., Pearse, D. E., Hearsey, J. W., ... & Garza, J. C. (2020). A complex phenotype in salmon controlled by a simple change in migratory timing. *Science*, *370*(6516), 609-613.
Thornton, P. E., Thornton, M., Mayer, B. W., Wei, Y., Devarakonda, R., Vose, R. S., Cook, R. B. (2018). Daymet: Daily Surface Weather Data on a 1-km Grid for North America, Version 3. *ORNL DAAC*, Oak Ridge, Tennessee, USA.
Thorley, J. B., & Lord, A. M. (2015). Laying date is a plastic and repeatable trait in a population of Blue Tits *Cyanistes caeruleus*. *Ardea*, *103*(1), 69-78.
de Villemereuil, P., Rutschmann, A., Ewen, J. G., Santure, A. W., & Brekke, P. (2019). Can threatened species adapt in a restored habitat? No expected evolutionary response in lay date for the New Zealand hihi. *Evolutionary applications*, *12*(3), 482-497.
Visser, M. E., & Both, C. (2005). Shifts in phenology due to global climate change: the need for a yardstick. *Proceedings of the Royal Society B: Biological Sciences*, *272*(1581), 2561-2569.
Visser, M. E., Holleman, L. J., & Gienapp, P. (2006). Shifts in caterpillar biomass phenology due to climate change and its impact on the breeding biology of an insectivorous bird. *Oecologia*, *147*(1), 164-172.
Visser, M. E., Caro, S. P., Van Oers, K., Schaper, S. V., & Helm, B. (2010). Phenology, seasonal timing and circannual rhythms: towards a unified framework. *Philosophical Transactions of the Royal Society B: Biological Sciences*, *365*(1555), 3113-3127.
Vogt, G. (2015). Stochastic developmental variation, an epigenetic source of phenotypic diversity with far-reaching biological consequences. *Journal of Biosciences*, *40*(1), 159-204.
Weber, F. (2009). Remodeling the clock: coactivators and signal transduction in the circadian clockworks. *Naturwissenschaften*, *96*(3), 321-337.
Wilson, A. J., Reale, D., Clements, M. N., Morrissey, M. M., Postma, E., Walling, C. A., ... & Nussey, D. H. (2010). An ecologist's guide to the animal model. *Journal of Animal Ecology*, *79*(1), 13-26.
Zeileis, A., & Hothorn, T. (2002). Diagnostic checking in regression relationships.

Zhang, S., Xu, X., Wang, W., Yang, W., & Liang, W. (2017). Clock gene is associated with individual variation in the activation of reproductive endocrine and behavior of Asian short toed lark. *Scientific Reports*, *7*(1), 1-8.

Chapter 3. Genetic and ecological mechanisms underlying nesting phenology shifts

Julie A. Heath, Jason M. Winiarski, Benjamin P. Pauli, Stephanie J. Galla, Breanna F. Powers, Christopher J. W. McClure, Anjolene R. Hunt

Abstract

Managers need reliable predictive models of whether and how populations may cope or adapt to climate change to identify vulnerable species, particularly those with the potential to constrain military testing and training. Critical knowledge gaps remain, however, about the underlying genetic and environmental factors that affect the potential for populations to undergo phenological shifts in response to climate change. Individual-based models (IBMs) provide a method to forecast phenological shifts using empirical data that is representative of risk exposure (i.e., climate projections), species sensitivity (i.e., fitness), and adaptive capacity (i.e., evolutionary mechanisms). We developed an integrative IBM that combined evolutionary mechanisms affecting circannual rhythms (i.e., putatively functional genetic markers and heritability), and ecological mechanisms (i.e., demographic and life-history traits), to explore shifts in egg-laying dates in a small raptor, the American kestrel (*Falco sparverius*). We created experiments within the IBM to examine how genetic composition and diversity, and demographic and life-history traits affect nesting phenology shifts and population trends. Interestingly, genetic composition and diversity had small effects on nesting phenology shifts. However, if heritability and genetic mechanisms were removed from the model, advancement of egg-laying was slower and populations tended to decline, reflecting the importance of representing evolutionary processes in biological IBMs. In our ecological experiments, phenological mismatch-driven declines in adult survival, as well as competition for nest sites and mates were the strongest drivers of earlier nesting. These were surprising results because previous research has focused on the effects of phenological mismatch on productivity as a driver of early nesting, rather than survival and competition. Carry-over effects from changes in migration tendency and distance had a small effect on the rate of egg-laying phenology advancement, suggesting that migration does not constrain earlier nesting, as previously hypothesized. Results from IBM experiments reinforce the risk assessment and management recommendations in Chapter 1. Specifically, large populations that lack seasonal trade-offs in reproduction and survival are likely to be resilient. Whereas large populations that have seasonal trade-offs between reproduction and survival, declining populations where competition for nest sites and mates is decreased, or small populations with limited genetic potential are likely to be vulnerable to mismatch. This work provides methodological approaches for integrating genetic and ecological information into models that simulate both evolutionary and ecological processes, which is an important advancement for understanding and predicting population responses to environmental change and increases our understanding of the mechanisms underlying phenology shifts.

Objectives

In this chapter, we used empirical data to develop an individual-based simulation model to test hypotheses about mechanisms underlying climate-based phenology shifts. Although earlier breeding is a common pattern affecting diverse taxa, most hypotheses regarding climate change and breeding phenology have been generated from studies of insectivorous passerine

birds in Europe (Crick et al. 1997, Forchhammer et al. 1998, Both et al. 2004, and others). In these systems, warming spring temperatures have affected plant phenology and insect emergence. Because birds benefit from timing their reproduction to coincide with periods of high food availability, early peaks in prey availability increase the selective pressure to nest earlier. Indeed, for some species, nesting phenology has advanced (Crick et al. 1997, Dunn and Winkler 1999, Both and Visser 2005, Pearce-Higgins et al. 2005, Bauer et al. 2010), whereas, some temperate species have not advanced nesting phenology, despite temporal advances in prey availability (Visser et al. 2003). In these cases, previously coinciding cycles between predators and prey may become decoupled, resulting in a temporal mismatch between reproduction and resources (Miller-Rushing et al. 2010), and significant negative consequences for population viability (Both et al. 2010). Extensive within- and between- species variation in phenological shifts suggests that several mechanisms may underlie changes in breeding phenology. Given the population-level consequences of mismatch, more information on the mechanisms that affect phenology shifts is necessary for making predictions about population abundance and distributions in changing climates.

We used the field-based data collected on the fitness consequences of nesting phenology (Chapter 1) and the genetic correlates of nesting phenology (Chapter 2) to develop a genetically- and spatially-explicit individual-based simulation model (IBM) called SCOPE: Simulation of Carry-Over and Phenology Effects. Within SCOPE we tested the following hypotheses:

H1: Composition and diversity within circadian rhythm candidate genes affect nesting phenology shifts.

H2: Seasonal timing effects on *nesting success* facilitate earlier nesting (i.e., advancing nesting phenology is driven by earlier nesting birds having higher nesting success than later nesters).

H3: Seasonal timing effects on *adult survival* facilitate earlier nesting (i.e., advancing nesting phenology is driven by earlier nesting birds having higher survival than later nesters).

H4: Carry-over effects from migration strategy, migration distance, or both affect nesting phenology shifts.

This research addresses the two important components within the SERDP SON:

Increase understanding of specific genetic factors. We explored polymorphisms at seven candidate genes (*top1, peak1, nacc2, mybbp1a, scn5a1, cpne4, cry1*) that are linked to circadian rhythms to investigate the role of genetic diversity and composition on the potential for evolutionary adaptation under an RCP 8.5 climate scenario.

Life-cycle modeling to assess emerging theoretical understanding of phenology and its role in maintaining species viability. A fundamental theme in our approach was to study phenology shifts within the context of a full annual cycle. This approach was critical to testing hypotheses about carry-over effects and generational changes, and for predicting population changes over time.

Background

Among the most dramatic signals of climate change are advances in the phenology (i.e., seasonal timing of life-history events) in plants and animals (Parmesan and Yohe 2003). Of particular concern is the role that climate change may play in disrupting synchrony in phenology among different trophic levels. In such cases, previously coinciding cycles between predators and prey may become decoupled, resulting in a temporal mismatch between reproduction and peak resources (Reed et al. 2013). In birds, climate-driven phenological mismatches can result in

decreased individual fitness and can have significant negative consequences for population viability (Visser and Both 2005, Both et al. 2006, Miller-Rushing et al. 2010). Unfortunately, the factors that constrain or enable phenology shifts for many species remain poorly understood (Visser 2008, Wingfield 2008). Given the population-level consequences of mismatch, a better understanding of the mechanisms underlying phenology shifts is urgently needed to accurately forecast the effects of climate change on birds. This could be particularly important on Department of Defense (DoD) lands, which have the highest density of threatened and endangered species of any federal land management agency (Stein et al. 2008), and for whom listing of additional species on the Endangered Species Act can impact mission activities.

The mechanisms underpinning phenology in birds are often a combination of internal timekeeping and external environmental cues. Endogenous circadian clocks—which regulate hormones for reproduction and migratory restlessness—are controlled by a series of genes and are triggered by light sensors and photoperiod as a proximal indicator of peak resource availability for reproduction in birds with non-equatorial distributions (Helm et al. 2013, Walker et al. 2019, but see also non-photic cues reviewed in Chmura et al. 2020). Polymorphisms in genes that underlie circadian and circannual rhythms create distinct early or late circannual phenotypes (hereafter: chronotypes, Liedvogel et al. 2009, Saino et al. 2019). Further, research across several species shows that the timing of egg-laying is heritable (Sheldon et al. 2003, Nussey et al. 2005, Chapter 2), indicating that variation in chronotypes is determined to some degree by genetics. It is therefore likely that genetic diversity, composition, or both, could affect the adaptive capacity of organisms to change phenology. Specifically, if populations have limited variation in circadian rhythm genes, they may not have sufficient genetic or phenotypic variation for selection to act upon for long-term resilience.

In addition to the evidence that there are genetic mechanisms underlying nesting phenology, there also is strong evidence of seasonal declines in fitness (Heath et al. 2012). Typically, individuals who nest earlier have higher reproductive success compared to individuals that nest later in the season (Møller et al. 2008). Earlier nesting individuals may be in better condition and able to secure higher-quality territories or mates compared to later nesting individuals, or seasonal declines in food may contribute to decreased fecundity (Hipfner et al. 2010), or both. Additionally, individuals that nest earlier in the season may have higher survival than later nesting individuals, and hence are more likely to return in subsequent breeding seasons (Chapter 1). If earlier nesters have higher fitness and reproductive timing is heritable (van Noordwijk et al. 1995, Sheldon et al. 2003), then directional selection could result in advances in nesting phenology (Gienapp et al. 2006). However, if seasonal declines in reproductive success or survival are not present (e.g., in the case of seasonal trade-offs) then there may be stabilizing selection that constrains against earlier nesting with climate-driven advancement in springs (Chapter 1).

Carry-over effects (i.e., events in one season affecting events in subsequent seasons, Sherry and Holmes 1996, Webster et al. 2002) from warming winters may be another important, but overlooked, driver of earlier nesting (Williams et al. 2015). For example, warmer winter temperatures may permit birds to remain closer to breeding areas (Berthold et al. 1992, Visser et al. 2009, Smallegange et al. 2010) or to stop migrating altogether (Van Vliet et al. 2009). Shorter migration distances can have carry-over effects on breeding phenology via earlier access to territories or mates (Cristol et al. 1990, Drent et al. 2006), or earlier clutch initiation (Warkentin et al. 1990, Anderson et al. 2016). Warmer winters may also weaken former thermoregulatory constraints, so that individuals attain reproductive condition sooner (McCleery and Perrins

1998), especially in resident birds that maintain mates or territories year-round. Further, assortative mating arising from the temporal segregation of resident and migratory individuals may provide a mechanism for rapid changes in migration strategies and the timing of breeding (Pulido and Berthold 2010).

The mechanisms underpinning shifting avian phenology—and the demographic implications of these shifts—remain elusive, and research can be challenging as trends are likely to occur over time scales that are greater than the period of a single research project. At the same time, there is a pressing need for DoD managers to identify vulnerable species and develop management strategies for systems that are changing relatively rapidly in ecological-time frames. Rigorous and reliable modeling can help us better understand the full annual cycle of birds in a changing environment (Knudsen et al. 2011), make management of DoD species of concern more effective and cost-efficient, and support the objectives of the DoD Coordinated Bird Monitoring Plan (Bart et al. 2012). The individual-based model (IBM) is one tool available for elucidating complex evolutionary and ecological processes in a changing environment. For over 50 years, IBMs have been used in the biological sciences to leverage ecological and evolutionary information, and simulate and track interactions between individuals and their environments over space and time (DeAngelis and Grimm 2014, Shugart et al. 2018). Unlike species distribution models, IBMs harness the decisions made by individuals based on their physiology and interactions, and are flexible to incorporate additional evolutionary mechanisms and environmental layers (Xuereb et al. 2021). In relation to climate change, IBMs have elucidated the roles of individual physiology, plant greening, and photoperiod for migration timing in pink-footed goose (*Anser brachyrhynchus*, Duriez et al. 2009). Another IBM in great tits (*Parus major*) revealed that climate change will likely cause directional selection for consumer-based phenology shifts (Gienapp et al. 2014). While IBMs can reveal some factors that contribute toward phenological shifts across diverse lifeforms, few have incorporated genetic mechanisms into these models to understand resilience to climate change (Seaborn et al. 2021). Genetic-based phenotypic plasticity (e.g., Sauve et al. 2019) and adaptive diversity (e.g., Bossu et al. 2022) are foundational for short- and long-term changes in avian phenology, and therefore are important parameters to consider for IBMs.

A combination of environmental, ecological, and genetic resources is advantageous for developing IBMs that are genetically explicit and capable of exploring both evolutionary and ecological consequences of climate change. American Kestrels (*Falco sparverius*) are a small falcon and one of the most well-studied raptors in North America, with long-term data sets to understand demographics and phenology available from small-scale study sites (e.g., southwest Idaho, USA; Steenhoff and Peterson 2009), to large-scale citizen science nest box programs (e.g., The American Kestrel Partnership, Schulwitz et al. 2021), and citizen science bird monitoring efforts (e.g., eBird, the Breeding Bird Survey, and Christmas Bird Counts). We developed genetic resources for American kestrels, including a reference genome, reduced representation sequencing, and a targeted SNP assay, and showed patterns of neutral and functional diversity across the North American range of American kestrels (Chapter 2, Ruegg et al. 2021, Bossu et al. 2022). Further, we showed that western and eastern American kestrels had different genetic compositions and diversity at functional loci associated with circadian rhythms, which may explain differences in rates of the phenology shifts (Chapter 2).

Here, we developed an IBM called SCOPE (**S**imulation of **C**arry-**O**ver and **P**henological **E**ffects) to evaluate and test these potential mechanisms underlying shifts in bird breeding phenology. Specifically, we tested four hypotheses: 1) composition and diversity within

circadian rhythm candidate genes affect nesting phenology shifts; 2) seasonal timing (mismatch) effects on *nesting success* facilitate earlier nesting; 3) seasonal timing (mismatch) effects on *adult survival* facilitate earlier nesting, and 4) carry-over effects from migration strategy, migration distance, or effect nesting shifts. We developed experiments within SCOPE by inoculating kestrels with different genotypes that varied in composition and diversity, and by turning hypothesized ecological factors on and off within the model. We measured the amount of change in nesting phenology and its effects on population size from 1980 – 2099.

Materials and Methods

Summary model description

A "TRAnsparent and Comprehensive model Evaludation" (TRACE) document providing extensive details to show that the SCOPE model was thoughtfully designed, correctly implemented, thoroughly tested, well understood, and appropriately used for its intended purpose (Schmolke et al. 2010) is available in Appendix 3. Here, we will summarize the model components and processes, and explain our experiments. Our model represented a full-annual-cycle model (Hostetler et al. 2015) consisting of individual kestrels, a virtual landscape representing different North American flyway regions, and landscape patches representing geographic locations (i.e., latitude/longitude values), ecoregion designation (Environmental Protection Agency [EPA] level III ecoregions), carrying capacity, and annual environmental conditions (see below). We integrated Partners in Flight population estimates (Partners in Flight 2020) and eBird relative abundance maps (eBird 2021) to create a raster layer that determines the maximum number of pairs that a patch is capable of supporting to ensure realistic population sizes and incorporate density-dependence in the model (i.e., carrying capacity). Individuals are characterized by a set of static and dynamic attributes, which are outlined in Table 3.1.

The model "starts" on day 1 of a breeding season that spans 212 days. Although the span of 212 days was a longer breeding season than any one individual would experience, it represented the span of time between the pairing of the earliest nesters until the migration departure for the latest nesters (Chapter 1). The non-breeding season events and the passage of 1 year (i.e., year t) occured on day 213 and then the year starts again with day 1. Within the model and during output writing, these tick values were adjusted to realistic days of the year by adding 31 days to calculate dates. We chose to organize time steps in this way because of constraints of the NetLogo software and to simplify programming, as non-breeding season events such as survival and

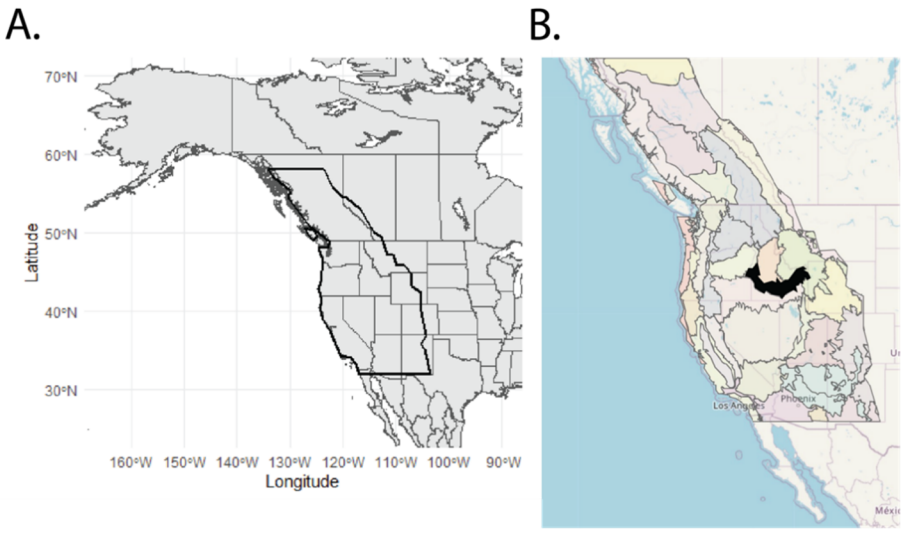

Figure 3.1 A) Map illustrating the western flyway (outlined in black) used in the SCOPE American kestrel model. B) Map illustrating individual ecoregions within the SCOPE model, with the ecoregion used in the genetics experiments (Snake River Plain) outlined in black.

Table 3.1 A list of attributes of individual birds, whether each attribute is static or dynamic, and how attributes are assigned in SCOPE, American kestrel version.

Bird Attributes	Status	Assignment
Sex	Static	Randomly assigned
Age	Dynamic	Increases each year by 1
Hatch date	Static	Date an individual hatched (randomly assigned for 1st generation)
Genotype for *top1*, *peak1*, *nacc2*, *mybbo1a*, *scn5a1*, *cpne4*, *cry1* genes	Static	Inherited from parents via Mendelian inheritance (experimentally assigned for 1st generation)
Migration strategy (migrant or resident)	Dynamic	Depends on latitude and winter minimum temperature anomaly
Migration distance	Dynamic	Depends on latitude and winter minimum temperature anomaly
Date of availability	Dynamic	Depends on migration distance (migrants), the extended spring index (SI-x, residents), and genotype (both migrants and residents)
Egg-laying date	Dynamic	Depends on the date of availability, and locating a nest site and mate
Mismatch	Dynamic	Difference between egg-laying date and SI-x
Early?	Dynamic	Whether or not an individual laid eggs before the median date of mismatch (17 days before SI-x)
Nest success and productivity	Dynamic	Depends on mismatch, longitude, latitude, and interactions among these variables
Probability of survival (juvenile)	Dynamic	Depends on hatch date, sex, and minimum winter temperature anomalies
Probability of survival (adult)	Dynamic	Depends on Early?, sex, and minimum temperature anomalies
Breeding dispersal distance and direction	Dynamic	Drawn from distribution
Natal dispersal distance and direction	Dynamic	Depends on sex, maximum temperature anomalies in August, and latitude
Long-distance disperser?	Dynamic	Drawn from distribution for hatch-year individuals
Parent identity	Static	Identity of both parents
Parent availability	Static	Date of availability for both parents
Mating status (mate or floater)	Dynamic	Depends on whether an individual finds an available mate

mortality could occur in a single time step. Simulations were run between 1980 – 2099. Additionally, we included the option for a burn-in period of 10, 15, or 20 years to allow the simulated kestrel population to reach a stable state.

The original version of SCOPE was developed to cover the range of American kestrels breeding in the western United States and Canada, or the western flyway region (Figure 3.1). The second version of SCOPE was developed for the eastern flyway and covers eastern North

America (Figure 3A.1). Although model coverage did not contain the full range of American kestrels in North America, it covered areas where there were reliable data for parameter estimates and where there were different apparent kestrel responses to climate change. Specifically, the flyway maps are based on the United States and Canada border, band return data from the USGS Bird Banding Lab, and a spatially-explicit map of kestrel population genetic structure (Ruegg et al. 2021). The flyway was composed of 28.5 km^2 patches. Patch size was based on the resolution of Regional Climate Models (RCMs) used to represent climatic conditions in the model. Each patch contained information about latitude, longitude, ecoregion, August maximum temperature anomaly, the extended spring estimate (SI-x), winter minimum temperature anomaly, and the number of pairs that a patch can support. Patch attributes were derived from raster files imported at initialization or annually, depending on the layer. Patches were grouped into Environmental Protection Agency (EPA) level III ecoregions. The spatial input and output scale of the model was set to 1 or more ecoregions per run. Output was printed at the individual level (best for genetic experiments) or patch level. Patch-level output reported average, min, and max values for all individuals within a patch and is preferable for large-scale (i.e., more than one ecoregion) experiments.

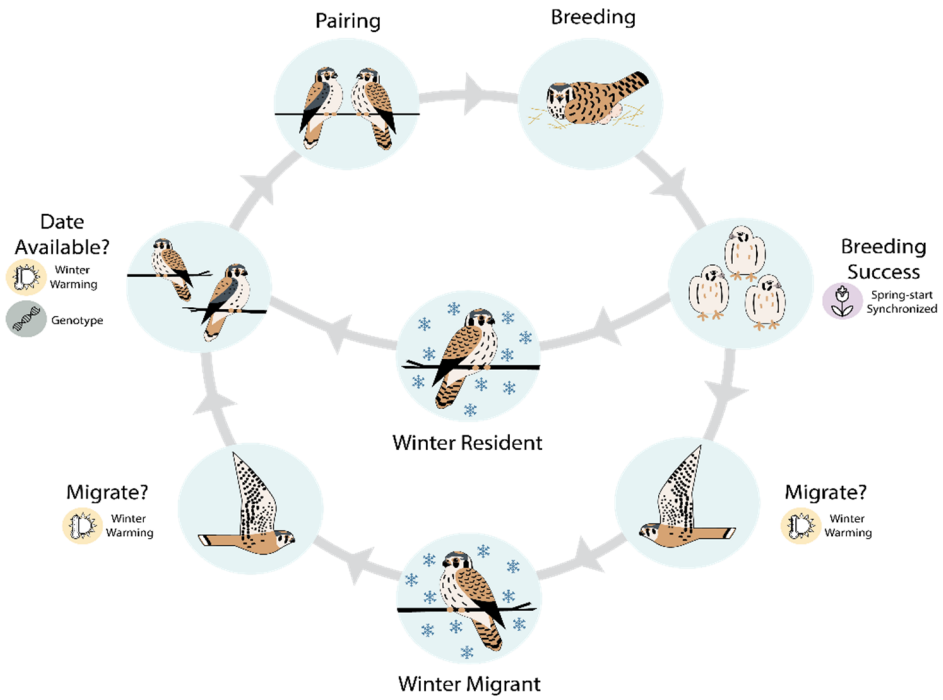

Figure 3.2 Simplified flow diagram of main model processes in the SCOPE model for American kestrels within the context of an avian annual cycle. Distinct paths represent the cycle of migrants and residents. Icons represent environmental input.

The model approximated the annual cycle of the American kestrel (Figure 3.2, Figure 3A.3). During the breeding season, individuals tracked their availability date; this was analogous to reproductive readiness. Date of availability depended on genotype and, for migrants, migration distance. For residents, date of availability depended genotype and environmental cues of spring (SI-x). If a male was available for breeding, males dispersed (Appendix 3) to a breeding patch that had the capacity for nesting and set their availability to true. Females that reached their date of availability dispersed (Appendix 3) to a patch with an available male that had not paired with a female and set their availability to true. If no available and unpaired males existed on the landscape, the female moved her available date to one day in the future and repeated the pairing process in the subsequent time-steps. Individuals that were unsuccessful at

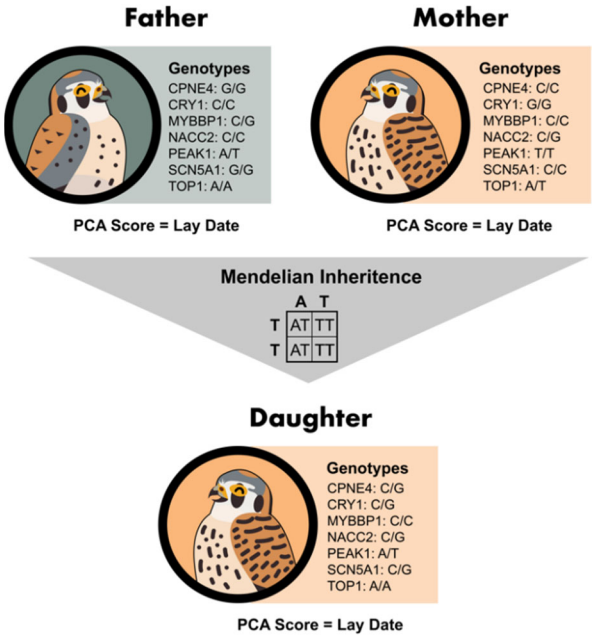

Figure 3.3 Inheritance of candidate gene alleles in the SCOPE model for American kestrels. Offspring inherit their parents' alleles following Mendelian inheritance patterns.

pairing remained in the population as non-breeding 'floaters.' Once paired, individuals set an egg-laying date. Paired females determined their probability of nest success based upon their egg-laying date in relation to the SI-x and geographic location. If the nest was successful, then the number of offspring for that nest was determined. These offspring were randomly assigned as male or female, tracked the egg-laying date of their parents, and whether or not they were from an early or late nest (i.e., the egg-laying date was before or after the SI-x of the patch where they hatched). Offspring inherited their parents' genotype following a Mendelian inheritance process (Figure 3.3). At the beginning of the non-breeding season, the age of each individual was increased by 1, their date of availability and migration distance were reset and the climate and environmental conditions for that year were determined.

The probability of surviving to the following year was determined for each individual on the last day of the annual cycle. For juveniles, survival probability was dependent on whether they were from an early or late nest, their sex, and the winter minimum temperature anomaly (Chapter 1). For adults, survival probability was dependent on their egg-laying date, whether they were successful, their sex, and winter minimum temperature anomaly (Chapter 1). Individuals then updated their migration strategy (whether to migrate or remain as a resident) based upon minimum winter temperature and breeding latitude (Appendix). For migrants, distance to the wintering grounds was determined in response to the minimum winter temperature anomaly and their breeding latitude (Heath et al. 2012).

Simulated individuals in SCOPE sensed the climate and vegetation phenology (i.e., extended spring index) conditions in the patch that they reside in, and these conditions were used to inform different SCOPE submodels (e.g., timing, movement, and demographic rates). To forecast changes in weather, we used RCM data from the NA-CORDEX project (Mearns et al. 2017) that was bias-corrected using the Daymet historical gridded dataset (Thornton et al. 1997). This bias-correction provides continuity between the historical climate data used to parameterize bird-weather-vegetation phenology relationships, and future changes in climate. We obtained climate data for representative concentration pathways (RCPs) 4.5 from 1 RCM, and RCP 8.5 from 12 RCMs (Table 3A.2) NA-CORDEX projections used in SCOPE were converted from netcdf format into annual raster layers.

Several key patterns emerged from this model. With warming winter temperatures, migration propensity and distances decreased. For migrants, shorter migration distances resulted in advancing availability dates in the spring. Additionally, warming winters had a positive effect on annual survival rates for adults and juveniles. Resident individuals that remained year-round on their breeding grounds tracked earlier springs, which advanced their date of availability.

Together, these changes resulted in overall advances in breeding phenology, and a pattern of assortative mating (i.e., migrant-migrant, resident-resident pairs) emerged as resident and migrant individuals shift their timing in the spring at different rates. Further, selection for earlier nesting created changes in allele frequencies over time. Finally, because we set carrying capacity levels within patches, at high densities individuals must compete for nest sites and mates. This density-dependent effect created an additional driver and selection for earlier nesting.

We compared model output under the RCP 4.5 scenario to known empirical patterns of American kestrel ecology to assess the ability of SCOPE to capture the fundamental drivers of system dynamics (Wiegand et al. 2003, Grimm et al. 2006) and assessed the sensitivity of the model to individual parameters. We used the western version of the SCOPE model for pattern matching and sensitivity analyses and ran the model at the full flyway scale. For details on the pattern matching procedure or sensitivity analyses, see the corresponding TRACE documentation (Appendix 3).

Genetic and evolution experiments

We ran four experiments to test the effects of genetic composition and diversity on nesting phenology shifts. In the first experiment (western seed), we seeded the first generation of individuals so that the population's allele frequencies matched the current (2016 – 2020) allele frequencies of western kestrels at the *top1*, *peak1*, *nacc2*, *mybbp1a*, *scn5a1*, *cpne4*, and *cry1* loci. In the second experiment (eastern seed), we seeded the first generation of individuals so that the population's allele frequencies matched the current (2016 – 2020) allele frequency of eastern kestrels at the *top1*, *peak1*, *nacc2*, *mybbp1a*, *scn5a1*, *cpne4*, and *cry1* loci. In the third experiment (heterozygous seed) each individual was heterozygous at all alleles, to show the impacts of maximized diversity. In the last experiment (no genetics), all genetic and heritability effect values were set to zero. We predicted that the allele frequency seed of the original population would affect the advancement of egg-laying dates over time and that models without genetic effects would not advance as quickly as models with genetics turned "on".

These experiments were run at RCP 8.5 across the full western scale of the SCOPE model. We used a 20-year burn-in period and ran models from 1980 until 2099. We ran 20 replicates of each experiment at the flyway scale. Output was produced at the individual level for Snake River Plain ecoregion only. Changes in allele frequencies, advancement of egg-laying dates, and population sizes were recorded for each experiment.

Life history and carry-over experiments

We ran eight experiments to investigate the effects of climate, genetic, and ecological mechanisms on nesting phenology. The first model scenario was the baseline western model that matched real-world patterns with all-climate, genetic, and ecological factors turned "on". We tested hypotheses by removing effects and comparing altered scenarios to the baseline. To turn "off" an effect, we set effect values to zero. Additional scenarios consisted of:

1) turning all climate, genetic, and ecological factors "off "(static model with no climate change)
2) turning the effect of mismatch on nesting success "off"
3) turning the effect of mismatch and winter temperatures on adult and juvenile survival "off"
4) turning the effect of winter temperature on migration strategy "off"
5) turning the effect of winter temperature on migration distance "off"
6) turning genetic and heritability of egg-laying "off"

7) and the final scenario was a baseline run of the eastern kestrel version, with all factors "on". We compared model outputs to the baseline model to evaluate the effects of turning different mechanisms off. Because of the stochastic nature of SCOPE, each scenario was replicated 20 times.

We focused on general trends and effect size of experiments rather than statistical significance because classical hypothesis-testing statistics may be misleading with simulated data (White et al. 2014). Credible intervals of 95% were calculated from linear models of the parameter of interest changing over time.

Results and Discussion

Model development

We successfully developed a full flyway-scale model for American kestrels that incorporated genetic and life-history traits, and evolutionary and ecological processes. Patterns from SCOPE simulations from 1980 – 2019 matched observed patterns of nesting phenology shifts, average nest success, and productivity from a long-term study in southern Idaho over those same years. Further, we matched flyway-wide patterns of migration distances and distance changes, and ecoregion population trends (Figure 3A.5). Finally, we developed a set of assumptions and criteria to consider when developing an IBM with functional genetics (Appendix 3). While the genetic basis of phenological traits has been explored, it is difficult to understand the demographic and phenological ramifications of this functional diversity over time. To date, functional genetic information has been incorporated into IBMs in two ways: 1) quantitative approaches, through parameterizing the heritability of phenotypic traits (e.g. Piou and Prevost 2012), and 2) through the addition of genetic markers that can be passed down from one generation to the next in simulations (e.g. Hogg et al. 2020). This is the first IBM to represent allele inheritance, functional effects on traits (nesting phenology), and selection pressures at a large spatial and temporal scale with realistic dispersal patterns and processes. Specifically, we explicitly represented allele diversity in loci of genes that have single- and multi-gene effects on nesting phenology. Rarely are traits underpinned by a single locus of large effect (Tam et al. 2019); therefore, developing modeling approaches to understand how these mechanisms work will be advantageous to ecologists and geneticists alike.

Genetic and evolutionary experiments

We recorded genotypes of American kestrels within the Snake River Plain ecoregion for four different experiments where initial populations were seeded with different allele frequencies (Western, Eastern, Heterozygous) or genetic effects were turned off. Over the span of the simulated time period (i.e., 120 years), both allele frequencies (Table 3.2, Figure 3.4) and heterozygosity (Table 3.3, Figure 3.4) changed, except in the case where genetics and heritability were turned off. In the western, eastern, and heterozygous seed experiments, all loci trended towards fixation for alleles favorable for earlier egg-laying dates, with *cpne4*, *cry1*, *mybbp1a*, *peak1*, and *top1* trending towards fixation for major or minor alleles (Figure 3.4). These shifts in allele frequencies were consistent across all experiments with genetic effects activated, regardless of seeded allele frequencies.

In population genetic theory, changes in allele frequencies are hypothesized to occur faster than heterozygosity, and as such are the first signs of shifting dynamics of populations (Schwartz et al. 2007). In the SCOPE model, we see a rapid shift in allele frequencies across all seven loci in a 120-year period, with many alleles going to fixation and heterozygosity

subsequently decreasing over time. In the SCOPE model, a decrease in heterozygosity indicates strong selection for adaptive loci. Because selection within the model is acting on only seven loci, and it is likely that empirical egg-laying date is a polygenic trait based on many more loci of small effect than represented in this model, we anticipate that changes in allele frequencies will occur faster than in empirical populations (Slate 2013). Allele frequencies and heterozygosity in the experiment with no genetic effects or heritability did not significantly change throughout the experiment. Unlike small populations that will have stochastic changes in allele frequency due to chance (Masel 2011), the large populations in the American kestrel SCOPE model are robust to genetic drift. This indicates that changes in allele frequency in the western, eastern, and heterozygous experiments are driven by directional selection (Hadfield and Reed 2022).

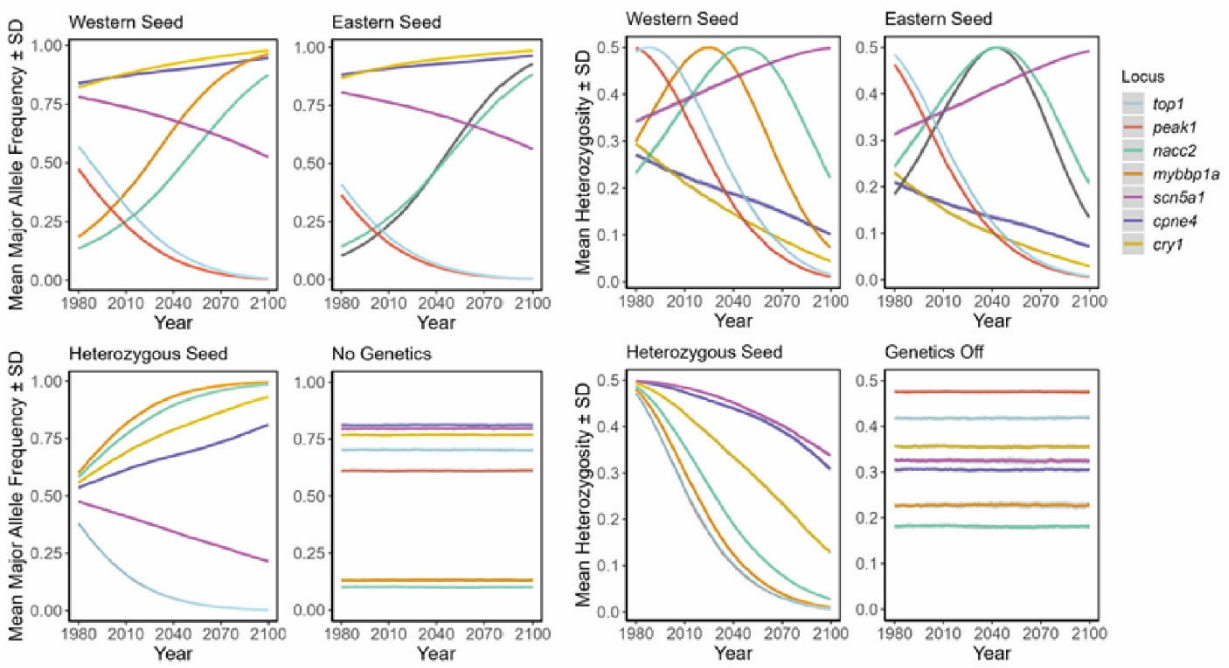

Figure 3.4 Average and standard deviation of major allele frequencies (left) and heterozygosity (right) at seven loci within circadian rhythm candidate genes from 1980 – 2099 for four different experiments seeded with different first-generation allele frequencies or with the genetic effects turned off in SCOPE.

Table 3.2 Major allele frequencies (mean across 20 model iterations ± SD) for seven candidate gene loci during the beginning (1980) and end (2099) of the SCOPE model for four different experiments: western, eastern, and heterozygous seeds, and one experiment where genetics was turned off.

	Western Seed		Eastern Seed		Heterozygous Seed		No Genetics	
Locus	1980	2099	1980	2099	1980	2099	1980	2099
cpne4	0.84 ± 0.00	0.95 ± 0.00	0.88 ± 0.00	0.96 ± 0.00	0.54 ± 0.00	0.81 ± 0.01	0.81 ± 0.01	0.81 ± 0.00
cry1	0.82 ± 0.00	0.98 ± 0.00	0.87 ± 0.00	0.99 ± 0.00	0.56 ± 0.01	0.93 ± 0.00	0.77 ± 0.00	0.77 ± 0.01
mybbp1a	0.18 ± 0.00	0.96 ± 0.00	0.10 ± 0.00	0.93 ± 0.00	0.60 ± 0.00	0.99 ± 0.00	0.13 ± 0.00	0.13 ± 0.01
nacc2	0.13 ± 0.01	0.87 ± 0.01	0.14 ± 0.00	0.88 ± 0.01	0.58 ± 0.01	0.99 ± 0.00	0.10 ± 0.00	0.10 ± 0.00
peak1	0.47 ± 0.01	0.01 ± 0.00	0.36 ± 0.00	0.00 ± 0.00	0.38 ± 0.00	0.00 ± 0.00	0.61 ± 0.00	0.61 ± 0.01
scn5a1	0.78 ± 0.00	0.53 ± 0.01	0.81 ± 0.00	0.56 ± 0.01	0.48 ± 0.01	0.22 ± 0.00	0.80 ± 0.00	0.80 ± 0.01
top1	0.57 ± 0.01	0.01 ± 0.00	0.41 ± 0.00	0.00 ± 0.00	0.38 ± 0.01	0.00 ± 0.00	0.70 ± 0.01	0.70 ± 0.01

Table 3.3 Average heterozygosity (mean across 20 model iterations ± SD) for seven candidate gene loci during the beginning (1980) and end (2099) of the SCOPE model for four different experiments: western, eastern, and heterozygous seeds, and one experiment where genetics was turned off.

	Western Seed		Eastern Seed		Heterozygous Seed		No Genetics	
Locus	1980	2099	1980	2099	1980	2099	1980	2099
cpne4	0.27 ± 0.00	0.10 ± 0.00	0.21 ± 0.01	0.07 ± 0.00	0.50 ± 0.00	0.31 ± 0.01	0.31 ± 0.01	0.31 ± 0.00
cry 1	0.29 ± 0.00	0.04 ± 0.00	0.23 ± 0.00	0.03 ± 0.00	0.50 ± 0.00	0.13 ± 0.00	0.36 ± 0.00	0.36 ± 0.01
mybbp1	0.30 ± 0.00	0.07 ± 0.00	0.18 ± 0.01	0.14 ± 0.00	0.48 ± 0.00	0.01 ± 0.00	0.23 ± 0.01	0.23 ± 0.01
nacc2	0.23 ± 0.01	0.22 ± 0.01	0.24 ± 0.00	0.21 ± 0.01	0.49 ± 0.00	0.03 ± 0.00	0.18 ± 0.00	0.18 ± 0.01
peak1	0.50 ± 0.00	0.01 ± 0.00	0.46 ± 0.00	0.01 ± 0.00	0.47 ± 0.00	0.01 ± 0.00	0.48 ± 0.00	0.48 ± 0.00
scn5a1	0.34 ± 0.00	0.50 ± 0.00	0.31 ± 0.00	0.49 ± 0.00	0.50 ± 0.00	0.34 ± 0.00	0.33 ± 0.00	0.32 ± 0.01
top1	0.49 ± 0.00	0.01 ± 0.00	0.48 ± 0.00	0.01 ± 0.00	0.47 ± 0.00	0.01 ± 0.00	0.42 ± 0.00	0.42 ± 0.01

In addition to information about genetic change over time, we recorded ecological changes of kestrels in the Snake River Plain ecoregion during the genetic experiments. Egg-laying dates advanced in all SCOPE genetic experiments (Figure 3.5). The fastest egg-laying date advancement occurred in populations seeded with western alleles (mean slope: -0.210, 95%: -0.212 – -0.208) and the smallest negative slope occurred in the experiment with no evolutionary mechanisms (mean slope: -0.117, 95%: -0.119 – -0.116). Differences in the rate of phenology shifts amongst western, eastern, and heterozygous seeding experiments were small (a difference of one day over 20 years between the western seed and heterozygous seed experiments). Though these results suggest that allele frequency at these putatively functional markers can impact the advancement of egg-laying dates, the difference in effect sizes between different experiments (i.e., allele frequencies) are relatively small. Importantly, the inclusion of evolutionary mechanisms in SCOPE improved the realism of the model and generated results that better represent empirical advancement rates in the Snake River Plain study field site, compared to the genetics off experiment. This provides a powerful example of how evolutionary mechanisms—including genetic markers—can improve the predictive power of IBMs (Seaborn et al. 2021). Further, given the evidence that these same markers reflect migratory chronotypes (Chapter 2) and that the biological clocks are highly conserved (Bradshaw et al. 2007, Krabbenhoft et al. 2014), these markers may be important in understanding genetic constraints to the adaptive capacity of other migratory

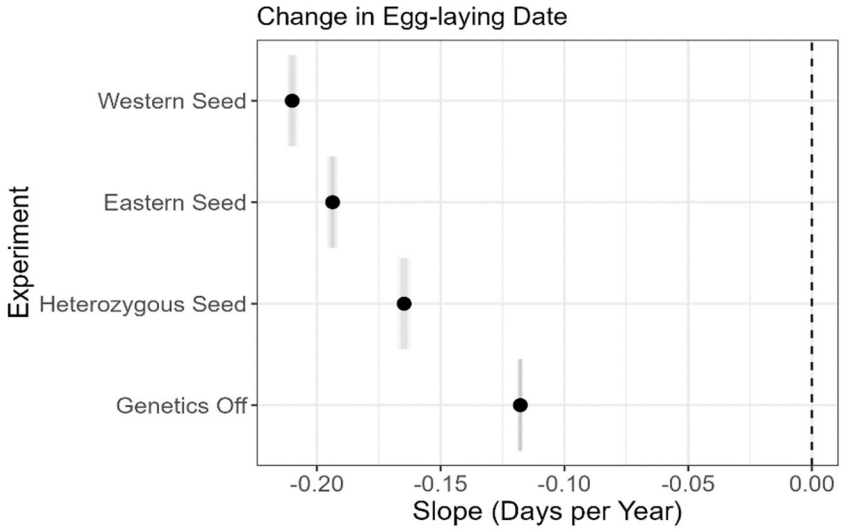

Figure 3.5 Average slope (days per year, dark circle) and standard error (gray line) of egg-laying date shifts from 1980 – 2099 for American kestrels in the Snake River Plain ecoregion of the western SCOPE version for four genetic experiments.

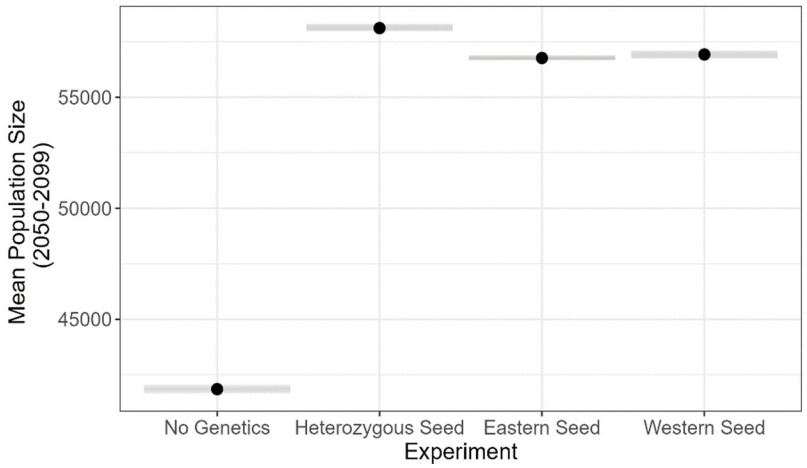

Figure 3.6 Average population size (dark circle) and standard error (gray line) of American kestrels in the Snake River Plain ecoregion in the last 49 years of a 120-year simulation in the western SCOPE model for four different genetic experiments.

birds or vertebrates. Specifically, in large populations, genetic composition and diversity may not limit the adaptive capacity of species responses to climate change and earlier springs. However, this may not be the case for smaller populations that may have very limited genetic diversity (Willi et al. 2009)

Population size in the final 49 years varied significantly between all experiments, with population size being largest with heterozygous seed (average ± SD = 60,552 ± 4474.254 individuals) and smallest in the genetics off experiment (average ± SD = 44,376 ± 5137.40 individuals, Figure 3.6). It is unclear why the heterozygous seed experiment had a higher population size in the final years of the experiment compared to the western and eastern seed experiments. However, like the rate of egg-laying advancements, the differences between the "seeded" experiments are small (< 2000 individuals). Experiments with evolutionary mechanisms included (i.e., the genetic seed experiment) had similar population sizes in comparison to the model with no genetics or heritability included (Figure 3.6). The experiments with evolutionary mechanisms provided an additional opportunity for populations to select for adaptive traits, allowing for higher survival, productivity, and population sizes. Further, populations were smaller in the genetics off experiments because the slow rate of egg-laying date advancement and increased mismatch had negative effects on productivity and adult survival compared to the "seeded" experiments.

In sum, genetic composition and diversity did not limit egg-laying date advancement from 1980 – 2099. Strong fitness advantages of "early" nesting individuals compared to "later" nesting individuals created strong directional selection for early nesting, and allele frequencies trended toward fixation of an early chronotype. Experiments performed here do not support the hypothesis that genetic diversity or composition of eastern American kestrels are constraining their ability to nest earlier (Chapter 2).

Life history and carry-over experiments

We ran seven experiments at the full flyway scale and output data at the patch-level to summarize changes across the western range and one experiment across the eastern range. We considered the model with all effects "on" as the baseline model. We considered another experiment with all the climate and genetic effects "off" as a static-environmental model (i.e., no climate change). In the remaining experiments, we turned off different effects of the environment or traits one-by-one to test hypotheses (see above). We examined effects on egg-laying dates, nest success, population size, and adult survival.

The rate of egg-laying date change was affected by the experimental scenario (Figure 3.7). In the baseline model, individuals advanced their nesting by 0.215 (95%: -0.216 – -0.215) days per year over the course of 120 years. With climate change turned off, egg-laying dates did not advance over time (mean slope: 0). Interestingly, when the effect of phenological mismatch on nesting success was turned off, kestrels advanced egg-laying dates at a faster rate (mean slope: -0.233, 95%: -0.233 – -0.232) compared to the baseline scenario. With the effect of phenological mismatch on productivity turned off, kestrels had higher nesting success (Figure 3.8) and the population size grew larger than any other scenario (Figure 3.9). At higher population sizes there was higher competition for mates and nest sites compared to lower population sizes. This density-dependent effect created additional selection pressure to nest earlier, thus driving the faster advancement of nesting. This result was unexpected because the effect of mismatch on nesting success and productivity is thought to be one of the main drivers

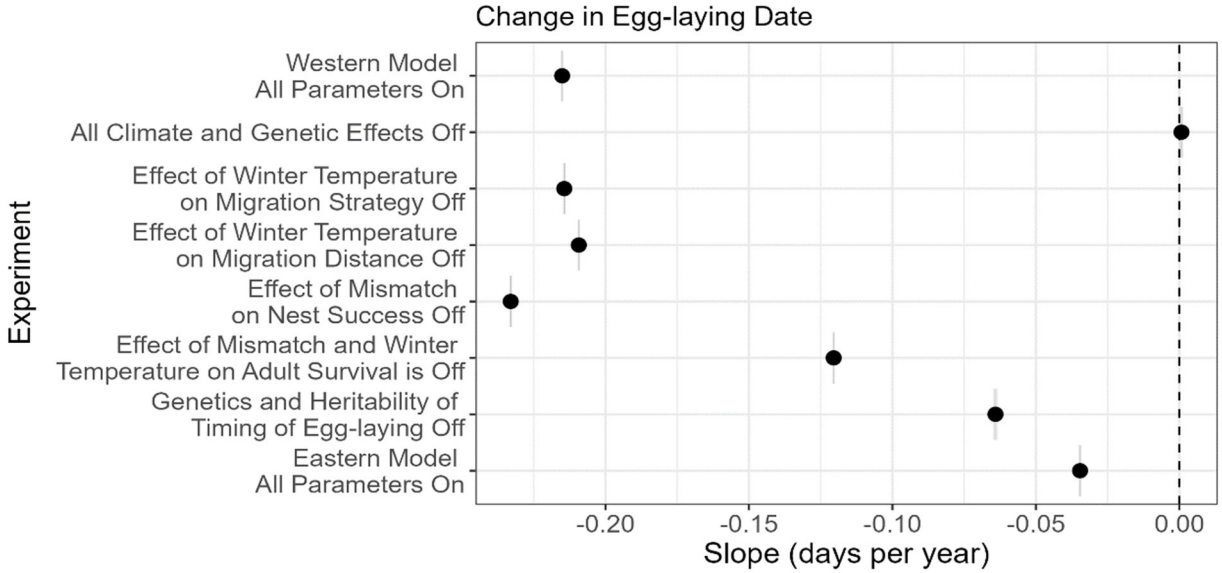

Figure 3.7 Average change in egg-laying date per year (dark circle) and standard error (gray line width) of American kestrels during a 120-year (1980 – 2099) simulation for eight different ecological experiments. More negative values reflect faster advancement of egg-laying dates compared to no shift (0 value).

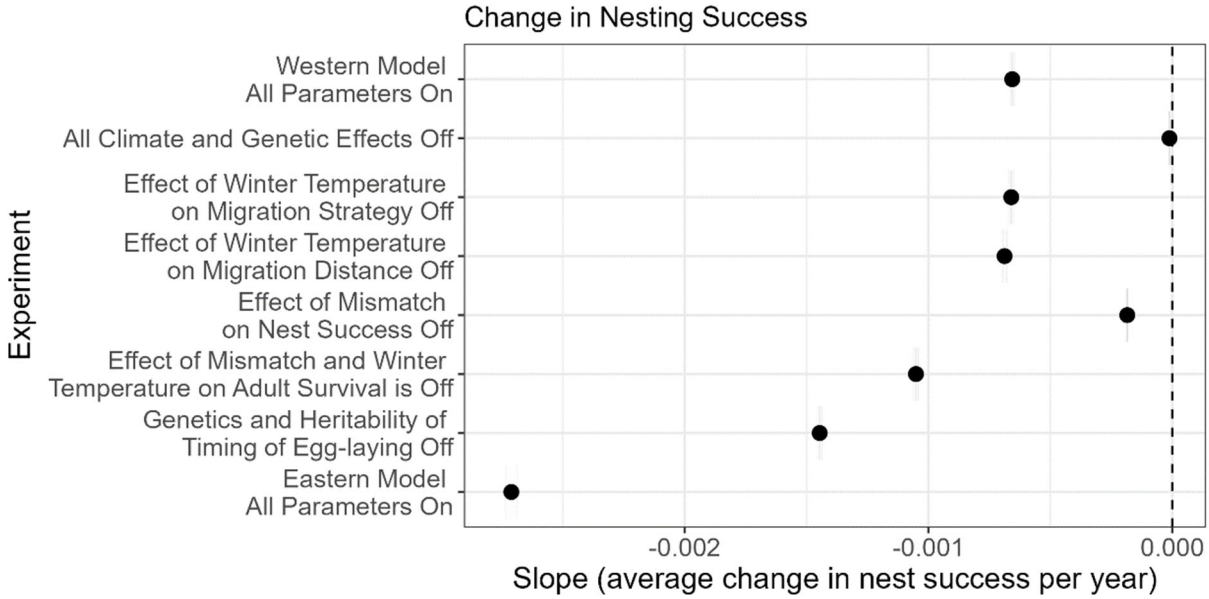

Figure 3.8 Average change in nesting success (dark circle) and standard error (gray line) of American kestrels during a 120-year simulation (1980 – 2099) for eight different ecological experiments. More negative values represent a faster decline in nesting success compared to no change (0 value).

of earlier nesting (Perrins 1970, Verhulst and Nilsson 2008). However, if populations are declining because of mismatch effects on nest success or productivity, then it is less likely that density-dependent effects, such as competing for nest sites or mates, would drive earlier nesting. Thus, contrary to current belief, the effect of phenological mismatch on productivity may not be the main driver of earlier nesting. Instead, phenological mismatch effects on productivity may

slow phenological advancement because of negative effects on productivity and decreased population sizes that reduce density-dependent drivers for earlier nesting. For example, when the phenological mismatch effect on nest success was turned "on" in the model (i.e., baseline experiment) it slowed the rate of advancement compared to the effect of mismatch on nesting success turned "off".

In general, adult survival increased in experimental runs because of increasing winter minimum temperatures (Figure 3.10). Interestingly, when the effects of phenological mismatch and minimum temperatures on adult and juvenile survival were removed, the rate of egg-laying advancement drastically slowed (Figure 3.7), suggesting that mismatch effects on survival are important drivers of earlier nesting, even more so than the effects of phenological mismatch on productivity. This conclusion is further supported by the results from the eastern flyway model. The eastern model has similar sub-models to the western model, with the exception of the survival model which reflects the seasonal trade-off between productivity and adult survival discussed in Chapter 1 (Figure 1.10). In this case, successful adults that nest earlier, have lower survival than successful adults that nest later. The trade-off between survival and reproduction constrained egg-laying advancement (Figure 3.7), resulting in declining nest success (Figure 3.8) as individuals became more mismatched, and populations declined. Results from SCOPE reinforce that seasonal trade-offs are likely to limit changes in nesting phenology and may be a reliable indicator of phenological vulnerability in migratory birds.

Interestingly, turning off the effects of temperature on migration distance and turning off the effects of temperature on migration strategy did not significantly slow the egg-laying date advancement rate (Figure 3.8). Carry-over effects from migration have been purported to be a constraint for nesting earlier. However, these results suggest that individuals can overcome these constraints as long as there are genetic mechanisms (heritable chronotypes) and directional selection through seasonal declines in fitness. Not all migratory birds may be vulnerable to phenological mismatch just because a migration stage precedes nesting.

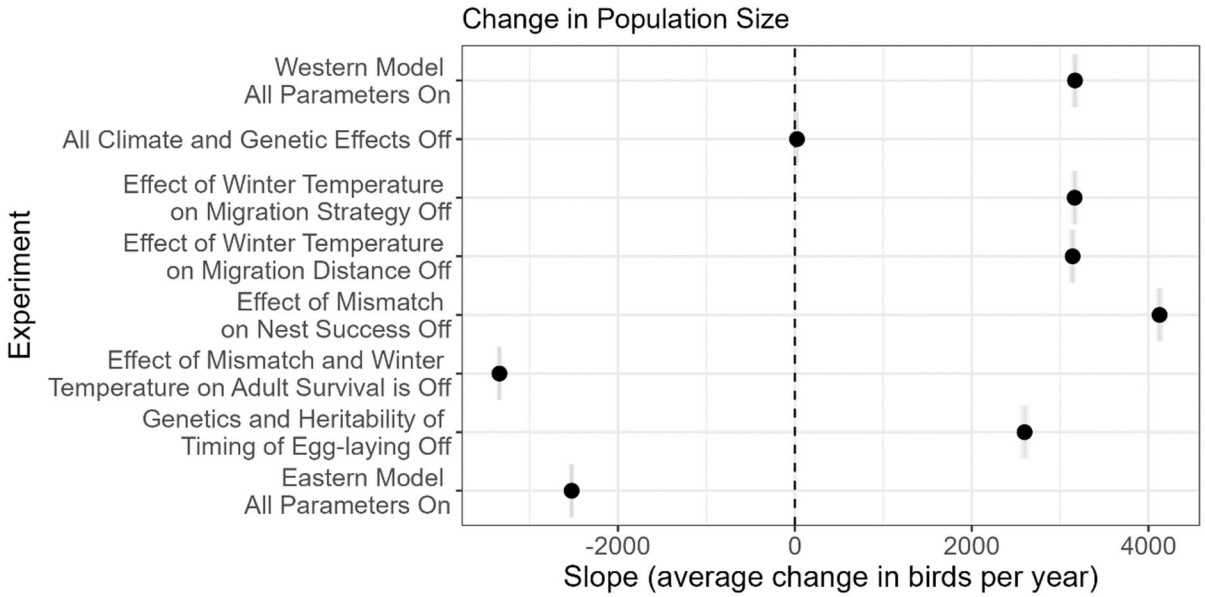

Figure 3.9 Average change in population size (dark circle) and standard error (gray line) of American kestrels during a 120-year simulation (1980 – 2099) for eight different ecological experiments. More negative values represent a decline in populations and more positive values represent population growth.

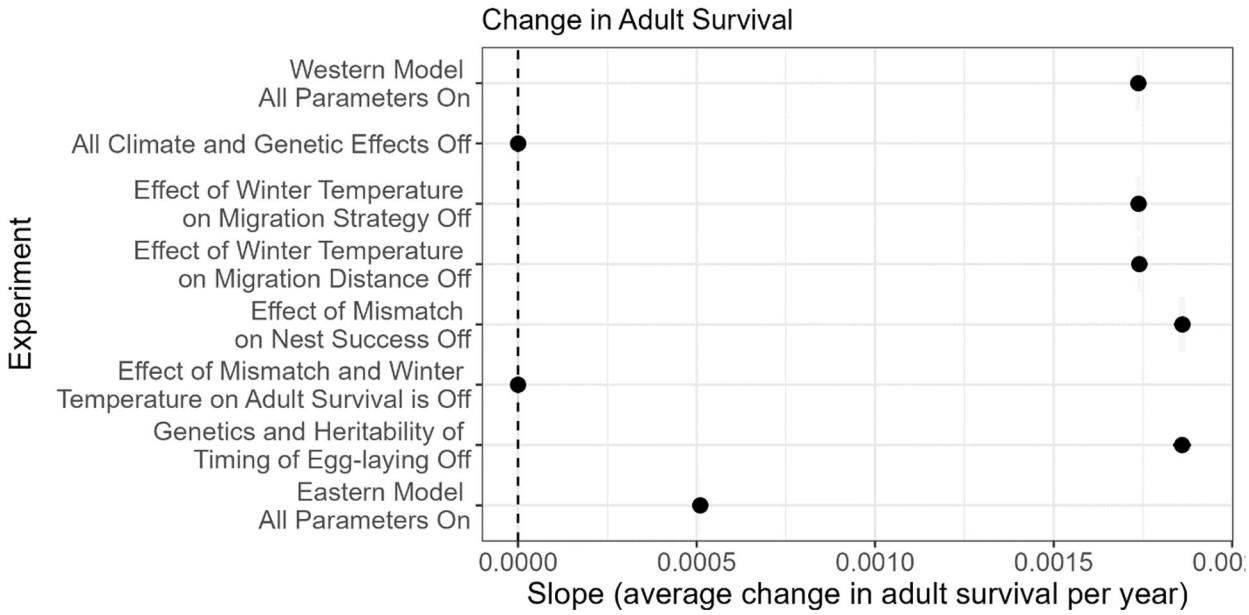

Figure 3.10 Average change in adult survival (dark circle) and standard error (gray line) of American kestrels during a 120-year simulation (1980 – 2099) for eight different ecological experiments. More positive values represent an increase in adult survival compared to no change (0 value).

Finally, similar to the individual results in the Snake River Plain ecoregion experiment, if we turned off the genetic and heritability components in SCOPE, egg-laying dates did not advance quickly (Figure 3.8) and nesting success decreased (Figure 3.9). However, population sizes stayed stable (Figure 3.10), most likely because of higher adult survival (Figure 3.11) from warmer winter temperatures. The implementation of explicit genetic traits in the model was important for representing evolutionary processes. Without those processes, there was still some advancement in egg-laying date, most likely because each year individuals with early availability were most likely to find a nest site and mate.

Overall, if simulated populations did not advance their egg-laying date, nesting success declined as mismatch increased. Even within our base model, which had a relatively rapid rate of nest advancement, nesting success declined over time. However, population growth rates were positive in all scenarios where warmer winter temperatures led to higher adult (and juvenile) survival rates, with the exception of the eastern scenario model. Though adult survival increased over time in the eastern scenario, it was not enough to compensate for declines in nesting success caused by increasing phenological mismatch.

Conclusions and Implications for Future Research/Implementation

We aimed to build an IBM using field data we collected on the genetic correlates and fitness consequences of nesting phenology to test hypotheses about genetic and ecological mechanisms underlying nesting phenology shifts. We fulfilled that objective and tested our research hypotheses. Specifically, we found no evidence that, in large populations, composition or diversity within circadian rhythm candidate genes limited nesting phenology shifts. If ecological patterns (seasonal declines in nesting success and adult survival) were present, allele frequencies quickly trended towards earlier nesting phenotypes. This conclusion may not be true for all populations, though. For example, if populations experienced a bottleneck and were significantly smaller (e.g., <500 individuals), some of these alleles may move towards fixation

because of drift, as opposed to selection (Masel 2011). While populations of American kestrels have seen recent declines—especially in eastern North America (McClure et al. 2021, McClure and Schulwitz 2022)—we anticipate that populations have not experienced population bottlenecks at this point that will cause drift at these loci. However, our model could be modified to test this idea for kestrels or other species.

We found mixed support for the hypotheses that mismatch drives nesting phenology shifts. There was no evidence that mismatch effects on nesting success facilitated earlier nesting. In fact, mismatch effects on nesting success *slowed* the rate of egg-laying date advancement. This was because mismatch has negative effects on nesting success, leading to lower population sizes and reduced competition for mates and nest sites. However, when nesting success was not affected by mismatch, individuals had higher nesting success and population sizes grew leading to increased competition for nest sites and mates, which was a strong driver of earlier nesting. These results were very surprising because the effects of mismatch on productivity is one of the predominant hypotheses explaining earlier nesting (Perrins 1970, Verhulst and Nilsson 2008). Only through having "complete" knowledge of individual behavior and population patterns via SCOPE, were we able to identify these interactive mechanisms. The same finding would be difficult to demonstrate in a field setting and take many years of high-effort work.

We did find strong support that mismatch effects on adult survival were a strong factor driving the advancement of nesting phenology. The effects of mismatch on survival have not been studied as much as the effects on productivity, in part because survival studies are very data-intensive (Reed et al. 2013, Tarwater and Beissinger 2013, Bastianelli et al. 2021). However, it is reasonable to consider survival impacts given the energetic costs of raising young in areas or years with low food supply (Nilsson and Svensson 1996, Thomas et al. 2001, Reed et al. 2013). Further, the parallel pattern of seasonal declines in both productivity and survival was important for advancing egg-laying dates in the west (see baseline experiment). In our eastern experiment, seasonal trade-offs between productivity and survival constrained the advancement of egg-laying dates and caused the population to decline. The SCOPE model provided the ability to directly compare two hypotheses to explain why eastern American kestrels are not advancing their egg-laying dates: 1) lack of genetic diversity, or 2) seasonal trade-offs between reproduction and survival. Results clearly demonstrate that seasonal trade-offs constrain phenology shifts and eastern kestrels are not limited by genetic diversity (see Eastern Seed experiment).

While SCOPE enables several new insights into mechanisms underlying phenology shifts, there are some limitations to the model. For example, we are cautious about interpreting the flyway-wide decline of kestrels in the eastern part of North America. The pattern of seasonal trade-offs between reproduction and survival comes from survival data collected at one long-term study site in New Jersey, but was used to populate all of the eastern model. These trade-offs may not exist throughout the eastern flyway. Similarly, we used long-term data from our Idaho site to populate survival parameters for all of the western flyway model. This extrapolation may not represent sites at northern or high elevation latitudes where short breeding windows may create seasonal trade-offs. More information about survival, and how mismatch effects survival, across a spatial range is needed. In addition to extrapolation issues, SCOPE does not explicitly include habitat quality or changes in drastic weather events, like early spring snow storms, both of which could affect phenology shifts and population resilience.

Despite model limitations, we created new knowledge about the mechanisms underlying phenology shifts. Specifically, the effect of phenology mismatch on adult survival, competition

for nest sites and mates, and evolutionary processes are key mechanisms driving earlier nesting. The effect of phenological mismatch on nesting success was not a stronger driver of earlier nesting, and migration was only a weak constraint to earlier nesting. In addition to this new knowledge, these experiments provide DoD land managers insight into populations that are resilient to and those that are vulnerable to climate-driven phenological mismatch. Results from SCOPE experiments reinforce the risk assessment and management recommendations in Chapter 1. Specifically, large populations that lack seasonal trade-offs in reproduction and survival are likely to be resilient. Whereas large populations that have seasonal trade-offs between reproduction and survival, declining populations where competition for nest sites and mates is decreased, or small populations with limited genetic potential are likely to be vulnerable to mismatch. Finally, the development of SCOPE resulted in novel methodological approaches for integrating genetic and ecological information into models that simulate both evolutionary and ecological processes, which is an important advancement for understanding and predicting population responses to environmental change and increases our understanding of the mechanisms underlying phenology shifts.

Literature Cited

Anderson, A. M., Novak, S. J., Smith, J. F., Steenhof, K., & Heath, J. A. (2016). Nesting phenology, mate choice, and genetic divergence within a partially migratory population of American Kestrels. *The Auk: Ornithological Advances*, *133*(1), 99-109.

Augusiak, J., Van den Brink, P. J., & Grimm, V. (2014). Merging validation and evaluation of ecological models to 'evaludation': A review of terminology and a practical approach. *Ecological Modelling*, *280*, 117-128.

Bart, J., Manning, A., Dunn, L., Fischer, R., & Eberly, C. (2012). Coordinated bird monitoring: Technical recommendations for military lands: *U.S. Geological Survey Open-File Report* 20101078.

Bastianelli, O., Charmantier, A., Biard, C., Bonamour, S., Teplitsky, C., & Robert, A. (2021). Is earlier reproduction associated with higher or lower survival? Antagonistic results between individual and population scales in the blue tit. *bioRxiv*.

Bauer, Z., Trnka, M., Bauerová, J., Možný, M., Štěpánek, P., Bartošová, L., & Žalud, Z. (2010). Changing climate and the phenological response of great tit and collared flycatcher populations in floodplain forest ecosystems in Central Europe. *International journal of biometeorology*, *54*(1), 99-111.

Berthold, P., & Helbig, A. J. (1992). The genetics of bird migration: stimulus, timing, and direction. *Ibis*, *134*, 35-40.

Bossu, C. M., Heath, J. A., Kaltenecker, G. S., Helm, B., & Ruegg, K. C. (2022). Clock-linked genes underlie seasonal migratory timing in a diurnal raptor. *Proceedings of the Royal Society B*, *289*(1974), 20212507.

Both, C., Artemyev, A. V., Blaauw, B., Cowie, R. J., Dekhuijzen, A. J., Eeva, T., ... and Visser, M. E. (2004). Large–scale geographical variation confirms that climate change causes birds to lay earlier. *Proceedings of the Royal Society of London. Series B: Biological Sciences*, *271*(1549), 1657-1662.

Both, C., and Visser, M. E. (2005). The effect of climate change on the correlation between avian life-history traits. *Global Change Biology*, *11*(10), 1606-1613.

Both, C., Bouwhuis, S., Lessells, C. M., & Visser, M. E. (2006). Climate change and population declines in a long-distance migratory bird. *Nature*, *441*(7089), 81-83.

Both, C., Van Turnhout, C. A., Bijlsma, R. G., Siepel, H., Van Strien, A. J., & Foppen, R. P. (2010). Avian population consequences of climate change are most severe for long-distance migrants in seasonal habitats. *Proceedings of the Royal Society B: Biological Sciences*, *277*(1685), 1259-1266.

Bradshaw, W. E., & Holzapfel, C. M. (2007). Evolution of animal photoperiodism. *Annual Review of Ecology, Evolution, and Systematics*, 1-25.

Chmura, H. E., Wingfield, J. C., & Hahn, T. P. (2020). Non-photic environmental cues and avian reproduction in an era of global change. *Journal of Avian Biology*, *51*(3).

Crick, H. Q., Dudley, C., Glue, D. E., & Thomson, D. L. (1997). UK birds are laying eggs earlier. *Nature*, *388*(6642), 526-526.

Cristol, D.A., Nolan Jr, V. & Ketterson, E.D. (1990). Effect of prior residence on dominance status of dark-eyed juncos, *Junco hyemalis*. *Animal Behaviour*, *40*, 580–586.

DeAngelis, D. L., & Grimm, V. (2014). Individual-based models in ecology after four decades. F1000prime reports, 6.

Drent, R. H., Fox, A. D., & Stahl, J. (2006). Travelling to breed. *Journal of Ornithology*, *147*(2), 122-134.

Dunn, P. O., & Winkler, D. W. (1999). Climate change has affected the breeding date of tree swallows throughout North America. *Proceedings of the Royal Society of London. Series B: Biological Sciences*, *266*(1437), 2487-2490.

Duriez, O., Bauer, S., Destin, A., Madsen, J., Nolet, B. A., Stillman, R. A., & Klaassen, M. (2009). What decision rules might pink-footed geese use to depart on migration? An individual-based model. *Behavioral Ecology*, *20*(3), 560-569.

eBird. 2021. eBird: An online database of bird distribution and abundance [web application]. eBird, Cornell Lab of Ornithology, Ithaca, New York. Available: http://www.ebird.org. (Accessed: Date [e.g., February 2, 2021]).

Forchhammer, M. C., Post, E., & Stenseth, N. C. (1998). Breeding phenology and climate. *Nature*, *391*(6662), 29-30.

Gienapp, P., Postma, E., & Visser, M. E. (2006). Why breeding time has not responded to selection for earlier breeding in a songbird population. *Evolution*, *60*(11), 2381-2388.

Gienapp, P., Reed, T. E., & Visser, M. E. (2014). Why climate change will invariably alter selection pressures on phenology. *Proceedings of the Royal Society B: Biological Sciences*, *281*(1793), 20141611.

Grimm, V., Berger, U., Bastiansen, F., Eliassen, S., Ginot, V., Giske, J., Goss-Custard, J., Grand, T., Heinz, S.K., Huse, G. & others. (2006). A standard protocol for describing individual-based and agent-based models. *Ecological Modelling*, *198*, 115–126.

Grimm, V., Augusiak, J., Focks, A., Frank, B. M., Gabsi, F., Johnston, A. S., ... & Railsback, S. F. (2014). Towards better modelling and decision support: documenting model development, testing, and analysis using TRACE. *Ecological modelling*, *280*, 129-139.

Hadfield, J. D., & Reed, T. E. (2022). Directional selection and the evolution of breeding date in birds, revisited: Hard selection and the evolution of plasticity. *Evolution Letters*, *6*(2), 178-188.

Heath, J. A., Steenhof, K., and Foster, M. A. (2012). Shorter migration distances associated with higher winter temperatures suggest a mechanism for advancing nesting phenology of American kestrels *Falco sparverius*. *Journal of Avian Biology*, *43*(4), 376-384.

Helm, B., Ben-Shlomo, R., Sheriff, M. J., Hut, R. A., Foster, R., Barnes, B. M., & Dominoni, D. (2013). Annual rhythms that underlie phenology: biological time-keeping meets environmental change. *Proceedings of the Royal Society B: Biological Sciences*, *280*(1765), 20130016.

Hipfner, J. M., McFarlane-Tranquilla, L. A., & Addison, B. (2010). Experimental evidence that both timing and parental quality affect breeding success in a zooplanktivorous seabird. *The Auk*, *127*(1), 195-203.

Hogg, C. J., McLennan, E. A., Wise, P., Lee, A. V., Pemberton, D., Fox, S., ... & Grueber, C. E. (2020). Preserving the demographic and genetic integrity of a single source population during multiple translocations. *Biological Conservation*, *241*, 108318.

Hostetler, J. A., Sillett, T. S., & Marra, P. P. (2015). Full-annual-cycle population models for migratory birds. *The Auk: Ornithological Advances*, *132*(2), 433-449.

Knudsen, E., Lindén, A., Both, C., Jonzén, N., Pulido, F., Saino, N., ... & Stenseth, N. C. (2011). Challenging claims in the study of migratory birds and climate change. *Biological Reviews*, *86*(4), 928-946.

Krabbenhoft, T. J., & Turner, T. F. (2014). Clock gene evolution: seasonal timing, phylogenetic signal, or functional constraint?. *Journal of Heredity*, *105*(3), 407-415.

Liedvogel, M., Szulkin, M., Knowles, S. C., Wood, M. J., & Sheldon, B. C. (2009). Phenotypic correlates of Clock gene variation in a wild blue tit population: evidence for a role in seasonal timing of reproduction. *Molecular Ecology*, *18*(11), 2444-2456.

Masel, J. (2011). Genetic drift. *Current Biology*, 21(20), R837-R838.

McClure, C. J., Brown, J. L., Schulwitz, S. E., Smallwood, J., Farley, K. E., Therrien, J. F., Miller K.E., Steenhof, K., & Heath, J. A. (2021). Demography of a widespread raptor across disparate regions. *Ibis*, *163*(2), 658-670.

McClure, C. J., & Schulwitz, S. E. (2022). Historical Accounts Provide Inference into Population Dynamics of American Kestrels (*Falco sparverius*) in the Northeastern USA. *Journal of Raptor Research*, *56*(1), 89-94.

McCleery, R. H., & Perrins, C. M. (1998). ¨temperature and egg-laying trends. *Nature*, *391*(6662), 30-31.

Mearns, L.O., et al., 2017: The NA-CORDEX dataset, version 1.0. NCAR Climate Data Gateway, Boulder CO, https://doi.org/10.5065/D6SJ1JCH

Miller-Rushing, A. J., Høye, T. T., Inouye, D. W., & Post, E. (2010). The effects of phenological mismatches on demography. *Philosophical Transactions of the Royal Society B: Biological Sciences*, *365*(1555), 3177-3186.

Møller, A. P., Rubolini, D., Lehikoinen, E. (2008). Populations of migratory bird species that did not show a phenological response to climate change are declining. *Proceedings of the National Academy of Sciences 105*, 16195-16200.

Nilsson, J. Å., Svensson, E. (1996). The cost of reproduction: a new link between current reproductive effort and future reproductive success. *Proceedings of the Royal Society of London Series B: Biological Sciences 263*, 711-714.

Nussey, D. H., Postma, E., Gienapp, P., & Visser, M. E. (2005). Selection on heritable phenotypic plasticity in a wild bird population. *Science*, *310*(5746), 304-306.

Parmesan, C., & Yohe, G. (2003). A globally coherent fingerprint of climate change impacts across natural systems. *nature*, *421*(6918), 37-42.

Partners in Flight. 2020. Population Estimates Database, version 3.1. Available at http://pif.birdconservancy.org/PopEstimates. Accessed on 1/4/2020.

Pearce-Higgins, J. W., Yalden, D. W., & Whittingham, M. J. (2005). Warmer springs advance the breeding phenology of golden plovers *Pluvialis apricaria* and their prey (Tipulidae). *Oecologia*, *143*(3), 470-476.
Perrins, C. M. (1970). The timing of birds 'breeding seasons. *Ibis*, *112*(2), 242-255.
Piou, C., & Prévost, E. (2012). A demo-genetic individual-based model for Atlantic salmon populations: Model structure, parameterization and sensitivity. *Ecological modelling*, *231*, 37-52.
Pulido, F., & Berthold, P. (2010). Current selection for lower migratory activity will drive the evolution of residency in a migratory bird population. *Proceedings of the National Academy of Sciences*, *107*(16), 7341-7346.
Reed, T. E., Grøtan, V., Jenouvrier, S., Sæther, B. E., & Visser, M. E. (2013). Population growth in a wild bird is buffered against phenological mismatch. Science, 340(6131), 488-491.
Ruegg, K. C., Brinkmeyer, M., Bossu, C. M., Bay, R. A., Anderson, E. C., Boal, C. W., ... & Heath, J. A. (2021). The American Kestrel (Falco sparverius) genoscape: Implications for monitoring, management, and subspecies boundaries. The Auk, 138(2), ukaa051.
Saino, N., Albetti, B., Ambrosini, R., Caprioli, M., Costanzo, A., Mariani, J., ... & Bollati, V. (2019). Inter-generational resemblance of methylation levels at circadian genes and associations with phenology in the barn swallow. *Scientific reports*, *9*(1), 1-16.
Sauve, D., Divoky, G., & Friesen, V. L. (2019). Phenotypic plasticity or evolutionary change? An examination of the phenological response of an arctic seabird to climate change. Functional Ecology, 33(11), 2180-2190.
Schmolke A., P. Thorbek, D.L. DeAngelis, and V. Grimm. 2010. Ecological modelling supporting environmental decision making: a strategy for the future. Trends in Ecology and Evolution 25:479–486.
Schulwitz, S. E., Hill, G. C., Fry, V., & McClure, C. J. (2021). Evaluating citizen science outreach: A case-study with The Peregrine Fund's American Kestrel Partnership. PloS one, 16(3), e0248948.
Schwartz, M. K., Luikart, G., & Waples, R. S. (2007). Genetic monitoring as a promising tool for conservation and management. Trends in ecology & evolution, 22(1), 25-33.
Seaborn, T., Andrews, K. R., Applestein, C. V., Breech, T. M., Garrett, M. J., Zaiats, A., & Caughlin, T. T. (2021). Integrating genomics in population models to forecast translocation success. Restoration Ecology, e13395.
Sheldon, B. C., Kruuk, L. E. B., & Merila, J. (2003). Natural selection and inheritance of breeding time and clutch size in the collared flycatcher. *Evolution*, *57*(2), 406-420.
Sherry, T. W., & Holmes, R. T. (1996). Winter habitat quality, population limitation, and conservation of Neotropical-Nearctic migrant birds. *Ecology*, *77*(1), 36-48.
Shugart, H. H., Wang, B., Fischer, R., Ma, J., Fang, J., Yan, X., ... & Armstrong, A. H. (2018). Gap models and their individual-based relatives in the assessment of the consequences of global change. Environmental Research Letters, 13(3), 033001.
Slate, J. (2013). From Beavis to beak color: a simulation study to examine how much QTL mapping can reveal about the genetic architecture of quantitative traits. Evolution, 67(5), 1251-1262.
Smallegange, I. M., Fiedler, W., Köppen, U., Geiter, O., & Bairlein, F. (2010). Tits on the move: exploring the impact of environmental change on blue tit and great tit migration distance. *Journal of Animal Ecology*, *79*(2), 350-357.

Steenhof, K., & Peterson, B. E. (2009). American Kestrel reproduction in southwestern Idaho: annual variation and long-term trends. Journal of Raptor Research, 43(4), 283-290.
Tam, V., Patel, N., Turcotte, M., Bossé, Y., Paré, G., & Meyre, D. (2019). Benefits and limitations of genome-wide association studies. Nature Reviews Genetics, 20(8), 467-484.
Tarwater, C. E., & Beissinger, S. R. (2013). Opposing selection and environmental variation modify optimal timing of breeding. *Proceedings of the National Academy of Sciences*, *110*(38), 15365-15370.
Thomas DW, Blondel J, Perret P, Lambrechts MM, Speakman JR (2001) Energetic and fitness costs of mismatching resource supply and demand in seasonally breeding birds. Science 291:2598-2600.
Thornton, P.E., Running, S.W. & White, M.A. (1997). Generating surfaces of daily meteorological variables over large regions of complex terrain. *Journal of Hydrology*, **190**, 214–251.
Van Noordwijk, A. J., McCleery, R. H., & Perrins, C. M. (1995). Selection for the timing of great tit breeding in relation to caterpillar growth and temperature. *Journal of animal ecology*, 451-458.
Van Vliet, J., Musters, C. & Ter Keurs, W.J. (2009). Changes in migration behaviour of blackbirds *Turdus merula* from the Netherlands. *Bird Study*, **56**, 276–281.
Verhulst, S., & Nilsson, J. Å. (2008). The timing of birds' breeding seasons: a review of experiments that manipulated timing of breeding. *Philosophical Transactions of the Royal Society B: Biological Sciences*, *363*(1490), 399-410.
Visser, M. E., Adriaensen, F., van Balen, J. H., Blondel J., Dhondt A. A., van Dongen, S., du Feu, C., Ivankina, E. V., Kerimov, A. B., de Laet, J., Matthysen, E., McCleery, R., Orell, M., and Thomson, D. L. (2003) Variable responses to large-scale climate change in European Parus populations. *Proceedings of the Royal Society of London. Series B: Biological Sciences*, *270*(1513), 367-372.
Visser, M. E. (2008). Keeping up with a warming world; assessing the rate of adaptation to climate change. *Proceedings of the Royal Society B: Biological Sciences*, *275*(1635), 649-659.
Visser, M. E., Holleman, L. J., & Caro, S. P. (2009). Temperature has a causal effect on avian timing of reproduction. *Proceedings of the Royal Society B: Biological Sciences*, *276*(1665), 2323-2331.
Walker, W. H., Meléndez-Fernández, O. H., Nelson, R. J., & Reiter, R. J. (2019). Global climate change and invariable photoperiods: A mismatch that jeopardizes animal fitness. *Ecology and evolution*, *9*(17), 10044-10054.
Warkentin, I. G., James, P. C., & Oliphant, L. W. (1992). Assortative mating in urban-breeding Merlins. *The Condor*, *94*(2), 418-426.
Webster, M. S., Marra, P. P., Haig, S. M., Bensch, S., & Holmes, R. T. (2002). Links between worlds: unraveling migratory connectivity. *Trends in ecology & evolution*, *17*(2), 76-83.
White, J. W., Rassweiler, A., Samhouri, J. F., Stier, A. C., & White, C. (2014). Ecologists should not use statistical significance tests to interpret simulation model results. *Oikos*, *123*(4), 385-388.
Wiegand, T., Jeltsch, F., Hanski, I., & Grimm, V. (2003). Using pattern-oriented modeling for revealing hidden information: a key for reconciling ecological theory and application. *Oikos*, *100*(2), 209-222.

Willi, Y., & Hoffmann, A. A. (2009). Demographic factors and genetic variation influence population persistence under environmental change. *Journal of evolutionary biology*, *22*(1), 124-133.

Williams, T. D., Bourgeon, S., Cornell, A., Ferguson, L., Fowler, M., Fronstin, R. B., & Love, O. P. (2015). Mid-winter temperatures, not spring temperatures, predict breeding phenology in the European starling Sturnus vulgaris. *Royal Society Open Science*, *2*(1), 140301.

Wingfield, J. C. (2008). Comparative endocrinology, environment and global change. *General and comparative endocrinology*, *157*(3), 207-216.

Xuereb, A., Rougemont, Q., Tiffin, P., Xue, H., & Phifer-Rixey, M. (2021). Individual-based eco-evolutionary models for understanding adaptation in changing seas. *Proceedings of the Royal Society B, 288*(1962), 20212006.

Chapter 4. Demonstrating the portability of an annual-cycle modeling framework for Department of Defense species of concern: Canada warbler (*Cardellina canadensis*) and burrowing owl (*Athene cunicularia*)

Julie A. Heath, Breanna F. Powers, Benjamin P. Pauli, Anjolene R. Hunt, Jason M. Winiarski

Abstract

The Department of Defense manages more threatened and endangered species than any other federal land manager. Threatened and endangered species on military installations can be particularly vulnerable to impacts of climate change because of their small or declining populations and their limited ability to colonize new ranges. Natural resource managers need tools to predict which species may be vulnerable to phenological mismatch. We developed the individual-based model (IBM) Simulated Carry Over and Phenology Effects (SCOPE) under the premise that multi-generational, full annual cycle models are better than single-season (e.g., breeding season) models at providing information on a species' ability to shift the timing of phases in their annual cycle, and full-spatial scale models that allow for dispersal may be important for capturing dispersal and evolutionary processes that affect phenology. Here, we demonstrate the portability of this modeling framework by parameterizing SCOPE for a DoD Partners in Flight (PIF) Mission-sensitive Species (burrowing owl, *Athene cunicularia*), and a DoD PIF Tier 2 species (Canada warbler, *Cardellina canadensis,* DoD PIF 2019), that are likely vulnerable to climate change impacts. We collated data for each species from previous research, used data mining approaches, and collected expert opinions from collaborators. Then, we re-parameterized SCOPE with the appropriate spatial, climate, and environmental variables and the species-specific biology-environmental parameters for each model sub-process. We obtained high-quality data on Canada warbler biology from Monitoring Avian Productivity and Survival (MAPS) sites and other sources and learned that Canada warbler reproduction and survival were sensitive to phenology. Within SCOPE simulations, we found that Canada warbler nesting phenology did not advance at the same pace as climate-driven advances in spring, leading to increased mismatch over time, decreased adult survival, and declining population trends. It was challenging to find high-quality raw data on burrowing owl life history. To parameterize SCOPE, we used published information about nest success and survival that contained little to no information about sensitivity to mismatch. Within SCOPE simulations, burrowing owls did not advance their phenology to keep pace with earlier springs, but their populations remained relatively stable, likely because of inadequate representation of sensitivity to mismatch. Together, these results highlight the importance of data curation and availability. Developing tools to assess climate vulnerability will require access to longitudinal data that can be challenging for individuals to manage and share. Improved resources for data management could aid in capturing archival data that would be useful for creating natural resource management tools. In sum, though SCOPE was initially developed for a data-rich species, American kestrels, the sub-processes within the model were made to be generalizable to other species of migratory birds. Parameterization of SCOPE for Canada warblers revealed that phenological mismatch is likely to become a threat for this species. Alternatively, parameterization of SCOPE for burrowing owls suggested the phenological mismatch would not be an emerging threat for owls, but challenges in obtaining quality data for burrowing owls make this result tenuous.

Objectives

In this chapter, our main objective was to demonstrate the portability of the SCOPE modeling framework to forecast population changes and the resilience of Department of Defense (DoD) Species of Concern to phenological mismatch. We selected two migratory land bird species, Canada warblers (*Cardellina canadensis*) and burrowing owls (*Athene cunicularia*) for this demonstration. To accomplish our objective, we collated data for each species from previous research, used data mining approaches, and collected expert opinions from collaborators. Then, we re-parameterized SCOPE with the appropriate spatial, climate, and environmental variables for each species, and the species-specific biology-environmental parameters for each model sub-process.

This work addresses the following SERDP Statement of Need (SON) 17-01: *Life-cycle modeling to (a) assess emerging theoretical understanding of phenology and its role in maintaining species viability and (b) address resultant conservation and management challenges within relevant, testable, and adaptable conceptual frameworks.* Using the modeling framework, we developed for the American kestrel (*Falco sparverius*), a data-rich land bird species that shows phenology variation and differential responses to climate change across its range, we parameterized SCOPE with data for Canada warblers and burrowing owls to forecast changes in phenology, phenological mismatch, nest success, survival, and population sizes from 1980 – 2099 under resource concentration pathways (RCP) 4.5 and 8.5.

Background

Department of Defense lands have the highest density of threatened and endangered species of any federal land management agency (Stein et al. 2008). Preserving these species on DoD lands is not only a legal obligation but also plays a role in ensuring that personnel have access to realistic and varied land cover conditions for military training, thereby improving training and combat readiness (Benton et al. 2008). Particular attention is given to proactively addressing the conservation and management of DoD Partners in Flight Mission Sensitive Species (MSS), those listed as species of concern that would have the greatest impact on the military mission if federally listed under the Endangered Species Act (ESA). However, management and conservation are becoming more challenging and costlier as climate-driven changes in distribution, abundance, life history, and vital rates of species alter local biodiversity and community composition, and in some cases, lead to population declines (Trautmann 2018). Threatened and endangered species can be particularly vulnerable to impacts of climate change as they tend to have specialized habitat requirements, narrow environmental tolerances, are dependent on specific environmental cues and interspecific interactions, and have limited ability to colonize new ranges (Foden et al. 2009). Furthermore, because they have small or declining populations, direct and indirect effects of climate change can have extreme consequences for species persistence (USEPA 2009). One potentially adaptive response of plants and animals to climate-driven shifts in environmental conditions and resource availability is a shift in phenology (i.e., the timing of seasonal life events) to match seasonal needs with food availability (Visser and Gienapp 2019). However, not all species will shift phenology, and in many cases, the rate of spring advancement outpaces species' capacities for adaptation (Visser et al. 2012). Species that have shifted timing the least in response to climate change have experienced more severe population declines than species that have shifted the most (Møller et al. 2008). Understanding

whether species are vulnerable to climate-driven changes in ecosystem phenology and mismatch is critical for predicting population trends and managing DoD Species of Concern.

Research on biological responses to climate change can be challenging as trends are likely to occur over time scales that are greater than the period of a single research project. At the same time, there is a pressing need to identify vulnerable species and develop management strategies for systems that are changing relatively rapidly in ecological-time frames. One approach to overcome this challenge is to use existing empirical information to develop simulation models to test hypotheses across extended temporal scales. Individual-based models (IBMs) are simulation models that can be used to predict how animal (and plant) populations respond to environmental change, wherein "agents" represent individual animals within a virtual physical and biological environment that make decisions to maximize survival and reproduction. Rules that govern individuals are informed by the natural history of the focal species. Individual behaviors and interactions result in emergent patterns that match those observed in real-world populations. IBMs allow researchers to manipulate virtual environments and measure population response in a manner that would not be feasible in the field. Model development requires empirical estimates of the relationships underlying the hypothesized drivers and constraints of species responses. Though, this can prove challenging for species of concern as they are often rare, have small population sizes, or both, which can result in limited data availability (Szaro 2008). One possible solution to this challenge is to use model frameworks developed for representative, data-rich species, and then re-parameterized for data-limited species. In this way, testing model portability can help us highlight areas of uncertainty and suggest future avenues for research.

Canada warbler (*Cardellina canadensis,* CAWA) and burrowing owl (*Athene cunicularia,* BUOW) are two species on the MSS list that are likely vulnerable to climate change impacts. They have different life-history traits, habitat preferences, and ranges, which makes them interesting case studies to test model portability and examine the impacts of climate change. The Canada warbler is a small, neotropical migratory songbird associated with wet forest and riparian areas (Reitsma et al. 2020), while the burrowing owl is a medium-sized partially-migratory raptor associated with open grassland and agricultural areas (Poulin et al. 2020). Canada warblers and burrowing owls have experienced population declines over the last 50 years (63% and 33%, respectively: Sauer et al. 2017, Wilson et al. 2018) and habitat loss and degradation are proposed as the primary driver of these trends (Environment Canada 2007, 2016). Climate change could exacerbate threats to critical habitat for these species, as well as cause other direct and indirect fitness impacts. For Canada warblers, drier, warmer conditions will likely result in increased drought, wildfires, and insect outbreaks, decreasing habitat suitability and affecting vital rates. Both body condition and survival of Canada warblers wintering in Columbia were negatively impacted by El Niño drought conditions (Gonzalez et al. 2020). Further, the significant northward shift of the breeding distribution of Canada warblers in the eastern region (McCaslin et al. 2020) and decreased density and population growth rates of southernmost breeders with warmer temperatures and lower precipitation (Merker and Chandler 2021) could suggest a distributional response to changing climatic suitability. Lastly, as a long-distance migrant with a very short breeding window (Flockhart 2010) Canada warblers may be particularly vulnerable to climate-induced phenological mismatch (Both et al. 2010, see Chapter 1). Indeed, Culp et al (2017) assessed Canada warblers as one of the species highly vulnerable to climate change based on climate exposure, climate sensitivity, adaptive capacity, and indirect effects. For burrowing owls, extreme rainfall events on the breeding grounds (Fisher 2015, Haley

and Rosenberg 2013), storms during fall migration and increased precipitation on the wintering grounds (Wellicome et al. 2014), and drought across the annual cycle (Cruz-McDonnell and Wolf 2016, Porro et al. 2020) have been shown to negatively affect both survival and productivity. Burrowing owls in their southwest range are arriving later and later, with negative effects on breeding success (Cruz-McDonnell and Wolf 2016), whereas later nesting burrowing owls had higher nest success in a Wyoming breeding population (Lantz and Conway 2009) suggesting that climate responses and vulnerabilities may vary regionally.

Simulation of Carry-Over and Phenology Effects (SCOPE) is an individual-based model of the full annual cycle of migratory birds (see Chapter 3). SCOPE consists of individual birds, a virtual landscape representing the North American breeding range for the species of interest, and landscape patches within the breeding range that contain information about geographic locations (i.e., latitude and longitude values), climate, the start of spring, and carrying capacity. Birds interact with each other and with the landscape to make decisions about dispersal, reproduction, migration, and survival. We developed this model with the premise that 1) multi-generational, full annual cycle models are better than single-season (e.g., breeding season) models at providing information on a species' ability to shift the timing of phases in their annual cycle, and 2) full-spatial scale models that allow for dispersal may be important for capturing dispersal and evolutionary processes that affect phenology. Here, we tested the portability of the SCOPE modeling framework developed for American kestrels (Chapter 3) by parameterizing the model for DoD Species of Concern: Canada warblers and burrowing owls to understand how these species may, or may not, have the adaptive potential to shift phenology in response to climate change. Specifically, we used previous research, data mining approaches, and solicited expert opinion and collaboration to parameterize SCOPE for each species and forecast population viability under RCPs 4.5 and 8.5.

Materials and Methods

Summary model description

SCOPE begins on the first day of the breeding season and advances each day throughout the full breeding season across the North American range. This range provides opportunities for individuals in different ecoregions and with different migratory strategies to breed at different times of the year. The non-breeding season was represented by a single day when individuals calculate their annual survival probability and go through the mortality subprocess. The model simulated the years 1980 – 2099 at two RCPs, 4.5 and 8.5. Information from 1980 to the present could be used for hindcasting and pattern matching to empirical information. Additionally, we included the option for a burn-in period of 10, 15, or 20 years with constant climate data. The burn-in period allowed the simulated population to reach a stable state before environmental change begins. We used regional climate model (RCM) data from the NA-CORDEX project (Mearns et al. 2017) that was bias-corrected using the Daymet historical gridded dataset (Thornton et al. 1997). This bias-correction provided continuity between the historical climate data used to parameterize bird-weather-vegetation phenology relationships, and future changes in climate. We obtained climate data for RCP 4.5 from 1 RCM, and RCP 8.5 from 12 RCMs (Tables 4A.2 and 5A.2). NA-CORDEX projections used in SCOPE were converted from netcdf format into annual raster layers.

The spatial patch size (28.5 km^2) was based on the resolution of RCMs used to represent climatic conditions in the model. Each patch contained information about latitude, longitude, the Environmental Protection Agency (EPA) level III ecoregions, and climate and seasonal variables

relevant to the species. Output could be printed at the patch level and reports average, min, and max values for all individuals within a patch.

During the breeding season, individuals tracked their "date of availability"; this was analogous to reproductive readiness. Date of availability depended on several factors latitude, and spring weather conditions. Once a male was available for breeding they dispersed to a breeding patch that had the capacity for nesting and set their availability to true. Females that had reached their date of availability dispersed to a patch with an available male that had not paired with a female and set their availability to true. If there were no unpaired, available males on the landscape, the female moved her available date to one day in the future and repeated the pairing process in the subsequent time steps. Individuals that were unsuccessful at pairing remain in the population as non-breeding 'floaters.' Once paired, individuals set an egg-laying date. Paired females determined their probability of nest success based on species-specific biology. If the nest was successful, then the number of offspring for that nest was determined. These offspring were randomly assigned as male or female and can track information about their natal site or parents.

At the beginning of the non-breeding season, the age of each individual was increased by 1 and the probability of surviving to the following year was determined for each individual. Survival could be dependent on life-history traits or drawn from a random distribution. After the survival sub-model was run, individuals made decisions about whether or not to migrate and how far to migrate based on environmental conditions. Before the next year starts, all dynamic bird attributes were reset and the next year starts.

Population patterns emerged from the decisions individuals make within SCOPE. Population-level patterns from past years were used to calibrate and validate SCOPE. Population-level patterns in future years allowed for forecasting of how phenology, fitness, and population sizes may change under different climate scenarios. For each species-specific version of the model we created a TRAnsparent and Comprehensive Ecological (TRACE) document (Augusiak et al. 2014, Grimm et al. 2014) to record details on the purpose of the model, the process and parameterization of the model, and validation and sensitivity testing (Appendix 4, Appendix 5).

Parameter estimation

The model is parameterized with equations and variables that capture key life-history processes such as dispersal, survival, reproduction, and migration. Here we describe how we approached estimating these parameters for CAWA- and BUOW-specific submodels in SCOPE.

Dispersal. We estimated distances and directions of natal dispersal (i.e., movement from the place of birth to a breeding site) and breeding dispersal (i.e., movement between breeding sites) separately because patterns of natal dispersal and breeding dispersal can be very different (Greenwood and Harvey 1982, Whitfield et al. 2009), suggesting that they are driven by different processes (Greenwood and Harvey 1982, Clobert 2012). We used the United States Geological Survey's (USGS) Bird Banding Lab (BBL) data to estimate dispersal. We requested all banding and encounter data for each species and then filtered the data to contain only records where birds were captured and encountered during a breeding season. We used records of individuals first banded as a nestling (i.e., "local") and then encountered in a subsequent year during the breeding season to parameterize natal dispersal. We used records of individuals originally captured as an adult and subsequently captured again in another breeding season to parameterize breeding dispersal. We calculated the straight-line distance between banding and encounter locations, and

the direction of dispersal. For both CAWA and BUOW, we did not have enough data to evaluate the effects of environmental covariates on dispersal distance or direction, though these covariates can be incorporated into SCOPE (see Chapter 3). Further, we had very few dispersal records for Canada warblers (1 natal dispersal, 4 breeding dispersal) so we included BBL records for a congeneric species, Wilson's warblers (*Cardellina pusilla*). We created intercept-only models with a Gamma-distributed random variable to represent the natal dispersal and breeding dispersal process in SCOPE. Dispersal directions (in degrees) were drawn from a wrapped cauchy distribution.

Survival. We obtained banding and encounter data collected from 1992 – 2019 at Monitoring Avian Productivity and Survivorship (MAPS) sites (DeSante et al. 1995, Figure 4.1) to estimate adult survival of Canada warblers using a multi-state mark-recapture model developed in RMark (Laake 2013). The sample size was sufficient to include a covariate, so we categorized whether adult birds nested relatively early or late. To classify the timing of each individual we estimated the extended spring index (SI-x, Appendix 4) for each MAPS capture station, each year. We used "breeding status" variables within MAPS data to classify whether birds were breeding. Next, we estimated breeding windows (i.e., earliest egg-laying to latest fledge) for Canada warblers in three distinct regions: Boreal, Great Lakes, and Appalachian. The breeding window estimated for the Boreal region was June 5 to July 16 (Flockhart 2010), the Great Lakes region was May 31 to July 19 (Bird Studies Canada 2006), and the Appalachian region was from May 12 to July 6 (Becker 2012). Finally, we calculated the median difference between egg-laying date and SI-x for each region and categorically classified whether an individual was breeding before (early) or after (late) the median date of asynchrony. Represented by the variable *early?* in SCOPE.

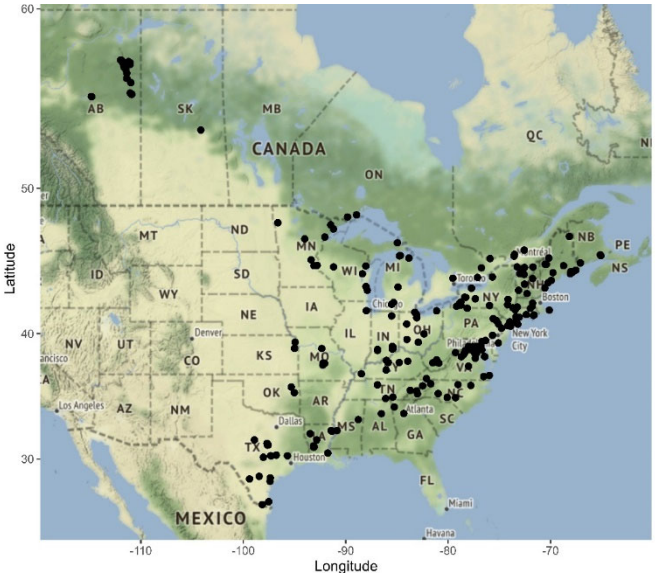

Figure 4.1 Banding and encounter locations for Canada warbler records used to estimate adult survival. Some banding and encounters were at migration and wintering sites, outside the range of the breeding area. Overall, there was good coverage for sampling survival.

We did not successfully obtain a mark and recapture dataset that was sufficient to estimate survival with environmental or life-history parameters for burrowing owls. Therefore, the probability of adult and juvenile survival was drawn from a random distribution centered on average adult and juvenile survival (Poulin et al. 2020). The lack of mark-and-recapture data on BUOW constrained our ability to study the effects of mismatch on an important component of individual fitness and population demographics.

Reproduction. The process of reproduction contained two key submodels: drawDateAvailable and NestSuccess. The drawDateAvailable process determined what day of the year (i.e., date of availability) individuals become available for pairing for the upcoming breeding season. The

date of availability equation typically depended on whether individuals are migrants or residents. For Canada warblers, all individuals were migrants (Reitsma et al. 2020). Therefore, we used a modified approach from Powers et al. (2021) to model spatially-explicit arrival dates derived from eBird checklists (eBird 2019) in relation to latitude and spring climate conditions (i.e., minimum temperature anomalies). Date of availability was modeled as Gamma-distributed random variable with a fixed effect of latitude, spring T_{min} anomaly, and a random effect of year. Burrowing owls had migratory and resident individuals (Poulin et al. 2020). For migrant BUOW, we used a similar approach as above to model spatially-explicit arrival dates derived from eBird checklists in relation to latitude and spring climate conditions (i.e., minimum temperature anomalies). Date of availability was modeled as Gamma-distributed random variable with a fixed effect of latitude and spring minimum temperature anomaly and a random effect of year. Once migrant BUOWs arrive they are delayed by a constant (35 days) to represent the biological process of obtaining resources to produce eggs and to match patterns from empirical data. Unfortunately, poor access to raw data limited our ability to estimate the factors that govern timing of nesting of resident individuals. We used an equation similar to resident American kestrels, where resident date of availability was driven by the extended spring index, with variation in year accounted for by a random intercept in a Gamma mixed effects model. Residents obtained a date of availability from this equation and the extended spring index of the patch they occupied for the breeding season. Once individuals became available to breed, they go through the process of finding a nest site and mate (see above).

After pairing, females of the pair went through the submodel NestSuccess. Canada warbler nest success depended on phenological mismatch. Individuals that nested earlier in the season (compared to the SI-x) generally had higher nest success than individuals that nested later. To estimate this relationship, we compiled data from MAPS programs and professional scientists (Reitsma pers. comm., Hunt pers. comm.). We modeled nest success as a Bernoulli-distributed random variable and as a function of phenological mismatch (i.e., the difference in days between egg-laying date and SI-x) and a random year effect. After drawing a nest success probability, a uniform random number between 0 and 1 is drawn and compared to the nest success probability. If the random value is less than the calculated probability, the nest survives and both the female and associated male set their success value to true (otherwise they set success as false). Burrowing owl nest success varies with weather (Cruz-McDonnell and Wolf 2016). We used parameter estimates from Cruz-McDonnell and Wolf (2016) to represent nest success. Nest success was modeled as a Bernoulli-distributed random variable, and as a function of monthly mean maximum temperatures in spring and total monthly precipitation in spring. To draw their probability of nesting success, females sensed the spring maximum temperatures and spring precipitation at their patch in that year. Using this information, females obtained a nest success probability and then went through the process described above.

For successful CAWA females, the number of offspring produced was drawn by rounding to the nearest integer a value from a normal distribution with a mean of 3.8 and standard deviation of 1.03. For BUOW females, the number of offspring produced was drawn by rounding to the nearest integer a value from a normal distribution with a mean of 5 and standard deviation of 1.65. If the calculated value was negative, it was set to 0; if the value was greater than 6 for CAWA and greater than 8 for BUOW, it was set to six or eight, respectively, to prevent unrealistically productive nests. Offspring were randomly assigned as male or female and given an age of 0.

Migration. All Canada warblers migrate. There was no sub-model for individuals to determine whether to remain resident on the breeding grounds or migrate. Further, there was no sub-process to calculate migration distance because of a lack of empirical data. Individuals moved to an arbitrary location (patch 0,0) in the winter range (migrate) in which location was not influential to other processes.

Burrowing owls decided whether to migrate or remain resident on the breeding/natal grounds. For the updateStrategy submodel, we used BBL band records (1980–2019) to calculate migration distances of individuals that were banded in year *t* during the breeding (April–August) or non-breeding season (November–February), and encountered in the subsequent year on the non-breeding or breeding grounds, respectively. We calculated migration distances with coordinates from banding and encounter locations using the *geosphere* package in R (Hijmans et al. 2021). We assigned migration strategy based upon distances between breeding/natal sites and subsequent non-breeding sites, where individuals that traveled ≤ 100 km were considered residents. We modeled the decision to migrate or not dependent upon an individual's breeding latitude and the upcoming winter mean minimum temperature anomaly at the breeding/natal patch. Then, a random uniform number between 0 and 1 was generated. If that value was less than the probability of not migrating (1–the probability of migrating), an individual set its migration strategy to false (i.e., resident strategy). Once individuals adopted a resident strategy, they did not migrate in subsequent years.

Migrant BUOW obtained a distance (in km) to migrate to the non-breeding grounds. We parameterized migration distance using band encounters from the BBL (1980–2019) as described above. We modeled migration distance (distances ≥ 100 km) as a function of fixed effects of breeding/natal latitude and winter mean minimum temperature anomaly, and a random year effect in a Gamma mixed effects model. To prevent drawing unrealistically high migration distances, we set any distances over ≥ 4500 km equal to 4500 (a plausible distance based on BBL records). Migratory birds then moved to the 'non-breeding grounds' (i.e., NetLogo patch coordinate 0,0). This arbitrary location was selected to simplify programming and was not influential to other processes. This submodel did not apply to resident BUOW.

Simulations

We ran 2 experiments for each species, one at RCP 4.5 and another at RCP 8.5, for 120 years from 1980 – 2099. Each experiment had a 20-year burn-in and was replicated 20 times. We examined changes in population size, egg-laying date and phenological mismatch with the start of spring, nesting success, and adult and juvenile survival. As in Chapter 3, we focused on general trends and effect size of experiments rather than statistical significance because classical hypothesis-testing statistics may be misleading with simulated data (White et al. 2014). Credible intervals of 95% were calculated from linear models of the parameter of interest changing over time. For Canada warblers, we show output for the Appalachian ecoregion separately from the combined Canada and Northeastern ecoregions because Appalachian populations are genetically distinct from Canada and Northeastern populations (Ferrari et al. 2018). For burrowing owls, there is a distinct separation between western populations of BUOW and Florida BUOW (Desmond et al. 2001), so we show results separately for these populations.

Results and Discussion

Canada warblers

We found evidence that Canada warbler reproduction and adult survival were sensitive to the timing of nesting. Individuals that nested relatively early had higher nesting success (0.13, 95% CI: 0.003 – 0.31) and adult survival (0.10, 95% CI: 0.09 – 0.11) compared to later nesting individuals. Further, the arrival of Canada warblers to breeding grounds was weakly affected by spring minimum temperature anomalies (-0.001, 95% CI: -0.003 – 0). We used this information to parameterize SCOPE for Canada warblers. We evaluated the CAWA version of SCOPE and matched several patterns (Figure 4A.3). Specifically, SCOPE_CAWA matched egg-laying dates at two sites, in New Hampshire and Alberta. In addition, we matched nest success and productivity patterns in New Hampshire. In general, model estimates had less variance than empirical estimates of nest success and productivity, suggesting that we are not including all factors that contribute to these metrics, however we captured the central tendency of the metrics and considered the model reliable.

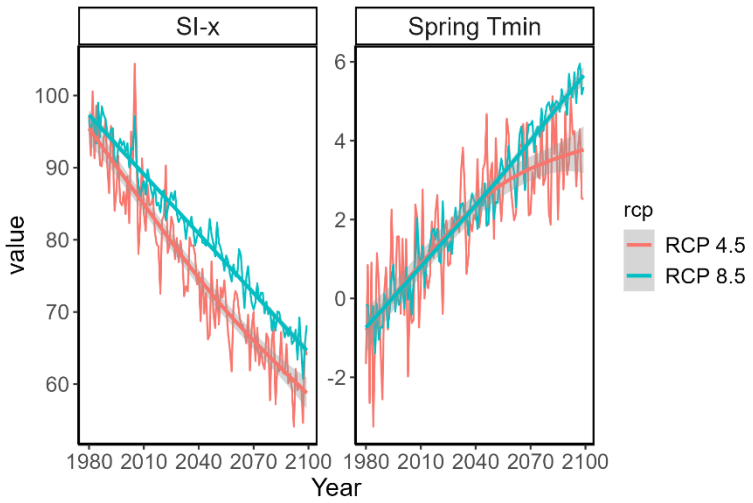

Figure 4.2 Changes in the extended spring index (SI-x, days) and spring minimum temperature anomalies (˚C) from 1980 – 2099 in the SCOPE Canada warbler model at RCP 4.5 and 8.5.

From 1980 – 2099 in SCOPE_CAWA, there were significant changes in SI-x and the spring minimum temperature anomalies at both RCP 4.5 (SI-x: -0.31, 95% CI -0.33 – -0.29; spring Tmin: 0.04, 95% CI 0.03 – 0.05) and 8.5 (SI-x: -0.27, 95% CI -0.28 – -0.26; spring Tmin: 0.05, 95% CI 0.05 – 0.06; Figure 4.2). Despite advancing springs the mean egg-laying date tended to get a later over time (Figure 4.3, Table 4.1). Later egg-laying resulted in greater phenological mismatch between the SI-x and egg-laying dates (Figure 4.4, Table 4.1). Though mismatch increased, there was no significant change in nest success (Figure 4.5, Table 4.1). However, adult survival did decline over time (Figure 4.6, Table 4.1), likely because of phenological mismatch. As a result, Canada warbler populations increased initially and then declined (Figure 4.7, Table 4.1). This was especially true in the Appalachian region, where some simulations went to zero.

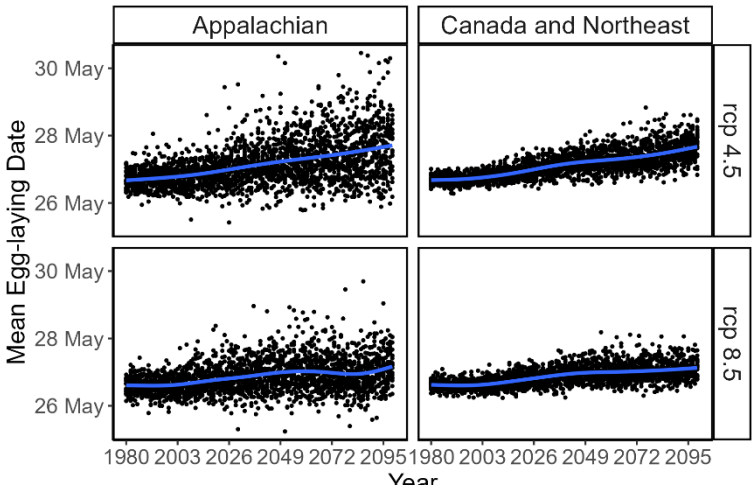

Figure 4.3 Changes in the mean egg-laying date for Canada warblers in the Appalachian and Canada and Northeast regions at RCP 4.5 and 8.5. Black dots represent annual means, the blue line represents smoothed averages.

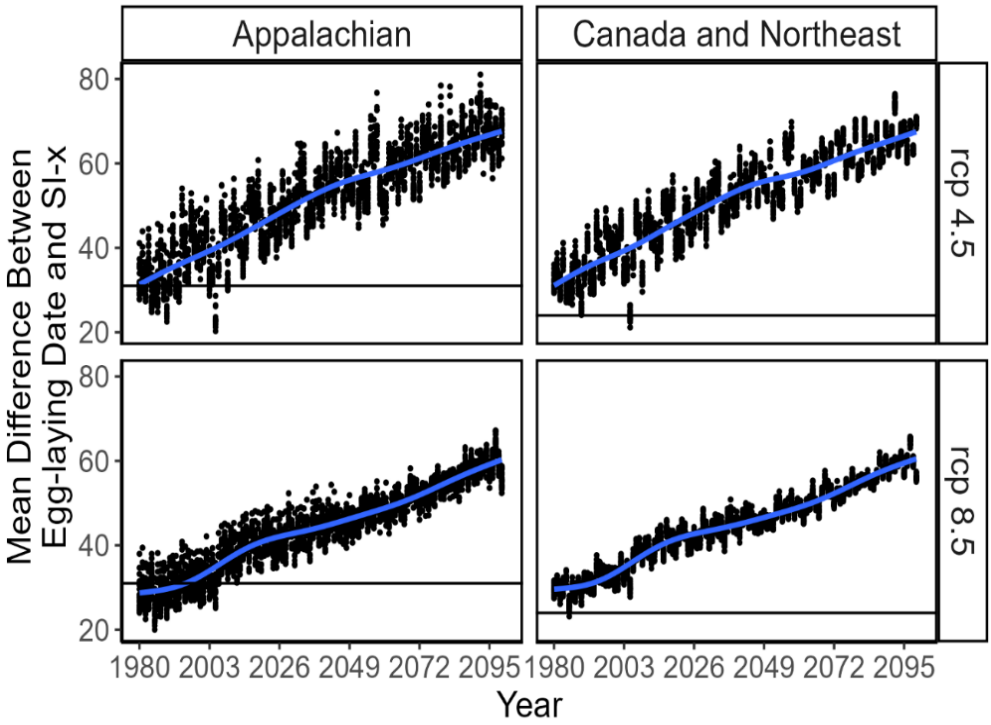

Figure 4.4 Changes in the mean mismatch (i.e., difference between egg-laying date and SI-x) for Canada warblers in the Appalachian and Canada and northeastern US regions at RCP 4.5 and 8.5. Black dots represent annual means, the blue line represents the smoothed average.

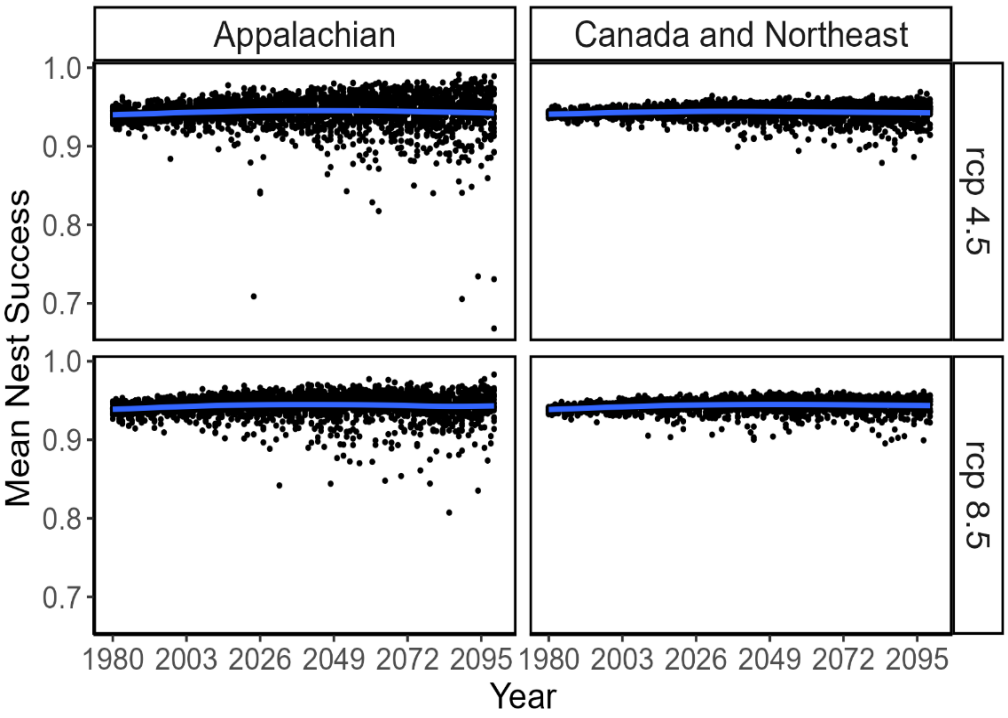

Figure 4.5 Changes in mean nest success (i.e., probability a pair produces ≥1oung) for Canada warblers in the Appalachian and Canada and northeastern US regions at RCP 4.5 and 8.5. Black dots represent annual means, the blue line represents the smoothed average.

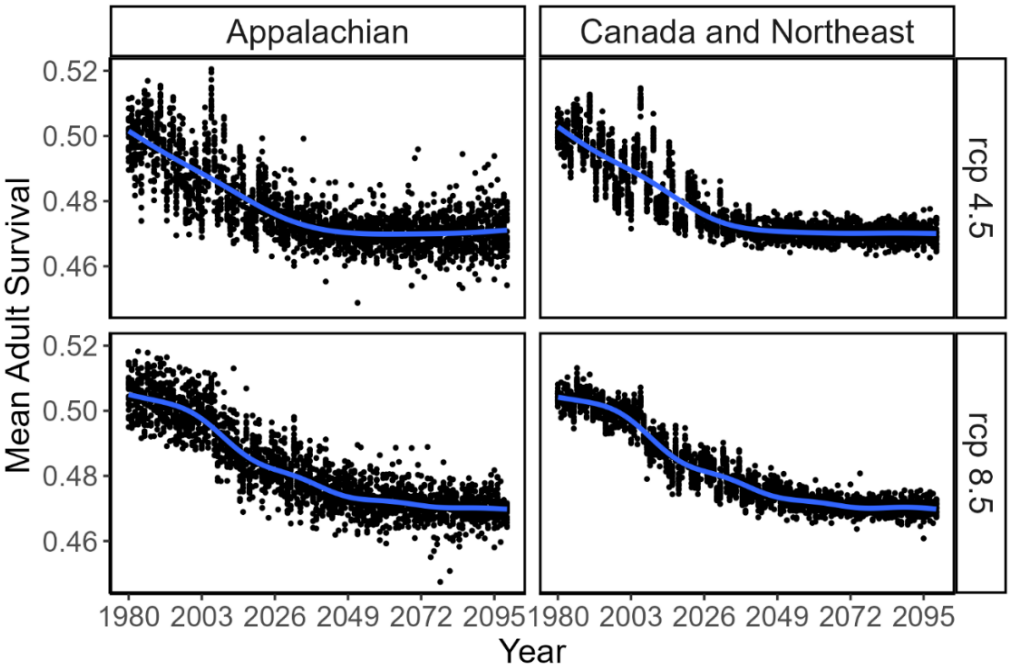

Figure 4.6 Changes in mean adult survival of Canada warblers in the Appalachian and Canada and northeastern US regions at RCP 4.5 and 8.5. Black dots represent annual means, the blue line represents the smoothed average.

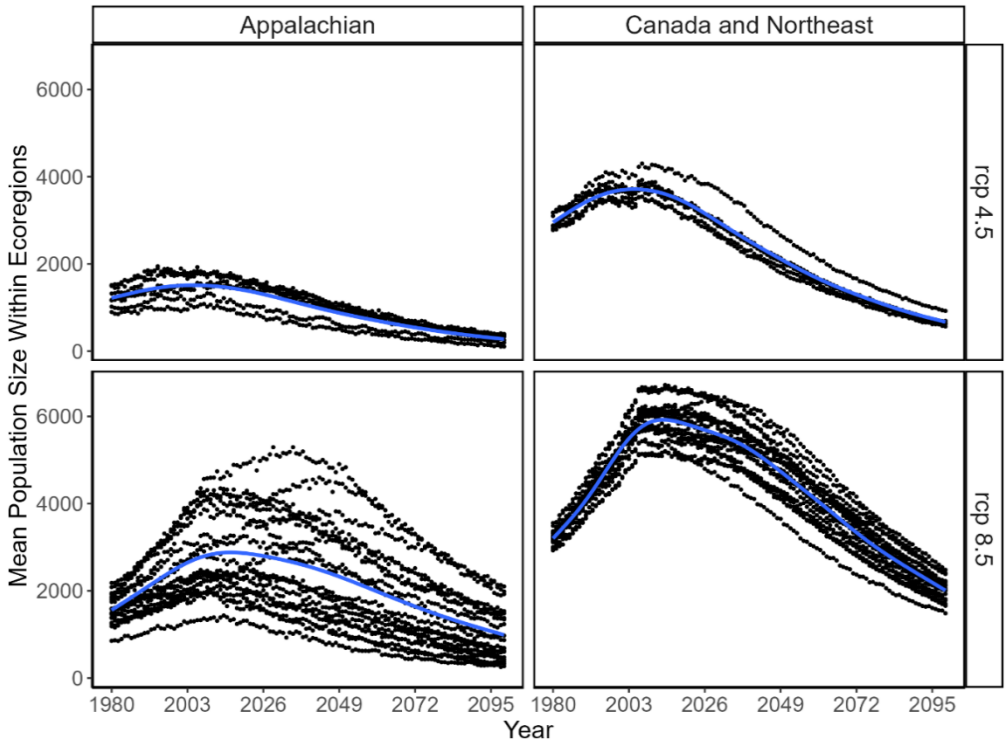

Figure 4.7 Changes in the mean population size of Canada warblers within the Appalachian and Canada and northeastern US regions at RCP 4.5 and 8.5. Black dots represent annual means, the blue line represents the smoothed average.

Table 4.1 Annual change (β) and 95% confidence interval (CI) of Canada warbler biological variables from 1980 – 2099 by region for RCP 4.5 and 8.5 experiments. Each RCP experiment was run 20 times in SCOPE.

		Appalachian			Canada and Northeast		
Variable	RCP	β	Lower 95% CI	Upper 95 % CI	β	Lower 95% CI	Upper 95 % CI
Egg-laying date	4.5	0.009	0.008	0.01	0.009	0.008	0.009
	8.5	0.0045	0.004	0.005	0.005	0.005	0.005
Mismatch	4.5	0.31	0.30	0.32	0.3	0.29	0.31
	8.5	0.26	0.26	0.26	0.26	0.25	0.27
Nest Success	4.5	0.0005	-0.003	0.001	0.0003	-0.00007	0.0006
	8.5	0.0007	0.0001	0.001	0.001	0.0009	0.002
Adult Survival	4.5	-0.00025	-0.00026	-0.00024	-0.00026	-0.00027	-0.00025
	8.5	-0.00033	-0.00034	-0.00032	-0.00032	-0.00033	-0.00032
Population Size	4.5	-11.5	-11.9	-11.2	-28.6	-29.3	-27.9
	8.5	-10.8	-11.6	-10.2	-22.2	-23.3	-21.1

Burrowing Owls

Unfortunately, it was very difficult to obtain sufficient data to evaluate the relationships between the timing of nesting and survival or reproduction for burrowing owls. Though there was some mark and recapture data from the BBL, we did not have the breeding information to link to banding data. We attempted to collaborate with several long-term projects with these types of data but, unfortunately, partners could not produce the needed information because of curation issues with legacy data or COVID-19-related delays. Though we did not have information about whether BUOW were sensitive to climate-driven phenological mismatch, there were excellent publications about the effects of weather and nesting success of burrowing owls. Further, we used BBL data to evaluate the effects of weather on migration and eBird data to examine effects of weather on spring arrival – two key components of nesting phenology.

We evaluated the SCOPE burrowing owl model and pattern-matched egg-laying dates at three sites, in New Mexico, Idaho, and Florida (Poulin et al. 2020). In addition, we matched nest success and productivity patterns in Idaho. Finally, we were able to compare model estimates of changes in migration distance over time to empirical estimates of migration changes (Figure 5A.3). Similar to the Canada warbler results, model estimates had less variance than empirical estimates of nest success and productivity, suggesting that we are not including all factors that contribute to these metrics, however, we captured the central tendency of the metrics and considered the model reliable.

From 1980 – 2099 there were significant changes in SI-x and weather variables at both RCP 4.5 and 8.5 of SCOPE_BUOW (Figure 4.8). We saw a weak advancement in the timing of egg-laying in burrowing owls (Figure 4.9, Table 4.2). Egg-laying date advancement was likely the result of competition for nest sites and mates and changes in migration distance. Despite weak advancement in egg-laying dates, differences between SI-x and egg-laying dates increased over time (Figure 4.10, Table 4.2). Nest success weakly declined (Figure 4.11, Table 4.2) likely because of increases in spring maximum temperatures. Unsurprisingly, adult survival did not change over time as this parameter was drawn from a mean value and not sensitive to environmental change (Figure 4.12, Table 4.2). This is not surprising as we were unable to assess the effects of timing on these metrics, populations remained relatively stable over time, Though, in Florida, at least one simulation went to extinction, likely because of overall smaller population sizes and stochastic events in the model

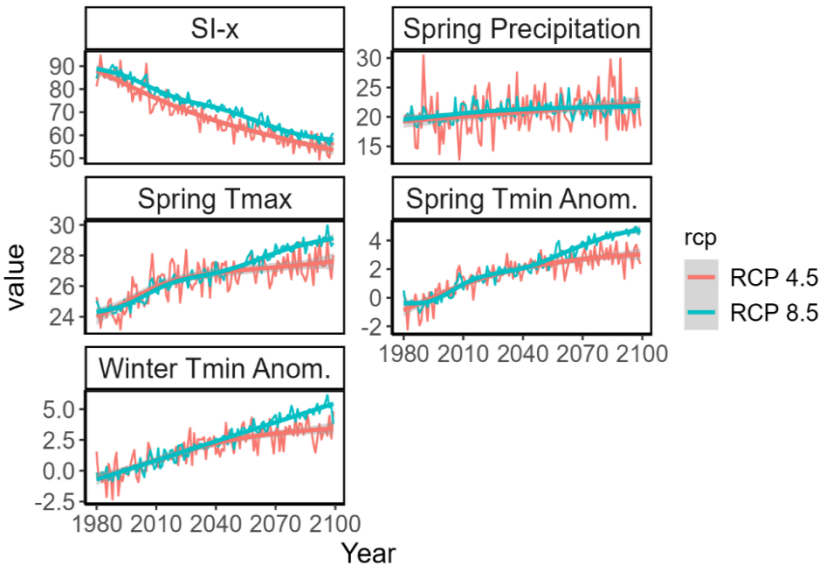

Figure 4.8 Changes in the extended spring index (SI-x, days), spring precipitation (cm), spring temperature maximums (˚C), spring minimum temperature anomalies (˚C), and winter minimum temperature anomalies (˚C) from 1980 – 2099 in the SCOPE burrowing owl model at RCP 4.5 and 8.5.

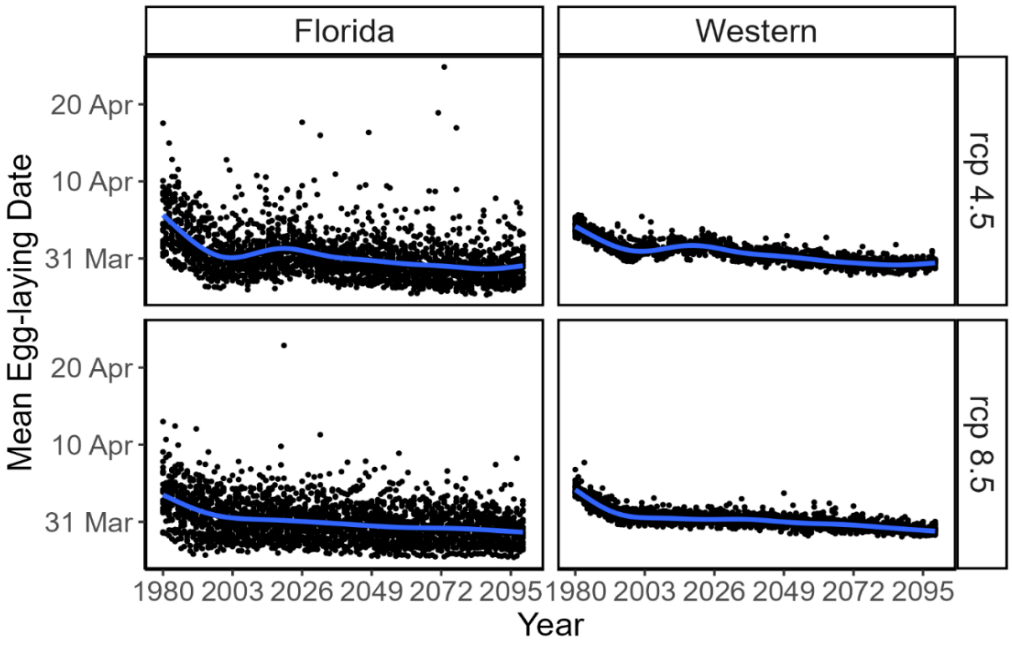

Figure 4.9 Changes in the mean egg-laying date for burrowing owls in the Florida and Western regions at RCP 4.5 and 8.5. Black dots represent annual means, the blue line represents smoothed average.

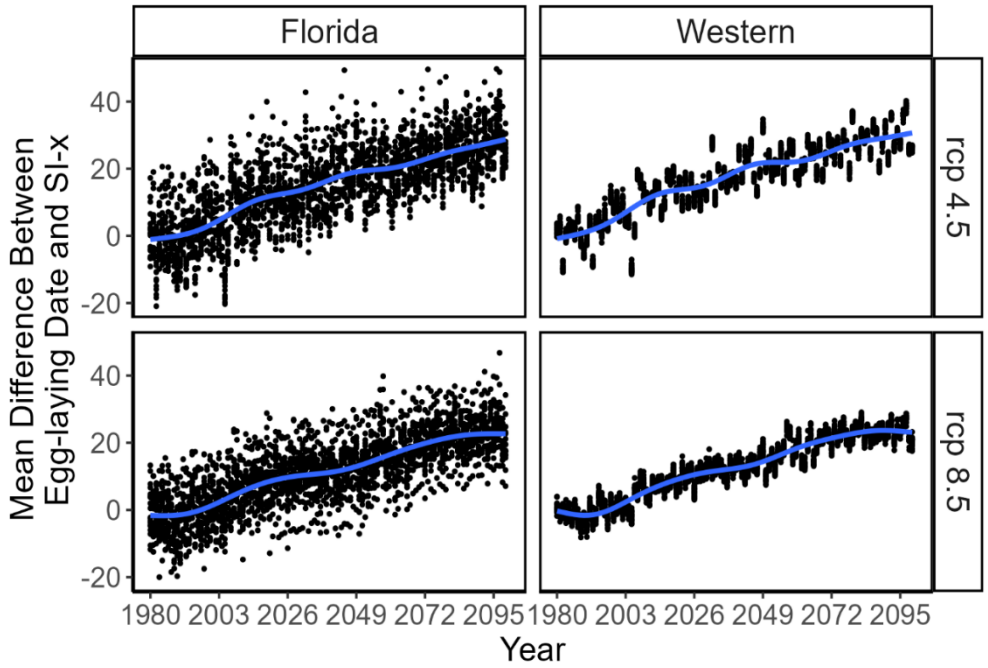

Figure 4.10 Changes in mean mismatch (i.e., difference between egg-laying date and SI-x) for burrowing owls in the Florida and Western regions at RCP 4.5 and 8.5. Black dots represent annual means, the blue line represents smoothed average.

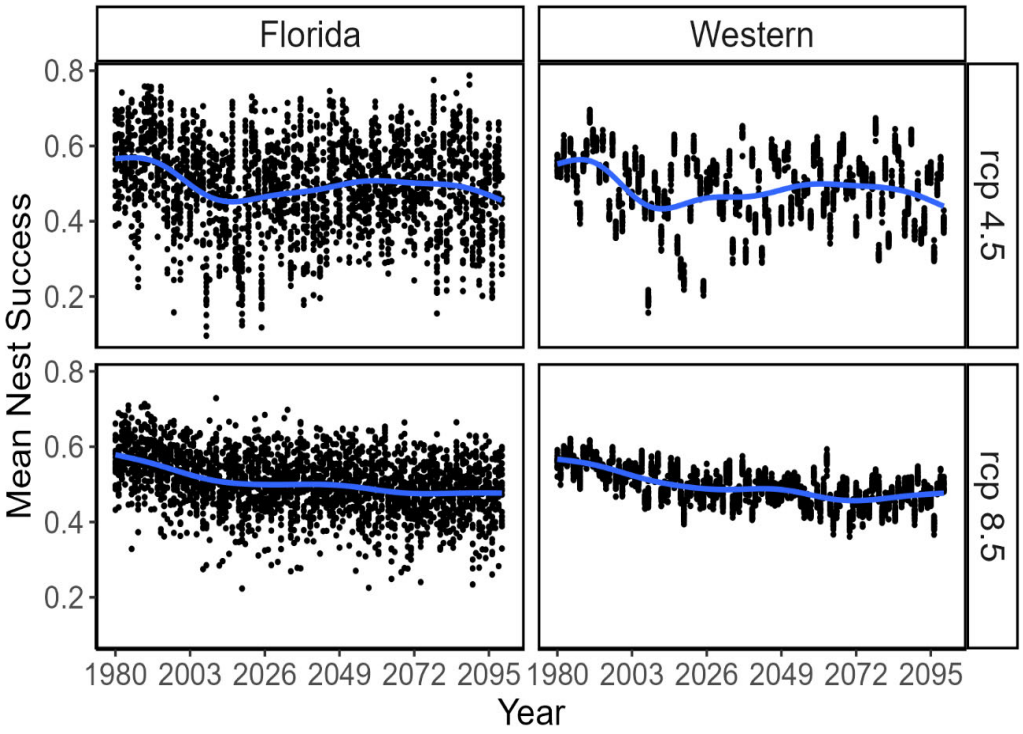

Figure 4.11 Changes in mean nest success (i.e., probability that a pair produces ≥1 young) for burrowing owls in the Florida and Western regions at RCP 4.5 and 8.5. Black dots represent annual means, the blue line represents smoothed average.

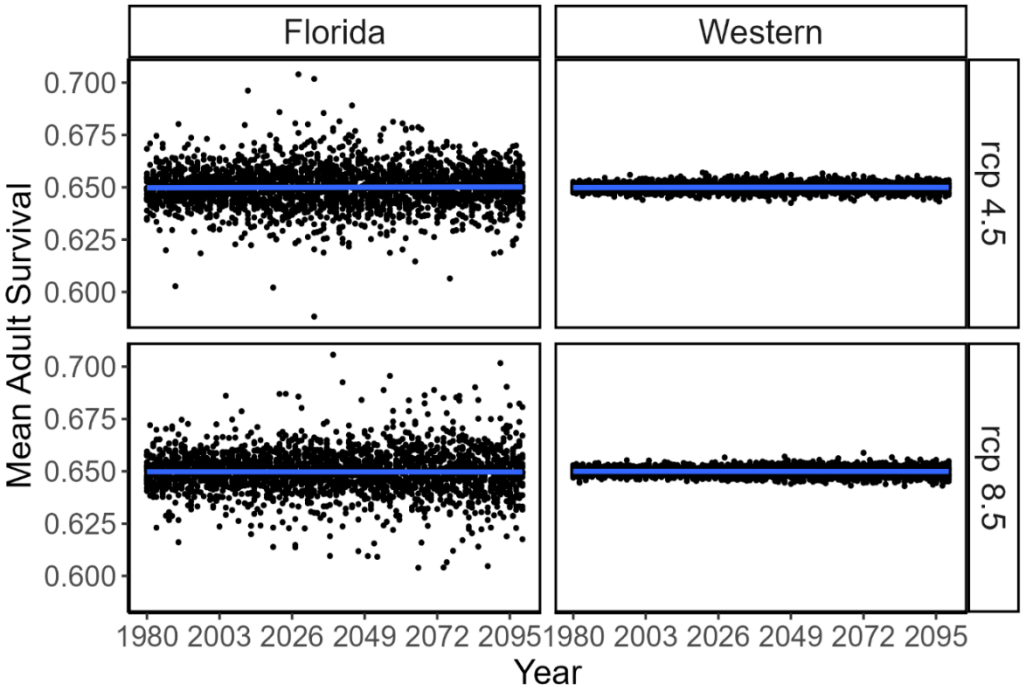

Figure 4.12 Changes in mean adult survival for burrowing owls in the Florida and Western regions at RCP 4.5 and 8.5. Black dots represent annual means, the blue line represents smoothed average.

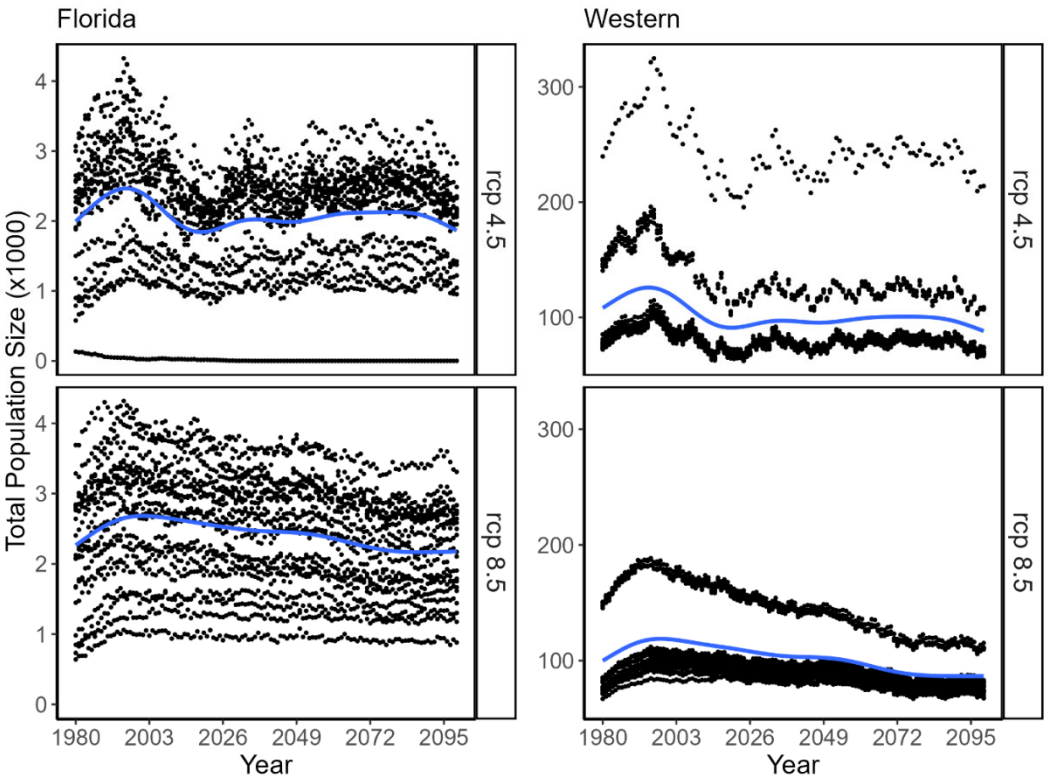

Figure 4.13 Changes in the total population size (x1000) for burrowing owls in the Florida and Western regions at RCP 4.5 and 8.5. Black dots represent annual means, the blue line represents smoothed average.

Table 4.2 Annual change (β) and 95% confidence interval (CI) of burrowing owl biological variables from 1980 – 2099 by region for RCP 4.5 and 8.5 experiments. Each experiment was run 20 times in SCOPE. Zero values for adult survival represent no change in adult survival over time.

		Florida			Western		
Variable	RCP	β	Lower 95% CI	Upper 95 % CI	β	Lower 95% CI	Upper 95 % CI
Egg-laying date	4.5	-0.035	-0.038	-0.03	-0.03	-0.03	-0.03
	8.5	-0.028	-0.03	-0.03	-0.03	-0.03	-0.03
Mismatch	4.5	0.26	0.25	0.27	0.27	0.26	0.28
	8.5	0.23	0.22	0.24	0.24	0.24	0.25
Nest Success	4.5	-0.0004	-0.0005	-0.0002	-0.0003	-0.0004	-0.0002
	8.5	-0.0007	-0.0008	-0.0006	-0.0008	-0.0009	-0.0007
Adult Survival	4.5	0	0	0	0	0	0
	8.5	0	0	0	0	0	0
Population Size	4.5	-0.001	-0.002	-0.001	-0.19	-0.20	-0.17
	8.5	-0.004	-0.004	-0.003	-0.28	-0.29	-0.27

Synthesis

We successfully parameterized SCOPE for two DoD Species of concern, Canada warblers, and burrowing owls. We found that Canada warbler reproduction and survival were sensitive to phenological mismatch. Similar to American kestrels (Chapter 1) and consistent with previous literature (Goodenough et al. 2010, Bastianelli et al. 2021), Canada warbler nest success and survival was lower in individuals that nested later compared to early nesters. However, unlike kestrels (Chapter 3), Canada warbler egg-laying dates did not advance at a rate to keep up with changes in the start of spring, resulting in increased mismatch, lower adult survival, and declining populations. The lack of advancement may be the result of very few birds being categorized as "early", particularly after ~ 2005. Canada warblers have the shortest known breeding window of wood warblers (Flockhart 2010) which suggests on-time nesting is likely important, and may constrain their ability to shift nesting phenology appropriately in response to advancing springs (see Chapter 1). They are long-distance migrants, and so have incomplete knowledge of breeding ground conditions, which may impede their ability to adjust the timing of migration departure, duration, and arrival to match resource peaks (Rubolini et al. 2010). Furthermore, drought conditions on their wintering grounds result in decreased body condition (Gonzalez et al. 2020), which could delay spring migration and time to attain breeding condition, and hence have carry-over effects on egg-laying phenology (Marra et al. 1998). Interestingly, and similar to our results of Chapter 3, phenological mismatch had the strongest effect on survival, not productivity (nest success), which is particularly concerning as Canada warbler declines are driven by decreases in survival and recruitment, rather than in productivity (Wilson et al. 2018). This result emphasizes the need to understand the energetic consequences of raising young at suboptimal times on the health of adults, an understudied phenomenon. Although population declines were predicted in all three regions, declines were steepest in the Appalachian region. This result is consistent with Wilson et al. (2018) who also found that populations in the south and east had lower survival and recruitment rates, resulting in steeper population declines, than central and western regions. Canada warblers in the Appalachian region are a trailing-edge population which is genetically distinct from leading-edge and central populations, so climate-induced extirpation could have negative genetic consequences for the species overall (Ferrari et al. 2018).

The SCOPE burrowing owl model lacked information about the sensitivity of burrowing owl reproduction and survival to phenological mismatch because data on this topic were unavailable. Nonetheless, we used published estimates about the relationship between weather and reproductive success, and used BBL data to estimate relationships between weather and burrowing owl migration strategies and distance to parameterize SCOPE. Burrowing owls egg-laying dates advanced slowly, likely because of competition for nest sites and mates, when population sizes were highest, in the early simulation years. There is evidence that in some regions (e.g. southwest) burrowing owls are arriving later and experiencing lower nest success as a result (Cruz-McDonnell and Wolf 2016), whereas later nesting individuals in other regions (e.g. Wyoming) are experiencing higher nest success. We found that predicted nest success weakly declined over time, likely because of increases in spring maximum temperature. Predicted survival rates did not change over time, likely of our inability to parameterize any environmental effects on survival. Other climatic variables, such as precipitation or frequency of extreme weather events may be important (Haley and Rosenberg 2013, Wellicome et al. 2014, Fisher 2015).

It is important to note that both of these species face multiple threats that were not represented in the SCOPE model. Specifically, both species are limited and threatened by changes in habitat. Loss and degradation of breeding and non-breeding habitat (e.g. deforestation, understory removal, land conversion) and accidental mortality (i.e. collisions with anthropogenic features) are considered high-level threats to Canada warblers (Environment Canada 2016). For burrowing owls, cumulative impacts of habitat loss (e.g. through cultivation, oil and gas development, urban sprawl), loss of burrows, and decreased prey availability are considered the main threats to the species. So results here should not be viewed as predictions but rather scenarios for the effects of phenological mismatch. Furthermore, climate change will likely exacerbate many of these existing threats. Climate projection scenarios predict a decrease in suitable Canada warbler habitat in their boreal range (i.e., old-growth, wet forest, and riparian areas) because of drier, warmer conditions and increased wildfires (Cadieux et al. 2020). Decreased density and population growth rates in Appalachian populations linked to warmer temperatures and lower precipitation are hypothesized to be the result of changes in prey availability and thermal-physiological limits (Merker and Chandler, 2020), and because these populations occur only at the highest elevations, upslope shifts in response to climate change will not be possible (Ferrari et al. 2016). Both body condition and survival of Canada warblers wintering in Columbia were negatively impacted by El Niño drought conditions, likely because of decreased habitat quality and food availability (Gonzalez et al. 2020). For burrowing owls, extreme precipitation is increasing on their breeding grounds in the Great Plains, and resulting in increased nestling mortality linked to burrow flooding and decreases in food availability (Fisher 2015). Storms during fall migration and increased precipitation on the wintering grounds decreased apparent survival, possibly because of direct mortality or decreased prey accessibility (Wellicome et al. 2014), and drought during the non-breeding period decreased survival and productivity, possibly as a result of reduced prey availability (Porro et al. 2020).

We used large data collections like eBird, BBL, and MAPS, and some data from research collaborators to parameterize the models. At times, it was difficult to obtain sufficient data for model parameterization because of small samples (e.g., Canada warbler migration) or data curation and sharing challenges (e.g., burrowing owl phenology and survival). More than ever, BBL, MAPS, eBird – large-scale projects that have longtitudinal data are critical for creating accurate demographic estimates that are needed for forecasting population changes. The contrast between reaching out to individuals versus a program like MAPS was stark. Given how important it is to have data for producing models for species of concern – it is important that resources and emphasis be placed on managing and cataloging data and making it publicly available.

Conclusions and Implications for Future Research/Implementation

We parameterized SCOPE for DoD species of concern, but challenges in data accessibility and small sample sizes limited our ability to use SCOPE to the full extent. Developing tools to assess climate vulnerability will require access to longitudinal data that can be challenging for individuals to manage and share. Improved resources for data management could aid in capturing archival data that would be useful for creating natural resource management tools.

In sum, though SCOPE was initially developed for a data-rich species, American kestrels, the sub-processes within the model were generalizable to other species of migratory birds. Parameterization of SCOPE for Canada warblers revealed that phenological mismatch is likely to

become a threat for this species, and cumulatively with other threats, could be contributing to documented population declines. Particularly steep predicted declines in Appalachian populations, which are genetically distinct from other populations, suggests that conservation actions at DoD sites in this region may be particularly important. Additionally, we add to the body of evidence suggesting that survival, rather than productivity, might be a more valuable area of research to understand population declines in this species. Alternatively, parameterization of SCOPE for burrowing owls suggested the phenological mismatch may not be an emerging threat, but challenges in obtaining quality data for burrowing owls make this result tenuous.

Literature Cited

Augusiak, J., Van den Brink, P. J., & Grimm, V. (2014). Merging validation and evaluation of ecological models to 'evaludation': A review of terminology and a practical approach. *Ecological Modelling*, *280*, 117-128.

Bastianelli O, Charmantier A, Biard C, Bonamour S, Teplitsky C, Robert A. (2021). Is earlier reproduction associated with higher or lower survival? Antagonistic results between individual and population scales in the blue tit. *bioRxiv*

Becker, D. A., Wood, P. B., & Keyser, P. D. (2012). Canada Warbler use of harvested stands following timber management in the southern portion of their range. *Forest Ecology and Management*, *276*, 1-9.

Benton, N., Ripley, J. D., & Powledge, F. (2008). Conserving biodiversity on military lands: A guide for natural resources managers. *NatureServe, Arlington, Virginia*.

Bird Studies Canada, Environment Canada's Canadian Wildlife Service, Ontario Nature, Ontario Field Ornithologists and Ontario Ministry of Natural Resources. (2006). Ontario Breeding Bird Atlas Database, 31 January 2008. http://www.birdsontario.org/atlas/aboutdata.jsp?lang=en

Both, C., Van Turnhout, C. A. M., Bijlsma, R. G., Siepel, H., Van Strien, A. J., and Foppen, R. P. B. (2010). Avian population consequences of climate change are most severe for long-distance migrants in seasonal habitats. *Proceedings of the Royal Society B: Biological Sciences*, 277(1685), 1259-1266.

Cadieux, P., Boulanger, Y., Cyr, D., Taylor, A. R., Price, D. T., Sólymos, P., ... & Tremblay, J. A. (2020). Projected effects of climate change on boreal bird community accentuated by anthropogenic disturbances in western boreal forest, Canada. *Diversity and Distributions*, *26*(6), 668-682.

Clobert, J., Baguette, M., Benton, T. G., & Bullovk, J. M. (2012) Dispersal Ecology and Evolution. Oxford: Oxford University Press.

Cruz-McDonnell, K. K., & Wolf, B. O. (2016). Rapid warming and drought negatively impact population size and reproductive dynamics of an avian predator in the arid southwest. *Global Change Biology*, *22*(1), 237-253.

Culp, L. A., Cohen, E. B., Scarpignato, A. L., Thogmartin, W. E., & Marra, P. P. (2017). Full annual cycle climate change vulnerability assessment for migratory birds. *Ecosphere*, *8*(3), e01565.

Department of Defense Partners in Flight. (2019). Annal Report. https://partnersinflight.org/resources/dod-pif-annual-report-2019/

Desante, D. F., Burton, K. M., Saracco, J. F., & Walker, B. L. (1995). Productivity indices and survival rate estimates from MAPS, a continent-wide programme of constant-effort mist-netting in North America. *Journal of Applied Statistics*, *22*(5-6), 935-948.

Desmond, M. J., Parsons, T. J., Powers, T. O., & Savidge, J. A. (2001). An initial examination of mitochondrial DNA structure in Burrowing Owl populations. *Journal of Raptor Research*, *35*(4), 274-281.

eBird. (2019). eBird: An online database of bird distribution and abundance [web application]. eBird, Cornell Lab of Ornithology, Ithaca, New York. Available: http://www.ebird.org. (Accessed: Date, October 11, 2019]).

Environment Canada. (2012). Recovery Strategy for the Burrowing Owl (*Athene cunicularia*) in Canada. *Species at Risk Act Recovery Strategy Series.* Environment Canada, Ottawa. viii + 34 pp.

Environment Canada. (2016). Recovery Strategy for the Canada Warbler *(Cardellina canadensis)* in Canada. *Species at Risk Act Recovery Strategy Series.* Environment Canada, Ottawa. vii + 56 pp.

Ferrari, B., Shamblin, B., Chandler, R., Tumas, H., Hache, S., Reitsma, L., & Nairn, C. (2018). Canada Warbler (Cardellina canadensis): novel molecular markers and a preliminary analysis of genetic diversity and structure. *Avian Conservation and Ecology*, *13*(1).

Fisher, R. J., Wellicome, T. I., Bayne, E. M., Poulin, R. G., Todd, L. D., & Ford, A. T. (2015). Extreme precipitation reduces reproductive output of an endangered raptor. *Journal of Applied Ecology*, *52*(6), 1500-1508.

Flockhart, D. T. (2010). Timing of events on the breeding grounds for five species of sympatric warblers. *Journal of Field Ornithology*, *81*(4), 373-382.

Foden, W., Mace, G. M., Vié, J. C., Angulo, A., Butchart, S. H., DeVantier, L., ... & Turak, E. (2009). Species susceptibility to climate change impacts. *Wildlife in a changing world–an analysis of the 2008 IUCN Red List of threatened species*, *77*.

González, A. M., Wilson, S., Bayly, N. J., & Hobson, K. A. (2020). Contrasting the suitability of shade coffee agriculture and native forest as overwinter habitat for Canada Warbler (*Cardellina canadensis*) in the Colombian Andes. *The Condor*, *122*(2), duaa011.

Goodenough, A. E., Hart, A. G., & Stafford, R. (2010). Is adjustment of breeding phenology keeping pace with the need for change? Linking observed response in woodland birds to changes in temperature and selection pressure. *Climatic change*, *102*(3), 687-697.

Greenwood, P. J., & Harvey, P. H. (1982). The natal and breeding dispersal of birds. *Annual review of ecology and systematics*, *13*, 1-21.

Grimm, V., Augusiak, J., Focks, A., Frank, B. M., Gabsi, F., Johnston, A. S., ... & Railsback, S. F. (2014). Towards better modelling and decision support: documenting model development, testing, and analysis using TRACE. *Ecological modelling*, *280*, 129-139.

Haley, K. L. & Rosenberg, D. K. (2013) Influence of food limitation on reproductive performance of Burrowing Owls. *Journal of Raptor Research, 47*, 365–376.

Hijmans, R. J. (2021). Introduction to the" geosphere" package (Version 1.5-14).

Laake, J. (2013). RMark: An R Interface for Analysis of Capture-Recapture Data with MARK. AFSC Processed Rep. 2013-01, Alaska Fish. Sci. Cent., NOAA, Natl. Mar. Fish. Serv.,Seattle, WA. http://www.afsc.noaa.gov/Publications/ProcRpt/PR2013-01.pdf.

Lantz, S. J., & Conway, C. J. (2009). Factors affecting daily nest survival of burrowing owls within black-tailed prairie dog colonies. *The Journal of Wildlife Management*, *73*(2), 232–241.

Marra, P. P., Hobson, K. A., & Holmes, R. T. (1998). Linking winter and summer events in a migratory bird by using stable-carbon isotopes. *Science*, *282*(5395), 1884-1886.

McCaslin, H. M., & Heath, J. A. (2020). Patterns and mechanisms of heterogeneous breeding distribution shifts of North American migratory birds. *Journal of Avian Biology*, *51*(3).
Møller, A. P., Rubolini, D., & Lehikoinen, E. (2008). Populations of migratory bird species that did not show a phenological response to climate change are declining. *Proceedings of theNational Academy of Sciences*, *105*(42), 16195-16200.
Mearns, L. O., McGinnis, S., Korytina, D., Arritt, R., Biner, S., Bukovsky, M., ... & Gutowski, W. (2017). The NA-CORDEX dataset, version 1.0. NCAR climate data gateway. BoulderCO.
Merker, S. A., & Chandler, R. B. (2021). An experimental test of the Allee effect range limitation hypothesis. *Journal of Animal Ecology*, *90*(3), 585-593.
Porro, C. M., Desmond, M. J., Savidge, J. A., Abadi, F., Cruz-McDonnell, K. K., Davis, J. L., ... & Rodríguez, N. H. (2020). Burrowing Owl (*Athene cunicularia*) nest phenology influenced by drought on nonbreeding grounds. *The Auk*, *137*(2), ukaa008.
Poulin, R. G., L. D. Todd, E. A. Haug, B. A. Millsap, and M. S. Martell (2020). Burrowing Owl (*Athene cunicularia*), version 1.0. In Birds of the World (A. F. Poole, Editor). Cornell Lab of Ornithology, Ithaca, NY, USA. https://doi.org/10.2173/bow.burowl.01
Powers, B. F., Winiarski, J. M., Requena-Mullor, J. M., & Heath, J. A. (2021). Intra-specific variation in migration phenology of American Kestrels (*Falco sparverius*) in response to spring temperatures. *Ibis*, *163*(4), 1448-1456.
Reitsma, L. R., M. T. Hallworth, M. McMahon, and C. J. Conway (2020). Canada Warbler (*Cardellina canadensis*), version 2.0. In Birds of the World (P. G. Rodewald and B. K. Keeney, Editors). Cornell Lab of Ornithology, Ithaca, NY, USA. https://doi.org/10.2173/bow.canwar.02
Rubolini, D., Saino, N., & Møller, A. P. (2010). Migratory behaviour constrains the phenological response of birds to climate change. *Climate Research*, *42*(1), 45-55.
Sauer, J. R., Niven, D. K., Hines, J. E., Ziolkowski Jr., D. J., Pardieck, K. L., Fallon, J. E., & Link , W.A. (2017). The North American breeding bird survey, results and analysis 1966–2015. Version 2.07.2017. U.S. Geological Survey, Patuxent Wildlife Research Center, Laurel, Maryland, USA.
Stein, B. A., Scott, C., & Benton, N. (2008). Federal lands and endangered species: the role of Military and other federal lands in sustaining biodiversity. *BioScience*, *58*(4), 339-347.
Szaro, R. C. (2008). Endangered species and nature conservation: science issues and challenges. *Integrative Zoology*, *3*(2), 75-82.
Thornton, P.E., Running, S.W. & White, M.A. (1997). Generating surfaces of daily meteorological variables over large regions of complex terrain. *Journal of Hydrology*, 190, 214–251.
Trautmann, S. (2018). Climate change impacts on bird species. In *Bird Species* (pp. 217-234). Springer, Cham.
U.S. Environmental Protection Agency (2009). A framework for categorizing the relative vulnerability of threatened and endangered species to climate change. *National Center for Environmental Assessment*, Washington, D.C.: EPA/600/R-09/011. Available from the National Technical Information Service, Springfield, VA, http://www.epa.gov/ncea
Visser, M. E., and Gienapp, P. (2019). Evolutionary and demographic consequences of phenological mismatches. *Nature ecology & evolution*, *3*(6), 879-885.
Visser, M. E., te Marvelde, L., and Lof, M. E. (2012). Adaptive phenological mismatches of birds and their food in a warming world. *Journal of Ornithology*, 153(1), 75-84.

Wellicome, T. I., Fisher, R. J., Poulin, R. G., Todd, L. D., Bayne, E. M., Flockhart, D. T., ... & James, P. C. (2014). Apparent survival of adult Burrowing Owls that breed in Canada is influenced by weather during migration and on their wintering grounds. *The Condor: Ornithological Applications*, *116*(3), 446-458.

White, J. W., Rassweiler, A., Samhouri, J. F., Stier, A. C., & White, C. (2014). Ecologists should not use statistical significance tests to interpret simulation model results. *Oikos*, *123*(4), 385-388.

Whitfield, D. P., Douse, A., Evans, R. J., Grant, J., Love, J., McLeod, D. R., ... & Wilson, J. D. (2009). Natal and breeding dispersal in a reintroduced population of White-tailed Eagles *Haliaeetus albicilla*. *Bird Study*, *56*(2), 177-186.

Wilson, S., Saracco, J. F., Krikun, R., Flockhart, D. T., Godwin, C. M., & Foster, K. R. (2018). Drivers of demographic decline across the annual cycle of a threatened migratory bird. *Scientific Reports*, *8*(1), 1-11.

Appendix 1. Supplemental material for Chapter 1
Effects of phenological mismatch on American kestrel (*Falco sparverius*) demography

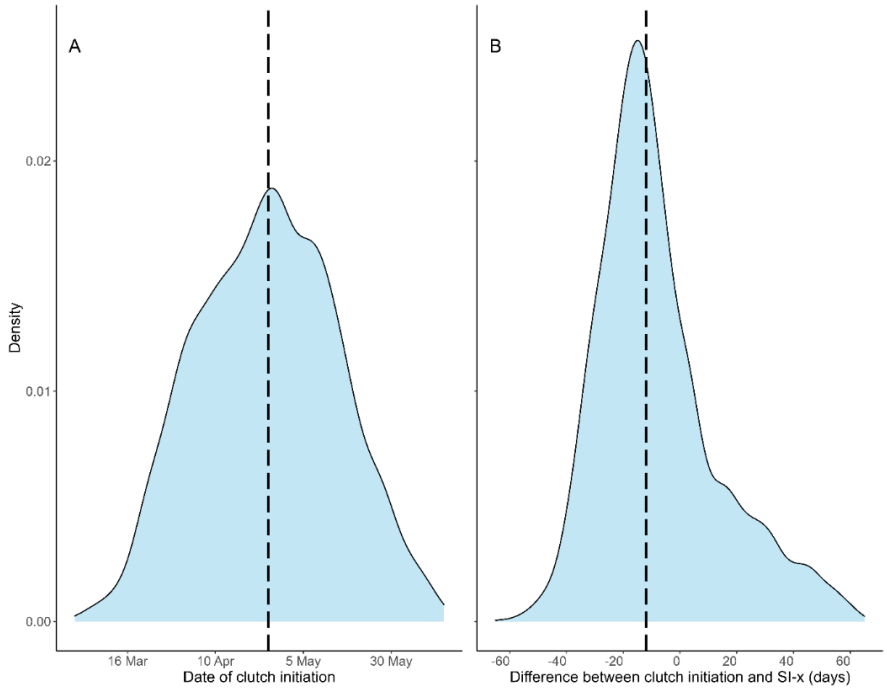

Figure A1.1 Density distributions of A) clutch initiation dates and B) the difference between clutch initiation date and extended spring index date (SI-x) for American kestrel nests in North America (1997 – 2019, n = 2144). The black dashed line represents the median overall clutch initiation date (25 April) and the overall median difference between clutch initiation date and SI-x (-12 days).

NDVI and seasonal resources at representative sites across the US

We extracted Normalized Difference Vegetation Index (NDVI) values from points within 1 km of three nest boxes at study sites in California, Washington, North Carolina, and New York (below) and three nest boxes in Idaho and New Jersey (see Chapter 1) using Google Earth Engine. We used the satellite view to sample NDVI of likely foraging areas of kestrels (i.e., we attempted to select fields and avoid streets, water, or other non-habitat). We extracted NDVI estimates from 1 Jan 2001 through 31 Dec 2020 based on data collected from the Terra Moderate Resolution Imaging Spectroradiometer (MODIS) Version 6 data generated every 16 days at 250 m spatial resolution (Didan 2015). We graphed annual patterns of NDVI over the calendar year and fit data with geom_smooth from the *tidyverse* package (Wickham et al. 2019) in R (Figure A1.2).

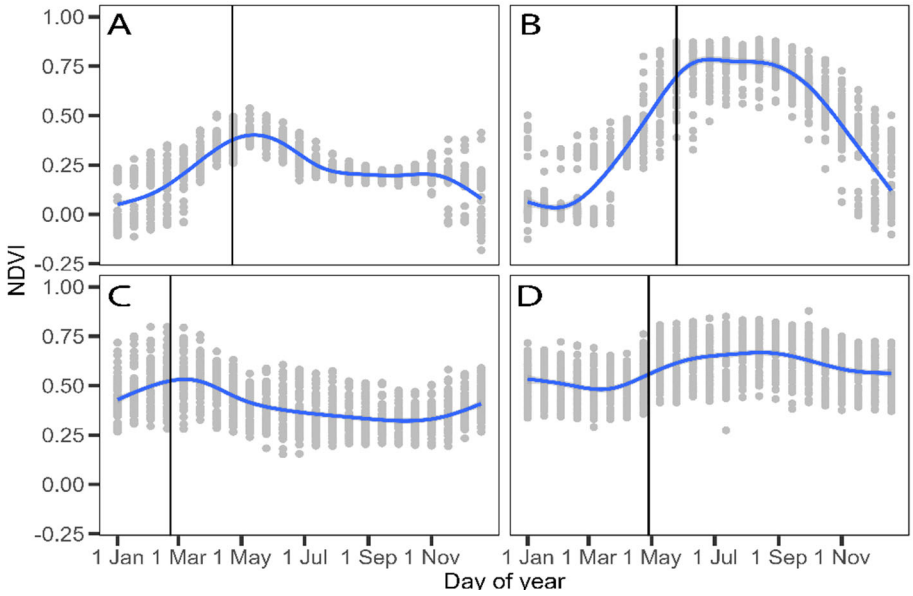

Figure A1.2 Annual Normalized Difference Vegetation Index (NDVI) values of three different American kestrel territories (2001 – 2020) at four different locations including A) Yakima Training Center, Washington; B) Fort Drum, New York; C) Camp Pendleton, California; and D) Fort Bragg, North Carolina. Gray points represent values, the blue line represents smoothed average, and the black vertical line is the average extended spring estimate (SI-x) for each site.

Methods for monitoring nest contents

Cornell's NestWatch

NestWatch (https://nestwatch.org/) is a long-term community science project administered by the Cornell Lab of Ornithology that engages participants in monitoring the breeding biology of North American birds (Phillips and Dickinson, 2009). NestWatch asks volunteers to observe nests 1 – 2 times per week, although the protocol is flexible (Phillips et al., 2007). Specifically, NestWatch volunteers use standardized data forms to record nest metadata (e.g., species, year, unique site names, location, and nest substrate) and breeding parameters for each nest visit. These include date and time, numbers of eggs, live young, and dead young for host and brood parasite species, and descriptions of adult activity, nest maintenance activity, and developmental stages of nests and young via standardized codes. In addition, volunteers are encouraged to provide a summary of the host species' estimated first egg, hatch and fledge dates, maximum clutch size, numbers of unhatched eggs, live young, and fledged birds, and any anecdotal evidence for why they believe a nest was successful or failed. Volunteers enter their nest observations online after each visit or at the end of the breeding season. The NestWatch database uses built-in error checks and filters (e.g., the number of young cannot exceed the maximum clutch size) to ensure accurate data entry by participants (Phillips and Dickinson, 2009).

American Kestrel Partnership

The Peregrine Fund's American Kestrel Partnership (AKP; https://kestrel.peregrinefund.org/) coordinates a network of community and professional scientists monitoring nest boxes across the western hemisphere, with the goal of addressing long-

term kestrel population declines. Initiated in 2012, the AKP enlists volunteers to install and monitor nest boxes and to contribute their data to a centralized database. AKP partners submit characteristics for each nest box they monitor (e.g., nest box ID, geographic coordinates, substrate, orientation), date and time of each visit, and corresponding nest contents (e.g., count of adults, eggs, live and dead nestlings, nest box use by other species). If possible, the oldest nestling is aged using plumage characteristics according to a photographic guide of kestrel nestling development (Klucsarits and Rusbuldt, 2007). The AKP protocol encourages partners to check nests once every other week beginning in late winter or early spring (in North America, early March). At a minimum, partners are asked to make at least one more visit within 30 days to check for nestlings. If eggs are still present on this second visit, partners are then asked to return again within 30 days. This nest check interval guarantees at least one visit when there are eggs and one visit when there should be nestlings present. Partners are encouraged to enter nest data on the same day that observations are made or after each breeding season.

Full Cycle Phenology Project

The Full Cycle Phenology Project (FCPP; https://fullcyclephenology.com/) seeks to understand the impacts of climate change on American kestrel phenology and demographics in North America. FCPP established a network of 284 nest boxes at 13 Department of Defense installations and partner sites (Table A1.1). At each DoD site, nest monitoring began two

Table A1.1 A list of Department of Defense installations and sites managed by the Army Corps of Engineers where American kestrel nest boxes were posted to study clutch initiation and productivity.

Location	State
Marine Corps Base Camp Pendleton	California
Yakima Training Center	Washington
U. S. Army Fort Bragg	North Carolina
U. S. Army Fort Hood	Texas
U. S. Army Fort Drum	New York
White Sands Missile Range	New Mexico
U. S. Army Fort Riley	Kansas
Eglin Air Force Base	Florida
U. S. Army Fort Wainwright	Alaska
Big Oaks National Wildlife Refuge	Indiana
U. S. Army Dugway Proving Ground	Utah
Minot Air Force Base	North Dakota
Lucky Peak Reservoir	Idaho

weeks prior to the earliest clutch initiation date records for kestrels in the region. Depending on the study site, nests were monitored remotely via cellular trail cameras (Spypoint Link-Evo, Victoriaville, Québec, CA) located inside nest boxes, monthly in-person visits by DoD biologists to nest boxes equipped with non-cellular trail cameras (Spypoint Force-10, Victoriaville, Québec, CA and Reconyx Hyperfire 2, Holmen, Wisconsin, USA), or bi-weekly in-person visits to nest boxes without trail cameras. Cameras were placed inside a false lid located at the top of

the nest box, with the camera's field-of-view aimed toward the bottom of the box. Non-cellular and cellular cameras were programmed on time-lapse mode to record photos three times per day (3:00, 9:00, 15:00), and were switched to hourly intervals once the first egg was detected in images or in-person visits. During in-person visits and time-lapse imagery review, nest contents were assessed by determining the presence, sex, and incubation behavior of adults, and the number of eggs and nestlings. Time-lapse imagery was reviewed and annotated at the end of each breeding season using the ViXeN software package (Ramachandran and Devarajan 2018). In addition to regularly-scheduled visits and time-lapse imagery, additional visits were made on or near the estimated hatch date (30 days after a complete clutch was laid) to confirm hatching, and again prior to fledging (23 – 25 days the after the first egg hatched) to band and record the age of nestlings.

Southwestern Idaho Kestrel Study

The breeding biology of American kestrels in southwestern Idaho (43°N 116°W) has been monitored as part of a long-term study (Steenhof and Peterson 2009; Anderson et al. 2016; Smith et al. 2017). The study area includes approximately 98 – 113 nest boxes (depending on the year; Smith et al. 2017) located in rural, residential, and agricultural areas near Boise, Kuna, and Meridian, Idaho. Beginning in March, nest boxes are visited every 7 – 20 days to determine occupancy and nest initiation date. After capturing adults, nest boxes are checked again on estimated hatch dates, when the oldest nestling is approximately 10 days old, and again at approximately 25 days old, prior to fledging. Nest contents (number of eggs, live and dead young) are recorded during each visit. Nest failure is determined based on the presence or absence of eggs, nestlings, or adult birds (Strasser and Heath 2013).

Data curation

NestWatch

We restricted our sample of NestWatch nests to attempts with a known clutch initiation date, hatch date or fledge date, and known outcomes (either success or failure).

American Kestrel Partnership

A primary objective of the AKP is determining the drivers of nest box occupancy, and submitting records of unoccupied boxes is highly encouraged. As a first step, we discarded nests that did not contain kestrel eggs or nestlings. We then restricted our sample to nests within the USA and Canada and removed nests occupied by other species. We also excluded nest attempts that included nestling observations only and no age reported (which prevented back-calculating clutch initiation date), and attempts with a single egg observation (which did not contain nest outcome or productivity information). We conducted an additional manual screening of the data to remove nest records containing unclear observations (e.g., the appearance of multiple attempts entered per record) or comments that indicated problematic data entries. Finally, we retained nests during this step that had some indication of success or failure (i.e., ≥ 25-day-old nestlings, anecdotal evidence of fledging or predation), and provided a count of nestlings or fledglings from the nest record or comments used to determine nest outcome.

Full Cycle Phenology Project

The majority of the FCPP's nest boxes were equipped with cellular or non-cellular trail cameras, generally allowing direct observation of clutch initiation date, nest success, and productivity. We discarded nests that had low frequency or no time-lapse imagery due to camera failures, and infrequent in-person visits that prohibited reliable estimation of phenology and nest outcome.

Southwestern Idaho Kestrel Study
We restricted our sample of southwestern Idaho nest records to attempts with a known clutch initiation date and known outcomes (either success or failure).

Clutch initiation date, nest outcome, and productivity determinations
NestWatch
We relied on user-specified fields in the NestWatch database to determine clutch initiation dates and nest outcomes (Phillips and Dickinson, 2009). To assign the clutch initiation date, we used the first egg date (FIRST_LAY_DT) field. If the first egg date contained an NA value, we back-calculated from the hatch (HATCH_DT) or fledge date (FLEDGE_DT) assuming 1 egg laid every other day, 30 days for incubation, and 30 days until fledging (Bird and Palmer, 1988; Anderson et al., 2016). We used the 's' or 'f' prefix in the OUTCOME_CODE_LIST field to assign nest success or failure, respectively. If a nest was successful, we set productivity equal to the YOUNG_HOST_TOTAL_ATLEAST field value; otherwise, productivity was set to zero.
American Kestrel Partnership, Full Cycle Phenology Project, and Southwestern Idaho Kestrel Study
We estimated the clutch initiation date for each nesting attempt in several ways. When we discovered an incomplete clutch of eggs in a nest box, the clutch initiation date was calculated by subtracting the number of eggs in the clutch multiplied by two from the date that the clutch was discovered (AKP, FCPP, Southwestern Idaho Kestrel Study; Anderson et al., 2016), because kestrels tend to lay 1 egg every other day (Bird and Palmer, 1988). For nest attempts discovered with a complete clutch or already hatched, we used nestling age as determined by plumage characteristics (Griggs and Steenhof, 1993; Klucsarits and Rusbuldt, 2007) to back-calculate the clutch-initiation date by subtracting the age of the most mature nestling, 30 days for incubation, and twice the number of nestlings from the hatching date. For FCPP nest boxes with functioning cameras, we directly measured clutch initiation date from time-lapse imagery. For nest attempts in which the view of the nest box floor was obstructed, we relied on in-person nest visits and used the back-calculation methods described above.
We used the following criteria to determine nest outcome: successful nests produced at least one ≥ 25-day-old nestling (85% of fledging age; Strasser and Heath, 2013) as indicated by aging during nest visits or from time-lapse imagery (FCPP), or based on anecdotal evidence of nest success or failure provided by volunteers (AKP). Finally, the number of young fledged from successful nests was estimated using the count of live nestlings when at least one ≥ 25-day-old nestling was present or from participant comments (AKP).

American kestrel breeding phenology and the extended spring index
We used data from the AKP (https://kestrel.peregrinefund.org/) and the Cornell Lab of Ornithology's NestWatch Program (https://www.nestwatch.org/) to examine environmental predictors of nest timing (see above). Nest data were also obtained from a long-term kestrel demographic study in southwestern Idaho and the FCPP (https://fullcyclephenology.com/, see above). Clutch initiation dates for these sources were estimated as described above. Our final data set included nest records from 2012 – 2019 that spanned the contiguous USA, Alaska, and southern Canada (Figure A1.3).

Breeding phenology covariates

We hypothesized that kestrels would time their breeding to coincide with vegetation green-up, which is an indicator of peak prey abundance (Smith et al. 2017). We used the extended spring index (SI-x; Schwartz et al. 2013, Ault et al. 2015) to determine spring green-up for each nest record. This data set provides the start-of-spring date (day-of-year), which is determined primarily by accumulated springtime warmth needed for leaf-out and bloom of lilac (*Syringa chinensis*) and honeysuckle species (*Lonicera tatarica* and *L. korolkowii*; Ault et al. 2015). Leaf-out dates are generally aligned with plant species that are active earliest in the spring, while bloom dates are associated with species that are active later in the spring. Extended spring indices have been shown to be strongly correlated with the timing of phenological events for native species and crops alike (Schwartz et al. 2013, Rosemartin et al. 2015, Gerst et al. 2020). Annual SI-x raster layers for leaf-out and first bloom dates were created using Google Earth Engine (Gorelick et al. 2017, Izquierdo-Verdiguier et al. 2018) and derived for each nest location using the raster package in R (Hijmans 2021).

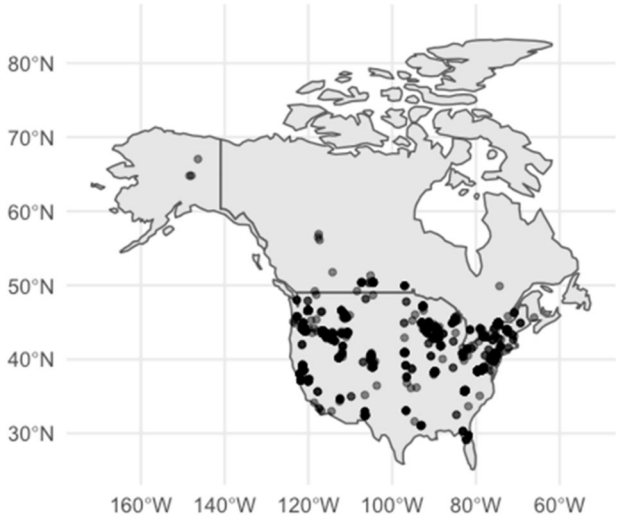

Figure A1.3 Distribution of American kestrel nests (n = 3212) monitored in the continental US, 2012 – 2019 that were used to assess environmental predictors of clutch initiation dates.

We expected warmer spring temperatures to be associated with earlier clutch initiation dates, while colder winter temperatures and higher precipitation in spring could result in longer migration distances (Heath et al. 2012) or increase kestrel energetic demands, respectively, leading to later clutch initiation. Therefore, we included winter minimum temperature (November – February average), spring minimum temperature (March – May average), and spring precipitation (March – May total) in the analysis. Weather variables were obtained from the NASA Daymet daily surface weather and climatological summary dataset (Thornton et al. 1997). Daymet has a 1 km spatial resolution and provides daily modeled estimates of several weather variables. Data were extracted for each nest record using the *daymetr* package in R (Hufkens et al. 2018).

Statistical analysis

We tested for associations between environmental covariates and kestrel clutch initiation dates by fitting hierarchical generalized linear models in a Bayesian framework using integrated nested Laplace approximation (INLA; Rue et al. 2009). INLA is a fast and reliable alternative to Markov chain Monte Carlo, and allows for an efficient way of approximating Gaussian random fields (GRFs) to incorporate spatial effects in models (Simpson et al. 2016). We fit clutch initiation models using the R package *inlabru* (Bachl et al. 2019), which provides accessible and user-friendly functions for the widely-used *RINLA* package (Lindgren and Rue 2015).
In this framework, the spatial random effect represents processes that cannot be explained by covariates, including spatial dependence between observations. The spatial random effect was modeled as a continuous GRF using the stochastic partial differential equation (SPDE) approach

(Lindgren et al. 2011). The INLA-SPDE approach overcomes the computational challenges of modeling spatial data by approximating GRFs with sparser Gaussian Markov random fields (Lindgren et al. 2011, Blangiardo and Cameletti 2015, Krainski et al. 2019). The Gaussian Markov random fields was modeled across most of the United States and Canada using a spatial mesh created with constrained refined Delaunay triangulation. To build the mesh, a boundary layer of small triangles was created to cover the domain of kestrel nest records, and an outer layer of larger triangles was added to reduce boundary effects. We used the the inla.mesh.assessment function in the *inlabru* package to determine the appropriate triangle size for the inner portion of the mesh, which can affect the accuracy of model parameters. This tool visualizes the standard deviation, which should be uniform across the mesh (both at mesh nodes and inside triangles) when triangle edge lengths are properly chosen.

We analyzed kestrel breeding phenology using gamma-distributed models because clutch initiation dates (day-of-year) are always positive. We used default non-informative prior distributions from R-INLA for all regression coefficients and hyperparameters. Prior to analysis, we followed the data exploration and variable collinearity guidelines outlined by Zuur et al. (2017). As many of the covariates were highly correlated, we ran a null model (no spatial effect), and a null model and univariate models with a spatial random effect included. Models also contained a random effect for year to account for temporal variation in clutch initiation date. All covariates were centered and scaled by subtracting the mean value and dividing by the standard deviation prior to analysis.

Log pseudo-marginal likelihood (LPML) or the sum of the log conditional predictive ordinate values (Lindgren et al. 2011) was used to compare models. Calculation of conditional predictive ordinate occurs as part of the model fitting process (Held et al. 2010) and is a leave-one-out cross-validation score (Hooten and Hobbs 2015). The top model was selected based on the lowest LPML value, and a covariate was considered significant if the 85% credible interval did not overlap zero. Finally, we used the mean absolute error to evaluate the predictive ability of the top model.

Results

We analyzed predictors of breeding phenology from 3212 American kestrel nests (Figure A1.3). Comparing the spatial random effect models by LPML value, the best model included the effect of the extended spring index first bloom date (Table A1.2), which had a strong positive relationship with clutch initiation date (β = 0.07, 95% CI = 0.06 – 0.08; Figure A1.4). The second-highest-ranking model included the effect of the first leaf date but differed in LPML value by ~3 (Table A1.2).

The posterior mean of the range parameter, which is representative of the distance at which the spatial autocorrelation declines to a negligible level, was approximately 255 km (Figure A1.5). Predicted clutch initiation dates from the top model were heterogeneous across the study area (Figure A1.6). The model predicted the earliest clutch initiation dates in the Central Valley region of California, the interior Pacific Northwest, the Midwest, and mid-Atlantic states. Later clutch initiation dates were predicted for kestrels breeding in southern California, New Mexico, Florida, New England, and the Northern Great Plains. mean absolute error for clutch initiation dates was ~11 days.

Table A1.2 Candidate models and model selection results using log pseudo-marginal likelihoods (LPMLs) for gamma regression of American kestrel nesting phenology in North America, 2012 – 2019. We used two versions of the extended spring index (SI-x) estimates of first bloom (SI-x-bloom) and leaf out (SI-x-leaf). SI-x-bloom best predicted nesting phenology.

Model	**LPML**
SI-x-bloom + site(map = coordinates, model = spde1) + year(map = year_id, model = "iid", n = n_years)	13019
SI-x-leaf + site(map = coordinates, model = spde1) + year(map = year_id, model = "iid", n = n_years)	13022
spring_tmin + site(map = coordinates, model = spde1) + year(map = year_id, model = "iid", n = n_years)	13030
winter_tmin + site(map = coordinates, model = spde1) + year(map = year_id, model = "iid", n = n_years)	13045
spring_prcp + site(map = coordinates, model = spde1) + year(map = year_id, model = "iid", n = n_years)	13047
site(map = coordinates, model = spde1) + year(map = year_id, model = "iid", n = n_years)	13048
1 + year(map = year_id, model = "iid", n = n_years)	13880

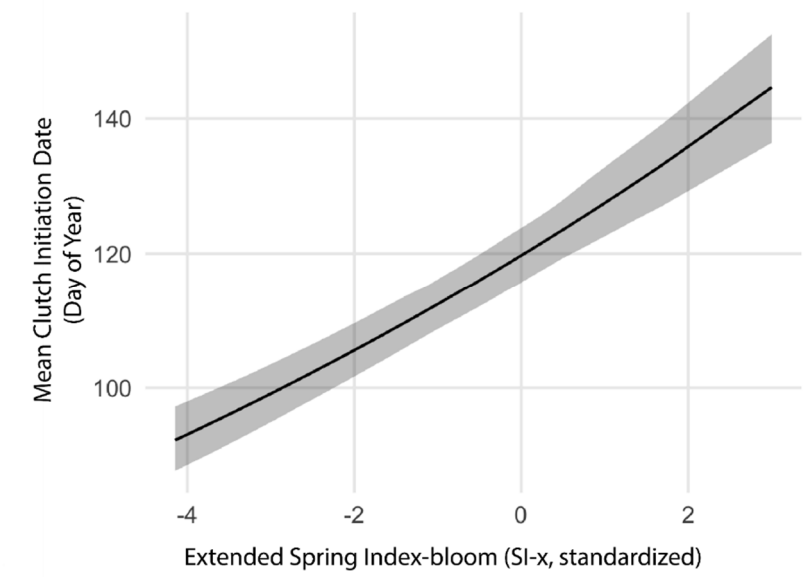

Figure A1.4 Relationship between clutch initiation date and the extended spring index estimating first bloom date (standardized). Black line and gray ribbon indicate mean predicted values and 95% credible intervals, respectively.

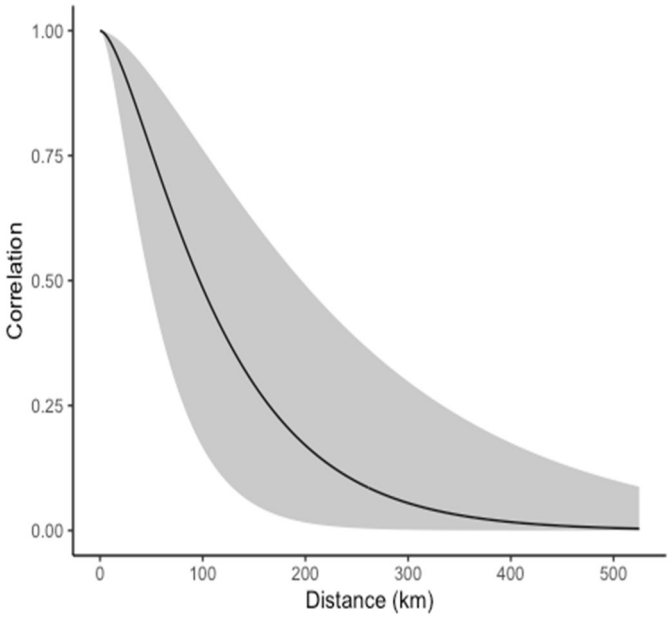

Figure A1.5 Matern correlation values showing spatial autocorrelation for American kestrel clutch initiation dates for nest records up to ~255 km apart from each other. Black line and gray ribbon indicate mean correlation values and 95% credible intervals, respectively.

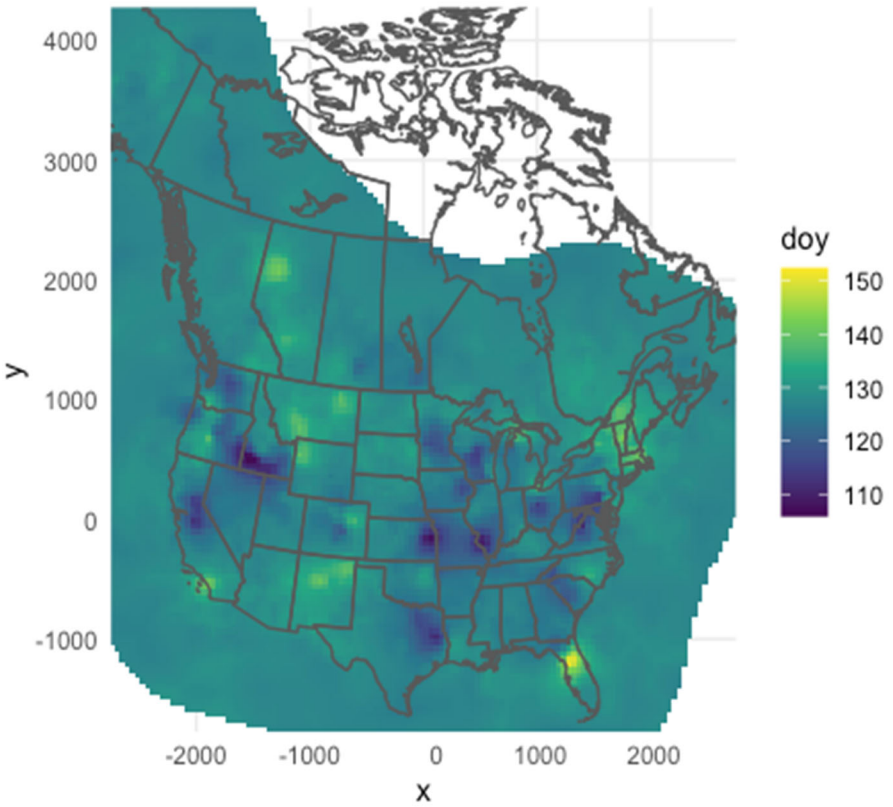

Figure A1.6 Posterior mean predicted clutch initiation dates shown as day-of-year (doy) from the inlabru model including SI-x as a fixed effect with a random spatial effect. Cooler colors represent earlier predicted clutch initiation dates, and warmer colors represent later predicted clutch initiation dates.

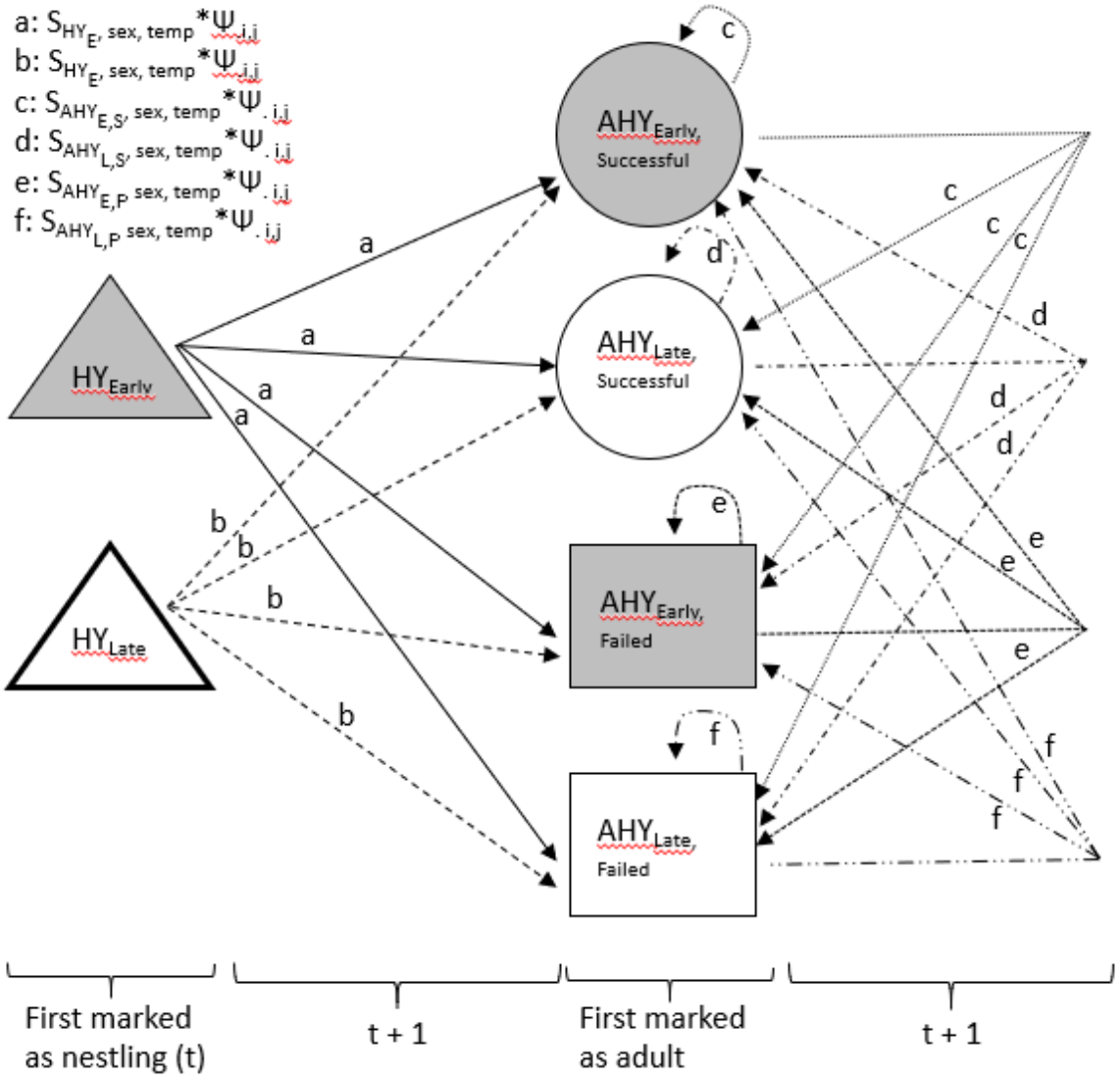

Figure A1.7 Model structure for the top model of apparent survival of American kestrels at the western (Idaho) site showing the 6 levels of strata stratified by age (HY or AHY), nesting timing (Early or Late), and whether adults were successful (Successful, Failed). The probability of a kestrel surviving and transitioning between the first state (i) and next state (j) is shown in lettered paths. Transition probabilities between HY groups and from AHY groups to HY were fixed to zero and are not shown.

Supplemental tables showing candidate model sets for recapture probability and transition probability

Table A1.3 Candidate model set to estimate recapture probability (p) of American kestrels in the western (Idaho) site captured between 2008 – 2017. The table includes the model, number of model parameters (K), delta AIC_c (ΔAIC_c), and model weights (w_i). The transition probability and apparent survival terms included an intercept-only term for these models.

Recapture (p)	K	ΔAIC_c	w_i
Sex	23	0	0.44
Winter temperature	23	0.8	0.29
Intercept-only	22	0.9	0.27

Table A1.4 Candidate model set to estimate recapture probability (p) of American kestrels in the eastern (New Jersey) site captured between 1997 – 2017. The table includes the model, number of model parameters (K), delta AIC_c (ΔAIC_c), and model weights (w_i). The transition probability and apparent survival terms included an intercept-only term for these models.

Recapture (p)	K	ΔAICc	wi
Sex	23	0	0.99
Intercept-only	22	11.7	0.01
Winter temperature	23	12.9	0

Table A1.5 Candidate model set to estimate transition probability (Ψ) of American kestrels in the western (Idaho) site captured between 2008 – 2017. The table includes the model, number of model parameters (K), delta AICc (ΔAIC_c), and model weights (w_i). The recapture probability and apparent survival terms included an intercept-only term for these models.

Transition (Ψ)	K	ΔAIC_c	w_i
Intercept-only	23	0	0.74
Stratum	24	2.07	0.26

Table A1.6 Candidate model set to estimate transition probability (Ψ) of American kestrels in the eastern (New Jersey) site captured between 1997 – 2017. The table includes the model, number of model parameters (K), delta AICc (ΔAIC_c), and model weights (w_i). The recapture probability and apparent survival terms included an intercept-only term for these models.

Transition (Ψ)	K	ΔAIC_c	w_i
Intercept-only	23	0	0.68
Stratum	24	1.5	0.32

Literature cited

Anderson, A. M., Novak, S. J., Smith, J. F., Steenhof, K., & Heath, J. A. (2016). Nesting phenology, mate choice, and genetic divergence within a partially migratory population of American Kestrels. *The Auk: Ornithological Advances*, *133*(1), 99-109.

Ault, T. R., Schwartz, M. D., Zurita-Milla, R., Weltzin, J. F., & Betancourt, J. L. (2015). Trends and natural variability of spring onset in the conterminous United States as evaluated by a new gridded dataset of spring indices. *Journal of Climate*, *28*(21), 8363-8378.

Bachl, F. E., Lindgren, F., Borchers, D. L., Simpson, D., & Scott-Hayward, L. (2018). inlabru: Spatial inference using integrated nested Laplace approximation. *R package version*, *2*(3).

Bird, D. M., & Palmer, R. S. (1988). American kestrel. Handbook of North American birds (Vol. 5, pp. 253–290).

Didan, K. (2015). MOD13Q1 MODIS/Terra vegetation indices 16-day L3 global 250m SIN grid V006. *NASA EOSDIS Land Processes DAAC*, *10*, 415.

Gerst, K. L., Crimmins, T. M., Posthumus, E. E., Rosemartin, A. H., & Schwartz, M. D. (2020). How well do the spring indices predict phenological activity across plant species? *International Journal of Biometeorology*, *64*(5), 889-901.

Gorelick, N., Hancher, M., Dixon, M., Ilyushchenko, S., Thau, D., & Moore, R. (2017). Google Earth Engine: Planetary-scale geospatial analysis for everyone. *Remote sensing of Environment*, *202*, 18-27.

Griggs, G. R., & Steenhof, K. (1993). Photographic guide for aging nestling American Kestrels. USDI Bureau of Land Management. *Raptor Research Technical Assistance Center, Boise, ID USA*.

Heath, J. A., Steenhof, K., & Foster, M. A. (2012). Shorter migration distances associated with higher winter temperatures suggest a mechanism for advancing nesting phenology of American kestrels *Falco sparverius*. *Journal of Avian Biology*, *43*(4), 376-384.

Hijmans R. J. (2021). raster: Geographic Data Analysis and Modeling. https://CRAN.R-project.org/package=raster

Hufkens, K., Basler, D., Milliman, T., Melaas, E. K., & Richardson, A. D. (2018). An integrated phenology modelling framework in R. *Methods in Ecology and Evolution*, *9*(5), 1276-1285.

Izquierdo-Verdiguier, E., Zurita-Milla, R., Ault, T. R., & Schwartz, M. D. (2018). Development and analysis of spring plant phenology products: 36 years of 1-km grids over the conterminous US. *Agricultural and Forest Meteorology*, *262*, 34-41.

Klucsarits, J. R., & Rusbuldt, J. J. (2007). *A photographic timeline of Hawk Mountain Sanctuary's American kestrel nestlings*. Zip Publishing.

Krainski E. T., Lindgren F., Simpson D., Rue H. (2019). The R-INLA tutorial on SPDE models. https://www.math.ntnu.no/inla/r-inla.org/tutorials/spde/spde-tutorial.pdf

Lindgren, F., Rue, H., & Lindström, J. (2011). An explicit link between Gaussian fields and Gaussian Markov random fields: the stochastic partial differential equation approach. *Journal of the Royal Statistical Society: Series B (Statistical Methodology)*, *73*(4), 423-498.

Lindgren, F., & Rue, H. (2015). Bayesian spatial modelling with R-INLA. *Journal of Statistical Software*, *63*, 1-25.

Phillips, T., Cooper, C., Dickinson, J., Lowe, J., Rietsma, R., Gifford, K., & Bonney, R. (2007). NestWatch Nest Monitoring Manual. *Ithaca, NY: Cornell Lab of Ornithology*, *28*.

Phillips, T. I., & Dickinson, J. L. (2009). Tracking the nesting success of North America's breeding birds through public participation in NestWatch. In *Proceedings of the Fourth International Partners in Flight Conference. McAllen: Partners in Flight* (pp. 633-640).

Ramachandran, P., & Devarajan, K. (2018). ViXeN: An open-source package for managing multimedia data. *Methods in Ecology and Evolution*, *9*(3), 785-792.

Rosemartin, A. H., Denny, E. G., Weltzin, J. F., Lee Marsh, R., Wilson, B. E., Mehdipoor, H., ... & Schwartz, M. D. (2015). Lilac and honeysuckle phenology data 1956–2014. *Scientific Data*, *2*(1), 1-8.

Rue, H., Martino, S., & Chopin, N. (2009). Approximate Bayesian inference for latent Gaussian models by using integrated nested Laplace approximations. *Journal of the Royal Statistical Society: Series B (Statistical Methodology)*, *71*(2), 319-392.

Schwartz, M. D., Ault, T. R., & Betancourt, J. L. (2013). Spring onset variations and trends in the continental United States: past and regional assessment using temperature-based indices. *International Journal of Climatology*, *33*(13), 2917-2922.

Smith, S. H., Steenhof, K., McClure, C. J., & Heath, J. A. (2017). Earlier nesting by generalist predatory bird is associated with human responses to climate change. *Journal of Animal Ecology*, *86*(1), 98-107.

Steenhof, K., & Peterson, B. E. (2009). American Kestrel reproduction in southwestern Idaho: annual variation and long-term trends. *Journal of Raptor Research*, *43*(4), 283-290.

Strasser, E. H., & Heath, J. A. (2013). Reproductive failure of a human-tolerant species, the American kestrel, is associated with stress and human disturbance. *Journal of Applied Ecology*, *50*(4), 912-919.

Thornton, P. E., Running, S. W., & White, M. A. (1997). Generating surfaces of daily meteorological variables over large regions of complex terrain. *Journal of Hydrology*, *190*(3-4), 214-251.

Wickham, H., Averick, M., Bryan, J., Chang, W., McGowan, L. D. A., François, R., ... & Yutani, H. (2019). Welcome to the Tidyverse. *Journal of Open Source Software*, *4*(43), 1686.

Zuur, A. F., Elena, N. I., & Anatoly, A. S. (2017). Beginner's guide to spatial, temporal, and spatial temporal ecological data analysis with R-INLA Volume I: using GLM and GLMM. Highland Statistics Ltd. *Newburgh United Kingdom*.

Appendix 2. Supplemental material for Chapter 2
Genetic correlates of avian phenology

Heritability analysis

The heritability model chosen for our study passed Heidelberger stationary and halfwidth mean tests, indicating model convergence. The effective size of all parameters used in this study was high (>4000) and the deviance information criterion of this model was low relative to other models tested (DIC = -1157.122).

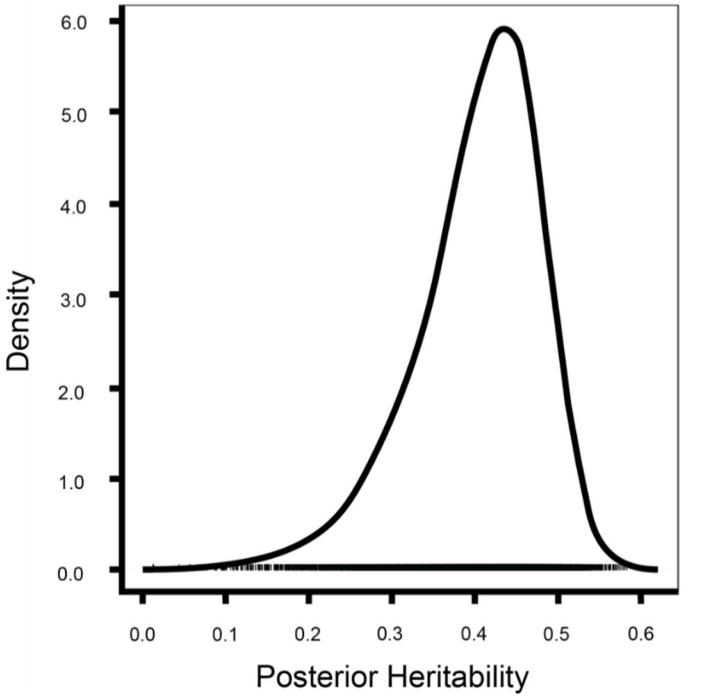

Figure 2A.1 The heritability posterior distribution of American kestrel clutch initiation dates of individuals nesting in southwestern Idaho 1992 – 2019.

Table 2A.1 Simulated heritability (h^2), the average median (± SD), mode (± SD), and 90% confidence interval bounds for estimated h^2 of American kestrel clutch initiation from 100 iterations.

Simulated h^2	Average median h^2 ± SD	Average mode h^2 ± SD	Average L90 ± SD	Average H90 ± SD
0.01	0.033 ± 0.018	0.001 ± 0.000	0.000 ± 0.000	0.123 ± 0.035
0.05	0.055 ± 0.038	0.011 ± 0.038	0.001 ± 0.006	0.153 ± 0.047
0.1	0.103 ± 0.057	0.058 ± 0.086	0.009 ± 0.022	0.218 ± 0.053
0.2	0.171 ± 0.075	0.139 ± 0.123	0.032 ± 0.047	0.304 ± 0.064
0.25	0.214 ± 0.074	0.188 ± 0.136	0.052 ± 0.074	0.351 ± 0.059
0.42	0.392 ± 0.077	0.400 ± 0.131	0.210 ± 0.104	0.528 ± 0.047

Table 2A.2 Principal component loadings of 10 single-nucleotide polymorphisms (SNPs) located within genes associated with circadian rhythms or annual cycles of American kestrels, based on 971 nestling samples. The first $PC_{nesting}$ accounted for 17.7% of the variance and $PC_{nesting}$ 2 accounted for 12.6% of the variance. Loadings > 0.5 are in bold. Blank spaces represent loadings < 0.09.

Gene	$PC_{nesting}$ 1	$PC_{nesting}$ 2	$PC_{nesting}$ 3
top1	0.75	0.32	
peak1	0.75	0.33	0.17
nacc2		0.24	-0.32
mybbp1a		-0.65	0.13
scn5a1		0.39	
phllp1			0.46
lmbr1	-0.12		0.66
npas2	-0.16	0.10	-0.49
cpne4	-0.51	0.54	0.11
cry1	-0.58	0.32	0.18

Table 2A.3 Principal component loadings of 9 SNPs located within genes associated with circadian rhythms or annual cycles of American kestrels, based on 165 migration samples and 738 nestling samples. The first $PC_{migration}$ accounted for 17.5% of the variance and $PC_{migration}$ 2 accounted for 13.1% of the variance. Loadings > 0.5 are in bold. Blank spaces represent loadings < 0.09.

Gene	$PC_{migration}$ 1	$PC_{migration}$ 2	$PC_{migration}$ 3
top1	**0.88**		
peak1	**0.84**	-0.22	
nacc2		0.24	-0.62
scn5a	0.12	0.32	-0.38
phlpp1	**-0.23**	-0.49	-0.17
lmbr1		0.48	0.14
npas2		-0.42	
cpne4	**-0.15**	-0.55	-0.39
cry1		0.17	-0.57

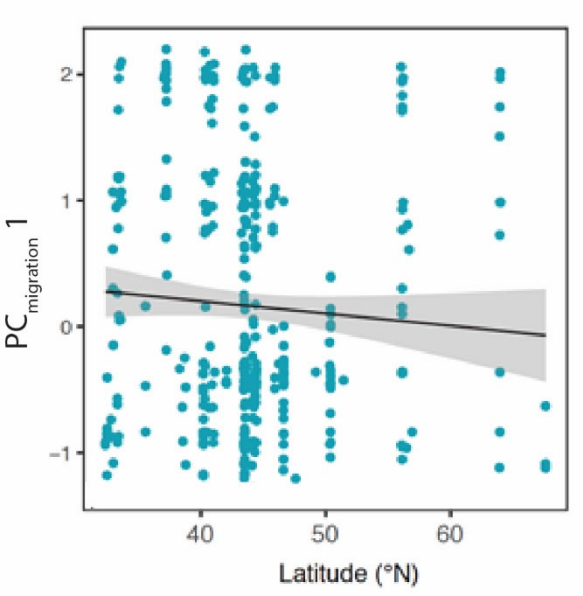

Figure 2A.2 The relationship between candidate gene $PC_{migration}$ 1 values of migrating American kestrels and breeding latitude (°N). We did not find a significant association between $PC_{migration}1$ and breeding latitude, suggesting variation in migration timing is not confounded by breeding origin.

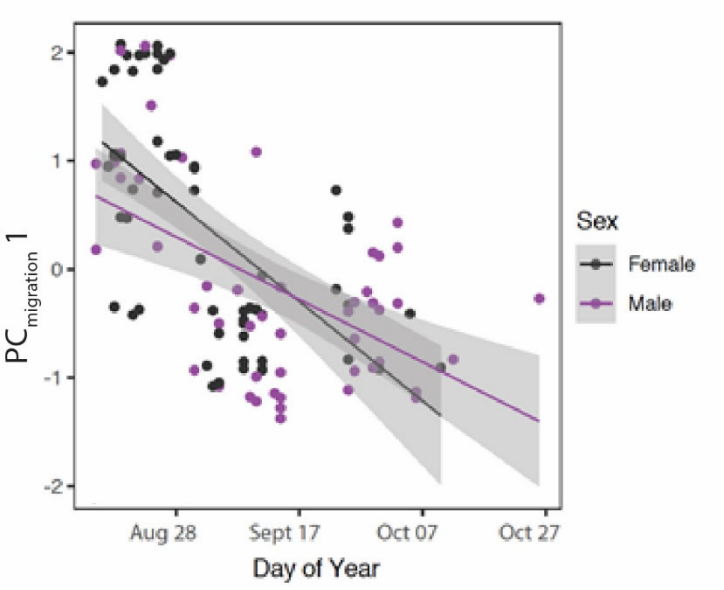

Figure 2A.3 Sex-specific autumn migration timing of American kestrels in Idaho and candidate gene $PC_{migration}$ 1 values. There was no evidence that the effect of $PC_{migration}$ 1 on autumn migration differed between females and males.

Table 2A.4 Mean and standard deviation of allele frequencies at loci associated with the timing of American kestrel clutch initiation from eastern and western populations, *P*-value, beta estimate (β), and standard error from comparisons of allele frequency estimates between eastern and western American kestrels.

Gene	Eastern	Western	*P*-value	β	Std Error
top1	0.561 + 0.344	0.692 + 0.233	0.32	-0.56	0.56
peak1	0.519 + 0.247	0.589 + 0.205	0.16	-0.65	0.46
nacc2	0.881 + 0.046	0.891 + 0.054	0.17	-0.43	0.32
mybbp1	0.867 + 0.066	0.882 + 0.056	0.56	-0.13	0.23
scn5a1	0.831 + 0.057	0.828 + 0.066	0.98	0.01	0.19
phllp1	0.870 + 0.045	0.839 + 0.103	0.54	-0.22	0.36
lmbr1	0.832 + 0.085	0.801 + 0.075	0.24	0.27	0.23
npas2	0.644 + 0.106	0.678 + 0.104	0.37	-0.20	0.22
cpne4	0.869 + 0.086	0.883 + 0.053	0.87	-0.04	0.26
cry1	0.830 + 0.083	0.825 + 0.127	0.28	-0.40	0.37

Table 2A.5 Mean and standard deviation of heterozygosity estimates at loci associated with the timing of American kestrel clutch initiation from eastern and western populations, *P*-value, beta estimate (β), and standard error from comparisons of heterozygosity estimates between eastern and western American kestrels. Bolded genes are significantly different or tend to be different between populations.

Gene	Eastern	Western	*P*-value	β	Std Error
top1	0.288 + 0.204	0.334+0.184	0.07	0.95	0.52
peak1	0.400 + 0.101	0.417+0.168	0.07	-0.94	0.52
nacc2	0.212 + 0.073	0.194 +0.090	0.02	-1.04	0.45
mybbp1	0.229 + 0.100	0.208 + 0.088	0.58	-0.13	0.23
scn5a1	0.280 + 0.077	0.284+0.091	0.97	0.01	0.19
phllp1	0.228 + 0.069	0.258+0.134	0.06	-0.89	0.47
lmbr1	0.271 + 0.118	0.317 + 0.091	0.21	0.28	0.22
npas2	0.449 + 0.060	0.427 +0.108	0.50	-0.13	0.19
cpne4	0.219 + 0.119	0.207 + 0.085	0.93	-0.02	0.25
cry1	0.276 + 0.090	0.267 + 0.157	0.03	-1.03	0.48

Appendix 3. TRACE document for SCOPE: An individual-based model of carry-over effects and phenological shifts in migratory birds, American kestrel version

TRACE document background

This is a TRACE document ("TRAnsparent and Comprehensive model Evaludation") which provides supporting evidence that our model was thoughtfully designed, correctly implemented, thoroughly tested, well understood, and appropriately used for its intended purpose.

The rationale of this document follows:

> Schmolke A., P. Thorbek, D.L. DeAngelis, and V. Grimm. 2010. Ecological modelling supporting environmental decision making: a strategy for the future. Trends in Ecology and Evolution 25:479–486.

and uses the updated standard terminology and document structure in:

> Grimm V., J. Augusiak, A. Focks, B. Frank, F. Gabsi, A.S.A Johnston, K. Kulakowska, C. Liu, B.T. Martin, M. Meli, V. Radchuk, A. Schmolke, P. Thorbek, and S.F. Railsback. 2014. Towards better modelling and decision support: documenting model development, testing, and analysis using TRACE. Ecological Modelling 280:129–139.

and

> Augusiak J., P.J. Van den Brink, and V. Grimm. 2014. Merging validation and evaluation of ecological models to 'evaludation': a review of terminology and a practical approach. Ecological Modelling 280:117–128.

Problem formulation

We built an Individual-based model (IBM) called SCOPE (Simulation of Carry-over and Phenological Effects) to test hypotheses of the potential mechanisms underlying phenological shifts in migratory land birds, and to forecast how breeding phenology and other aspects of their life-history will be impacted by a changing climate. Specifically, the purpose of this model is to understand what environmental and genetic factors constrain or enable phenological shifts. We developed SCOPE initially for the American kestrel (*Falco sparverius*), a widespread raptor species exhibiting different migration strategies (Smallwood and Bird 2020) and responses to climate change across its range (Chapter 1). Winter warming in western North America has been linked to northward shifts in winter distributions and decreased migratory distances for American kestrels (Heath et al. 2012, Paprocki et al. 2014). Resident kestrels in this focal population nest earlier (Anderson et al. 2016), have higher nest success (Chapter 1), produce more offspring (Steenhof and Heath 2013), and have higher apparent survival (Steenhof and Heath 2009) than later-breeding migrant birds. Whereas in eastern North America, American kestrels have not shifted their timing of nesting (Chapter 1), and do not show changes in migration behavior (Heath unpub. data). We built 2 versions of SCOPE for American kestrels, one for the western flyway, and another for the eastern flyway. SCOPE has the capacity to output data on the individual-level, which is useful for studies of evolution, genetic change, and heritability; and on the patch-level, which is useful for widespread studies of ecological processes. Submodels within SCOPE can be turned on and

off to test hypotheses about mechanisms affecting phenology, demographics, and population health.

Model description

Below is a complete model description of the IBM of American kestrel phenology described using the ODD protocol. The model description follows the ODD (Overview, Design concepts, Details) protocol for describing IBMs (Grimm *et al.* 2006, 2010). This model was written in NetLogo 6.2.2 (Wilensky 1999).

Purpose

We built an IBM to test hypotheses of the potential mechanisms underlying phenological shifts in migratory landbirds, and to forecast how breeding phenology and other aspects of their life-history will be impacted by a changing climate. Specifically, the purpose of this model is to understand what environmental and genetic factors constrain or enable phenological shifts. We developed SCOPE initially for the American kestrel, a widespread raptor species exhibiting variable migration strategies and responses to climate change in different parts of their range. The SCOPE modeling framework is portable to other migratory species.

Entities, state variables, and scales

Our model is a full-annual-cycle model (Hostetler et al. 2015) consisting of individual birds, a virtual landscape representing different North American flyway regions, and landscape patches representing geographic locations (i.e., latitude/longitude values), ecoregion designation, carrying capacity, and annual environmental conditions. Individuals are characterized by a set of static and dynamic attributes, which are outlined in Table 3A.1.

We employed a time scale in which non-breeding season events and the passage of 1 year (i.e., year *t*) occurs on day 213, and the breeding season occurs during days 1–212 (i.e., breeding season$_{t1–t212}$). Within the model and during output writing, these tick values are adjusted by adding 31 days to calculate real calendar dates. We chose to organize time steps in this way because of constraints of the NetLogo software and to simplify programming, as non-breeding season events such as survival and mortality could occur in a single time step. Although the span of 212 days is a longer breeding season than any one individual would experience, it represents the span of time between pairing of the earliest breeders until migration departure for the latest breeders (Chapter 1). To match the temporal resolution of the climate and empirical data used in the model, simulations can be run between 1980 – 2099. Additionally, we included the option for a burn-in period of 10, 15, or 20 years to allow the simulated bird population to reach a stable state.

Version 1 of SCOPE covers the range of American kestrels breeding in the western United States and Canada, or the ‘western flyway’ region (Figure 3A.1). Version 2 covered the range of American kestrel breeding in the eastern United States and Canada (Figure 3A.1). Our flyway maps were based upon the United States/Canada border, band return data from the USGS Bird Banding Lab, and a spatially-explicit map of kestrel genetic structure (Ruegg et al. 2021). The flyway was composed of 28.5 km^2 patches. Patch size was based on the resolution of Regional Climate Models (RCMs) used to represent climatic conditions in the model. Each patch contains information about latitude, longitude, ecoregion, August maximum temperature

Table 3A.1 A list of individual bird attributes, whether each attribute is static or dynamic, and how attributes are assigned in SCOPE, American kestrel version.

Bird Attributes	Status	Assignment
Sex	Static	Randomly assigned
Age	Dynamic	Increases each year by 1
Hatch date	Static	Date an individual hatched (randomly assigned for 1st generation)
Genotype for *top1*, *peak1*, *nacc2*, *mybbo1a*, *scn5a1*, *cpne4*, *cry1* genes	Static	Inherited from parents via Mendelian inheritance (experimentally assigned for 1st generation)
Migration strategy (migrant or resident)	Dynamic	Depends on latitude and winter minimum temperature anomaly
Migration distance	Dynamic	Depends on latitude and winter minimum temperature anomaly
Date of availability	Dynamic	Depends on migration distance (migrants), the extended spring index (SI-x, residents), and genotype (both migrants and residents)
Egg-laying date	Dynamic	Depends on the date of availability, and locating a nest site and mate
Mismatch	Dynamic	Difference between egg-laying date and SI-x
Early?	Dynamic	Whether or not an individual laid eggs before or after the median date of mismatch (17 days before SI-x)
Nest success and productivity	Dynamic	Depends on mismatch, longitude, latitude, and interactions among these variables
Probability of survival (juvenile)	Dynamic	Depends on hatch date, sex, and minimum winter temperature anomalies
Probability of survival (adult)	Dynamic	Depends on Early?, sex, and minimum temperature anomalies
Breeding dispersal distance and direction	Dynamic	Drawn from distribution
Natal dispersal distance and direction	Dynamic	Depends on sex, maximum temperature anomalies in August, and latitude
Long-distance disperser?	Dynamic	Drawn from distribution for hatch-year individuals
Parent identity	Static	Identity of both parents
Parent availability	Static	Date of availability for both parents
Mating status (mate or floater)	Dynamic	Depends on whether an individual finds an available mate

anomaly, SI-x, winter minimum temperature anomaly, and the number of pairs that a patch can support. Patch attributes are derived from raster files imported at initialization or annually, depending on the layer.

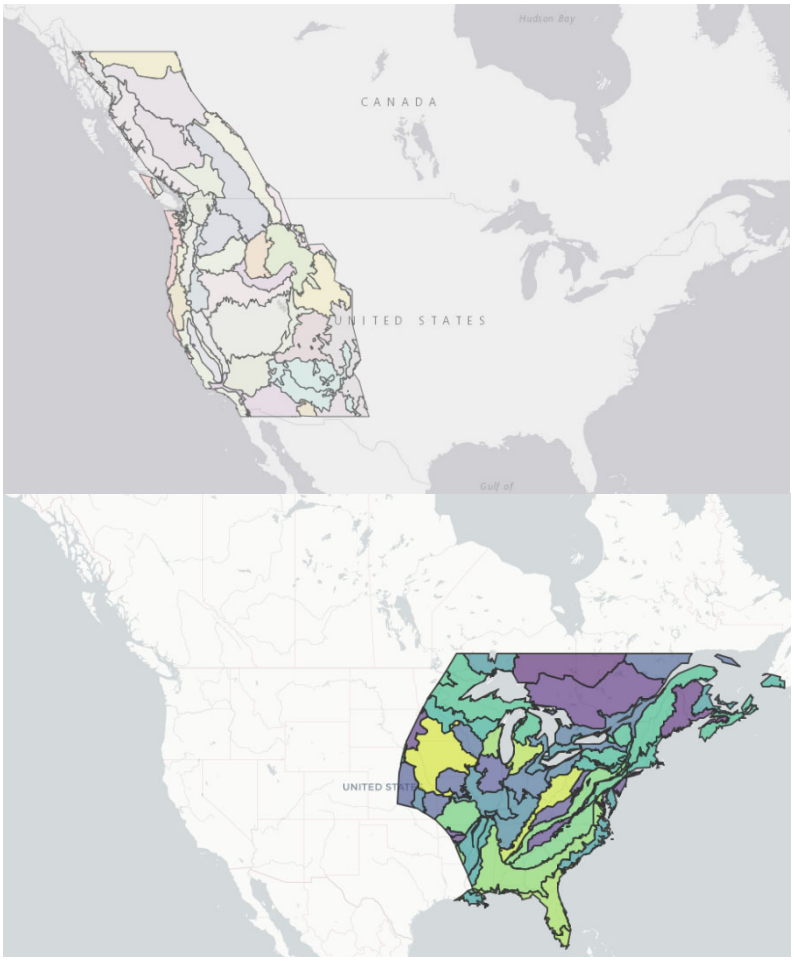

Figure 3A.1 Spatial extent of the western flyway (top) and eastern flyway (bottom) versions of SCOPE for American kestrels. Colored polygons represent EPA level III ecoregions.

Process overview and scheduling

Our model approximates the full-annual-cycle of the American kestrel (Figure 3A.2); the exact sequence of model procedures and submodels are as follows. During the breeding season, individuals check to see if their date of availability has arrived; this is analogous to reproductive readiness. If so, males move to an unoccupied breeding patch and set their availability to true. Females that have reached their date of availability move to a patch with an available male that has not paired with a female and set their availability to true. If there are no unpaired, available males on the landscape, the female moves her available date to one day in the future and repeats the pairing process in the subsequent time-steps. Individuals that are unsuccessful at pairing remain in the population as non-breeding 'floaters.'

At the end of the breeding season (but before migration), paired females determine their probability of nest success based upon their egg-laying date in relation to the SI-x (?) date and geographic location. If the nest is successful, then the number of offspring for that nest is determined. These offspring are randomly assigned as male or female, track the egg-laying date of their mother, and whether or not they were from an early or late nest (i.e., the egg-laying date was before or after the extended spring index (SI-x) date of the patch where they hatched).

At the beginning of the non-breeding season, the age of each individual is increased by 1, their date of availability and migration distance is reset and the climate and environmental conditions for that year are determined.

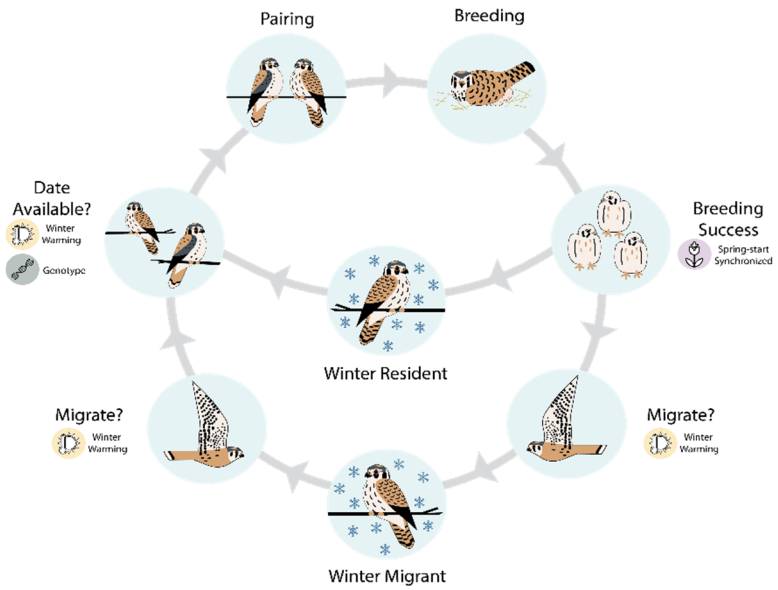

Figure 3A.2 Simplified flow diagram of main model processes in the SCOPE model for American kestrels within the context of an avian annual cycle. Distinct paths represent the cycle of migrants and residents. Icons represent environmental input.

The probability of surviving to the following year is determined for each individual. For juveniles, survival probability is dependent upon whether they were from an early or late nest, their sex, and, the winter minimum temperature anomaly. For adults, survival probability is dependent upon their previous egg-laying date, whether they were successful, their sex, and winter minimum temperature anomaly. Individuals then update their migration strategy (whether to migrate or remain as a resident) based upon minimum winter temperature and breeding latitude. For migrants, distance to the wintering grounds is determined in response to the minimum winter temperature anomaly and their breeding latitude. Migrant individuals then determine their date of availability based on the distance they travelled to the non-breeding grounds. Resident individuals determine their date of availability based on the SI-x date of patch that they remain in year-round. A detailed schematic of submodel scheduling is provided in Figure 3A.3.

Design concepts

Basic Principles

Within SCOPE, we simulate full-annual-cycle events of birds, and include a carry-over effect of winter minimum temperature on arrival date in the subsequent spring (via effects of temperature on migration propensity and distance). In this use of SCOPE, life-history events and scheduling are guided by the biology of American kestrels, either from previously published research or our own analyses of empirical data sets.

Emergence

Several patterns emerge from this model. With warming winter temperatures, migration propensity and distances decrease. For migrants, shorter migration distances result in advancing availability dates in the spring. Additionally, warming winters have a positive effect on annual survival rates for adults and juveniles. Resident kestrels that remain year-round on their breeding grounds track earlier springs, which advances their date of availability. Although kestrels advance their timing in the spring, phenological mismatch increases over time, resulting in lower nest success and productivity. Together, these changes result in overall advances in breeding phenology, and a pattern of assortative mating (i.e., migrant-migrant, resident-resident) emerges as resident and migrant kestrels shift their timing in the spring at different rates. As population sizes grow, individuals compete for nest sites and mates, driving earlier nesting over time.

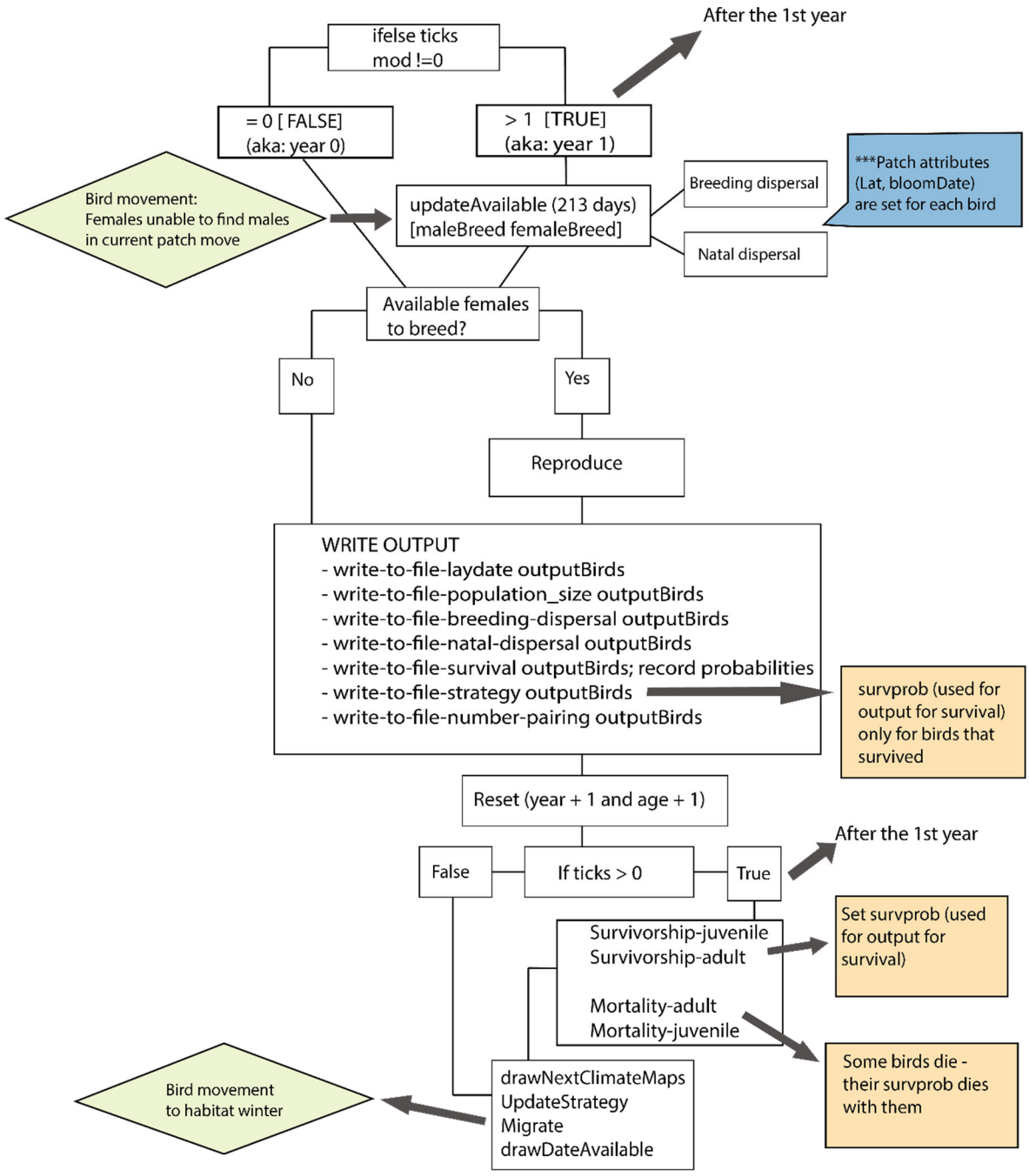

Figure 3A.3 A detailed flowchart of model processes in SCOPE.

Adaptation

Within the IBM modeling framework, adaptation is the term for individual decisions that maximize fitness. When individuals become available, males establish territories and females choose from one of the available males. There are a limited number of pairs on each patch. Competition for mates and patches, as well as the effects of phenological mismatch on nest success and survival drives the selection for earlier nesting. Individuals maximize fitness through establishing nests as early as possible.

Objectives

The objective for individuals is to pair with a mate, successfully nest, produce offspring, make migration decisions and survive until the following year.

Learning

No learning occurs within our model.

Prediction

Individuals in the model use simple predictive models that incorporate climatic and environmental conditions of breeding or natal patches to make decisions on whether and how far to migrate, and how far they disperse as juveniles.

Sensing

Individuals can sense the climatic conditions of the patch they occupied during the breeding season. Average minimum temperature during the subsequent non-breeding period in years t and $t + 1$ (15 November$_t$–15 February$_{t+1}$) informs migration propensity, migration distance, and annual survival probability of adults and juveniles. Average maximum temperature experienced during the post-breeding period in year t (August$_t$) also influences natal dispersal distance of juvenile males. In addition, individuals can determine whether a potential breeding patch within their assigned dispersal distance and direction has available mates, or has reached carrying capacity.

Interaction

Adult individuals attempt to find mates to pair and reproduce, and offspring inherit genetic attributes from both parents when they are born. The density of individuals within potential breeding patches can also indirectly impact the reproductive status of individuals, potentially resulting in reduced survival for individuals that are unable to secure a mate and become non-breeders (i.e., ‘floaters’).

Stochasticity

The majority of submodels in our IBM are parameterized from individual regression models. This approach allowed us to incorporate parameter uncertainty by drawing parameter values from the posterior distribution of each regression model. For the survival submodel, calibrated mean values from a multi-state mark-recapture model analyzed in RMark (Laake 2013) were used to generate survival probabilities. Further stochasticity was included by randomly drawing values from the appropriate response distribution. Although we included random effect of year in some of the submodel regressions, we did not include this form of environmental stochasticity (i.e., year-to-year variation in the submodel process) in the IBM.

Collectives

Male and female individuals form pairs during the breeding season and produce offspring with genetic attributes from their parents. Pairing status is reset before the start of the next breeding season. Otherwise, social structure is not included in the model.

Observation

Our model records several phenological and demographic metrics each simulation year, but the resolution of these observations differs depending on the objective. For 'genetic experiments' that test the effect of genetic diversity on phenological shifts, full pedigree information is required and metrics are written each year and for each individual (typically for just one or a few ecoregions due to memory constraints). Otherwise, output metrics are summarized at the patch- and ecoregion-level because of the large spatial extent and number of individuals in the model. These different observation types are described below.

Individual-level observations

We record 10 different individual-level outputs in .csv format:

- Laydate output
  - *birdID*: unique bird identifier (female)
  - *mateID*: unique bird identifier (male)
  - *laydate*: day-of-year when nest is initiated
  - *lat*: latitude (degrees)
  - *migStrat*: migration strategy (resident or migrant)
  - *migDist*: migration distance (km) if migrant
  - *sync_bloom*: difference between laydate and SI-x (days)
  - *success*: nest status (successful or failed)
  - *xcor*: NetLogo x coordinate
  - *ycor*: NetLogo y coordinate
  - *early?*: mismatch status (early or late compared to SI-x)
  - *nestProb*: nest survival probability
  - *dateAvail*: day-of-year when an individual is available to pair
  - *ecoregion*: level III ecoregion designation
- Offspring output
  - *femaleID*: unique female identifier
  - *offspring*: number of offspring produced
  - *ecoregion*: level III ecoregion designation
- Population size output
  - *populationSize*: number of adults
  - *ecoregion*: level III ecoregion designation
- Allele frequencies output
  - *birdID*: unique bird identifier
  - *top1*: genotype for *top1* as number of minor alleles at locus (0,1,2)
  - *peak1*: genotype for *peak1* as number of minor alleles at locus (0,1,2)

    - *mybbp1a*: genotype for *mybbp1a* as number of minor alleles at locus (0,1,2)
    - *cpne4*: genotype for *cpne4* as number of minor alleles at locus (0,1,2)
    - *cry1*: genotype for *cry1* as number of minor alleles at locus (0,1,2)
    - *nacc2:* genotype for *nacc2* as number of minor alleles at locus (0,1,2)
    - *scn5a1:* genotype for *scn5a1* as number of minor alleles at locus (0,1,2)
    - *ecoregion*: level III ecoregion designation
- Breeding dispersal output
    - *distance*: breeding dispersal distance (km)
    - *direction*: breeding dispersal direction (degrees)
    - *ecoregion*: level III ecoregion designation
- Natal dispersal output
    - *birdID*: unique bird identifier
    - *lat*: latitude (degrees)
    - *xcor*: NetLogo x coordinate
    - *ycor*: NetLogo y coordinate
    - *distance*: natal dispersal distance (km)
    - *direction*: natal dispersal direction (degrees)
    - *tmax*: August average maximum temperature anomaly (degrees C)
    - *sex*: sex of individual (male or female)
    - *ecoregion*: level III ecoregion designation
- Strategy output
    - *birdID*: unique bird identifier
    - *lat*: latitude (degrees)
    - *age*: age (years)
    - *mig?*: migration strategy (resident or migrant)
    - *migDist*: migration distance (km)
    - *sex*: sex of individual (male or female)
    - *mate*: unique bird identifier (for mate)
    - *mate_mig?*: migration strategy of mate (resident or migrant)
    - *ecoregion*: level III ecoregion designation
- Number pairing output
    - *birdID*: unique bird identifier
    - *mig?*: migration strategy (resident or migrant)
    - *daysBWAvailPairing*: difference between date of availability and day an individual paired (days)
    - *ecoregion*: level III ecoregion designation
- Parentage output
    - *birdID*: unique bird identifier
    - *fatherID*: unique identifier of father
    - *motherID*: unique identifier of mother
- Survival output

- *birdID*: unique bird identifier
- *age*: age (years)
- *sex*: sex
- *lat*: latitude (degrees)
- *syncBloom*: difference between laydate (or birthdate) and SI-x (days)
- *xcor*: NetLogo x coordinate
- *ycor*: NetLogo y coordinate
- *mig?*: migration strategy (resident or migrant)
- *early?*: mismatch status (early or late relative to SI-x)
- *juvProb*: juvenile survival probability
- *adultProb*: adult survival probability
- *ecoregion*: level III ecoregion designation

Patch- and ecoregion-level observations

We record 11 different patch- and ecoregion-level outputs in .csv format. Most of the metrics are summarized by patch, and we record summary statistics (mean, min, max, standard deviation, and count) for each metric:

- Environmental output
  - *pxcor*: NetLogo patch x coordinate
  - *pycor*: NetLogo patch y coordinate
  - *latitude*: latitude of patch
  - *tmax*: August average maximum temperature anomaly of patch
  - *tmin*: winter average minimum temperature anomaly of patch
  - *bloomDate*: SI-x of patch
- Laydate output
  - *nestProb*: summary statistics of nest success probability
  - *syncBloom*: summary statistics of synchrony with bloom date
  - *dateAvail*: summary statistics of date of availability
  - *laydate*: summary statistics of laydate
- Offspring output
  - *offspring*: summary statistics of offspring produced
- Population size output
  - *populationSize*: number of adults
  - *migPop*: number of migrant adults
  - *resPop*: number of resident adults
- Breeding dispersal output
  - *distance*: summary statistics of breeding dispersal distance
  - *direction*: mean and dispersion of breeding dispersal direction
- Natal dispersal output
  - *distance*: summary statistics of natal dispersal distance
  - *direction*: mean and dispersion of natal dispersal direction
- Strategy output
  - *strategy*: count of resident and migrant individuals

    - *distance*: summary statistics of migration distance
- Number pairing output
    - *daysBWAvailPairing*: summary statistics of days between date of availability and pairing date
- Adult survival output
    - *age*: summary statistics of age
    - *probSurvAdult*: summary statistics of survival probability
- Juvenile survival output
    - *probSurvJuvenile*: summary statistics of survival probability

Initialization

At the beginning of the model simulation, values for the patches in the landscape and agent parameters are set. The first year the model begins is determined by the user; here we initialized the landscape with climate data starting in 1980 (to allow for pattern-matching with our Idaho empirical data). The simulation begins with 50,000 males and 50,000 females (or whatever the user chooses) randomly distributed on breeding habitat patches within the landscape. Each patch consists of a number for the maximum pairs allowed, derived by calculating the maximum number of kestrel home ranges that can fit within a patch (see Input data: eBird denisty). A number of bird attributes are then determined: each individual is randomly assigned an age between 0 and 6 (where ages less than or equal to 1 are considered juveniles and ages greater than 1 are considered adults); sex is randomly assigned; migration strategy is set to true; availability, natal dispersal success, nesting status, and early are set to false; hatch date is set to a random number between 1 and 212; mate identity is set to nobody; and dispersal distances and directions, asynchrony, and nest success probability are set to 0. All individuals are also given a genotype which can be determined by the user at the start of the simulation. Males move to an unoccupied breeding patch first and females move to any breeding patch.

Input data

Input data for our IBM included 7 different environmental and geographic variables in raster format to represent time-varying processes and static attributes. We prepared all raster layers for NetLogo using R (R Core Team 2021). We clipped rasters for SCOPE to match the western flyway, projected into an equal area projection, re-sampled to match the resolution of climate or start-of-spring rasters derived from regional climate model (RCM) projections, and written in ESRI ASCII Grid file format for compatibility with the Netlogo GIS extension.

Regional climate model projections

Simulated individuals in SCOPE sense the climate and vegetation phenology (i.e., start-of-spring date) conditions in the 'patch' or raster cell that they reside in, and these conditions are used to inform different SCOPE submodels (e.g., timing, movement, and demographic rates). To forecast changes in weather, we used regional climate model (RCM) data from the NA-CORDEX project (Mearns et al. 2017) that was bias-corrected using the Daymet historical gridded dataset (Thornton et al. 1997). This bias-correction provides continuity between the historical climate data used to parameterize kestrel-weather-vegetation phenology relationships, and future changes in climate. We obtained climate data for two representative concentration pathways (RCPs) that represent scenarios where moderate effort or no action is taken to curb

emissions: RCP 4.5 (only 1 bias-corrected RCM was available) and RCP 8.5 (12 RCMs, Table 3A.2). NA-CORDEX projections used in SCOPE were available at a ~25 km^2 resolution for the period 1980–2099, and converted from netcdf format into annual raster layers.

Table 3A.2 Names of regional climate models used to produce ensemble climate layers and extended spring index estimates for SCOPE at RCP 8.5 and the regional climate model used for climate and extended spring index estimates at RCP 4.5.

Regional Climate Model	RCP
CanESM2.CanRCM4	8.5
CanESM2.CRCM5-UQAM UQAM	8.5
GEMatm-Can.CRCM5-UQAM	8.5
GFDL-ESM2M.RegCM4	8.5
GFDL-ESM2M.WRF	8.5
HadGEM2-ES.RegCM4	8.5
HadGEM2-ES.WRF	8.5
MPI-ESM-LR.CRCM5-UQAM	8.5
MPI-ESM-LR.RegCM4	8.5
MPI-ESM-LR.WRF	8.5
MPI-ESM-MR.CRCM5-UQAM	8.5
CanESM2.CanRCM4	4.5

We calculated daily temperature anomaly values for each raster cell by subtracting 30-year average temperatures (1980–2009) from annual temperature values. Next, we averaged the daily temperature anomalies for each season in each year of the climate projections. To represent the mean minimum temperature base for winter anomalies we averaged 15 November–15 February minimum temperatures. August maximum temperatures were averaged for the base period used to calculate summer mean maximum temperature anomalies. Finally, we created a multi-model ensemble (i.e., average winter T_{min} anomaly and August T_{max} anomaly rasters across all available RCMs) for the RCP 8.5 pathway. Only one RCM was available for RCP 4.5 (CanESM2.CanRCM4); therefore, we were unable to produce ensemble climate layers and used the single RCM for this pathway.

Start-of-spring date

We quantified start-of-spring dates in SCOPE using the extended spring indices (SI-x, Schwartz et al. 2006, 2013). The extended spring indices are mathematical models that predict the start-of-spring (i.e., date of leaf-out or first bloom) based on weather at a particular location. These models were constructed using historical observations of the timing of first leaf and first bloom in a cloned lilac cultivar and two cloned honeysuckle cultivars, which were selected based on the availability of historical observations from across a wide geographic area (Schwartz et al. 2006). Extended spring indices also reflect spring phenological transitions in native species and crops (Rosemartin et al. 2015), and estimates for start-of-spring dates derived from extended spring indices are generally in good agreement with estimates derived from near-surface time-lapse cameras (Richardson et al. 2018, 2019).

Primary inputs to estimate extended spring indices are daily minimum and maximum temperatures beginning January 1 of each year, and daylength derived from latitude (Ault et al.

2015). Spring index models were built with bias-corrected NA-CORDEX RCM data and the Go Programming Language (Cox et al. 2022), and we verified our model output against spring index code and projections developed by Allstadt et al. (2015). Similar to the temperature rasters described above, only one RCM was available for RCP 4.5 (CanESM2.CanRCM4) and a multi-model ensemble was used for RCP 8.5 In SCOPE, we represented spatially-explicit estimates of start-of-spring in each year (1980–2099) using SI-x, as this spring index was positively associated with the timing of kestrel reproduction (Appendix 1).

eBird density

To ensure realistic population sizes and incorporate density-dependence in the model, we integrated Partners in Flight population estimates (Partners in Flight 2020) and eBird relative abundance maps (eBird 2021) to create a raster layer that determines the maximum number of pairs that a patch is capable of supporting. First, we used the ebirdst package (Auer et al. 2020) to create a spatially-explicit raster of kestrel relative abundance (estimated number of individuals detected by an eBirder during a traveling count at the optimal time of day) across North America. Second, we estimated the number of individuals that a cell could support by multiplying the relative abundance value by a scaling factor, such that the sum of all raster cells was approximately equal to the mean Partners in Flight population estimate for the western flyway. Finally, we divided each raster value by 2 to produce a raster with the total number of pairs allowed per cell.

Ecoregions

We divided flyways into United States Environmental Protection Agency (US EPA) level III ecoregions (Omernik 1987) for summarizing outputs. We rasterized the level III ecoregions shapefile retrieved from the US EPA website.

Geographic coordinates

We selected a random climate raster to calculate the latitudinal and longitudinal center of each raster cell, and created a separate raster file for the centroid latitude and longitude values.

Submodels

The model is organized under two distinct annual cycle periods, the "breeding" season and the "non-breeding" season. The following submodels represent all processes in the model. Actual names of submodel procedures used in the IBM code are included in parentheses. For regression-based submodels, we used Bayesian inference to fit models (unless otherwise noted) via the R package brms (Bürkner 2017), which provides a user-friendly interface for the STAN probabilistic programming language (Carpenter et al. 2017). Regression model details can be found in the supplementary material. All procedures occur for individuals in random order each time they are invoked, except for the updateAvailable submodel. Additional procedures underlying main submodels called in the go procedure are italicized in each submodel description.

Update date of availability (updateAvailable)

Prior to becoming available to pair (at this stage they are 'unavailable'), individual color is set to black (male) or white (female). Once individuals are available to pair, they begin the process of dispersing and finding a mate. During this submodel, date of availability in the spring

for each individual is updated on a daily basis, depending on whether an individual is available and if it is successfully paired.

maleBreed and *femaleBreed*.–Males are the first to occupy breeding patches, which may be the site that they occupied in the previous year, or a site they are dispersing to for the first time. Males determine whether the carrying capacity of a patch has been met; if not they occupy that patch and decrease the number of pairs that may occupy it. If the patch is occupied, they continue searching for breeding patches for a pre-determined number of tries (controlled by a slider on the NetLogo interface). If this number of breeding attempts is reached prior to locating a breeding patch, the male dies. Date of availability increases by a day if individuals are not successful in pairing. Once males pair, their color is changed to sky. Females use a similar process to locate an available male, and increase their date of availability if they are unsuccessful at finding a mate on a particular day. Once females pair, their color is changed to brown.

checkNeighboringPatches.–In this procedure, females also have the opportunity to check neighboring patches during their last attempt to find a mate.

These procedures repeat every day until an individual pairs, dies, or becomes a non-breeding individual or floater (i.e., they reach the maximum number of attempts to breed - 8). Floaters have their color set to orange (female) or cyan (male) and the early? and success? attributes are set to false, which puts them in a lower survival category.

Natal dispersal and direction (natalDispersal)

Juvenile individuals attempt to find a breeding patch in the year following birth. We parameterized natal dispersal distance using an approach modified from McCaslin et al. (2020). Natal dispersal distances (in km) were extracted from the United States Geological Survey's Bird Banding Laboratory (BBL) band encounters data set (1980–2019) with data processing and calculations following McCaslin et al. (2020). The dispersal distance of long-distance individuals (>30 km) was modeled as a Gamma-distributed random variable, with distance as a function of fixed effects of sex, an interactive effect of sex and mean maximum August temperature anomaly, latitude of the natal site, recovery status, percent agriculture in the matrix between natal and breeding sites, and a random year effect:

$$log(\mu) = \alpha + \beta_1 * sex + \beta_2 * T_{max} + \beta_3 * T_{max} * sex + \beta_4 * latitude + \beta_5 * status + \beta_6 * \%\ agriculture$$

To provide coherence with the historical gridded climate data used in SCOPE, we replaced mean August maximum temperature anomalies McCaslin et al. (2020) derived from Berkeley Earth (Rohde et al. 2013) with those from Daymet (Thornton et al. 1997). When generating natal dispersal distances, we also set percent agriculture to its mean centered value (i.e., zero) and recovery status as dead.

We used the same BBL data set to calculate mu and rho parameters in R and determine natal dispersal direction. Similar to McCaslin et al. (2020), natal dispersal direction was biased toward the southeast. Direction (in degrees) was drawn from a wrapped cauchy distribution. Only juveniles set as long-distance dispersers during the survivalJuvenile procedure undergo natal dispersal. Otherwise, juveniles become short-distance dispersers and undergo breeding dispersal instead (see survivalJuvenile below). Long-distance dispersers are permitted to make a pre-

determined number of attempts (natalattempts, controlled by a NetLogo slider) to locate an available breeding patch (i.e., a patch that has not reached maximum capacity and is within their drawn dispersal distance and direction). If the number of permitted natal dispersal attempts is exceeded, individuals die.

Breeding dispersal and direction (breedingDispersal)

Juvenile (only those assigned as short-distance natal dispersers; see survival) and adult individuals disperse from their natal or breeding patch in subsequent seasons. Individuals can remain on the same patch if it is available and they draw a short dispersal distance; otherwise, individuals locate a new, available breeding patch. We parameterized breeding dispersal based on band encounters from the BBL (1980–2019). We retained banding records for individuals banded during the breeding season in year t ($April_t$–$August_t$) and encountered in the subsequent breeding season in year $t + 1$ ($April_{t+1}$–$August_{t+1}$). Distances between breeding locations were calculated from pairs of latitude/longitude coordinates using the geosphere package (Hijmans 2019). Breeding dispersal distance (in km) was modeled as a Gamma-distributed random variable, with distance as a function of flyway (west or east):

$$log(\mu) = \alpha + \beta_1 * flyway$$

We used the same BBL data set to calculate mu and rho parameters in R to determine breeding dispersal direction. Breeding dispersal direction was random (i.e., there was no bias toward a particular compass bearing). Direction (in degrees) was drawn from a wrapped cauchy distribution.

Reproduction (reproduce)

Females that have found a mate initiate nesting and producing offspring. In our model, kestrel nest success varies geographically, and individuals that nest earlier in the season (as compared to the SI-x) generally have higher nest success (Chapter 1). Data were compiled from community and professional scientists; further details on the data set and processing are described in Appendix 1. We modeled nest success as a Bernoulli-distributed random variable, and as a function of asynchrony (i.e., difference in days between egg-laying date and SI-x), latitude, longitude, and interactive effects of these covariates (and a random year effect):

$$logit(\mu) = \alpha + \beta_1 * mismatch + \beta_2 * latitude + \beta_3 * longitude + \beta_4 * mismatch * latitude * longitude$$

To draw their probability of nesting success, females first determine how their egg-laying date (i.e., calculated as date of availability plus 14 days) compares with the SI-x of their breeding patch to calculate a 'mismatch' value. Negative mismatch values (i.e., earlier breeding) have a positive effect on nesting success, while positive mismatch values (i.e., later breeding) negatively affect nesting success. Using this information and the latitude and longitude of their breeding patch, females draw a nest success probability. Next, a uniform random number between 0 and 1 is drawn and compared to the nest success probability. If the random value is less than the calculated probability, the nest survives and both the female and associated male set their success value to true (otherwise they set success as false).

For successful females, the number of offspring produced is drawn by rounding to the nearest integer a value from a normal distribution with a mean of 3.94 and standard deviation of

1.13. If the calculated value is negative, it is set to 0; if the value is greater than 6 it is set to six to prevent unrealistically productive nests (Steenhof and Peterson 2009). Offspring are randomly assigned as male or female, given an age of 0, track their mother's egg-laying date, and record whether they were from a nest initiated before or after the local SI-x (i.e., early or late). Lastly, offspring inherit the genetic attributes of their parents by Mendelian inheritance. Offspring have a 50:50 chance of inheriting either allele from one parent. This genetic makeup can then influence the date of availability in subsequent years via single gene and multigene effects (Chapter 2).

Bird attribute, year, and patch updates (reset)

After reproduction, the next year begins and several updates occur. Year is incremented by one, and the day of year and the number of offspring in the population are set to 0. In addition, each individual resets several dynamic attributes: availability, nesting status, and long-distance disperser status are set to false, migration distance is set to 0, age is incremented by 1 year, mate is set to nobody, and individuals reset their color to black (males) or white (females). The number of pairs occupying each patch are also set to 0.

Survival (survival and mortality)

Individuals survive or die based upon an annual survival probability. We parameterized adult and juvenile apparent survival in SCOPE using equations derived from a multi-state mark-recapture model developed in RMark (Laake 2013) for kestrels breeding in southwest Idaho (Chapter 1) for the western version and New Jersey (Chapter 1) for the eastern version. These models estimated apparent annual survival rates for individuals banded as adults or nestlings, and in relation to relative difference between clutch initiation and SI-x, winter mean minimum temperature anomaly, and nest success (for adults only). These variables and states are recorded by each individual during the reproduction submodel, and are used in the survival equations to determine an annual apparent survival probability:

$$logit(\mu) = \alpha + \beta_1 * late,\ successful\ adult + \beta_2 * early,\ failed\ adult + \beta_3 * late,\ failed\ adult + \beta_4 * early\text{-}hatched\ juvenile + \beta_5 * late\text{-}hatched\ juvenile + \beta_7 * sex + \beta_8 * winter\ T_{min}$$

This value is then compared to a uniform random number between 0 and 1; if the random number is greater than the probability of survival, then the individual dies. We found that calibration was required to achieve realistic survival probabilities, so parameter values are modified from those reported in Chapter 1 but have the same relative pattern for each state. We also used the same survival probability from this initial survival step to classify a proportion of 'dead' juveniles as long-distance dispersers to account for the fact that emigration and mortality are confounded in our apparent survival rate. To determine the proportion, a uniform random number between 0 and 1 was drawn and compared to the probability of survival. If the random value is less than the calculated probability, the juvenile dies otherwise it becomes a long-distance disperser. Juveniles that did not become long-distance dispersers in this step died and were removed from the total population.

To kill individuals, we use a Bernoulli trial with the probability of success equal to the survival probability value generated in either survivalJuvenile or survivalAdult in a separate mortality procedure for juveniles and adults. Floater survival probability (adults only) is also

halved. The separate mortality procedures allow us to record survival probabilities prior to removing dead individuals from the population.

Update environmental rasters (drawNextClimateMaps)

Environmental layers that comprise the virtual world in NetLogo are updated on an annual basis by importing rasters in .asc format. This procedure uses the appropriate calendar year to pull in corresponding winter mean minimum temperature, SI-x, August mean maximum temperature anomaly layers. Thus, individuals can sense environmental conditions that are key to determining different components of a bird's life-history.

Migration strategy (updateStrategy)

Migrant individuals decide whether to change their migration strategy and remain on the breeding/natal grounds as a resident, or migrate to the non-breeding grounds. We used BBL band records (1980–2019) to calculate migration distances of individuals that were banded in year *t* during the breeding (April–August) or non-breeding season (November–February), and encountered in the subsequent year on the non-breeding or breeding grounds, respectively. We calculated migration distances with coordinates from banding and encounter locations using the geosphere package in R. We assigned migration strategy based upon distances between breeding/natal sites and subsequent non-breeding sites, where individuals that traveled ≤ 100 km were considered residents. We modeled the decision to migrate or not dependent upon an individual's breeding latitude and the upcoming winter mean minimum temperature anomaly at the breeding/natal patch. We account for random year variation by adding a random intercept:

$$logit(\mu) = \alpha + \beta_1 * latitude + \beta_2 * winter\ T_{min}$$

Then, a random uniform number between 0 and 1 is generated. If that value is less than the probability of not migrating (1–probability of migrating), an individual sets its migration strategy to false (i.e., resident strategy). Once individuals adopt a resident strategy, they do not migrate in subsequent years.

Migration distance (migrate)

Migrant individuals draw a distance (in km) to migrate to the non-breeding grounds, which constrains date of availability in the subsequent spring. We parameterized migration distance using band encounters from the BBL (1980–2019). Data processing was the same as described in migration strategy. We modeled migration distance (distances ≥ 100 km) as a function of fixed effects of breeding/natal latitude and and winter mean minimum temperature anomaly, and a random year effect in a Gamma mixed effects model:

$$log(\mu) = \alpha + \beta_1 * latitude + \beta_2 * winter\ T_{min}$$

To prevent drawing unrealistically high migration distances, we set any distances over ≥ 8500 km equal to 8500 (a plausible distance for very high latitude migrant kestrels based on BBL records). Migratory individuals then move to the 'non-breeding grounds' (i.e., NetLogo patch coordinate 0,0). This arbitrary location was selected to simplify programming and is not influential to other processes. This submodel does not apply to resident individuals.

Date of availability (drawDateAvailable)

This process determines what day of the year (i.e., date of availability) individuals will become available for pairing for the upcoming breeding season. The date of availability is dependent on whether an individual is a migrant or a resident. Migrant individuals are constrained by the distance they migrated to the non-breeding grounds, while residents are able to track changes in start-of-spring because they have remained on the breeding grounds.

Migrant date of availability.–For migrants, we used a modified approach from Powers et al. (2021) to model spatially-explicit arrival dates derived from eBird checklists in relation to expected migration distances from our migration distance model (see above). Date of availability was modeled as Gamma-distributed random variable with a fixed effect of log (migration distance) and a random effect of year:

$$log(\mu) = \alpha + \beta_1 * log(migration\ distance)$$

In SCOPE, migrants draw a date of availability from this equation and the migration distance they traveled to the non-breeding grounds.

Resident date of availability.–In contrast, resident date of availability was back-calculated from resident egg-laying dates from data sets provided by the American Kestrel Partnership, Cornell Nestwatch, and our own empirical data from DoD nest boxes and known residents breeding in Idaho (Chapter 1). Date of availability was driven by the SI-x, with variation in year accounted for by a random intercept in a Gamma mixed effects model:

$$log(\mu) = \alpha + \beta_1 * SI\text{-}x$$

Residents draw a date of availability from this equation and the SI-x of the patch they occupy for the breeding season.

Genetics and heritability.–When the genetic effect is activated, date of availability for both migrants and residents includes an additive effect of an individual's genotype. The incorporation of functional genetics into an ecologically realistic IBM is a novel feature of this model. We considered several assumptions and criteria for representing loci from candidate genes. First, we confirmed that egg-laying date was a heritable trait in American kestrels (Chapter 2). Second, we estimated the single- and multi-gene effects on the trait (Chapter 2). Next, we considered whether genes were linked (Chapter 2). Finally, because our loci were not likely linked (i.e., were located on separate chromosomes, or were separated by >17 million base pairs) we decided to employ Mendelian inheritance to pass alleles from one generation to the next. Offspring have a 50:50 chance of inheriting either allele from one parent. Because the model operates in a small time period (120 years), we did not include recombination or mutation (Ellegren 2007) as these are unlikely to affect our SNP markers or dissociate them functional coding regions during the specified model time period. Realistic processes, including mutation and recombination, could be added in future versions.

Individuals calculated 2 PC scores based on their genotypes across all seven loci (Chapter 2). Then they calculated a genetic effect with the following equation:

$$\mu = \alpha + \beta_1 * PC1 + \beta_2 * SI\text{-}x + \beta_3 * PC2 + \beta_4 * PC1 * SI\text{-}x + \beta_5 * nacc2 + \beta_6 * mybbp1a$$

This effect (negative or positive) is then added to the date available to advance or delay egg-laying. Offspring compare their date available to the average date available of their parents. Then either advance or delay their date available by 40% of the difference between offspring and parents. It is unlikely that we are representing all of the inherited material that affects egg-laying date. This step ensured that we matched realistic heritability values.

Delay.-For both migrant and resident individuals we added a constant value after they calculated their date available to both represent time when an individual may gain energy reserves for egg-laying and to improve pattern matching.

Output writing (write-to-file-")

We record a number of outputs (in the form of .csv files) for each simulation; see the Observation section for more details.

Data evaluation

We parameterized our model using multiple sources of data that are outlined in Input data. Here, we focus on the limitations and the quality of our input data sets.

Survival

Our data set for parameterizing survival came from long-term demographic study systems in Idaho and New Jersey. While these sites represent some of the few long-term mark-recapture data sets for this species, we lacked such information for kestrel populations across each of the flyways. Therefore, the positive relationships between winter minimum temperature anomaly derived from the multi-state model might not have applied across the entire flyway. For example, kestrels breeding in the southern portion of their range might not endure severe enough winter temperatures to experience reductions in annual survival. This submodel also required the most calibration to achieve survival rates that fell within a realistic range for this species.

Migration distance and strategy

Parameterizing the migration distance and migration strategy submodels relied on BBS data. We lacked BBS records at higher latitudes, possibly as a result of lower research efforts in these locations and lower encounter rates for long-distance migrants (i.e., birds wintering south of the US border are less likely to be found or reported compared to birds wintering in the US).

Migrant and resident date of availability

Our data sets to parameterize date of availability included records contributed by community scientists. It is possible that these records may have been more prone to errors or data entry mistakes compared with those from professional scientists.

Reproduction

As with date of availability above, a portion of records used to parameterize the nest success and productivity submodel came from community scientist researchers. It is possible that

these records may have been more prone to errors or data entry mistakes compared with those from professional scientists.

Population size and density

For computational and biological reasons, we set population size and density (kestrel pairs per patch) in the model. We used an estimate of population size from the Partners in Flight database to control the largest number of individuals allowed in the model, which had a high degree of uncertainty. We then used this number–along with eBird status and trend estimates of kestrels counted for ideal checklist conditions–to calculate the carrying capacity of each patch in SCOPE. Therefore, errors in the population size estimate or eBird counts could have contributed to the number of kestrels in each ecoregion and output summaries.

Conceptual model evaluation

Details regarding model design and conceptual framework are presented in the model description and data evaluation sections. While the assumptions of the empirical research underlying this model are not addressed here, the general framework for this model is discussed below.

This model is built from the basic framework that nesting phenology in bird populations is the product of external factors (e.g., climate), internal (e.g., inherited traits), and individual history (e.g., nesting success the previous year). The framework for this model is the simple assumption that the timing of nesting is conditional on acquisition of a breeding site (the timing of which is inversely proportional to migration distance or positively associated with start-of-spring date) and the energetic requirements necessary for egg production (and that this is inversely proportional to winter conditions). This model does not explicitly model bird energetics. However, there is empirical evidence, from this system and elsewhere that shows correlative relationships between winter conditions and timing of nesting, and migration distance and date of arrival. Also, we assume that pattern of seasonal decline in fecundity does not change with advancing phenology. This may not be the case if early birds are at risk of failure from periodic late winter/early spring storms or if the synchrony of breeding with peaks of prey availability becomes decoupled.

Implementation verification

Our flyway-scale model with many millions of individuals faced some tractability issues. We conducted smaller-scale simulations (i.e., by examining patterns in a single ecoregion) that were more tractable to verify our code. We did extensive checking of model outputs during simulations (by print statements of variables in NetLogo) and after simulations were completed via plotting in R.

Tests of model execution varied in their complexity and focus, but all were executed to ensure that the entire model was implemented properly. Throughout code development, the syntax was verified via the syntax checker in NetLogo to ensure that each line of code followed proper structuring. Visual testing was used extensively throughout model development to ensure proper functioning. For instance, parameters were simplified to isolate only pairing of individuals. Because of the color coding of both habitat and individual sexes, the improper association of individuals (e.g., >2 per pair, incorrect sex distribution, etc.) could be readily tested through visual inspection. The use of both immediate and summary output was employed throughout nearly every submodel. Most commonly, tracking of internal variables and processes

were done by simply writing out the values of variables (via show commands in NetLogo). In addition, summary output at the conclusion of simulations was also used to ensure that derived variables (e.g., slope of regression lines) were properly determined. Similarly, extensive spot checking of agents and habitat patches was conducted. This allowed for the examination of variables midstream and enabled us to compare the changes in particular variables to those calculated manually to ensure that they aligned properly.

Model output verification

The implementation of this model involved calibrating parameters within the survival submodel and calibrating migrant and resident arrival dates (drawDateAvailable submodel). Pattern-matching of model outputs to empirical observations is evaluated in the model output corroboration section.

Model analysis

We examined the sensitivity of the model to changes in a number of the model parameters. We examined the effect of systematic variation of each parameter on several key model outputs. Emergence of model output is explored more thoroughly in the model output corroboration section and the main manuscript.

The vast majority of parameters to represent submodels in SCOPE came from regression-based analyses. Because our model included a large number of parameters and was computationally intensive, we chose to conduct a local sensitivity analysis, primarily on submodel intercepts and coefficients related to important climate or environmental predictors. With local sensitivity analysis, small variations of input values (e.g., within a specified percentage around a mean value) are performed for one-factor-at-a-time (Saltelli et al. 2007). While this method provides less detailed information than global sensitivity analysis, it is still a widely-used sensitivity approach (Thiele et al. 2014) and was the most practical option given our model's large parameter set and computational demands.

For each focal parameter (n = 82), we conducted 20 simulations where all other parameters were held constant but the parameter of interest was varied by $\pm$ 10%. Simulations were run for 50 years with a burn-in period of 10 years. Including the baseline experiment (i.e., all parameters held at their mean value), this resulted in a total of 1660 simulations. We examined the effect of parameter perturbations on average laydate, nest success, adult and juvenile survival, and population size values. To do so, we calculated the mean percent change from the baseline simulation and the perturbation simulations for each parameter and output metric.

The local sensitivity analysis identified several parameters that had a large effect on output metrics (Figure 3A.4). In general, the SCOPE model was strongly influenced by uncertainty in the intercept from the equation determining resident date of availability (*resInt*). Adult survival was sensitive to variability in the survival model intercept (*mortInt*) and the effect of unsuccessful, late breeding (*mortAdultFailLate*), although the uncertainty in these variables affected adult survival rates by <5%. Juvenile survival was similarly driven by these same parameters and the parameters representing effects of breeding strata (i.e., early/late, successful/unsuccessful). Timing of breeding was most sensitive to resident date of availability (*resInt*), and to a lesser extent, migrant date of availability (*b_Intercept_mig_arrival*). Several nest success regression parameters influenced average nest success probability, but ended to have smaller effects than parameters associated with timing (i.e., *resInt* and

b_Intercept_mig_arrival). Finally, population size was relatively insensitive to parameter uncertainty except for these same two parameters associated with arrival timing.

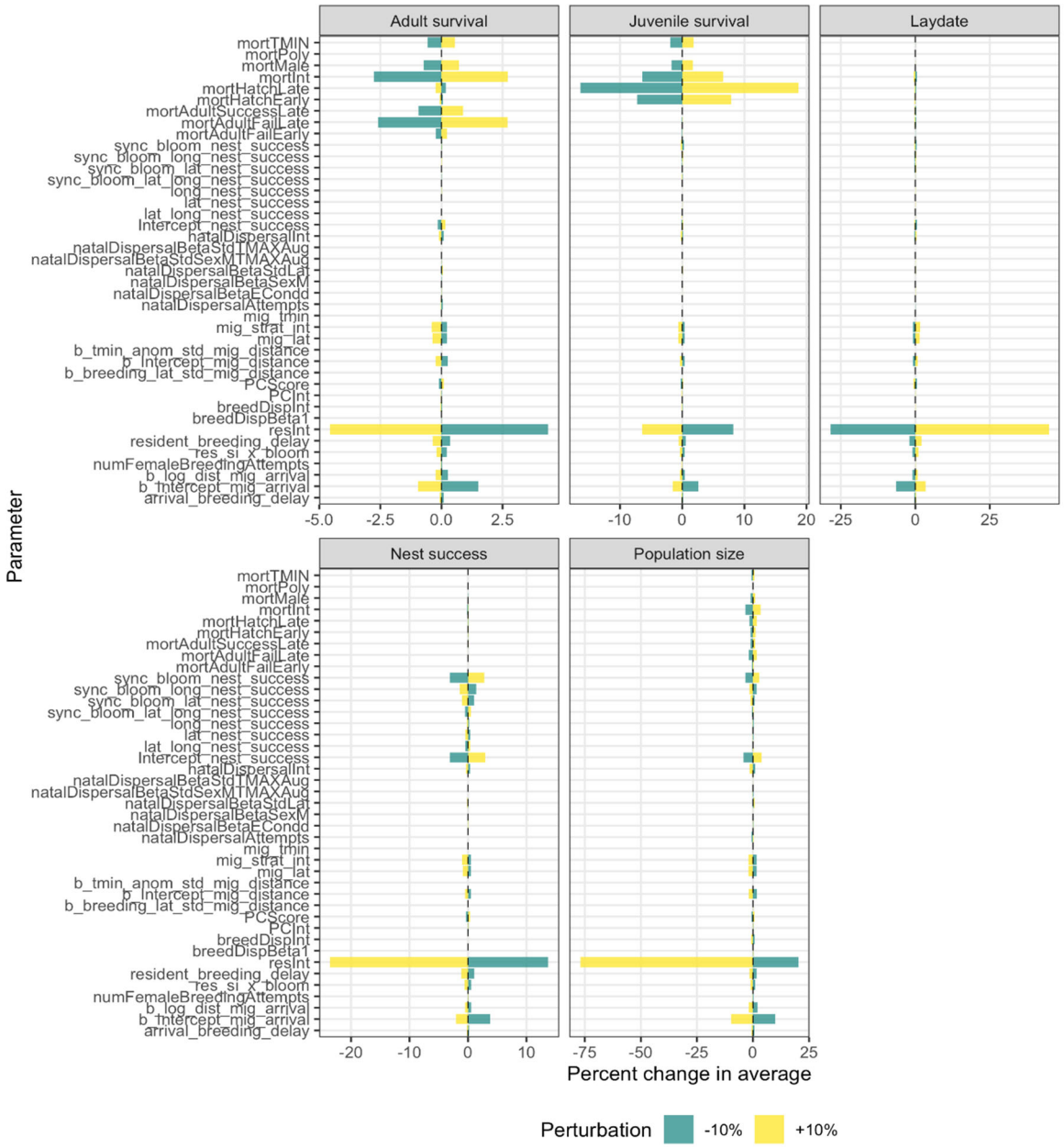

Figure 3A.4 Sensitivity analysis of average egg-laying date, nesting succezss, adult and juvenile survival, and population size for SCOPE input parameters. Bars indicate percent change in output metric average with -10% (green) and +10% (yellow) adjustments for each model parameter.

Model output corroboration

A number of patterns have been used to evaluate the ability of the model to realistically represent breeding phenology, migration distance, nest success, productivity, population trends, and latitudinal shift in abundance from empirical data sets.

Output metrics

Here, we provide 1) the temporal resolution and spatial extent of model output and empirical data sets, and 2) how we compared patterns for each output metric. Baseline simulations for both RCP4.5 and RCP8.5 were compared to empirical findings. All pattern matching analyses were conducted using the brms package (Bürkner 2017) in R (R Core Team 2021). To obtain average output metrics, we used intercept-only models with a random effect for simulation number. To estimate yearly trends in outputs, we used year (centered) as a fixed effect, with a random intercept for simulation number. Empirical data sets were modeled without random effects unless otherwise noted.

Egg-laying date

We compared average egg-laying date and trend in egg-laying dates over time of kestrels breeding in southwestern Idaho from 2008–2018 with egg-laying date output from the model over the same time period and across the Snake River Plain ecoregion. Empirical and model egg-laying dates were analyzed using linear (mixed) models.

Migration distance

We compared average migration distance and trend in migration distance over time of kestrels in the western flyway from 1980–2019 with migration distance output from the model over the same time period and spatial extent. Empirical and model migration distances were analyzed using linear (mixed) models.

Nest success

We compared average nest success rate and trend in nest success over time of kestrels breeding in southwestern Idaho from 2008–2018 with nest success output from the model over the same time period and across the Snake River Plain ecoregion. For the empirical data, we first modeled nest success as a Bernoulli-distributed random variable (0 = failure, 1 = success) with a random intercept of year. Next, we used the random intercept values to calculate the average nest success probability for each year which was matched model nest success probabilities. Because our responses were probability values, we used generalized linear models with a beta distribution and logit link function.

Productivity

We compared average productivity (young per pair) and trend in productivity over time of kestrels breeding in southwestern Idaho from 2008–2018 with productivity output from the model over the same time period and from kestrels across the Snake River Plain ecoregion. Empirical and model productivity rates were analyzed using linear (mixed) models.

Population trends

We compared the trend in kestrels counted per BBS route for the California Central Valley, Snake River Plain, Mojave, and Fraser Plain ecoregions from 1980–2017 (modified from McCaslin and Heath 2020) with population size output from the model over the same time period and same ecoregions. Trends in kestrels counted per BBS route (empirical) or total population size per year (model output) were analyzed using linear (mixed) models. For both data sets, we considered population trends to be decreasing if the 95% credible interval (CI) of

the slope did not overlap zero and was negative; stable if the 95% CI overlapped zero; and increasing if the 95% CI did not overlap zero and was positive.

Latitudinal shift in center of abundance

We compared the latitudinal shift in abundance of kestrels in the western flyway from 1994–2017 (McCaslin and Heath 2020) with the latitudinal shift in abundance over the same time period and similar spatial extent of kestrels in the model. Empirical and model shifts in the center of abundance (km per year) were analyzed using linear (mixed) models.

Pattern-matching results

We evaluated how well patterns were matched between model outputs and empirical data by visually comparing the intercept and/or beta estimates of the regression analyses described above. Specifically, we wanted to test whether model output metrics fell within 95% CIs of the same set of empirical intercept and beta estimates (Van Schmidt et al. 2019).

We found that model outputs mostly fell within reasonable ranges of the empirical data sets (Figure 3A.5). Change in egg-laying date matched the empirical trend, but average egg-laying date fell outside of the empirical estimate by 5-10 days. Both the average and slopes for migration distance were well matched with empirical estimates. Patterns of average nest success were closely matched to the empirical data, but change in nest success was negative in SCOPE compared to the empirical trend. Change in young per pair per year were closely matched to the empirical value, and model estimates fell very slightly outside of the 95% CI for average young per pair. SCOPE correctly predicted the population trend for the Snake River Plain and Mojave ecoregion, but did not predict the trend in the Central Valley of California and Okanagan Plateau in Canada. Finally, the shift in latitudinal center of abundance was approximately 2 times greater in the empirical data than in SCOPE, but the direction of shift was similar. We should note that slight mismatch in spatial scales (i.e., comparing data from a single study site in southwestern Idaho with model data from the Snake River Plain ecoregion) may have affected our ability to match certain patterns.

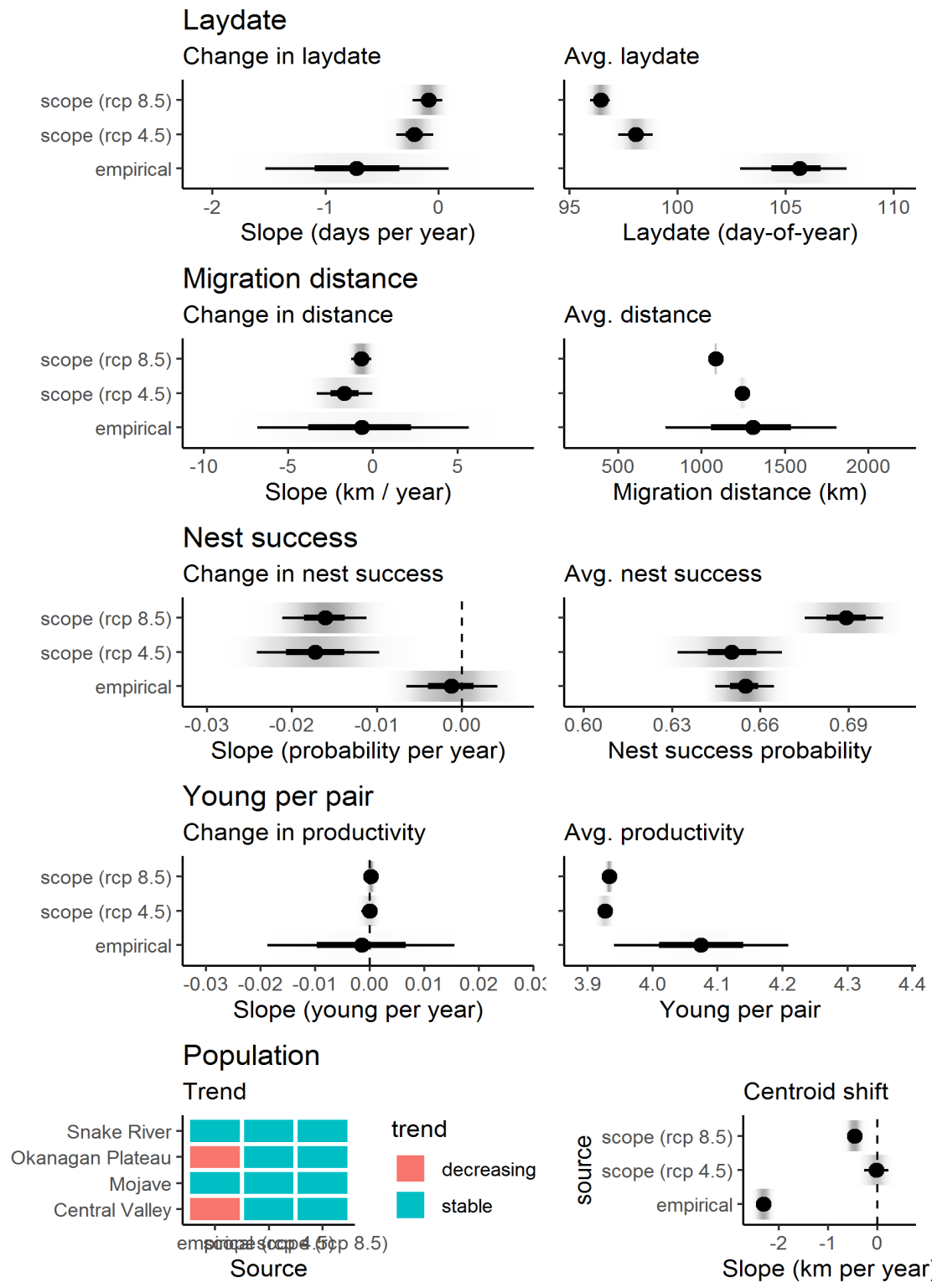

Figure 3A.5 Comparison of analyses of baseline SCOPE simulations (n = 20) and empirical data sets. Points represent mean estimates for each pattern. Thick and thin bars represent 50 and 95% posterior credible intervals, respectively.

Literature cited

Allstadt, A.J., Vavrus, S.J., Heglund, P.J., Pidgeon, A.M., Thogmartin, W.E. & Radeloff, V.C. (2015). Spring plant phenology and false springs in the conterminous US during the 21st century. *Environmental Research Letters*, *10*, 104008.

Anderson, A.M., Novak, S.J., Smith, J.F., Steenhof, K. & Heath, J.A. (2016). Nesting phenology, mate choice, and genetic divergence within a partially migratory population of American Kestrels. *The Auk*, *133*, 99–109.

Auer, T., Fink, D. & Strimas-Mackey, M. (2020). *Ebirdst: Tools for loading, plotting, mapping and analysis of eBird status and trends data products*.

Ault, T.R., Schwartz, M.D., Zurita-Milla, R., Weltzin, J.F. & Betancourt, J.L. (2015). Trends and natural variability of spring onset in the coterminous United States as evaluated by a new gridded dataset of spring indices. *Journal of Climate*, *28*, 8363–8378.

Bürkner, P.-C. (2017). Brms: An R package for Bayesian multilevel models using Stan. *Journal of Statistical Software*, *80*, 1–28.

Carpenter, B., Gelman, A., Hoffman, M.D., Lee, D., Goodrich, B., Betancourt, M., Brubaker, M., Guo, J., Li, P. & Riddell, A. (2017). Stan: A probabilistic programming language. *Journal of Statistical Software*, *76*, 1–32.

Cox, R., Griesemer, R., Pike, R., Taylor, I., & Thompson, K., (2022). The Go programming language and environment. *Communications of the ACM, 65* (5), (70-78).

eBird. 2021. eBird: An online database of bird distribution and abundance [web application]. eBird, Cornell Lab of Ornithology, Ithaca, New York. Available: http://www.ebird.org. (Accessed: Date [e.g., February 2, 2021]).

Ellegren, H. (2007). Molecular evolutionary genomics of birds. *Cytogenetic and Genome Research*, *117*, 120–130.

Grimm, V., Berger, U., Bastiansen, F., Eliassen, S., Ginot, V., Giske, J., Goss-Custard, J., Grand, T., Heinz, S.K., Huse, G. & others. (2006). A standard protocol for describing individual-based and agent-based models. *Ecological Modelling*, *198*, 115–126.

Grimm, V., Berger, U., DeAngelis, D.L., Polhill, J.G., Giske, J. & Railsback, S.F. (2010). The ODD protocol: A review and first update. *Ecological Modelling*, *221*, 2760–2768.

Heath, J.A., Steenhof, K. & Foster, M.A. (2012). Shorter migration distances associated with higher winter temperatures suggest a mechanism for advancing nesting phenology of American kestrels *Falco sparverius*. *Journal of Avian Biology*, *43*, 376–384.

Hijmans, R.J. (2019). *Geosphere: Spherical trigonometry*.

Hostetler, J.A., Sillett, T.S. & Marra, P.P. (2015). Full-annual-cycle population models for migratory birds. *The Auk*, *132*, 433–449.

Laake, J.L. (2013). *RMark: An R interface for analysis of capture-recapture data with MARK*. Alaska Fish. Sci. Cent., NOAA, Natl. Mar. Fish. Serv., Seattle, WA.

McCaslin, H.M., Caughlin, T.T. & Heath, J.A. (2020). Long-distance natal dispersal is relatively frequent and correlated with environmental factors in a widespread raptor. *Journal of Animal Ecology*, *89*, 2077–2088.

McCaslin, H.M. & Heath, J.A. (2020). Patterns and mechanisms of heterogeneous breeding distribution shifts of North American migratory birds. *Journal of Avian Biology*, 51, jav.02237.

Mearns, L.O., et al., 2017: The NA-CORDEX dataset, version 1.0. NCAR Climate Data Gateway, Boulder CO, https://doi.org/10.5065/D6SJ1JCH

Omernik, J.M. (1987). Ecoregions of the conterminous United States. *Annals of the Association of American Geographers*, *77*, 118–125.
Paprocki, N., Heath, J.A. & Novak, S.J. (2014). Regional distribution shifts help explain local changes in wintering raptor abundance: Implications for interpreting population trends. *PLoS ONE*, *9*, e86814.
Partners in Flight. 2020. Population Estimates Database, version 3.1. Available at http://pif.birdconservancy.org/PopEstimates. Accessed on 1/4/2020.
Powers, B. F., Winiarski, J. M., Requena-Mullor, J. M., & Heath, J. A. (2021). Intra-specific variation in migration phenology of American kestrels (*Falco sparverius*) in response to spring temperatures. *Ibis, 163,* 1448–1456.
R Core Team. (2021). *R: A language and environment for statistical computing*. R Foundation for Statistical Computing, Vienna, Austria.
Richardson, A.D., Hufkens, K., Li, X. & Ault, T.R. (2019). Testing Hopkins' bioclimatic law with PhenoCam data. *Applications in Plant Sciences*, *7*, e01228.
Richardson, A.D., Hufkens, K., Milliman, T. & Frolking, S. (2018). Intercomparison of phenological transition dates derived from the PhenoCam dataset V1.0 and MODIS satellite remote sensing. *Scientific Reports*, *8*, 1–12.
Rohde, R., Muller, R., Jacobsen, R., Perlmutter, S., Rosenfeld, A., Wurtele, J., Curry, J., Wickham, C. & Mosher, S. (2013). Berkeley Earth temperature averaging process. *Geoinformatics & Geostatistics: An Overview*, *1*, 1–13.
Rosemartin, A.H., Denny, E.G., Weltzin, J.F., Lee Marsh, R., Wilson, B.E., Mehdipoor, H., Zurita-Milla, R. & Schwartz, M.D. (2015). Lilac and honeysuckle phenology data 1956–2014. *Scientific Data*, *2*, 150038.
Ruegg, K.C., Brinkmeyer, M., Bossu, C.M., Bay, R.A., Anderson, E.C., Boal, C.W., Dawson, R.D., Eschenbauch, A., McClure, C.J.W., Miller, K.E., Morrow, L., Morrow, J., Oleyar, M.D., Ralph, B., Schulwitz, S., Swem, T., Therrien, J.-F., Van Buskirk, R., Smith, T.B. & Heath, J.A. (2021). The American Kestrel (*Falco sparverius*) genoscape: Implications for monitoring, management, and subspecies boundaries. *Ornithology*, *138*, ukaa051.
Saltelli, A., Ratto, M., Andres, T., Campolongo, F., Cariboni, J., Gatelli, D., Saisana, M. & Tarantola, S. (2007). *Global Sensitivity Analysis. The Primer*. John Wiley & Sons, Ltd, Chichester, UK.
Schwartz, M.D., Ahas, R. & Aasa, A. (2006). Onset of spring starting earlier across the Northern Hemisphere. *Global Change Biology*, *12*, 343–351.
Schwartz, M.D., Ault, T.R. & Betancourt, J.L. (2013). Spring onset variations and trends in the continental United States: Past and regional assessment using temperature-based indices. *International Journal of Climatology*, *33*, 2917–2922.
Smallwood, J.A. & Bird, D.M. (2020). American kestrel (*Falco sparverius*). *Birds of the World*.
Steenhof, K. & Heath, J.A. (2009). American Kestrel reproduction: Evidence for the selection hypothesis and the role of dispersal. *Ibis*, *151*, 493–501.
Steenhof, K. & Heath, J.A. (2013). Local recruitment and natal dispersal distances of American Kestrels. *The Condor*, *115*, 584–592.
Steenhof, K. & Peterson, B.E. (2009). American Kestrel reproduction in southwestern Idaho: Annual variation and long-term trends. *Journal of Raptor Research*, *43*, 283–290.
Thiele, J.C., Kurth, W. & Grimm, V. (2014). Facilitating Parameter Estimation and Sensitivity Analysis of Agent-Based Models: A Cookbook Using NetLogo and 'R'. *Journal of Artificial Societies and Social Simulation*, *17*, 11.

Thornton, P.E., Running, S.W. & White, M.A. (1997). Generating surfaces of daily meteorological variables over large regions of complex terrain. *Journal of Hydrology*, *190*, 214–251.

Van Schmidt, N.D., Kovach, T., Kilpatrick, A.M., Oviedo, J.L., Huntsinger, L., Hruska, T., Miller, N.L. & Beissinger, S.R. (2019). Integrating social and ecological data to model metapopulation dynamics in coupled human and natural systems. *Ecology*, *100*, e02711.

Wilensky, U. (1999). NetLogo. Evanston, IL: Center for Connected Learning and Computer-based Modeling, Northwestern University.

Wingfield, J.C. (2008). Organization of vertebrate annual cycles: Implications for control mechanisms. *Philosophical Transactions of the Royal Society of London B: Biological Sciences*, *363*, 425–441.

Appendix 4. TRACE document for SCOPE: Canada warbler version

This is a TRACE document ("TRAnsparent and Comprehensive model Evaludation") which provides supporting evidence that our model was thoughtfully designed, correctly implemented, thoroughly tested, well understood, and appropriately used for its intended purpose.

The rationale of this document follows:

Schmolke A., P. Thorbek, D.L. DeAngelis, and V. Grimm. 2010. Ecological modelling supporting environmental decision making: a strategy for the future. Trends in Ecology and Evolution 25:479–486.

and uses the updated standard terminology and document structure in:

Grimm V., J. Augusiak, A. Focks, B. Frank, F. Gabsi, A.S.A Johnston, K. Kulakowska, C. Liu, B.T. Martin, M. Meli, V. Radchuk, A. Schmolke, P. Thorbek, and S.F. Railsback. 2014. Towards better modelling and decision support: documenting model development, testing, and analysis using TRACE. Ecological Modelling 280:129–139.

and

Augusiak J., P.J. Van den Brink, and V. Grimm. 2014. Merging validation and evaluation of ecological models to 'evaludation': a review of terminology and a practical approach. Ecological Modelling 280:117–128.

Problem formulation

We built an IBM called SCOPE (Simulation of Carry-over and Phenological Effects) to test hypotheses of the potential mechanisms underlying phenological shifts in migratory landbirds, and to forecast how breeding phenology and other aspects of their life-history will be impacted by a changing climate. The model simulates the full annual cycle of migratory birds and was originally built to represent the biology of American kestrels (*Falco sparverius*). Here we demonstrate the portability of the SCOPE modeling framework by parameterizing the model for Canada warblers (*Cardellina canadensis*), a Department of Defense species of concern. SCOPE_Canada warbler can be used to forecast changes in Canada warbler breeding phenology, productivity, survival, and population trajectories from 1980 – 2099 under RCP 4.5 and RCP 8.5 scenarios

Model description

Below is a complete model description of the individual-based model of Canada warbler phenology described using the ODD protocol. The model description follows the ODD (Overview, Design concepts, Details) protocol for describing individual-based models (Grimm *et al.* 2006, 2010). This model was written in NetLogo 6.2.2 (Wilensky 1999).

Purpose

We parameterized this IBM to demonstrate the portability of a full annual cycle model to different species of migratory land birds for forecasting vulnerability to phenological mismatch. Here, we used data from eBirds, the Monitoring Avian Productivity and Survival (MAPS) program, the BBL, and published research to parameterize SCOPE for Canada warblers. Model results are a prediction of how breeding phenology, migration distance, and population sizes and distributions may change from 1980 – 2099 under different climate scenarios.

Entities, state variables, and scales

Our model is a full-annual-cycle model (Hostetler et al. 2015) consisting of individual birds, a virtual landscape representing the North American breeding range of Canada warblers, and landscape patches representing geographic locations (i.e., latitude/longitude values), ecoregion designation, carrying capacity, and annual environmental conditions. Birds are characterized by a set of static and dynamic attributes, which are outlined in Table 4A.1.

Table 4A.1 A list of bird attributes, whether each attribute is static or dynamic, and how attributes are assigned in SCOPE, Canada warbler version.

Bird Attributes	Status	Assignment
Sex	Static	Randomly assigned
Age	Dynamic	Increases each year by 1
Date of availability	Dynamic	Depends on latitude and spring minimum temperature anomaly
Egg-laying date	Dynamic	Depends on the date of availability, and locating a nest site and mate
Mismatch	Dynamic	Difference between egg-laying date and SI-x
Early?	Dynamic	Whether or not an individual laid eggs before or after the median date of mismatch (see text)
Nest success and productivity	Dynamic	Depends on mismatch
Probability of survival (juvenile)	Dynamic	Drawn from distribution
Probability of survival (adult)	Dynamic	Depends on Early?, sex, and minimum temperature anomalies
Breeding dispersal distance and direction	Dynamic	Drawn from distribution
Natal dispersal distance and direction	Dynamic	Drawn from distribution
Mating status (mate or floater)	Dynamic	Depends on whether individual finds an available mate

We employed a time scale in which non-breeding season events and the passage of 1 year (i.e., year *t*) occurs on day 161, and the breeding season occurs during days 1–160 (i.e., breeding season$_{t1–t212}$). Within the model and during output writing, these tick values are adjusted by adding 60 days to calculate real calendar dates. We chose to organize time steps in this way due to constraints of the NetLogo software and to simplify programming, as non-breeding season events such as survival and mortality could occur in a single time step. Although the span of 160 days is a longer breeding season than any one bird would experience, it represents the span of time between pairing of the earliest breeders until migration departure for the latest breeders (Reitsma et al. 2020). To match the temporal resolution of the climate and empirical data used in the model, simulations can be run between 1980–2099. Additionally, we included the option for

a burn-in period of 10, 15, or 20 years to allow the simulated bird population to reach a stable state.

The version of SCOPE presented here covers the breeding range of Canada warblers in the United States and Canada (Figure 4A.1). The range was composed of 28.5 km^2 patches. Patch size was based on the resolution of Regional Climate Models (RCMs) used to represent climatic conditions in the model. Each patch contains information about patch identity, latitude, longitude, ecoregion, the start of spring represented by the extended spring index (SI-x), spring minimum temperature anomaly, and the number of pairs that a patch can support. Patch attributes are derived from raster files imported at initialization or annually, depending on the layer.

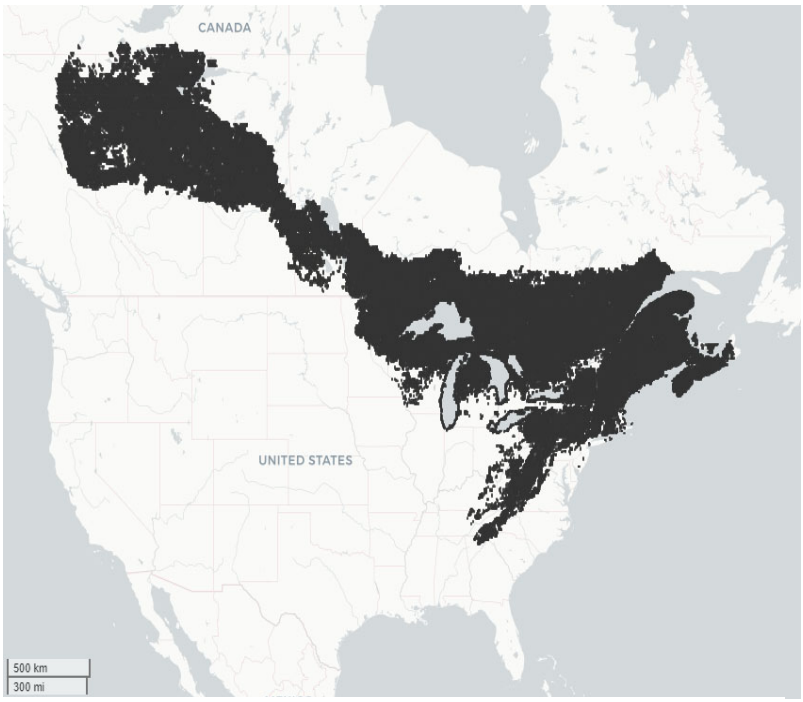

Figure 4A.1 Spatial extent of the North American breeding range of the Canada warbler within SCOPE.

Process overview and scheduling

Our model approximates the full-annual-cycle of Canada warblers; the exact sequence of model procedures and submodels are as follows. During the breeding season, warblers check to see if their date of availability has arrived; this is analogous to reproductive readiness. If so, males move to an unoccupied breeding patch and set their availability to true. Females that have reached their date of availability move to a patch with an available male that has not paired with a female and set their availability to true. If no unpaired, available males exist on the landscape, the female moves her available date to one day in the future and repeats the pairing process in the subsequent time-steps. Individuals that are unsuccessful at pairing remain in the population as non-breeding 'floaters.'

At the end of the breeding season (but before migration), paired females determine their probability of nest success based upon their egg-laying date in relation to the start-of-spring date. If the nest is successful, then the number of offspring for that nest is determined. These offspring are randomly assigned as male or female. At the beginning of the non-breeding season, the age

of each bird is increased by 1, their date of availability is reset and the climate and environmental conditions for that year are determined.

The probability of surviving to the following year is determined for each bird. For juveniles, survival probability is randomly drawn from a normal distribution with average and standard deviation of juvenile survival. For adults, survival probability is dependent upon the timing of egg-laying date. All Canada warbler migrate. Canada warblers determine their date of availability based on latitude and spring minimum temperature anomaly. Submodel processes follow the same flow as the American kestrel version (Figure 3A.3).

Design concepts

Basic Principles

Within SCOPE, we simulate full-annual-cycle events of birds, and include a carry-over effect of spring minimum temperature on arrival date in the subsequent spring. In this use of SCOPE, life-history events and scheduling are guided by the biology of Canada warblers, either from previously published research or our own analyses of empirical data sets.

Emergence

Several patterns emerge from this model. Trends in the phenology of egg-laying result from a combination of factors including changes in climate over time and date of availability. The mean mismatch increases over time as the extended spring index trends earlier and egg-laying dates trend later. Adult survival and population sizes decline as mismatch increases.

Adaptation

Within the IBM modeling framework, adaptation is the term for individual decisions that maximize fitness. When warblers become available, males establish territories and females choose from one of the available males. There are a limited number of pairs on each patch. Competition for mates and patches and the effect of phenological mismatch on nest success and adult survival drives the selection for earlier nesting. Individual warblers maximize fitness through establishing nests as early as possible.

Objectives

The objective for birds is to pair with a mate, successfully nest, produce offspring, migrate and survive until the following year.

Learning

No learning occurs within our model.

Prediction

Canada warblers use simple predictive models of that incorporate climatic and environmental conditions of breeding patches to make decisions about when to become available for breeding.

Sensing

Warblers can sense the climatic conditions of the patch they occupied during the breeding season. Phenological mismatch between the estimated start of spring and egg laying date affects nest success and adult survival. Spring minimum temperature anomalies (February – May)

influencing timing of availability to find a mate. In addition, birds can determine whether a potential breeding patch within their assigned dispersal distance and direction has available mates, or has reached carrying capacity.

Interaction

Adult birds attempt to find mates to pair and reproduce. The density of individuals within potential breeding patches can also indirectly impact the reproductive status of birds, potentially resulting in reduced survival for individuals that are unable to secure a mate and become non-breeders (i.e., 'floaters').

Stochasticity

The majority of submodels in our IBM are parameterized from individual regression models. This approach allowed use to incorporate parameter uncertainty by drawing values from a distribution of parameter values based on the mean value and the standard deviation of the parameter. Also, we included random effects of year and location in some of the submodel regressions.

Collectives

Male and female warblers form pairs during the breeding season. Pairing status is reset before the start of the next breeding season. Otherwise, social structure is not included in the model.

Observation

Our model records several phenological and demographic metrics each simulation year. Output metrics are summarized at the patch- and ecoregion-level because of the large spatial extent and number of individuals in the model. These different observation types are described below.

Patch- and ecoregion-level observations

We record 9 different patch- and ecoregion-level outputs in .csv format. Most of the metrics are summarized by patch, and we record summary statistics (mean, min, max, standard deviation, and count) for each metric:

- Environmental output
  - *pxcor*: NetLogo patch x coordinate
  - *pycor*: NetLogo patch y coordinate
  - *latitude*: latitude of patch
  - *spring.anom*: spring average minimum temperature anomaly of patch
  - *bloomDate*: first bloom date of patch
  - *ecoregion*
- Laydate output
  - *nestProb*: summary statistics of nest success probability
  - *syncBloom*: summary statistics of synchrony with bloom date
  - *dateAvail*: summary statistics of date of availability
  - *laydate*: summary statistics of laydate
- Offspring output
  - *offspring*: summary statistics of offspring produced

- Population size output
  - *populationSize*: number of adults
- Breeding dispersal output
  - *distance*: summary statistics of breeding dispersal distance
  - *direction*: mean and dispersion of breeding dispersal direction
- Natal dispersal output
  - *distance*: summary statistics of natal dispersal distance
  - *direction*: mean and dispersion of natal dispersal direction
- Number pairing output
  - *daysBWAvailPairing*: summary statistics of days between date of availability and pairing date
- Adult survival output
  - *age*: summary statistics of age
  - *probSurvAdult*: summary statistics of survival probability
- Juvenile survival output
  - *probSurvJuvenile*: summary statistics of survival probability

Initialization

At the beginning of the model simulation, values for the patches in the landscape and agent parameters are set. The first year the model begins is determined by the user; here we initialized the landscape with climate data starting in 1980. The simulation begins with 100,000 males and 100,000 females (or whatever the user chooses) randomly distributed on breeding habitat patches within the landscape. Each patch consists of a number for the maximum pairs allowed, derived by calculating the maximum number of Canada warbler home ranges that can fit within a patch. A number of warbler attributes are then determined: each bird is randomly assigned an age between 0 and 7 (where ages less than or equal to 1 are considered juveniles and ages greater than 1 are considered adults); sex is undefined; migration strategy is set to true; availability, natal dispersal success, nesting status, and early are set to false; mate identity is set to nobody; and dispersal distances and directions, phenological mismatch (asynchrony), and nest success probability are set to 0. Males move to an unoccupied breed patch first and females move to any breeding patch.

Input data

Input data for our IBM included 8 different environmental and geographic variables in raster format to represent time-varying processes and static attributes. We prepared all raster layers for NetLogo using R (R Core Team 2021). Rasters for SCOPE were clipped to match the North American Canada warbler breeding range, projected into an equal area projection, re-sampled to match the resolution of climate or start-of-spring rasters derived from regional climate model (RCM) projections, and written in ESRI ASCII Grid file format for compatibility with the Netlogo GIS extension.

Regional climate model projections

Simulated Canada warblers in SCOPE sense the climate and vegetation phenology (i.e., start-of-spring date) conditions in the ‘patch’ or raster cell that they reside in, and these conditions are used to inform different SCOPE submodels (e.g., timing and demographic rates). To forecast changes in weather, we used regional climate model (RCM) data from the NA-

CORDEX project (Mearns et al. 2017) that was bias-corrected using the Daymet historical gridded dataset (Thornton et al. 1997). This bias-correction provides continuity between the historical climate data used to parameterize warbler-weather-vegetation phenology relationships, and future changes in climate. We obtained climate data for two representative concentration pathways (RCPs) that represent scenarios where moderate effort or no action is taken to curb emmissions: RCP4.5 (1 bias-corrected RCM was available) and RCP8.5 (12 RCMs, Table 3A.2). NA-CORDEX projections used in SCOPE were available at a ~25 km^2 resolution for the period 1980–2099, and converted from netcdf format into annual raster layers.

We calculated daily temperature anomaly values for each raster cell by subtracting 30-year average temperatures (1980–2009) from annual temperature values. Next, we averaged the daily temperature anomalies for each spring in each year of the climate projections. To represent the mean minimum temperature (T_{min}) base for spring anomalies we averaged March – May minimum temperatures. Finally, we created a multi-model ensemble (i.e., average spring T_{min} anomaly across all available RCMs) for the RCP8.5 pathway. Only one RCM was available for RCP4.5 (CanESM2.CanRCM4); therefore, we were unable to produce ensemble climate layers and used the single RCM for this pathway.

Start-of-spring date

We quantified start-of-spring dates in SCOPE using the extended spring indices (Schwartz et al. 2006, 2013). The extended spring indices are mathematical models that predict the start-of-spring (i.e., date of leaf-out or first bloom) based on weather at a particular location. These models were constructed using historical observations of the timing of first leaf and first bloom in a cloned lilac cultivar and two cloned honeysuckle cultivars, which were selected based on the availability of historical observations from across a wide geographic area (Schwartz et al. 2006). Extended spring indices also reflect spring phenological transitions in native species and crops (Rosemartin et al. 2015), and estimates for start-of-spring dates derived from extended spring indices are generally in good agreement with estimates derived from near-surface time-lapse cameras (Richardson et al. 2018, 2019).

Primary inputs to estimate extended spring indices are daily minimum and maximum temperatures beginning January 1 of each year, and daylength derived from latitude (Ault et al. 2015). Spring index models were built with bias-corrected NA-CORDEX RCM data and the Go Programming Language (Cox et al. 2022), and we verified our model output against spring index code and projections developed by Allstadt et al. (2015). Similar to the temperature rasters described above, only one RCM was available for RCP4.5 (CanESM2.CanRCM4) and a multi-model ensemble was used for RCP8.5 In SCOPE, we represented spatially-explicit estimates of start-of-spring in each year (1980–2099) using first bloom date.

eBird density

To ensure realistic population sizes and incorporate density-dependence in the model, we integrated Partners in Flight population estimates and eBird relative abundance maps (eBird 2021) to create a raster layer that determines the maximum number of pairs that a patch is capable of supporting. First, we used the ebirdst package (Auer et al. 2020) to create a spatially-explicit raster of Canada warbler relative abundance (estimated number of Canada warblers detected by an eBirder during a traveling count at the optimal time of day) across their North American breeding range. Second, we estimated the number of individual warblers that a cell could support by multiplying the relative abundance value by a scaling factor, such that the sum

of all raster cells was approximately equal to the mean Partners in Flight population estimate for the species. Finally, we divided each raster value by 2 to produce a raster with the total number of pairs allowed per cell.

Ecoregions

We divided flyways into United States Environmental Protection Agency (US EPA) level III ecoregions (Omernik 1987) for summarizing outputs. We rasterized the level III ecoregions shapefile retrieved from the USA EPA website.

Geographic coordinates

We selected a random climate raster to calculate the latitudinal and longitudinal center of each raster cell, and created a separate raster file for the centroid latitude and longitude values.

Submodels

The model can organized under two distinct annual cycle periods, the "breeding" season and the "non-breeding" season. The following submodels represent all processes in the model. Actual names of submodel procedures used in the IBM code are included in parentheses. For regression-based submodels, we used Bayesian inference to fit models (unless otherwise noted) via the R package brms (Bürkner 2017), which provides a user-friendly interface for the STAN probabilistic programming language (Carpenter et al. 2017). Regression model details can be found in the supplementary material. All procedures occur for individuals in random order each time they are invoked, except for the updateAvailable submodel. Additional procedures underlying main submodels called in the go procedure are italicized in each submodel description.

Update date of availability (updateAvailable)

Prior to becoming available to pair (at this stage they are 'unavailable'), bird color is set to black (male) or white (female). Once birds are available to pair, they begin the process of dispersing and finding a mate. During this submodel, date of availability in the spring for each individual is updated on a daily basis, depending on whether an individual is available and if it is successfully paired.

maleBreed and *femaleBreed*.–Males are the first to occupy breeding patches, which may be the site that they occupied in the previous year, or a site they are dispersing to for the first time. Males determine whether the carrying capacity of a patch has been met; if not they occupy that patch and decrease the number of pairs that may occupy it. If the patch is occupied, they continue searching for breeding patches for a pre-determined number of tries (controlled by a slider on the NetLogo interface). If this number of breeding attempts is reached prior to locating a breeding patch, the male dies. Date of availability increases by a day if individuals are not successful in pairing. Once males pair, their color is changed to sky. Females use a similar process to locate an available male, and increase their date of availability if they are unsuccessful at finding a mate on a particular day. Once females pair, their color is changed to brown.

checkNeighboringPatches.–In this procedure, females also have the opportunity to check neighboring patches during their last attempt to find a mate.

These procedures repeat every day until an individual pairs, dies, or becomes a non-breeding individual or floater (i.e., they reach the maximum number of attempts to breed - 8). Floaters have their color set to orange (female) or cyan (male) and the early? and attributes are set to false, which puts them in a lower survival category.

Natal dispersal and direction (natalDispersal)

We parameterized natal dispersal distance using banding data. Natal dispersal distances (in km) were extracted from the United States Geological Survey's Bird Banding Laboratory (BBL) band encounters data set (1980–2019). Unfortunately, there were very few natal dispersal records for Canada warblers, so we included natal dispersal records for a closely related species, Wilson's warblers (*Cardellina pusilla*), in addition to Canada warbler records. Further, small samples sizes limited testing of covariates associated with natal dispersal. Therefore, we created a intercept model with a Gamma-distributed random variable.

$$\textit{Natal dispersal distance (km): } \log(\mu) = \alpha$$

We used the same BBL data set to calculate mu and rho parameters in R and determine natal dispersal direction. Direction (in degrees) was drawn from a wrapped cauchy distribution. Natal dispersers are permitted to make five attempts to locate an available breeding patch (i.e., a patch that has not reached maximum capacity and is within their drawn dispersal distance and direction). If the number of permitted natal dispersal attempts is exceeded, individuals die.

Breeding dispersal and direction (breedingDispersal)

Adult birds can disperse from a breeding patch in subsequent seasons. Birds can remain on the same patch if it is available and they draw a short dispersal distance; otherwise, individuals locate a new, available breeding patch. We parameterized breeding dispersal based on band encounters of Canada warblers and Wilson's warblers from the BBL (1980–2019). We retained banding records for individuals banded during the breeding season in year t (April_t–August_t) and encountered in the subsequent breeding season in year $t + 1$ (April_{t+1}–August_{t+1}). Distances between breeding locations were calculated from pairs of latitude/longitude coordinates using the geosphere package (Hijmans 2019). Breeding dispersal distance (in km) was modeled as a Gamma-distributed random variable.

$$\textit{Breeding dispersal distance (km): } \log(\mu) = \alpha$$

We used the same BBL data set to calculate mu and rho parameters in R to determine breeding dispersal direction. Breeding dispersal direction was random (i.e., there was no bias toward a particular compass bearing). Direction (in degrees) was drawn from a wrapped cauchy distribution.

Reproduction (reproduce)

Females that have found a mate initiate nesting and producing offspring. To estimate the relationship between mismatch and nest success, we compiled from MAPS programs and professional scientists. We modeled nest success as a Bernoulli-distributed random variable, and as a function of phenological mismatch (i.e., difference in days between egg-laying date and extended spring index date) and a random year effect.

$$P(\text{nest success}): \text{logit}(\mu) = \alpha_{[year]} + \beta_1 * \text{mismatch}$$

To draw their probability of nesting success, females first determine how their egg-laying date compares with the extended spring index date of their breeding patch to calculate an 'mismatch' value. Using this information, females draw a nest success probability. Next, a uniform random number between 0 and 1 is drawn and compared to the nest success probability. If the random value is less than the calculated probability, the nest survives and both the female and associated male set their success value to true (otherwise they set success as false).

Mismatch values are categorized as early or late by setting early? to *true* or *false*, respectively, for the adult survival submodel. Median mismatch values are different for different regions. Birds in the Great Lakes or Boreal regions have mismatch cut-off value of 24, where those birds are early if they are 24 and late if they are after the value of 24. The other region is Appalachian with an mismatch cut-off value of 31, where early is before 31 and late is after 31.

For successful females, the number of offspring produced is drawn by rounding to the nearest integer a value from a normal distribution with a mean of 3.8 and standard deviation of 1.03. If the calculated value is negative, it is set to 0; if the value is greater than 6 it is set to six to prevent unrealistically productive nests. Offspring are randomly assigned as male or female, given an age of 0.

Bird attribute, year, and patch updates (reset)

After reproduction, the next year begins and several updates occur. Year is incremented by one, and the day of year and the number of offspring in the population are set to 0. In addition, each bird resets several dynamic attributes: availability and nesting status are set to false, age is incremented by 1 year, mate is set to nobody, and individuals reset their color to black (males) or white (females). The number of pairs occupying each patch are also set to 0.

Survival (survival and mortality)

Birds survive or die based upon an annual survival probability. We parameterized adult survival (*survivalAdult*) in SCOPE using equations derived from a multi-state mark-recapture model developed in RMark (Laake 2013) using MAPS data spanning from 1992 to 2019 from stations within the breeding range of Canada warblers. We estimated the extended spring index (SI-x) for each capture station, each year. We used "breeding status" variables within MAPS data to classify whether birds were breeding. Next, we estimated breeding windows (earliest egg-laying to latest fledge) for Canada warblers in three distinct regions: Boreal, Great Lakes, and Appalachian. The breeding window estimated for the Boreal region is June 5 to July 16 (Flockhart 2010), the Great Lakes region was May 31 to July 19 (Ontario Breeding Bird Atlas), and the Appalachian region was from May 12 to July 6 (Becker 2012). Finally, we calculated the median difference between nesting and SI-x for each region and categorically classified (early?) whether a bird was breeding before (early) or after (late) the median date of asynchrony.

$$P(\text{survivalAdult}): \text{logit}(\mu) = \alpha + \beta_1 * \text{early?}$$

Juvenile survival (*survivalJuvenile)* was randomly drawn from an average and standard deviation estimates of juvenile survival of small warblers (Stewart 1988).

$$P(survivalJuvenile): logit(\mu) = \alpha$$

To kill individuals, we use a Bernoulli trial with the probability of success equal to the survival probability value generated in either *survivalJuvenile* or *survivalAdult* in a separate mortality procedure for juveniles and adults. Floater survival probability (adults only) is also halved. The separate mortality procedures allow us to record survival probabilities prior to removing dead individuals from the population. The survival probability value is then compared to a uniform random number between 0 and 1; if the random number is greater than the probability of survival, then the individual dies.

Update environmental rasters (drawNextClimateMaps)

Environmental layers that comprise the virtual world in NetLogo are updated on an annual basis by importing rasters in .asc format. This procedure uses the appropriate calendar year to pull in corresponding spring mean minimum temperature anomaly and extended spring index. Thus, birds can sense environmental conditions that are key to determining different components of a bird's life-history.

Migration

All Canada warblers migrate. There was no sub-model for individuals to determine whether to remain resident on the breeding grounds or migrate. Further, there was no sub-process to calculate migration distance because of a lack of empirical data. Migratory birds move to an arbitrary location (patch 0,0) in the winter range (migrate) in which location is not influential to other processes.

Date of availability (drawDateAvailable)

This process determines what day of the year (i.e., date of availability) individual birds will become available for pairing for the upcoming breeding season. We used a modified approach from Powers et al. (2021) to model spatially-explicit arrival dates derived from eBird checklists in relation to latitude and spring climate conditions (i.e., minimum temperature anomalies). Date of availability was modeled as Gamma-distributed random variable with a fixed effect of latitude, spring T_{min} anomaly, and a random effect of year:

$$Date\ of\ availability: log(\mu) = \alpha_{[year]} + \beta_1 * latitude + \beta_2 * spring\_T_{min}\_anomaly$$

Output writing (write-to-file-'')

We record a number of outputs (in the form of .csv files) for each simulation; see the Observation section for more details.

Data evaluation

We parameterized our model using multiple sources of data that are outlined above. Here, we focus on the limitations and the quality of our input data sets.

Dispersal

We did not have sufficient BBL records to estimate Canada warbler dispersal so we included data from a closely related species. This may be an inaccurate representation of Canada warbler dispersal.

Survival

We could not obtain a mark and recapture dataset that was sufficient to estimate juvenile survival with environmental or life-history parameters. Therefore, we used published estimates of averages. This constrains our ability to study the effects of mismatch on an important component of individual fitness and population demographics.

Migration distance and strategy

We did not have enough empirical data to estimate Canada warbler migration distance and environmental covariates on migration distance. Therefore the model does not forecast how climate change may influence changes in migration distance or strategy, and whether this has carry-over effects on nesting phenology.

Date of availability

Our data sets to parameterize date of availability included records contributed by community scientists. It is possible that these records may have been more prone to errors or data entry mistakes compared with those from professional scientists.

Reproduction

Canada warbler nests are difficult to find, especially early in the nesting cycle. Therefore, nest success data may be biased towards successful nests.

Population size and density

For computational and biological reasons, we set population size and density (birds pairs per patch) in the model. We used an estimate of population size from the Partners in Flight database to control the largest number of Canada warblers allowed in the model, which had a high degree of uncertainty. We then used this number–along with eBird status and trend estimates of Canada warblers counted for ideal checklist conditions–to calculate the carrying capacity of each patch in SCOPE. Therefore, errors in the population size estimate or eBird counts could have contributed to the number of Canada Warblers in each ecoregion and output summaries.

Conceptual model evaluation

Details regarding model design and conceptual framework are presented in the model description and data evaluation sections. While the assumptions of the empirical research underlying this model are not addressed here, the general framework for this model is discussed below.

This model is built from the basic framework that nesting phenology in bird populations is the product of external factors (e.g., climate) and life-history. The framework for this model is the simple assumption that the timing of nesting is conditional on acquisition of a breeding site (the timing of which is inversely proportional to latitude and spring T_{min} anomaly). This model does not explicitly model bird energetics. However, there is empirical evidence, from this system and elsewhere that shows correlative relationships between winter conditions and timing of nesting, and migration distance and date of arrival. Also, we assume that pattern of seasonal decline in fecundity does not change with advancing phenology. This may not be the case if early birds are at risk of failure from periodic late winter/early spring storms or if the synchrony of breeding with peaks of prey availability becomes decoupled.

Implementation verification

Our flyway-scale model with many millions of individuals faced some tractability issues. We conducted smaller-scale simulations (i.e., by examining patterns in a single ecoregion) that were more tractable to verify our code. We did extensive checking of model outputs during simulations (by print statements of variables in NetLogo) and after simulations were completed via plotting in R.

Tests of model execution varied in their complexity and focus but all were executed to ensure that the entire model was implemented properly. Throughout code development, the syntax was verified via the syntax checker in NetLogo to ensure that each line of code followed proper structuring. Visual testing was used extensively throughout model development to ensure proper functioning. For instance, parameters were simplified to isolate only pairing of birds. Because of the color coding of both habitat and individual sexes, the improper association of birds (e.g., >2 per pair, incorrect sex distribution, etc.) could be readily tested through visual inspection. The use of both immediate and summary output was employed throughout nearly every submodel. Most commonly, tracking of internal variables and processes were done by simply writing out the values of variables (via show commands in NetLogo). In addition, summary output at the conclusion of simulations was also used to ensure that derived variables (e.g., slope of regression lines) were properly determined. Similarly, extensive spot checking of agents and habitat patches was conducted. This allowed for the examination of variables midstream and enabled us to compare the changes in particular variables to those calculated manually to ensure that they aligned properly.

Model output verification

The implementation of this model involved calibrating parameters within the survival submodel and calibrating migrant arrival dates (drawDateAvailable submodel). Pattern-matching of model outputs to empirical observations is evaluated in the model output corroboration section.

Model analysis

We examined the sensitivity of the model to changes in a number of the model parameters. We examined the effect of systematic variation of each parameter on several key model outputs. Emergence of model output is explored more thoroughly in the model output corroboration section and the main manuscript.

The vast majority of parameters to represent submodels in SCOPE came from regression-based analyses. Because our model included a large number of parameters and was computationally intensive, we chose to conduct a local sensitivity analysis, primarily on submodel intercepts and coefficients related to important climate or environmental predictors. With local sensitivity analysis, small variations of input values (e.g., within a specified percentage around a mean value) are performed for one-factor-at-a-time (Saltelli et al. 2007). While this method provides less detailed information than global sensitivity analysis, it is still a widely-used sensitivity approach (Thiele et al. 2014) and was the most practical option given our model's large parameter set and computational demands.

For each focal parameter (n = 15), we conducted 20 simulations where all other parameters were held constant but the parameter of interest was varied by $\pm$ 10%. Simulations were run for 60 years with a burn-in period of 10 years. Including the baseline experiment (i.e.,

all parameters held at their mean value), this resulted in a total of 640 simulations. We examined the effect of parameter perturbations on average egg-laying date, nest success, adult and juvenile survival, and population size values. To do so, we calculated the mean percent change from the baseline simulation and the perturbation simulations for each parameter and output metric.

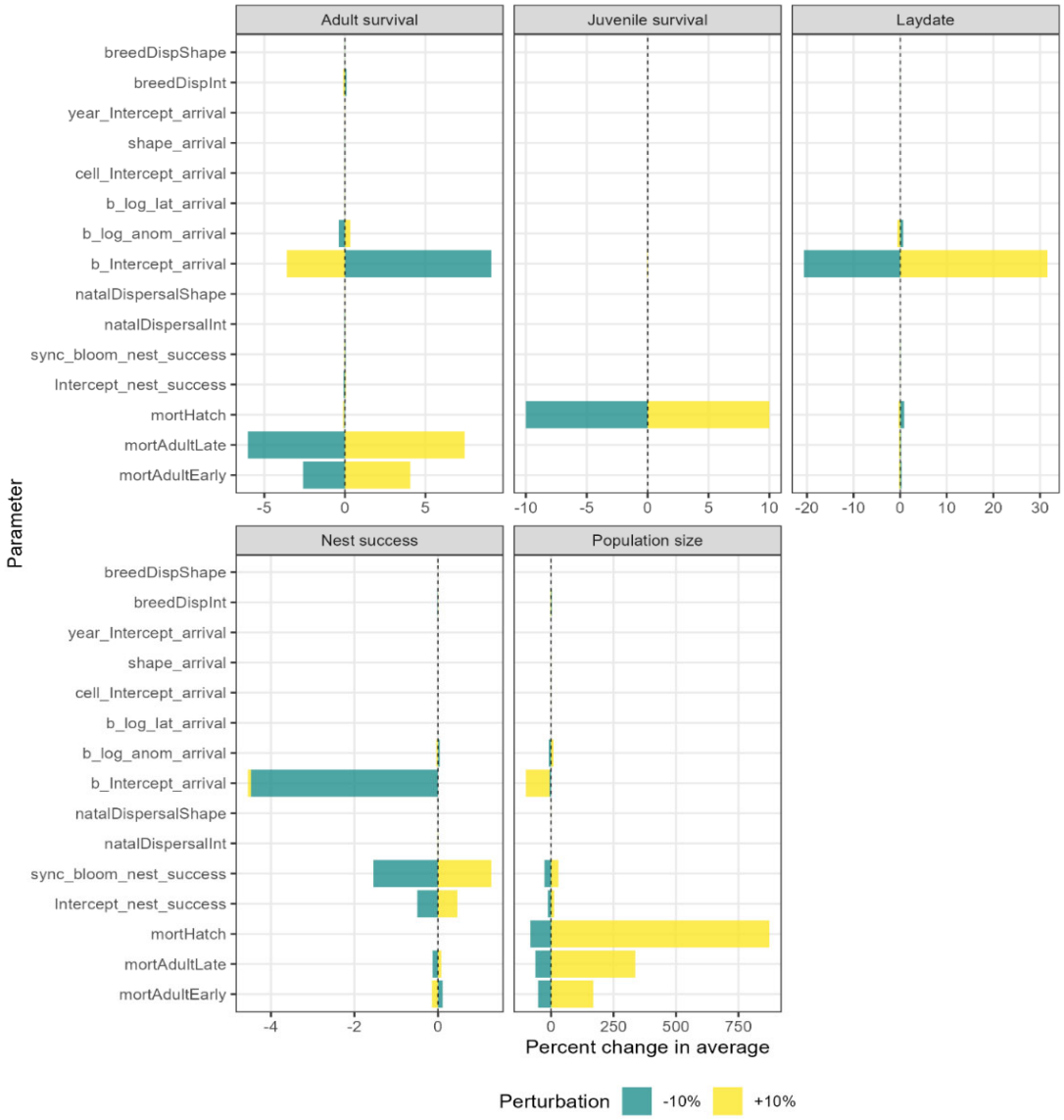

Figure 4A.2 Sensitivity analysis of average laydate, nesting success, adult and juvenile survival, and population size for SCOPE input parameters. Bars indicate percent change in output metric average with -10% (green) and +10% (yellow) adjustments for each model parameter.

The local sensitivity analysis identified several parameters that had a large effect on output metrics (Figure 4A.2). In general, the SCOPE model was strongly influenced by uncertainty in the intercept from the equation determining date of availability (*b_Intercept_arrival*). Adult survival was sensitive to variability in the survival model parameters for early (*mortAdultEarly*) and late nesters (*mortAdultLate*), and the timing of arrival from spring migration (*b_Intercept_arrival*). Juvenile survival was similarly driven by the

intercept we used for juvenile survival draws (*mortHatch*). Timing of breeding was most sensitive to migrant date of availability (*b_Intercept_arrival*). Nest success probability was influenced by date of availability (*b_Intercept_arrival*), the intercept term for nest success (*Intercept_nest_success*), and the effect of mismatch (*sync_bloom_nest_success*), and to a lesser extent survival parameters. Finally, population size was affected most by survival parameters (*mortAdultEarly, mortAdultLate, mortHatch)* and to a lesser extent nest success parameters.

Model output corroboration

A number of patterns have been used to evaluate the ability of the model to realistically represent breeding phenology, migration distance, nest success, productivity, population trends, and latitudinal shift in abundance from empirical data sets.

Output metrics

Here, we provide 1) the temporal resolution and spatial extent of model output and empirical data sets, and 2) how we compared patterns for each output metric. Baseline simulations for both RCP4.5 and RCP8.5 were compared to empirical findings. All pattern matching analyses were conducted using the brms package (Bürkner 2017) in R (R Core Team 2021). To obtain average output metrics, we used intercept-only models with a random effect for simulation number. Empirical data sets were modeled without random effects unless otherwise noted.

Egg laying date

We compared average egg laying dates at 2 study sites in different locations in the Canada warbler model: Alberta and New Hampshire with output from the model over the same time periods for the same ecoregions where the data were collected. Empirical and model egg-laying dates were analyzed using linear (mixed) models.

Nest success and productivity

We compared average nest success rate and productivity in nest success over time of Canada warblers at a long-term research site in New Hampshire with nest success output from the model over the same time period and across the Northeastern Highland ecoregion. For the empirical data, we first modeled nest success as a Bernoulli-distributed random variable (0 = failure, 1 = success) with a random intercept of year. Next, we used the random intercept values to calculate the average nest success probability for each year which was matched model nest success probabilities. Because our responses were probability values, we used generalized linear models with a beta distribution and logit link function. Empirical and model productivity rates were analyzed using linear (mixed) models.

Pattern-matching results

We evaluated how well patterns were matched between model outputs and empirical data by visually comparing the intercept and/or beta estimates of the regression analyses described above. We aimed to have model output metrics fall within 95% CIs of the same set of empirical intercept and beta estimates (van Schmidt et al. 2019). We found that model outputs mostly fell within reasonable ranges of the empirical data sets (Figure 4A.3). In general, average egg laying dates fell outside of the empirical estimate by 2–5 days. Patterns of average nest success and productivity were closely matched to the empirical data, though variance was significantly

underestimated, suggesting other important factors that contribute to nest success and productivity were not represented in SCOPE.

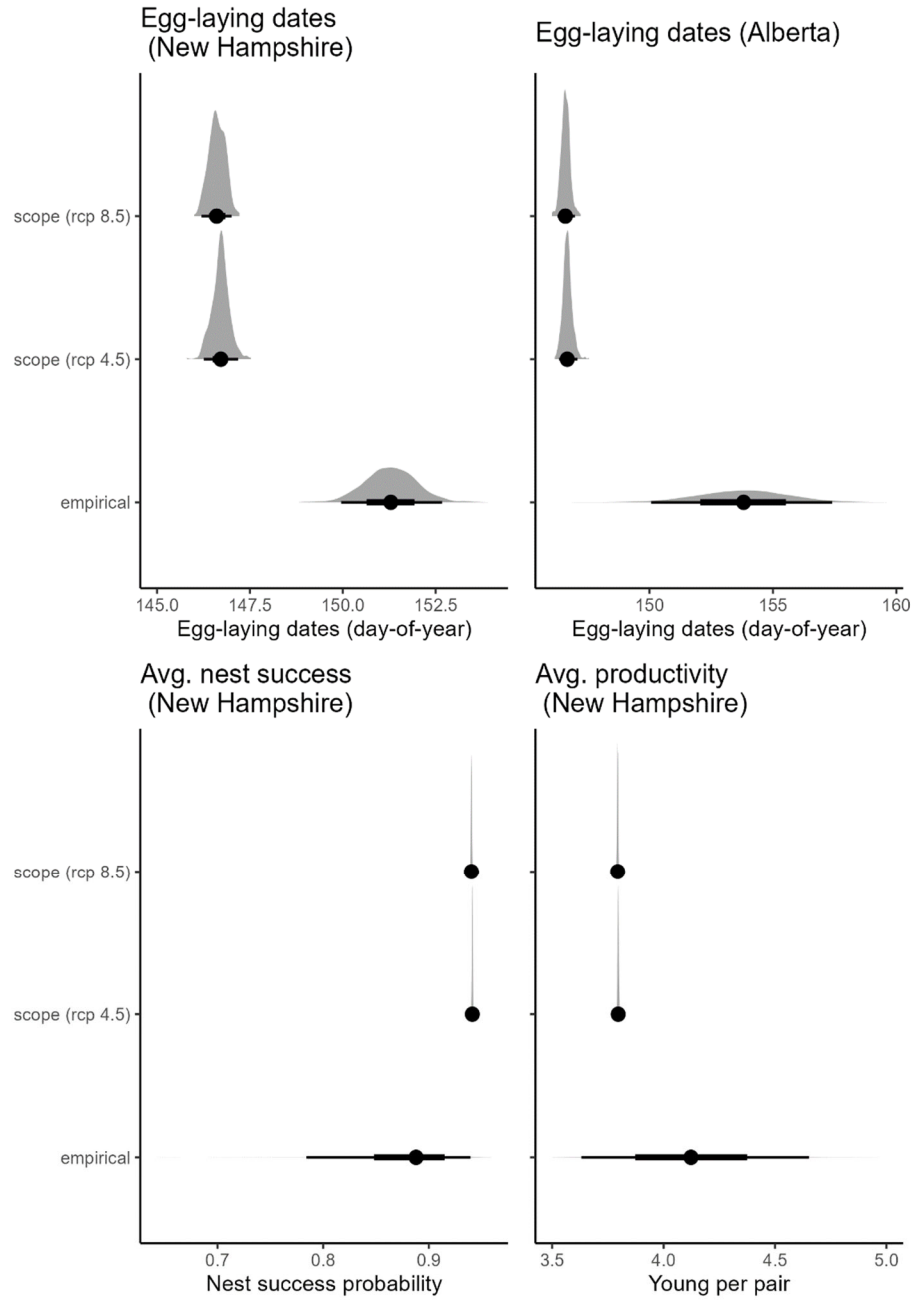

Figure 4A.3 Comparison of analyses of baseline SCOPE simulations (n = 20) and empirical data sets. Points represent mean estimates for each pattern. Thick and thin bars represent 50 and 95% posterior credible intervals, respectively. Polygons above points represent distribution of estimates.

Literature cited

Allstadt, A.J., Vavrus, S.J., Heglund, P.J., Pidgeon, A.M., Thogmartin, W.E. & Radeloff, V.C. (2015). Spring plant phenology and false springs in the conterminous US during the 21st century. *Environmental Research Letters*, *10*, 104008.

Auer, T., Fink, D. & Strimas-Mackey, M. (2020). *Ebirdst: Tools for loading, plotting, mapping and analysis of eBird status and trends data products*.

Ault, T.R., Schwartz, M.D., Zurita-Milla, R., Weltzin, J.F. & Betancourt, J.L. (2015). Trends and natural variability of spring onset in the coterminous United States as evaluated by a new gridded dataset of spring indices. *Journal of Climate*, *28*, 8363–8378.

Bürkner, P.-C. (2017). Brms: An R package for Bayesian multilevel models using Stan. *Journal of Statistical Software*, *80*, 1–28.

Carpenter, B., Gelman, A., Hoffman, M.D., Lee, D., Goodrich, B., Betancourt, M., Brubaker, M., Guo, J., Li, P. & Riddell, A. (2017). Stan: A probabilistic programming language. *Journal of Statistical Software*, *76*, 1–32.

Cox, R., Griesemer, R., Pike, R., Taylor, I., & Thompson, K., (2022). The Go programming language and environment. *Communications of the ACM, 65* (5), (70-78).

eBird. 2021. eBird: An online database of bird distribution and abundance [web application]. eBird, Cornell Lab of Ornithology, Ithaca, New York. Available: http://www.ebird.org. (Accessed: Date [e.g., February 2, 2021]).

Grimm, V., Berger, U., Bastiansen, F., Eliassen, S., Ginot, V., Giske, J., Goss-Custard, J., Grand, T., Heinz, S.K., Huse, G. & others. (2006). A standard protocol for describing individual-based and agent-based models. *Ecological Modelling*, *198*, 115–126.

Grimm, V., Berger, U., DeAngelis, D.L., Polhill, J.G., Giske, J. & Railsback, S.F. (2010). The ODD protocol: A review and first update. *Ecological Modelling*, *221*, 2760–2768.

Hijmans, R.J. (2019). *Geosphere: Spherical trigonometry*.

Hostetler, J.A., Sillett, T.S. & Marra, P.P. (2015). Full-annual-cycle population models for migratory birds. *The Auk*, *132*, 433–449.

Laake, J.L. (2013). *RMark: An R interface for analysis of capture-recapture data with MARK*. Alaska Fish. Sci. Cent., NOAA, Natl. Mar. Fish. Serv., Seattle, WA.

Mearns, L.O., et al., 2017: The NA-CORDEX dataset, version 1.0. NCAR Climate Data Gateway, Boulder CO, https://doi.org/10.5065/D6SJ1JCH

Omernik, J.M. (1987). Ecoregions of the conterminous United States. *Annals of the Association of American Geographers*, *77*, 118–125.

Powers, B. F., Winiarski, J. M., Requena-Mullor, J. M., & Heath, J. A. (2021). Intra-specific variation in migration phenology of American kestrels (*Falco sparverius*) in response to spring temperatures. *Ibis, 163,* 1448–1456.

R Core Team. (2021). *R: A language and environment for statistical computing*. R Foundation for Statistical Computing, Vienna, Austria.

Reitsma, L. R., M. T. Hallworth, M. McMahon, and C. J. Conway (2020). Canada Warbler (Cardellina canadensis), version 2.0. In Birds of the World (P. G. Rodewald and B. K. Keeney, Editors). Cornell Lab of Ornithology, Ithaca, NY, USA. https://doi.org/10.2173/bow.canwar.02

Richardson, A.D., Hufkens, K., Li, X. & Ault, T.R. (2019). Testing Hopkins' bioclimatic law with PhenoCam data. *Applications in Plant Sciences*, *7*, e01228.

Richardson, A.D., Hufkens, K., Milliman, T. & Frolking, S. (2018). Intercomparison of phenological transition dates derived from the PhenoCam dataset V1.0 and MODIS satellite remote sensing. *Scientific Reports*, *8*, 1–12.

Rosemartin, A.H., Denny, E.G., Weltzin, J.F., Lee Marsh, R., Wilson, B.E., Mehdipoor, H., Zurita-Milla, R. & Schwartz, M.D. (2015). Lilac and honeysuckle phenology data 1956–2014. *Scientific Data*, *2*, 150038.

Saltelli, A., Ratto, M., Andres, T., Campolongo, F., Cariboni, J., Gatelli, D., Saisana, M. & Tarantola, S. (2007). *Global Sensitivity Analysis. The Primer*. John Wiley & Sons, Ltd, Chichester, UK.

Schwartz, M.D., Ahas, R. & Aasa, A. (2006). Onset of spring starting earlier across the Northern Hemisphere. *Global Change Biology*, *12*, 343–351.

Schwartz, M.D., Ault, T.R. & Betancourt, J.L. (2013). Spring onset variations and trends in the continental United States: Past and regional assessment using temperature-based indices. *International Journal of Climatology*, *33*, 2917–2922.

Stewart, P.A. (1988). Annual survival rate of Yellow-rumped Warblers. *North American Bird Bander 13*, 106.

Thiele, J.C., Kurth, W. & Grimm, V. (2014). Facilitating Parameter Estimation and Sensitivity Analysis of Agent-Based Models: A Cookbook Using NetLogo and 'R'. *Journal of Artificial Societies and Social Simulation*, *17*, 11.

Thornton, P.E., Running, S.W. & White, M.A. (1997). Generating surfaces of daily meteorological variables over large regions of complex terrain. *Journal of Hydrology*, *190*, 214–251.

van Schmidt, N.D., Kovach, T., Kilpatrick, A.M., Oviedo, J.L., Huntsinger, L., Hruska, T., Miller, N.L. & Beissinger, S.R. (2019). Integrating social and ecological data to model metapopulation dynamics in coupled human and natural systems. *Ecology*, *100*, e02711.

Wilensky, U. (1999). NetLogo. Evanston, IL: Center for Connected Learning and Computer-based Modeling, Northwestern University.

Appendix 5. TRACE document for SCOPE: burrowing owl version

This is a TRACE document ("TRAnsparent and Comprehensive model Evaludation") which provides supporting evidence that our model presented was thoughtfully designed, correctly implemented, thoroughly tested, well understood, and appropriately used for its intended purpose.

The rationale of this document follows:

> Schmolke A., P. Thorbek, D.L. DeAngelis, and V. Grimm. 2010. Ecological modelling supporting environmental decision making: a strategy for the future. Trends in Ecology and Evolution 25:479–486.

and uses the updated standard terminology and document structure in:

> Grimm V., J. Augusiak, A. Focks, B. Frank, F. Gabsi, A.S.A Johnston, K. Kulakowska, C. Liu, B.T. Martin, M. Meli, V. Radchuk, A. Schmolke, P. Thorbek, and S.F. Railsback. 2014. Towards better modelling and decision support: documenting model development, testing, and analysis using TRACE. Ecological Modelling 280:129–139.

and

> Augusiak J., P.J. Van den Brink, and V. Grimm. 2014. Merging validation and evaluation of ecological models to 'evaludation': a review of terminology and a practical approach. Ecological Modelling 280:117–128.

Problem formulation

We built an IBM called SCOPE (Simulation of Carry-over and Phenological Effects) to test hypotheses of the potential mechanisms underlying phenological shifts in migratory landbirds, and to forecast how breeding phenology and other aspects of their life-history will be impacted by a changing climate. The model simulates the full annual cycle of migratory birds and was originally built to represent the biology of American kestrels (*Falco sparverius*). Here we demonstrate the portability of the SCOPE modeling framework by parameterizing the model for burrowing owls (*Athene cunicularia*), a Department of Defense species of concern. SCOPE_burrowing owl can be used to forecast changes in burrowing owl breeding phenology, productivity, survival, and population trajectories from 1980 – 2099 under RCP 4.5 and RCP 8.5 scenarios.

Model description

The model description follows the ODD (Overview, Design concepts, Details) protocol for describing individual-based models (Grimm et al. 2006, 2010). This model was written in NetLogo 6.2.2 (Wilensky 1999).

Purpose

We parameterized this IBM to demonstrate the portability of a full annual cycle model to different species of migratory land birds for forecasting vulnerability to phenological mismatch. Here, we used data from eBirds, the BBL, and published research to parameterize SCOPE for burrowing owls. Model results are a prediction of how breeding phenology, migration distance, and population sizes and distributions may change from 1980 – 2099 under different climate scenarios.

Entities, state variables, and scales

Our model is a full-annual-cycle model (Hostetler et al. 2015) consisting of individual birds, a virtual landscape representing the North American breeding range of burrowing owls, and landscape patches representing geographic locations (i.e., latitude/longitude values), ecoregion designation, carrying capacity, and annual environmental conditions. Birds are characterized by a set of static and dynamic attributes, which are outlined in Table 5A.1.

Table 5A.1 A list of bird attributes, whether each attribute is static or dynamic, and how attributes are assigned in SCOPE, burrowing owl version.

Bird Attributes	Status	Assignment
Sex	static	Randomly assigned
Age	dynamic	Increases each year by 1
Migration strategy (migrant or resident)	dynamic	Depends on latitude and winter minimum temperature anomaly
Migration distance	dynamic	Depends on latitude and winter minimum temperature anomaly
Date of availability	dynamic	Depends on latitude and spring minimum temperature anomaly (migrants) or extended spring index (residents)
Egg-laying date	Dynamic	Depends on the date of availability, and locating a nest site and mate
Nest success and productivity	dynamic	Depends on spring precipitation and maximum temperatures
Survival	dynamic	Drawn from distribution
Breeding dispersal distance and direction	dynamic	Drawn from distribution
Natal dispersal distance and direction	dynamic	Drawn from distribution
Mating status (mate or floater)	dynamic	Depends on whether individual finds an available mate

We employed a time scale in which non-breeding season events and the passage of 1 year (i.e., year *t*) occurs on day 151, and the breeding season occurs during days 1–150 (i.e., breeding season$_{t1–t150}$). Within the model and during output writing, these tick values are adjusted by adding 84 days to calculate real calendar dates. We chose to organize time steps in this way due to constraints of the NetLogo software and to simplify programming, as non-breeding season events such as survival and mortality could occur in a single time step. Although the span of 150 days is a longer breeding season than any one bird would experience, it represents the span of time between pairing of the earliest breeders until migration departure for the latest breeders (Poulin et al. 2020). To match the temporal resolution of the climate and empirical data used in the model, simulations can be run between 1980 – 2099. Additionally, we included the option for

a burn-in period of 10, 15, or 20 years to allow the simulated bird population to reach a stable state.

The version of SCOPE presented here covers the breeding range of burrowing owls in the United States and Canada (Figure 5A.1). The range was composed of 28.5 km^2 patches. Patch size was based on the resolution of Regional Climate Models (RCMs) used to represent climatic conditions in the model. Each patch contains information about patch identity, latitude, longitude, ecoregion, spring (March – June) precipitation, spring (March – June) maximum temperatures, the start of spring represented by the extended spring index (SI-x), spring (March – June) minimum temperature anomaly, winter (November – February) minimum temperature anomaly, and the number of pairs that a patch can support. Patch attributes are derived from raster files imported at initialization or annually, depending on the layer.

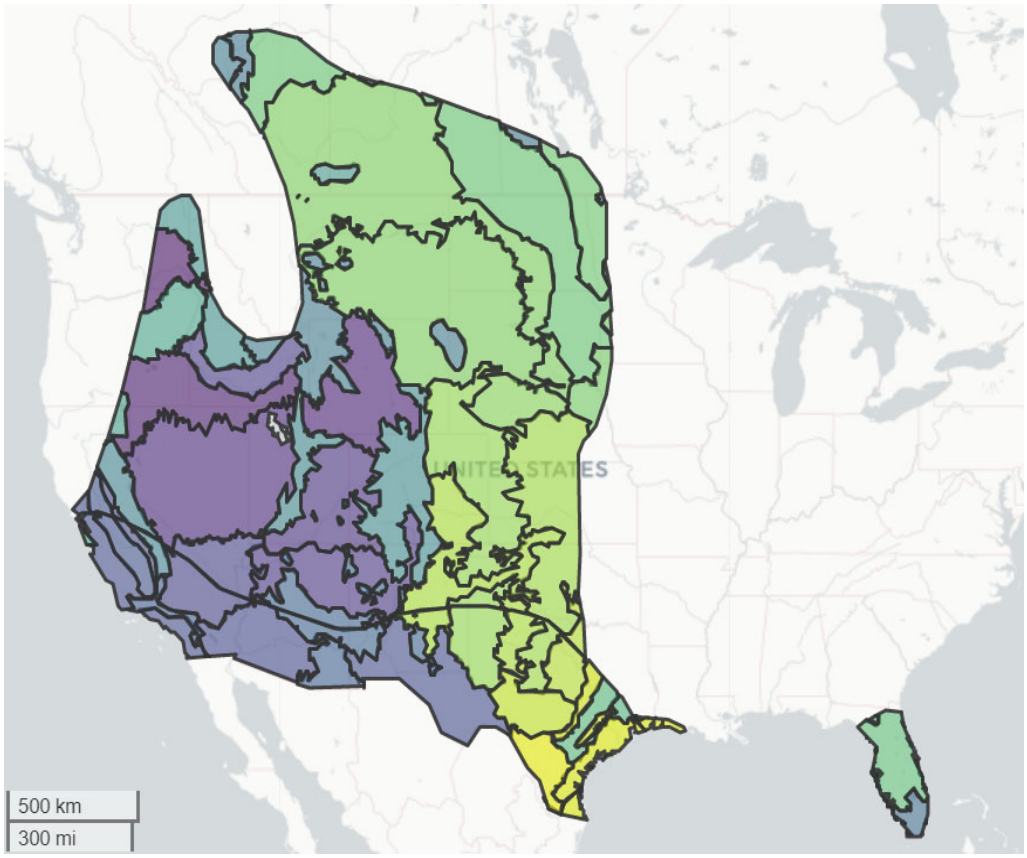

Figure 5A.1 Spatial extent of the North American breeding range of the burrowing owl within SCOPE. Each distinctly colored polygon represents an EPA level III ecoregion.

Process overview and scheduling

Our model approximates the full-annual-cycle of burrowing owls; the exact sequence of model procedures and submodels are as follows. During the breeding season, owls check to see if their date of availability has arrived; this is analogous to reproductive readiness. If so, males move to an unoccupied breeding patch and set their availability to *true*. Females that have reached their date of availability move to a patch with an available male that has not paired with a female and set their availability to *true*. If no unpaired, available males exist on the landscape, the female moves her available date to one day in the future and repeats the pairing process in the

subsequent time-steps. Individuals that are unsuccessful at pairing remain in the population as non-breeding 'floaters.'

At the end of the breeding season (but before migration), paired females determine their probability of nest success based upon spring maximum temperatures and spring precipitation at their location. If the nest is successful, then the number of offspring for that nest is determined. These offspring are randomly assigned as male or female and track the egg-laying date of their mother.

At the beginning of the non-breeding season, the age of each owl is increased by 1, their date of availability and migration distance is reset and the climate and environmental conditions for that year are determined.

The probability of surviving to the following year is determined for each owl. For juveniles and adults, survival probability is drawn from a normal distributions around average survival and standard deviation of survival values (Poulin et al. 2020). Owls then update their migration strategy (whether to migrate or remain as a resident) based upon minimum winter temperature and breeding latitude. For migrants, distance to the wintering grounds is determined in response to the minimum winter temperature anomaly and their breeding latitude. Migrant owls then determine their date of availability based on their latitude and spring temperature anomalies. Resident owls determine their date of availability based on the first-bloom date of their patch. Submodel processes follow the same flow as the American kestrel version (Figure 3A.3).

Design concepts

Basic Principles

Within SCOPE, we simulate full-annual-cycle events of birds, and include a carry-over effect of spring minimum temperature on arrival date in the subsequent spring. In this use of SCOPE, life-history events and scheduling are guided by the biology of burrowing owls, either from previously published research or our own analyses of empirical data sets.

Emergence

Several key patterns emerge from this model. With warming winter temperatures, migration propensity and distances decrease. Resident owls that remain year-round on their breeding grounds track earlier springs, which advances their date of availability. Although owls advance their timing in the spring, phenological mismatch increases over time, resulting in lower nest success and productivity. As populations size increase competition for nest sites and mates increases, driving earlier nesting. However, as population sizes decrease, decreased competition for nest sites and mates leads slows the rate of nesting phenology advancement and mismatch increases

Adaptation

Within the IBM modeling framework, adaptation is the term for individual decisions that maximize fitness. When owls become available, males establish territories and females choose from one of the available males. There are a limited number of pairs on each patch. Competition for mates and patches drives the selection for earlier nesting. Individual owls maximize fitness through establishing nests as early as possible.

Objectives

The objective for birds is to pair with a mate, successfully nest, produce offspring, make migration decisions and survive until the following year.

Learning

No learning occurs within our model.

Prediction

Owls in the model use simple predictive models of that incorporate climatic and environmental conditions of breeding or natal patches to make decisions on whether to migrate and how far, and how far they disperse as juveniles.

Sensing

Owls can sense the climatic conditions of the patch they occupied during the breeding season. Average minimum temperature during the subsequent non-breeding period in years t and $t + 1$ (15 November$_t$ – 15 February$_{t+1}$) informs migration propensity and migration distance. Average maximum temperatures and average monthly total precipitation amounts in spring (March – June) influences nest success. Spring minimum temperature anomalies (February – May) influencing timing of availability to find a mate for migrants and the start of spring (estimated by the extended spring index) influences availability to find a mate for residents. In addition, birds can determine whether a potential breeding patch within their assigned dispersal distance and direction has available mates, or has reached carrying capacity.

Interaction

Adult owls attempt to find mates to pair and reproduce. The density of individuals within potential breeding patches can also indirectly impact the reproductive status of birds, potentially resulting in reduced survival for individuals that are unable to secure a mate and become non-breeders (i.e., 'floaters').

Stochasticity

The majority of submodels in our IBM are parameterized from individual regression models. This approach allowed use to incorporate parameter uncertainty by drawing values from a distribution of parameter values based on the mean value and the standard deviation of the parameter. Also, we included random effects of year and location in some of the submodel regressions.

Collectives

Male and female owls form pairs during the breeding season and produce offspring. Pairing status is reset before the start of the next breeding season. Otherwise, social structure is not included in the model.

Observation

Our model records several phenological and demographic metrics each simulation year. Output metrics are summarized at the patch- and ecoregion-level because of the large spatial extent and number of individuals in the model. These different observation types are described below.

Patch- and ecoregion-level observations

We record 9 different patch- and ecoregion-level outputs in *.csv* format. Most of the metrics are summarized by patch. Each record has a patch identifier, and a column for year. We record summary statistics (mean, min, max, standard deviation, and count) for each metric:

- Environmental output
  - *year*: year of simulation
  - *patch-id*: individual patch identifier
  - *pxcor*: NetLogo patch x coordinate
  - *pycor*: NetLogo patch y coordinate
  - *latitude*: latitude of patch
  - *ecoregion*: EPA level III ecoregion membership
  - *tmin*: winter average minimum temperature anomaly of patch
  - *bloomDate*: earlier extended spring index estimate of patch
- Laydate output
  - *nestProb*: summary statistics of nest success probability
  - *syncBloom*: summary statistics of synchrony with bloom date
  - *dateAvail*: summary statistics of date of availability
  - *laydate*: summary statistics of laydate
- Offspring output
  - *offspring*: summary statistics of offspring produced
- Population size output
  - *populationSize*: number of adults
  - *migPop*: number of migrant adults
  - *resPop*: number of resident adults
- Breeding dispersal output
  - *distance*: summary statistics of breeding dispersal distance
  - *direction*: mean and dispersion of breeding dispersal direction
- Natal dispersal output
  - *distance*: summary statistics of natal dispersal distance
  - *direction*: mean and dispersion of natal dispersal direction
- Strategy output
  - *strategy*: count of resident and migrant individuals
  - *distance*: summary statistics of migration distance
- Adult survival output
  - *age*: summary statistics of age
  - *probSurvAdult*: summary statistics of survival probability
- Juvenile survival output
  - *probSurvJuvenile*: summary statistics of survival probability

Initialization

At the beginning of the model simulation, values for the patches in the landscape and agent parameters are set. The first year the model begins is determined by the user; here we initialized the landscape with climate data starting in 1980. The simulation begins with 100,000

males and 100,000 females (or whatever the user chooses) randomly distributed on breeding habitat patches within the landscape. Each patch consists of a number for the maximum pairs allowed, derived by calculating the maximum number of owl home ranges that can fit within a patch. A number of owl attributes are then determined: each bird is randomly assigned an age between 0 and 6 (where ages less than or equal to 1 are considered juveniles and ages greater than 1 are considered adults); sex is undefined; migration strategy is set to *true*; availability, natal dispersal success, and nesting status are set to *false*; hatch date is set to a random number between 1 and 84; mate identity is set to *nobody*; and dispersal distances and directions, asynchrony, and nest success probability are set to 0. Males move to an unoccupied breed patch first and females move to any breeding patch.

Input data

Input data for our IBM included 14 different environmental and geographic variables in raster format to represent time-varying processes and static attributes. We prepared all raster layers for NetLogo using R (R Core Team 2021). Rasters for SCOPE were clipped to match the North American breeding range of the burrowing owl, projected into an equal area projection, re-sampled to match the resolution of climate or start-of-spring rasters derived from regional climate model (RCM) projections, and written in ESRI ASCII Grid file format for compatibility with the Netlogo GIS extension.

Regional climate model projections

Simulated owls in SCOPE sense the climate and vegetation phenology (i.e., start-of-spring date) conditions in the 'patch' or raster cell that they reside in, and these conditions are used to inform different SCOPE submodels (e.g., timing, movement, and demographic rates). To forecast changes in weather, we used regional climate model (RCM) data from the NA-CORDEX project (Mearns et al. 2017) that was bias-corrected using the Daymet historical gridded dataset (Thornton et al. 1997). This bias-correction provides continuity between the historical climate data used to parameterize bird-weather-vegetation phenology relationships, and future changes in climate. We obtained climate data for two representative concentration pathways (RCPs) that represent scenarios where moderate effort or no action is taken to curb emmissions: RCP4.5 (1 bias-corrected RCM was available) and RCP8.5 (12 RCMs, Table 3A.2). NA-CORDEX projections used in SCOPE were available at a ~25 km^2 resolution for the period 1980–2099, and converted from netcdf format into annual raster layers.

We calculated daily temperature anomaly values for each raster cell by subtracting 30-year average temperatures (1980–2009) from annual temperature values. Next, we averaged the daily temperature anomalies for each season in each year of the climate projections. To represent the mean minimum temperature base for winter anomalies we averaged 15 November–15 February minimum temperatures. To represent the mean minimum temperature base for spring anomalies we averaged 15 February – 15 May. In addition, we averaged monthly total precipitation values for March – June to represent spring precipitation, and averaged monthly maximum temperature values to represent spring temperature maximums. Finally, we created a multi-model ensembles for each climate variable for the RCP8.5 pathway. Only one RCM was available for RCP4.5 (CanESM2.CanRCM4); therefore, we did not produce ensemble climate layers and used the single RCM for this pathway.

Start-of-spring date

We quantified start-of-spring dates in SCOPE using the extended spring indices (Schwartz et al. 2006, 2013). The extended spring indices are mathematical models that predict the start-of-spring (i.e., date of leaf-out or first bloom) based on weather at a particular location. These models were constructed using historical observations of the timing of first leaf and first bloom in a cloned lilac cultivar and two cloned honeysuckle cultivars, which were selected based on the availability of historical observations from across a wide geographic area (Schwartz et al. 2006). Extended spring indices also reflect spring phenological transitions in native species and crops (Rosemartin et al. 2015), and estimates for start-of-spring dates derived from extended spring indices are generally in good agreement with estimates derived from near-surface time-lapse cameras (Richardson et al. 2018, 2019).

Primary inputs to estimate extended spring indices are daily minimum and maximum temperatures beginning January 1 of each year, and daylength derived from latitude (Ault et al. 2015). Spring index models were built with bias-corrected NA-CORDEX RCM data and the Go Programming Language (Cox et al. 2022), and we verified our model output against spring index code and projections developed by Allstadt et al. (2015). Similar to the temperature rasters described above, only one RCM was available for RCP4.5 (CanESM2.CanRCM4) and a multi-model ensemble was used for RCP8.5 In SCOPE, we represented spatially-explicit estimates of start-of-spring in each year (1980–2099) using first bloom date.

eBird density

To ensure realistic population sizes and incorporate density-dependence in the model, we integrated Partners in Flight population estimates and eBird relative abundance maps (eBird 2021) to create a raster layer that determines the maximum number of pairs that a patch is capable of supporting. First, we used the ebirdst package (Auer et al. 2020) to create a spatially-explicit raster of owl relative abundance (estimated number of owls detected by an eBirder during a traveling count at the optimal time of day) across North America. Second, we estimated the number of individual owls that a cell could support by multiplying the relative abundance value by a scaling factor, such that the sum of all raster cells was approximately equal to the mean Partners in Flight population estimate for the North American breeding range. Finally, we divided each raster value by 2 to produce a raster with the total number of pairs allowed per cell.

Ecoregions

We divided flyways into United States Environmental Protection Agency (US EPA) level III ecoregions (Omernik 1987) for summarizing outputs. We rasterized the level III ecoregions shapefile retrieved from the USA EPA website.

Geographic coordinates

We selected a random climate raster to calculate the latitudinal and longitudinal center of each raster cell, and created a separate raster file for the centroid latitude and longitude values.

Submodels

The model can organized under two distinct annual cycle periods, the “breeding” season and the “non-breeding” season. The following submodels represent all processes in the model. Actual names of submodel procedures used in the IBM code are included in parentheses. For regression-based submodels, we used Bayesian inference to fit models (unless otherwise noted)

via the R package brms (Bürkner 2017), which provides a user-friendly interface for the STAN probabilistic programming language (Carpenter et al. 2017). All procedures occur for individuals in random order each time they are invoked, except for the *updateAvailable* submodel. Additional procedures underlying main submodels called in the *go* procedure are italicized in each submodel description.

Update date of availability (*updateAvailable*)

Prior to becoming available to pair (at this stage they are 'unavailable'), bird *color* is set to *black* (male) or *white* (female). Once birds are available to pair, they begin the process of dispersing and finding a mate. During this submodel, date of availability in the spring for each individual is updated on a daily basis, depending on whether an individual is available and if it is successfully paired.

maleBreed and *femaleBreed*.–Males are the first to occupy breeding patches, which may be the site that they occupied in the previous year, or a site they are dispersing to for the first time. Males determine whether the carrying capacity of a patch has been met; if not they occupy that patch and decrease the number of pairs that may occupy it. If the patch is occupied, they continue searching for breeding patches for a pre-determined number of tries (controlled by a slider on the NetLogo interface). If this number of breeding attempts is reached prior to locating a breeding patch, the male dies. Date of availability increases by a day if individuals are not successful in pairing. Once males pair, their *color* is changed to *sky*. Females use a similar process to locate an available male, and increase their date of availability if they are unsuccessful at finding a mate on a particular day. Once females pair, their *color* is changed to *brown*.

checkNeighboringPatches.–In this procedure, females also have the opportunity to check neighboring patches during their last attempt to find a mate.

These procedures repeat every day until an individual pairs, dies, or becomes a non-breeding individual or floater (i.e., they reach the maximum number of attempts to breed - 8). Floaters have their *color* set to *orange* (female) or *cyan* (male).

Natal dispersal and direction (*natalDispersal*)

Juvenile birds attempt to find a breeding patch in the year following birth. We parameterized natal dispersal distance using banding data. Natal dispersal distances (in km) were extracted from the United States Geological Survey's Bird Banding Laboratory (BBL) band encounters data set (1980–2019). Small samples sizes limited testing of covariates associated with natal dispersal. Therefore, we created an intercept model with a Gamma-distributed random variable.

$$\textit{Natal dispersal distance (km): } \log(\mu) = \alpha$$

We used the same BBL data set to calculate mu and rho parameters in R and determine natal dispersal direction. Direction (in degrees) was drawn from a wrapped cauchy distribution. Natal dispersers are permitted to make five attempts to locate an available breeding patch (i.e., a patch that has not reached maximum capacity and is within their drawn dispersal distance and direction). If the number of permitted natal dispersal attempts is exceeded, individuals die.

Breeding dispersal and direction (*breedingDispersal*)

Adult birds can disperse from a breeding patch in subsequent seasons. Birds can remain on the same patch if it is available and they draw a short dispersal distance; otherwise, individuals locate a new, available breeding patch. We parameterized breeding dispersal based on band encounters from the BBL (1980–2019). We retained banding records for individuals banded during the breeding season in year t ($April_t$–$August_t$) and encountered in the subsequent breeding season in year $t + 1$ ($April_{t+1}$–$August_{t+1}$). Distances between breeding locations were calculated from pairs of latitude/longitude coordinates using the geosphere package (Hijmans 2019). Breeding dispersal distance (in km) was modeled as a Gamma-distributed random variable.

$$\textit{Breeding dispersal distance (km): } log(\mu) = \alpha$$

We used the same BBL data set to calculate mu and rho parameters in R to determine breeding dispersal direction. Breeding dispersal direction was random (i.e., there was no bias toward a particular compass bearing). Direction (in degrees) was drawn from a wrapped cauchy distribution.

Reproduction (*reproduce*)

Females that have found a mate initiate nesting and producing offspring. Burrowing owl nest success varies with weather (Cruz-McDonnell and Wolf 2016). We used parameter estimates from Cruz-McDonnell and Wolf (2016) to represent nest success. Nest success was modeled as a Bernoulli-distributed random variable, and as a function of monthly mean maximum temperatures (SpTmax) and total monthly precipitation (SpPrec).

$$\textit{P(nest success): } logit(\mu) = \alpha + \beta_1 * SpTmax + \beta_2 * SpPrec$$

To draw their probability of nesting success, females sense the SpTmax and SpPrec at their patch in that year. Using this information, females draw a nest success probability. Next, a uniform random number between 0 and 1 is drawn and compared to the nest success probability. If the random value is less than the calculated probability, the nest survives and both the female and associated male set their success value to *true* (otherwise they set success as *false*).

For successful females, the number of offspring produced is drawn by rounding to the nearest integer a value from a normal distribution with a mean of 5 and standard deviation of 1.65. If the calculated value is negative, it is set to 0; if the value is greater than 8 it is set to eight to prevent unrealistically productive nests. Offspring are randomly assigned as male or female and given an age of 0.

Bird attribute, year, and patch updates (*reset*)

After reproduction, the next year begins and several updates occur. Year is incremented by one, and the day of year and the number of offspring in the population are set to 0. In addition, each bird resets several dynamic attributes: availability, migration distance is set to 0, age is incremented by 1 year, mate is set to *nobody*, and individuals reset their color to *black* (males) or *white* (females). The number of pairs occupying each patch are also set to 0.

Survival (*survival* and *mortality*)

Owls survive or die based upon an annual survival probability. We used values from the burrowing owl Birds of the World account to parameterize the model (Poulin et al. 2020).

$$P(survivalAdult): logit(\mu) = \alpha$$
$$P(survivalJuvenile): logit(\mu) = \alpha$$

To kill individuals, we use a Bernoulli trial with the probability of success equal to the survival probability value generated in either *survivalJuvenile* or *survivalAdult* in a separate *mortality* procedure for juveniles and adults. Floater survival probability (adults only) is also halved. The separate *mortality* procedures allow us to record survival probabilities prior to removing dead individuals from the population. The survival probability value is then compared to a uniform random number between 0 and 1; if the random number is greater than the probability of survival, then the individual dies.

Update environmental rasters (*drawNextClimateMaps*)

Environmental layers that comprise the virtual world in NetLogo are updated on an annual basis by importing rasters in *.asc* format. This procedure uses the appropriate calendar year to pull in corresponding winter mean minimum temperature, extended spring index estimate, spring mean minimum temperature, SpTmax, SpPrec. Thus, owls can sense environmental conditions that are key to determining different components of an owl's life-history.

Migration strategy (*updateStrategy*)

Birds decide whether to remain on the breeding/natal grounds as a resident, or migrate to the non-breeding grounds. We used BBL band records (1980–2019) to calculate migration distances of individuals that were banded in year *t* during the breeding (April–August) or non-breeding season (November–February), and encountered in the subsequent year on the non-breeding or breeding grounds, respectively. We calculated migration distances with coordinates from banding and encounter locations using the geosphere package in R. We assigned migration strategy based upon distances between breeding/natal sites and subsequent non-breeding sites, where individuals that traveled ≤ 100 km were considered residents. We modeled the decision to migrate or not dependent upon an individual's breeding latitude and the upcoming winter mean minimum temperature anomaly at the breeding/natal patch.

$$logit(\mu) = \alpha + \beta_1 * latitude + \beta_2 * winter\ T_{min}$$

Then, a random uniform number between 0 and 1 is generated. If that value is less than the probability of not migrating (1–probability of migrating), an individual sets its migration strategy to *false* (i.e., resident strategy). Once individuals adopt a resident strategy, they do not migrate in subsequent years.

Migration distance (*migrate*)

Migrant birds draw a distance (in km) to migrate to the non-breeding grounds. We parameterized migration distance using band encounters from the BBL (1980–2019). Data processing was the same as described in updateStrategy. We modeled migration distance

(distances ≥ 100 km) as a function of fixed effects of breeding/natal latitude and and winter mean minimum temperature anomaly, and a random year effect in a Gamma mixed effects model.

$$log(\mu) = \alpha + \beta_1 * latitude + \beta_2 * winter\ T_{min}$$

To prevent drawing unrealistically high migration distances, we set any distances over ≥ 4500 km equal to 4500 (a plausible distance based on BBL records). Migratory birds then move to the 'non-breeding grounds' (i.e., NetLogo patch coordinate 0,0). This arbitrary location was selected to simplify programming and is not influential to other processes. This submodel does not apply to resident birds.

Date of availability (*drawDateAvailable*)

This process determines what day of the year (i.e., date of availability) individual birds will become available for pairing for the upcoming breeding season. The date of availability is dependent on whether an individual is a migrant or a resident.

Migrant date of availability.–For migrants, we used a modified approach from Powers et al. (2021) to model spatially-explicit arrival dates derived from eBird checklists in relation to relation to latitude and spring climate conditions (i.e., minimum temperature anomalies). Date of availability was modeled as Gamma-distributed random variable with a fixed effect of latitude and spring minimum temperature anomaly and a random effect of year. Once birds arrive they are delayed by a constant (35 d) to represent the biological process of obtaining resources to produce eggs and to match patterns from empirical data.

$$Date\ of\ availability\_migrants:\ log(\mu) = \alpha_{[year]} + \beta_1 * latitude + \beta_2 * spring\_T_{min}\_anomaly$$

Resident date of availability.– Unfortunately, limited information constrained our ability to estimate the factors that govern timing of nesting of resident owls. We used an equation similar to resident kestrels, where resident date of availability was driven by the first bloom date, with variation in year accounted for by a random intercept in a Gamma mixed effects model. Residents draw a date of availability from this equation and the first bloom date of the patch they occupy for the breeding season.

$$Date\ of\ availability\_residents:\ log(\mu) = \alpha + \beta_1 * SI\text{-}x$$

Output writing (*write-to-file-"*)

We record a number of outputs (in the form of *.csv* files) for each simulation; see the Observation section for more details.

Data evaluation

We parameterized our model using multiple sources of data that are outlined above. Here, we focus on the limitations and the quality of our input data sets.

Survival

We could not obtain a mark and recapture dataset that was sufficient to estimate survival with environmental or life-history parameters. Therefore, we used published estimates of averages. This constrains our ability to study the effects of mismatch on an important component of individual fitness and population demographics.

Migration distance and strategy

Parameterizing the migration distance and migration strategy submodels relied on BBS data. We lacked BBS records at higher latitudes, possibly as a result of lower research efforts in these locations and lower encounter rates for long-distance migrants (i.e., birds wintering south of the US border are less likely to be found or reported compared to birds wintering in the US). Further, resident birds that remain on the study site are more likely to be recaptured. This may skew our estimate of migration strategy.

Migrant and resident date of availability

Our data sets to parameterize date of availability for migrants included records contributed by community scientists. It is possible that these records may have been more prone to errors or data entry mistakes compared with those from professional scientists. Data for environmental factors that cue timing of reproduction for resident owls were lacking. Use of an equation from an ecologically similar species may be incorrect.

Reproduction

Raw reproduction data were difficult to obtain. We used parameter estimates from published papers. It is difficult to assess alternative hypotheses about the effects of phenological mismatch without access to raw data.

Population size and density

For computational and biological reasons, we set population size and density (owls pairs per patch) in the model. We used an estimate of population size from the Partners in Flight database to control the largest number of owls allowed in the model, which had a high degree of uncertainty. We then used this number–along with eBird status and trend estimates of burrowing owls counted for ideal checklist conditions–to calculate the carrying capacity of each patch in SCOPE. Therefore, errors in the population size estimate or eBird counts could have contributed to the number of owls in each ecoregion and output summaries.

Conceptual model evaluation

Details regarding model design and conceptual framework are presented in the model description and data evaluation sections. While the assumptions of the empirical research underlying this model are not addressed here, the general framework for this model is discussed below.

This model is built from the basic framework that nesting phenology in bird populations is the product of external factors (e.g., climate) and life-history. The framework for this model is the simple assumption that the timing of nesting is conditional on acquisition of a breeding site (the timing of which is inversely proportional to spring minimum temperature anomalies or positively associated with start-of-spring date) and the energetic requirements necessary for egg production. This model does not explicitly model individual energetics. However, there is empirical evidence, from this system and elsewhere that shows correlative relationships between

winter conditions and timing of nesting, and migration distance and date of arrival. Also, we did not identify an effect of phenology on nesting success or survival, which may indicate the burrowing owls are less sensitive to phenological shifts and more sensitive to maximum temperatures and precipitation that are likely to be affected by climate change.

Implementation verification

We conducted smaller-scale simulations (i.e., by examining patterns in a single ecoregion) that were more tractable to verify our code. We did extensive checking of model outputs during simulations (by *print* statements of variables in NetLogo) and after simulations were completed via plotting in R.

Tests of model execution varied in their complexity and focus but all were executed to ensure that the entire model was implemented properly. Throughout code development, the syntax was verified via the syntax checker in NetLogo to ensure that each line of code followed proper structuring. Visual testing was used extensively throughout model development to ensure proper functioning. For instance, parameters were simplified to isolate only pairing of birds. Because of the color coding of both habitat and individual sexes, the improper association of birds (e.g., >2 per pair, incorrect sex distribution, etc.) could be readily tested through visual inspection. The use of both immediate and summary output was employed throughout nearly every submodel. Most commonly, tracking of internal variables and processes were done by simply writing out the values of variables (via show commands in NetLogo). In addition, summary output at the conclusion of simulations was also used to ensure that derived variables (e.g., slope of regression lines) were properly determined. Similarly, extensive spot checking of agents and habitat patches was conducted. This allowed for the examination of variables midstream and enabled us to compare the changes in particular variables to those calculated manually to ensure that they aligned properly.

Model output verification

The implementation of this model involved calibrating parameters within the migrant arrival dates (*drawDateAvailable* submodel). Pattern-matching of model outputs to empirical observations is evaluated in the model output corroboration section.

Model analysis

We examined the sensitivity of the model to changes in a number of the model parameters. We examined the effect of systematic variation of each parameter on several key model outputs. Emergence of model output is explored more thoroughly in the model output corroboration section and the main manuscript.

The vast majority of parameters to represent submodels in SCOPE came from regression-based analyses. Because our model included a large number of parameters and was computationally intensive, we chose to conduct a local sensitivity analysis, primarily on submodel intercepts and coefficients related to important climate or environmental predictors. With local sensitivity analysis, small variations of input values (e.g., within a specified percentage around a mean value) are performed for one-factor-at-a-time (Saltelli et al. 2007). While this method provides less detailed information than global sensitivity analysis, it is still a widely-used sensitivity approach (Thiele et al. 2014) and was the most practical option given our model's large parameter set and computational demands.

For each focal parameter (n = 25), we conducted 20 simulations where all other parameters were held constant but the parameter of interest was varied by ± 10%. Simulations were run for 60 years with a burn-in period of 10 years. Including the baseline experiment (i.e., all parameters held at their mean value). We examined the effect of parameter perturbations on average egg laying date, nest success, adult and juvenile survival, and population size values. To do so, we calculated the mean percent change from the baseline simulation and the perturbation simulations for each parameter and output metric.

The local sensitivity analysis identified several parameters that had a large effect on output metrics (Figure 5A.2). In general, the SCOPE burrowing owl model was strongly influenced by survival estimates. As expected the parameters for adult and juvenile survival affected individual survival estimate, and also population size. Timing of breeding was most sensitive to resident date of availability (*resInt*), and to a lesser extent, survival parameters and nest success parameters, both of which might lead to density dependent effects on lay data because of competition for nest sites and mates. Several nest success regression parameters influenced average nest success probability and so did survival parameters. Finally, population size was relatively more sensitive to nest success and survival parameters, compared to other parameters.

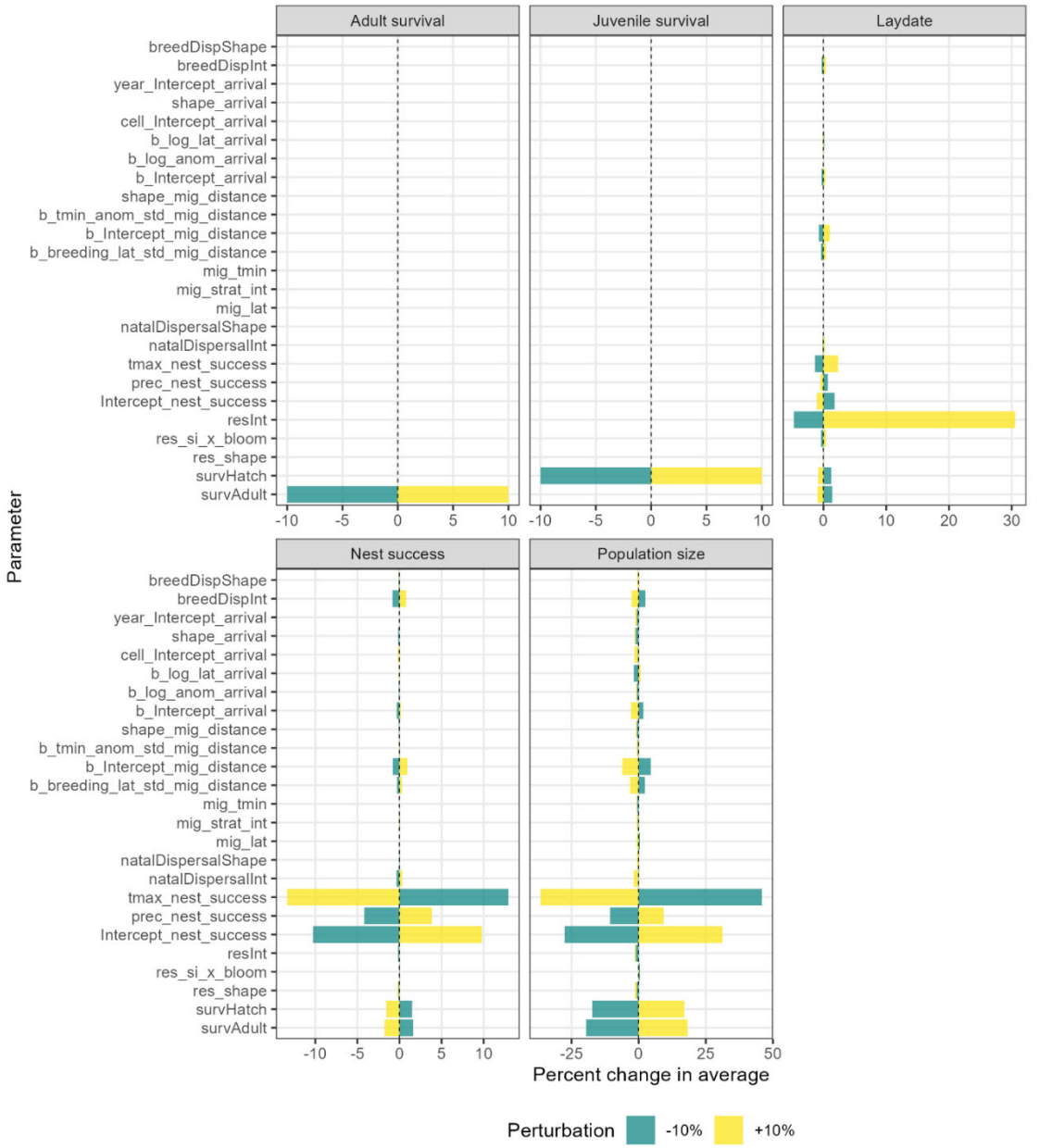

Figure 5A.2 Sensitivity analysis of average laydate, nesting success, adult and juvenile survival, and population size for SCOPE input parameters. Bars indicate percent change in output metric average with -10% (green) and +10% (yellow) adjustments for each model parameter.

Model output corroboration

A number of patterns have been used to evaluate the ability of the model to realistically represent breeding phenology, migration distance, nest success, productivity, population trends, and latitudinal shift in abundance from empirical data sets.

Output metrics

Here, we provide 1) the temporal resolution and spatial extent of model output and empirical data sets, and 2) how we compared patterns for each output metric. Baseline simulations for both

RCP4.5 and RCP8.5 were compared to empirical findings. All pattern matching analyses were conducted using the brms package (Bürkner 2017) in R (R Core Team 2021). To obtain average output metrics, we used intercept-only models with a random effect for simulation number. To estimate yearly trends in outputs, we used year (centered) as a fixed effect, with a random intercept for simulation number. Empirical data sets were modeled without random effects unless otherwise noted.

Egg-laying date

We compared average egg laying dates at 3 study sites in different locations of the burrowing owl model: Idaho, New Mexico, and Florida with output from the model over the same time periods for the same ecoregions where the data were collected. Empirical and model egg-laying dates were analyzed using linear (mixed) models.

Migration distance

We compared the trend in migration distance over time of burrowing owls apparent in the BBL data and in the model during the same years (1980–2019) with migration distance output from the model over the same time period and spatial extent. Empirical and model migration distances were analyzed using linear (mixed) models.

Nest success and productivity

We compared average nest success rate and productivity in nest success over time of burrowing owls breeding in southwestern Idaho from 2003–2016 with nest success output from the model over the same time period and across the Snake River Plain ecoregion. For the empirical data, we first modeled nest success as a Bernoulli-distributed random variable (0 = failure, 1 = success) with a random intercept of year. Next, we used the random intercept values to calculate the average nest success probability for each year which was matched model nest success probabilities. Because our responses were probability values, we used generalized linear models with a beta distribution and logit link function.

We compared average productivity (young per pair) and trend in productivity over time of owls breeding in southwestern Idaho from 2003–2016 with productivity output from the model over the same time period and from owls across the Snake River Plain ecoregion. Empirical and model productivity rates were analyzed using linear (mixed) models.

Pattern-matching results

We evaluated how well patterns were matched between model outputs and empirical data by visually comparing the intercept and/or beta estimates of the regression analyses described above. Specifically, we wanted to test whether model output metrics fell within 95% CIs of the same set of empirical intercept and beta estimates (van Schmidt et al. 2019).

We found that model outputs mostly fell within reasonable ranges of the empirical data sets (Figure 5A.3). In general, average egg laying dates fell outside of the empirical estimate by 2–5 days, with the largest difference in Florida. The slopes for migration distance was well

matched to empirical estimates. Patterns of average nest success and productivity were closely matched to the empirical data.

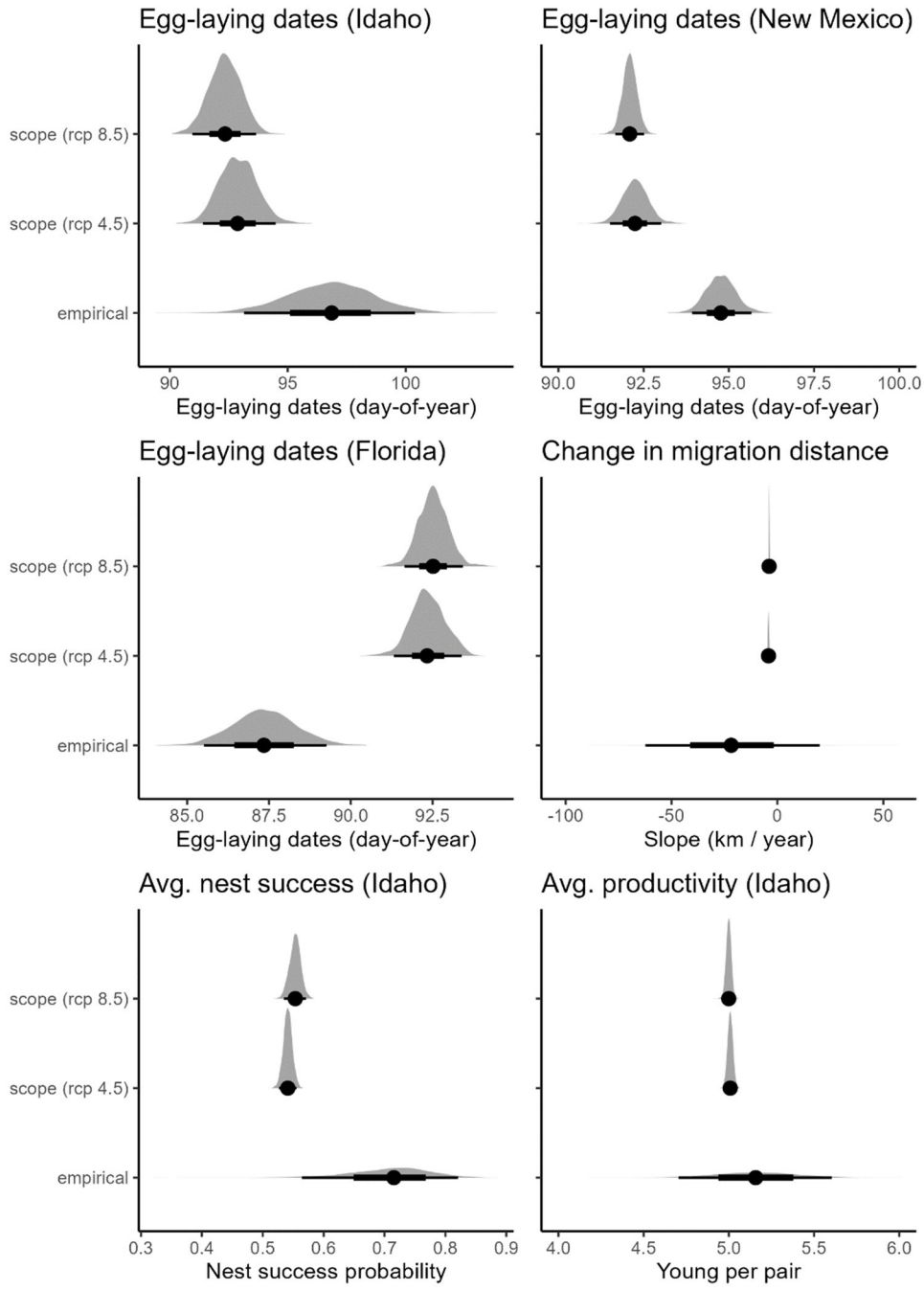

Figure 5A.3 Comparison of analyses of baseline SCOPE simulations (n = 20) and empirical data sets. Points represent mean estimates for each pattern. Thick and thin bars represent 50 and 95% posterior credible intervals, respectively. Polygons above points represent distribution of estimates.

Literature cited

Allstadt, A.J., Vavrus, S.J., Heglund, P.J., Pidgeon, A.M., Thogmartin, W.E. & Radeloff, V.C. (2015). Spring plant phenology and false springs in the conterminous US during the 21st century. *Environmental Research Letters*, *10*, 104008.

Auer, T., Fink, D. & Strimas-Mackey, M. (2020). *Ebirdst: Tools for loading, plotting, mapping and analysis of eBird status and trends data products*.

Ault, T.R., Schwartz, M.D., Zurita-Milla, R., Weltzin, J.F. & Betancourt, J.L. (2015). Trends and natural variability of spring onset in the coterminous United States as evaluated by a new gridded dataset of spring indices. *Journal of Climate*, *28*, 8363–8378.

Bürkner, P.-C. (2017). Brms: An R package for Bayesian multilevel models using Stan. *Journal of Statistical Software*, *80*, 1–28.

Carpenter, B., Gelman, A., Hoffman, M.D., Lee, D., Goodrich, B., Betancourt, M., Brubaker, M., Guo, J., Li, P. & Riddell, A. (2017). Stan: A probabilistic programming language. *Journal of Statistical Software*, *76*, 1–32.

Cox R, Griesemer R, Pike R, Taylor I and Thompson K (2022) , The Go programming language and environment, Communications of the ACM, *65*:5, (70-78)

eBird. 2021. eBird: An online database of bird distribution and abundance [web application]. eBird, Cornell Lab of Ornithology, Ithaca, New York. Available: http://www.ebird.org. (Accessed: Date [e.g., February 2, 2021]).

Grimm, V., Berger, U., Bastiansen, F., Eliassen, S., Ginot, V., Giske, J., Goss-Custard, J., Grand, T., Heinz, S.K., Huse, G. & others. (2006). A standard protocol for describing individual-based and agent-based models. *Ecological Modelling*, *198*, 115–126.

Grimm, V., Berger, U., DeAngelis, D.L., Polhill, J.G., Giske, J. & Railsback, S.F. (2010). The ODD protocol: A review and first update. *Ecological Modelling*, *221*, 2760–2768.

Hijmans, R.J. (2019). *Geosphere: Spherical trigonometry*.

Hostetler, J.A., Sillett, T.S. & Marra, P.P. (2015). Full-annual-cycle population models for migratory birds. *The Auk*, *132*, 433–449.

Mearns, L.O., et al., 2017: The NA-CORDEX dataset, version 1.0. NCAR Climate Data Gateway, Boulder CO, https://doi.org/10.5065/D6SJ1JCH

Omernik, J.M. (1987). Ecoregions of the conterminous United States. *Annals of the Association of American Geographers*, *77*, 118–125.

Poulin, R. G., L. D. Todd, E. A. Haug, B. A. Millsap, and M. S. Martell (2020). Burrowing Owl (Athene cunicularia), version 1.0. In Birds of the World (A. F. Poole, Editor). Cornell Lab of Ornithology, Ithaca, NY, USA. https://doi.org/10.2173/bow.burowl.01

Powers, B. F., Winiarski, J. M., Requena-Mullor, J. M., & Heath, J. A. (2021). Intra-specific variation in migration phenology of American kestrels (*Falco sparverius*) in response to spring temperatures. *Ibis, 163,* 1448–1456.

R Core Team. (2021). *R: A language and environment for statistical computing*. R Foundation for Statistical Computing, Vienna, Austria.

Richardson, A.D., Hufkens, K., Li, X. & Ault, T.R. (2019). Testing Hopkins' bioclimatic law with PhenoCam data. *Applications in Plant Sciences*, *7*, e01228.

Richardson, A.D., Hufkens, K., Milliman, T. & Frolking, S. (2018). Intercomparison of phenological transition dates derived from the PhenoCam dataset V1.0 and MODIS satellite remote sensing. *Scientific Reports*, *8*, 1–12.

Rosemartin, A.H., Denny, E.G., Weltzin, J.F., Lee Marsh, R., Wilson, B.E., Mehdipoor, H., Zurita-Milla, R. & Schwartz, M.D. (2015). Lilac and honeysuckle phenology data 1956–2014. *Scientific Data*, *2*, 150038.

Saltelli, A., Ratto, M., Andres, T., Campolongo, F., Cariboni, J., Gatelli, D., Saisana, M. & Tarantola, S. (2007). *Global Sensitivity Analysis. The Primer*. John Wiley & Sons, Ltd, Chichester, UK.

Schwartz, M.D., Ahas, R. & Aasa, A. (2006). Onset of spring starting earlier across the Northern Hemisphere. *Global Change Biology*, *12*, 343–351.

Schwartz, M.D., Ault, T.R. & Betancourt, J.L. (2013). Spring onset variations and trends in the continental United States: Past and regional assessment using temperature-based indices. *International Journal of Climatology*, *33*, 2917–2922.

Thiele, J.C., Kurth, W. & Grimm, V. (2014). Facilitating Parameter Estimation and Sensitivity Analysis of Agent-Based Models: A Cookbook Using NetLogo and 'R'. *Journal of Artificial Societies and Social Simulation*, *17*, 11.

Thornton, P.E., Running, S.W. & White, M.A. (1997). Generating surfaces of daily meteorological variables over large regions of complex terrain. *Journal of Hydrology*, *190*, 214–251.

van Schmidt, N.D., Kovach, T., Kilpatrick, A.M., Oviedo, J.L., Huntsinger, L., Hruska, T., Miller, N.L. & Beissinger, S.R. (2019). Integrating social and ecological data to model metapopulation dynamics in coupled human and natural systems. *Ecology*, *100*, e02711.

Wilensky, U. (1999). NetLogo. Evanston, IL: Center for Connected Learning and Computer-based Modeling, Northwestern University.

Appendix 6. List of Scientific/Technical Publications

Ranck, S. C., C. Garsvo, L. Reynard, M. Kohn, D. Schwartz, J. A. Heath (*submitted*) Sex, body size, and winter weather explain migration strategies in a partial migrant population of American Kestrels (*Falco sparverius*). *Ornithology*.

Hunt, A. R., J. L. Watson, J. M. Winiarski, R. P. Porter, J. A. Heath (*submitted*) Insights and challenges in tracking the migration of North America's smallest falcon, the American Kestrel (*Falco sparverius*). *Journal of Raptor Research*.

Bossu, C. M., J. A. Heath, B. Helm, G. M. Kaltenecker, K. C. Ruegg (2022) Clock-linked genes underlie seasonal migratory timing in a diurnal raptor. *Proceedings of the Royal Society B* 289: 20212507.

Callery, K. R., S. E. Schulwitz, A. R. Hunt, J. M. Winiarski, C. J. W. McClure, R. A. Fischer, J. A. Heath (2022) Phenology effects on productivity and hatching-asynchrony of American kestrels (*Falco sparverius*) across a continent. *Global Ecology and Conservation* 36: e02124

Callery, K. R., J. A. Smallwood, A. R. Hunt, E. R. Synder, J. A. Heath (2022) Seasonal trends in adult survival and reproductive trade-offs reveal potential constraints to earlier nesting a migratory bird. *Oecologia* 199:91–102.

Galla, S. J., L. B. Brown, Y. Couch-Lewis, I. Cubrinovska, D. Eason, R. Gooley, J. A. Hamilton, J. A. Heath, S. Hauser, E. Latch, M. Matocq, A. Richardson, J. Wold, C. Hogg, A. Santure, T. E. Steeves (2022) The relevance of pedigrees in the conservation genomics era. *Molecular Ecology* 31: 41– 54.

Galla, S. J., B. P. Pauli, J. Winiarski, B. F. Powers, K. Steenhof, J. A. Heath (2022) Invited Presentation. Creating a genetically explicit individual-based model to understand climate-driven egg laying date shifts in American Kestrels (*Falco sparverius*). NSF EPSCoR GUTT-C Modeling Workshop, Online.

Ranck, S.C. (2022) Sex, body size, and winter weather explain migration strategies in a partial migrant population of American Kestrels (*Falco sparverius*). Paper presentation to the Department of Biological Sciences, Boise State University.

Powers, B.P., J.M. Winiarski, J. Requena-Mullor, J.A. Heath (2021) Intra-specific variation in migration phenology of American Kestrels (*Falco sparverius*) in response to spring temperatures. *Ibis* 163:1448-1456.

McClure, C. J., J. L. Brown, S. E. Schulwitz, J. Smallwood, K. E. Farley, J.-F. Therrien, K. E. Miller, K. Steenhof, J. A. Heath (2021) Demography of a widespread raptor across disparate regions. *Ibis* 163:658-670.

Ruegg, K. C., M. S. Brinkmeyer, C. M. Bossu, R. Bay, E. C. Anderson, C. W. Boal, R. D. Dawson, A. Eschenbauch, C. J. W. McClure, K. E. Miller, L. Morrow, J. Morrow, M. D. Oleyar, B. Ralph, S. Schulwitz, T. Swem, J.-F. Therrien, R. van Buskirk, T. B. Smith, J. A. Heath (2021) The American kestrel genoscape (*Falco sparverius*): Implications for monitoring, management, and subspecies boundaries. *Ornithology* 138:1-14.

Heath, J.A. et al. (2021). Invited webinar. The American Kestrel. Bird Calls: US Fish and Wildlife Service.

Vazquez, S. B, S. C. Ranck, A. R. Hunt, J. A. Heath (2021) The influence of nesting habitat and migration strategy on the reproductive pace of American Kestrels (*Falco sparverius*). Poster presentation to the Raptor Research Foundation, Annual Meeting, Online.

Hunt, A. R., J. L. Watson, J. M. Winiarski, R. P. Porter, J. A. Heath (2021) Invited Symposium Presentation. Insights and challenges in tracking the migration of North America's smallest falcon, the American Kestrel (*Falco sparverius*). Raptor Research Foundation, Annual Meeting, Online.

Ranck, S. C., D. M. Schwartz, L. Reynard, M. J. Kohn, J. A. Heath (2021) Invited Symposium Presentation. Drivers and patterns of individual migration strategies in a partially migratory population of American Kestrels (*Falco sparverius*). Raptor Research Foundation, Annual Meeting, Online.

Galla, S. J., B. P. Pauli, J. Winiarski, B. F. Powers, K. Steenhof, J. A. Heath (2021) Invited Symposium Presentation. Creating a genetically explicit individual-based model to understand climate-driven egg laying date shifts in American Kestrels (*Falco sparverius*). Raptor Research Foundation, Annual Meeting, Online.

McCaslin, H.A., T. T. Caughlin, J. A. Heath (2020) Long-distance natal dispersal is relatively frequent and correlated with environmental factors in a widespread raptor. *Journal of Animal Ecology* 89:2077-2088

McCaslin, H. M., J. A. Heath (2020) Patterns and mechanisms of heterogeneous breeding distribution shifts of North American migratory birds. *Journal of Avian Biology* 51: doi:10.1111/jav.02237

Heath, J. A., S. J. Galla (2020) Invited Presentation: Creating a genetically explicit individual-based model to study migratory bird responses to climate driven phenology shifts. Idaho EPSCoR GEM3 Annual Meeting. Online.

Heath, J. A., C. M. Bossu, S. E. Simmonds, K. C. Ruegg (2020) Invited Symposium Paper: Standing genetic variation in CLOCK genes underlies phenological patterns of American kestrels. North American Ornithological Conference. Online.

Powers, B. F., J. M. Winiarski, J. Requena-Mullor, J. A. Heath (2020) Drivers of migration phenology in American kestrels (*Falco sparverius*) revealed with citizen science observations. Presentation for the Ecological Society of America annual conference.

Callery, K. C. (2020) Phenological mismatch is correlated with fitness outcomes and adaptive behavior in a generalist avian predator distributed across North America. Presentation for Master's thesis defense. Boise, Idaho.

Winiarski, J. M. (2020) It's about time: Using full cycle phenology to assess climate change vulnerability in North American birds. Presentation for Saint Mary's University of Minnesota Biology Department Seminar Series.

Ranck, S. C., J. A. Heath (2020) Patterns and consequences of individual migration strategy in a partially migratory population of American kestrels. Poster and paper presentation at the Biology Graduate Proposal Showcase for the Department of Biological Sciences at Boise State University.

Heath, J. A., C. M. Bossu, S. E. Simmonds, M. S. Brinkmeyer, M. D. Oleyar, K. C. Ruegg (2019) Spatial patterns in circadian rhythm and migration candidate genes of American kestrels: the key to phenology shifts? Invited Poster presented at the SERDP & ESTCP Symposium 2019: Enhancing DoD's Mission Effectiveness, Washington DC.

Callery, K. R., J. A. Smallwood, A. L. Eschenbauch, E. R. Luttmann, J. A. Heath (2019) The consequences of breeding phenology and mismatch on American kestrel fitness. Paper presentation to the Raptor Research Foundation, Annual Meeting, Fort Collins, CO.

Ranck, S. S. F. Hudon, J. A. Heath (2019) Heritability of telomere length in American kestrels. Poster presentation to the Raptor Research Foundation, Annual Meeting, Fort Collins, CO.

Hunt, A. R., J. M. Winiarski, S. Schulwitz, D. Oleyar, R. Fischer, J. A. Heath (2019) Collaboration across the geographic range and annual cycle of a widespread, migratory raptor (American kestrel; *Falco sparverius*) enhances scope and scale of phenology research. Poster presentation to the Raptor Research Foundation, Annual Meeting, Fort Collins, CO.

Winiarski, J. M., S. E. Schulwitz, C. J. W. McClure, J. A. Heath (2019) Spatial modeling of American kestrel breeding phenology across the continental U.S.A. Poster presentation to the Raptor Research Foundation, Annual Meeting, Fort Collins, CO.

Heath, J. A., C. M. Bossu, S. E. Simmonds, M. S. Brinkmeyer, M. D. Oleyar, K. C. Ruegg (2019) Spatial patterns in circadian rhythm and migration candidate genes of American kestrels. Paper presentation to the Raptor Research Foundation, Annual Meeting, Fort Collins, CO.

Heath, J. A., J. M. Winiarski (2019) Variation in phenological shifts: How do annual cycles and genetic diversity constrain or enable responses to climate change? Webinar #99 for SERDP & ESTCP Series.

Callery, K. C, J. A. Smallwood, A. L. Eschenbauch, E. R. Luttmann, J. A. Heath (2019) Timing is of the essence: does later breeding predict lower survival in American kestrels (*Falco sparverius*)? Paper presented at the American Ornithological Society Annual Meeting, Anchorage, AK.

Winiarski, J. M., J. A. Heath (2019) Predicting avian breeding phenology at a continental scale. Poster Presented at Boise State University's Graduate Student Showcase, Boise, ID.

Callery, K. C., J. A. Heath (2019) Later breeding predicts lower survival in American kestrels (*Falco sparverius*). Poster presented at Boise State University's Graduate Student Showcase, Boise, ID.

Winiarski, J. M., A. R. Hunt, S. E. Schulwitz, M. D. Oleyar, R. A. Fischer, J. A. Heath (2018) Collaborative partnerships enhance scope and scale of phenology research for DoD natural resource management. Poster presentation at the SERDP & ESTCP Symposium: Enhancing DoD's Mission Effectiveness, Washington DC

Heath, J. A., J. M. Winiarski, B. P. Pauli (2018) Poster presentation: Forecasting phenological responses of American kestrels to climate change: An individual-based modeling approach. Poster presentation at the SERDP & ESTCP Symposium: Enhancing DoD's Mission Effectiveness, Washington DC

Winiarski, J. M., B. P. Pauli, J. A. Heath (2018) Forecasting phenological responses of American kestrels to climate change: An individual-based modeling approach. Poster presented at the 9th Annual Northwest Climate Conference, Boise, ID

McCaslin, H. A., T. T. Caughlin, J. A. Heath (2018) Frequency and environmental correlates of long-distance natal dispersal in American kestrels (*Falco sparverius*). Poster presented at the 27th International Ornithological Conference, Vancouver, B.C.

Callery, K. C., J. M. Winiarski, J. A. Heath (2018) Consequences of mismatched breeding on the fitness of American kestrels. Paper presented at the 27th International Ornithological Conference, Vancouver, B.C.

Winiarski, J. M., B. P. Pauli, J. A. Heath (2018) Identifying the mechanisms driving earlier nesting by a partial migrant: an individual-based modeling approach. Paper presented at the 27th International Ornithological Conference, Vancouver, B.C.

Schulwitz, S., C. J. W. McClure, B. P. Pauli, J. A. Heath (2018) Research recommendations for understanding the American Kestrel decline. Paper presented at the 136th Stated Meeting of the American Ornithological Society Conference, Tucson, AZ.

M. S. Brinkmeyer, K. C. Ruegg, T. B. Smith, R. A. Bay, R. Harrigan, C. J.W. McClure, D. Oleyar, K. Miller, J. F. Therrien, T. Swem, C. W. Boal, R.D. Dawson, R. van Buskirk, L. Marrow, J. Marrow, J. A. Heath (2017) Using high-resolution genomic markers to identify discrete population structure in a continuously distributed raptor species. Paper presentation to the Raptor Research Foundation, Annual Meeting, Salt Lake City, UT.

Heath, J. A., B. P. Pauli, H. A. McCaslin, L. L. Dunn, C. J. W. McClure (2017) Insights from bird banding: Survival and causes of mortality of American kestrels. Paper presentation to the Raptor Research Foundation, Annual Meeting, Salt Lake City, UT.

McCaslin, H. A., J. A. Heath (2017) Environmental correlates of long-distance dispersal in American kestrels. Paper presentation to the Raptor Research Foundation, Annual Meeting, Salt Lake City, UT.